



Ca<sup>2+</sup>-sensitive Mef2c protein interactions  
and chromatin function in microglia-like  
cells

A thesis submitted for the degree of Doctor of  
Philosophy

At

Cardiff University  
School of Medicine

Cerys Ballard

2022



## Thesis Summary

Alzheimer's disease (AD) is a progressive neurodegenerative disorder for which there are no disease-modifying therapies. Genetic studies have identified over 50 susceptibility loci for sporadic AD including the locus encoding the transcription factor MEF2C. Most of the genes implicated in AD-risk are exclusively or preferentially expressed in microglia. Furthermore, AD-risk variants are enriched in microglial open chromatin regions that contain DNA binding motifs for MEF2C. Therefore, genetic variants that disrupt MEF2C binding to DNA in microglia may alter *cis*-gene expression, contributing to AD-risk. Understanding how MEF2C functions in microglia may provide valuable insights into the genetic basis of AD-risk.

To investigate the role of Mef2c in AD, mass spectrometry was used to identify proteins that co-purify with the endogenous protein in BV2 microglia-like cells. Two major Mef2c isoforms exist in BV2 cells that associate with 110 putative interactors including the transcriptional repressors, Hdac4, Hdac5, and Cabin1. Ionomycin treatment, that raises intracellular  $[Ca^{2+}]$ , caused the partial dissociation of these repressors from Mef2c and resulted in recruitment of the microglial amyloid- $\beta$  response proteins, Yes1 and Smpd13b to the Mef2c complex. However, no Mef2c-activating proteins were identified in the remodelled complex. Having demonstrated that ionomycin treatment remodels the Mef2c interactome, the effect of this treatment on chromatin accessibility in BV2 cells was investigated using ATAC-seq. This revealed that while the motifs for three transcription factors, Atf4, NFATC3 and p53, were enriched at  $Ca^{2+}$ -dependent differentially accessible sites, Mef2c sites were not similarly enriched. However, Mef2c motif-containing differentially accessible regions were associated with genes that control the microglial inflammatory response. This thesis investigated two mechanisms by which  $[Ca^{2+}]$  levels potentially influence gene regulation; altered protein interactions and chromatin accessibility and further contributes to our understanding of the transcription factor Mef2c,  $Ca^{2+}$  signalling, and chromatin function in BV2 cells. In conclusion,  $Ca^{2+}$  dysregulation in AD may result in remodelling of the Mef2c interactome leading to abnormal Mef2c-mediated inflammatory responses in microglia.

## Acknowledgements

Firstly, I would like to thank my supervisors Professor Derek Blake and Dr. Matt Hill for giving me the opportunity to work on this project. The experience has been both fascinating and challenging. I am so grateful for the invaluable support, advice, and guidance you have both given me throughout my PhD. You have provided me with so much experience allowing me to develop as a scientific researcher and set me up so well for my future career. Also, with your help, my PhD has become something I can really be proud of. Many thanks also go to Professor Phil Taylor and his lab group for adopting me along the way. It has been lovely to still feel part of the DRI and get to know members of the lab group better.

I would also like to especially thank Chris Smith who selflessly gave up his time and offered to help me. Thank you so much for showing me the ropes in the lab at the beginning of my PhD and for continuing to be the lab guru and fountain of all knowledge throughout my time at Cardiff.

There is no way I would have got through my PhD (and COVID!) without my fellow lab buddies. Thanks so much to Lauren Thorburn, Katy Widnall and Dina Fathalla for the numerous tea breaks and support. You guys have also been there and happy to listen to me even when you may not have wanted to! Working with you guys has been such a pleasure and I'm so glad I have had you to talk, complain and laugh with. I will miss you all immensely. Good luck Katy and Lauren with finishing your PhD's, I'm sure you will smash it!

Many thanks also to all the friends I have made during this PhD. You have all helped me really enjoy my time in Cardiff and helped me get through many a challenging day with some hilarious lunch and coffee breaks!

Last but definitely not least- my family. Mum, Dad, Eleri, Ben, and my wonderful husband Jonathan. Your continuous love, encouragement and support has been the main thing that has got me through the last 3 or so years. You have always been there for me in the hardest of times, always provide the right advice and always had faith in me, even when I didn't have any in myself. I cannot properly express my gratitude for all that you do for me so as a small gesture to show my appreciation, this thesis is dedicated to you.

## Abbreviations

AA: Alzheimer's Association

A $\beta$ : Amyloid beta

ACH: Amyloid cascade hypothesis

AChEIs: Acetylcholinesterase inhibitors

AD: Alzheimer's Disease

ADGC: Alzheimer's Disease Genetics Consortium

APS: Ammonium persulfate

ATAC-seq: Assay of transposase-accessible chromatin with sequencing

BFDR: Bayesian false discovery rate

BLAST: Basic local alignment search tool

BP: Base pair

CAA: Cerebral amyloid angiopathy

cDNA: Complementary DNA

CHARGE: Cohorts for Heart and Aging Research in Genomic Epidemiology

ChIP: Chromatin immunoprecipitation

CNS: Central nervous system

CRAPome: Contaminant repository for affinity purification

CSF: Cerebrospinal fluid

C-terminus: Carboxyl-terminus

DBD: DNA-binding domain

DMEM: Dulbecco's modified eagle medium

DMSO: Dimethyl sulfoxide

DNA: Deoxyribonucleic acid

dNTP: Deoxyribonucleotide triphosphates

DSM-5: Diagnostic and Statistical Manual of Mental Disorders Fifth Edition

DTT: Dithiothreitol

EMP: Erythromyeloid progenitor

ENCODE: Encyclopedia of DNA Elements

EOAD: Early onset Alzheimer's Disease

FAD: Familial Alzheimer's Disease

FBS: Foetal bovine serum

## Abbreviations

FDA: Food and Drug Administration  
GERAD: Genetic and Environmental Risk in AD  
GFP: Green fluorescent protein  
GOA: Gene ontology analysis  
GREAT: Genomic regions enrichment of annotations  
GWAS: Genome wide association study  
HJURP-C: Holliday junction recognition protein C-terminal  
HOMER: Hypergeometric optimisation of motif enrichment  
ICC: Immunocytochemistry  
IGAP: International Genomics of Alzheimer's Project  
IgG: Immunoglobulin G  
IGV: Integrative genomics viewer  
IP: Immunoprecipitation  
iPSC: Induced pluripotent stem cell  
kDa: Kilodalton  
LB: Luria-Bertani  
LD: Linkage disequilibrium  
LDTF: Lineage-determining transcription factor  
LOAD: Late onset Alzheimer's Disease  
MDAR: Mef2c motif-containing differentially accessible region  
mRNA: Messenger RNA  
MAPK: Mitogen activated protein kinases  
MS: Mass spectrometry  
NCBI: National Centre for Biotechnology Information  
NFT: Neurofibrillary tangles  
NGS: Next generation sequencing  
NIA: National Institute on Aging  
NLS: Nuclear localisation signal  
NMDA: N-methyl-D-aspartate  
N-terminus: Amino-terminus  
OCR: Open chromatin regions  
PAGE: Polyacrylamide gel electrophoresis

## Abbreviations

PBS: Phosphate buffered saline  
PCA: Principal components analysis  
PCR: Polymerase chain reaction  
PIC: Preinitiation complex  
RIPA: Radioimmunoprecipitation assay  
RiP: Reads in peaks  
RNA: Ribonucleic acid  
Rpm: Revolutions per minute  
RPMI: Roswell Park Memorial Institute  
SAD: Sporadic Alzheimer's Disease  
SAINT: Significance analysis of interactome  
SDS: Sodium dodecyl sulphate  
SDTF: Signal-dependent transcription factor  
SNP: Single nucleotide polymorphism  
SNV: Single nucleotide variant  
TAD: Transcription activation domain  
TBE: Tris-borate-Ethylenediaminetetraacetic acid  
TBST: Tris-buffered saline-Tween  
TEMED: N,N,N',N'-tetramethylethylenediamine  
TSS: Transcription start site  
TRE: Transcription response element  
UTR: Untranslated region  
v/v: volume/volume  
WB: Western blot  
WBR: Western blocking reagent  
w/v: weight/volume  
Y2H: Yeast two-hybrid

## Table of Contents

Thesis Summary .....	iii
Acknowledgements.....	iv
Abbreviations.....	v
Table of Contents.....	viii
Chapter 1 General Introduction .....	1
1.1 Alzheimer’s Disease.....	1
1.1.1 Clinical symptoms.....	1
1.1.2 Early theories & treatments .....	5
1.1.3 Aetiology of AD .....	9
1.2 Regulation of Gene Expression.....	12
1.2.1 Chromatin .....	13
1.2.2 Regulatory elements .....	14
1.2.3 Transcription factors .....	16
1.3 Microglia .....	20
1.3.1 Microglial ontogeny .....	21
1.3.2 Microglial function .....	22
1.3.3 Microglia and AD.....	25
1.3.4 Microglial gene <i>MEF2C</i> .....	28
1.4 MEF2C.....	29
1.4.1 MEF2 transcription factor family.....	29
1.4.2 <i>MEF2C</i> gene .....	30
1.4.3 MEF2C protein structure .....	31
1.4.4 MEF2C function .....	33
1.4.5 Regulation of MEF2C .....	35
1.4.6 MEF2C and disease.....	39
1.5 Protein-protein interactions.....	39
1.5.1 Protein-protein interaction detection methods .....	40
1.6 Thesis aims and structure.....	42
Chapter 2 Methods .....	43
2.1 Molecular Biology .....	43
2.1.1 Plasmid vectors .....	43
2.1.2 Plasmid construction .....	43
2.1.3 Polymerase chain reaction .....	44
2.1.4 Agarose gel electrophoresis .....	44



2.1.5 DNA extraction from gels .....	47
2.2 DNA Cloning .....	47
2.2.1 Restriction digestion of DNA .....	47
2.2.2 Ligation of DNA sequences into expression vectors .....	47
2.2.3 Transformation of bacteria .....	48
2.2.4 PCR colony screen .....	48
2.2.5 Plasmid DNA isolation .....	48
2.2.6 DNA sequencing .....	49
2.3 Cell Biology .....	49
2.3.1 Mammalian cell culture .....	49
2.3.2 Immunocytochemistry .....	50
2.3.3 Dual-luciferase reporter assays .....	50
2.4 Protein Analysis .....	51
2.4.1 Sample preparation .....	51
2.4.2 Sodium dodecyl sulphate-polyacrylamide gel electrophoresis .....	52
2.4.3 Western blotting .....	52
2.4.4 Antibodies .....	53
2.5 Proteomics .....	53
2.5.1 Crosslinking antibodies to protein G Dynabeads .....	53
2.5.2 Co-immunoprecipitation .....	54
2.5.3 Ionomycin stimulation .....	55
2.5.4 Co-IP sample preparation for mass spectrometry .....	55
2.5.5 Protein identification by mass spectrometry .....	56
2.5.6 HEK293T co-immunoprecipitation .....	56
2.6 Bioinformatics .....	58
2.6.1 General .....	58
2.6.2 Mass spectrometry data analysis .....	58
2.6.3 MAGMA .....	60
2.7 ATAC-seq .....	61
2.7.1 Library preparation .....	61
2.7.2 Sequencing, QC, and bed file preparation .....	63
2.7.3 Differential accessibility analysis .....	64
2.7.4 Principal components analysis .....	68
2.7.5 <i>De novo</i> motif enrichment analysis .....	68
2.7.6 Functional enrichment analysis .....	69
Chapter 3 Investigating the protein interactome of Mef2c in unstimulated BV2 cells .....	70

3.1 Introduction .....	70
3.2 Results.....	73
3.2.1 Co-immunoprecipitation of Mef2c in BV2 cells .....	73
3.2.2 MS analysis of Mef2c.....	73
3.2.3 Phosphoproteomic analysis of Mef2c .....	75
3.2.4 Proteomic analysis of Mef2c binding proteins .....	77
3.2.5 Functional annotation of Mef2c interactors.....	88
3.2.6 Validating putative interactors of Mef2c.....	94
3.3 Discussion.....	96
3.3.1 Distinct Mef2c isoforms in BV2 cells are detected by MS .....	96
3.3.2 Co-immunoprecipitation of known Mef2c interactors .....	97
3.3.3 Gene ontology analysis reveals involvement of Mef2c in several biological processes .....	99
3.3.4 Co-IP suggests Mef2c is being held in a partially repressed state in BV2 cells ..	100
3.3.5 Co-IP identifies potential novel Mef2c interactors .....	102
3.3.6 Mef2c directly interacts with Hdac4 but not Oasl1 .....	102
3.3.7 Limitations.....	103
3.3.8 Conclusions .....	103
Chapter 4 Investigating the effect of ionomycin treatment on the Mef2c interactome ....	105
4.1 Introduction .....	105
4.2 Results.....	108
4.2.1 Ionomycin stimulation optimisation.....	108
4.2.2 Mef2c co-immunoprecipitation in ionomycin-treated BV2 cells .....	108
4.2.3 MS analysis of Mef2c in ionomycin-treated cells .....	110
4.2.4 Phosphoproteomic analysis of Mef2c in ionomycin-treated cells .....	111
4.2.5 Proteomic analysis of Mef2c binding proteins in ionomycin-treated cells .....	113
4.2.6 Functional annotation of Mef2c interactors in ionomycin-treated cells .....	119
4.2.7 Comparison of unstimulated and stimulated datasets.....	120
4.3 Discussion.....	127
4.3.1 Further validation of distinct Mef2c isoforms in BV2 cells .....	127
4.3.2 Co-immunoprecipitation of the known interactor Mef2a .....	127
4.3.3 Gene ontology analysis reveals involvement of Mef2c in several biological processes .....	127
4.3.4 Ionomycin-treatment releases Mef2c from its repressed state .....	129
4.3.5 Co-IP identifies two potential novel interacting proteins.....	130
4.3.6 Limitations.....	130

4.3.7 Conclusions .....	131
Chapter 5 Assessing the effect of ionomycin treatment on the chromatin landscape.....	132
5.1 Introduction .....	132
5.2 Results.....	135
5.2.1 Principal components analysis .....	135
5.2.2 Differential accessibility analysis .....	136
5.2.3 <i>De novo</i> motif enrichment analysis .....	139
5.2.4 Peak annotation .....	147
5.2.5 Functional enrichment analysis .....	149
5.2.6 MAGMA.....	153
5.3 Discussion.....	154
5.3.1 Increases in intracellular [Ca <sup>2+</sup> ] result in changes to the chromatin landscape .	154
5.3.2 Atf4, NFATC3 and p53 motifs are associated with ionomycin-induced changes in chromatin accessibility in BV2 cells .....	154
5.3.3 App and immune-specific processes are potentially regulated by Mef2c in a Ca <sup>2+</sup> -dependent fashion .....	157
5.3.4 Ca <sup>2+</sup> potentially regulates genes and processes important for immune cell function which link to TREM2 signalling.....	158
5.3.5 Genes associated with Ca <sup>2+</sup> -regulated peaks are not enriched for AD-risk association signals.....	160
5.3.6 Limitations.....	161
5.3.7 Conclusions .....	161
Chapter 6 General Discussion .....	163
6.1 Elevated intracellular [Ca <sup>2+</sup> ] levels and Mef2c .....	165
6.2 Increases in intracellular [Ca <sup>2+</sup> ] may result in the regulation of the microglia inflammatory response by Mef2c .....	167
6.3 NFAT and Mef2c as downstream effectors of TREM2 signalling .....	168
6.4 Future directions .....	169
6.5 Final conclusions .....	173
References .....	174
Appendix.....	222
Appendix 1. Known interactors of Mef2c.....	222
Appendix 2. MDARs identified by HOMER .....	226

## Chapter 1 General Introduction

### 1.1 Alzheimer's Disease

Dementia is a general term used to describe a collection of symptoms that affect cognitive function. Alzheimer's Disease (AD), the most common cause of dementia, was first described in 1907 by Alois Alzheimer (Alzheimer, 1907). It is characterised as a progressive, multifarious, neurodegenerative disorder and accounts for more than 62% of dementia cases in the UK (Prince et al., 2014). In 2019, it was estimated that approximately 885,000 people in the UK had dementia with a prevalence rate of 7.1% in the older population. This number is projected to rise to around 1.6 million in 2040 if no disease-modifying treatments are found. The total cost of care for people with dementia in the UK in 2019 was £34.7 billion which is predicted to rise with the number of cases to around £94.1 billion in 2040 meaning the UK faces substantial costs associated with dementia (Wittenberg et al., 2019). This worldwide social and economic burden, which is greater than that for cancer, stroke and heart disease combined (Luengo-Fernandez et al., 2015), is expected to rise due to the ageing population and the increasing cost of full-time care. In 2020, 11.5% of all deaths had a primary cause attributed to dementia or AD. This was the second most common cause of death after COVID-19 (Office for National Statistics, 2021). AD is the only disease among the most common causes of death that has no disease-modifying therapies or vaccines, emphasising that research into novel treatment development is critical.

#### 1.1.1 Clinical symptoms

There are two main types of AD which, besides from age of onset, are clinically indistinguishable from each other. The most common form, late onset AD (LOAD), which is typically the sporadic form of AD (SAD), accounts for approximately 95% of cases whereas early onset (EOAD), which is typically the familial form of AD (FAD), accounts for around 5% (Bali et al., 2012; Zhu et al., 2015b). The first clinical symptoms for each develop at different ages with early onset at approximately 30-65 and late onset after 65 years of age. This thesis focuses primarily on LOAD/SAD which will be referred to as AD throughout, unless otherwise specified.

##### 1.1.1.1 Diagnostic Criteria

The current diagnostic standard for dementia diagnosis is the Diagnostic and Statistical Manual of Mental Disorders Fifth Edition (DSM-5) (American Psychiatric Association, 2013). The DSM-5 recognises two cognitive syndromes: mild neurocognitive impairment and

major neurocognitive impairment. Major impairment is defined as an objective severe cognitive decline that interferes with daily living activities but is not caused by delirium or another psychiatric, neurological, or medical disorder. On the other hand, mild impairment requires milder cognitive decline that does not impact the patient's ability to lead an independent lifestyle or complete complex daily tasks (e.g., driving a car). Interestingly, the DSM-5 criteria differ from previous DSM editions to account for dementias, such as frontotemporal and vascular, in which memory impairment is not a prominent or, in some cases present, symptom (Karantzoulis & Galvin, 2011). In the DSM-5, for a neurodegenerative dementia diagnosis, the presence of a memory impairment is no longer required.

More specifically to AD, the National Institute on Aging (NIA) and the Alzheimer's Association (AA) have developed diagnostic criteria that span the three main stages of AD; preclinical, prodromal, and overt (Albert et al., 2011; McKhann et al., 2011; Sperling et al., 2011). The NIA-AA criteria for dementia diagnosis requires a significant decline in daily functioning and objective impairment, either cognitive or behavioural, in at least two of the following: memory, reasoning and handling complex tasks, visuospatial abilities, language functions, or personality, behaviour, or comorbidity. The criteria for probable AD dementia diagnosis require that the dementia criteria are met along with the following: an insidious onset, gradual progression, initial cognitive symptoms either memory or non-memory related (e.g., language, executive function) and that the symptoms are not accounted for by another psychiatric, neurological, or medical disorder that can interfere with cognitive ability. Additionally, diagnostic certainty can be increased by the presence of positive biomarkers including cerebral spinal fluid (CSF) amyloid- $\beta$  ( $A\beta$ ) or tau and hippocampal atrophy detected by a magnetic resonance imaging (MRI) scan. A definite AD diagnosis requires histopathological confirmation from an autopsy or biopsy post-mortem.

#### *1.1.1.2 Cognitive, behavioural, and psychological symptoms*

AD progresses through several stages of severity over a time course of approximately 7-10 years. There are three main stages of AD progression; mild, moderate, and severe which account for approximately 127,000, 246,000 and 511,000 of the 885,000 UK cases, respectively (Wittenberg et al., 2019). A decline in cognitive abilities is a distinguishing feature of AD. Cognitive symptoms typically experienced by AD patients include memory impairment, including both recent episodic and long-term memories, a decline in language

and visuospatial abilities, executive dysfunction; issues with problem-solving or attention, and loss of insight (Apostolova, 2016). AD patients also eventually become entirely dependent on carers for all daily activities and in advanced stages often become unable to walk, speak or control bladder or bowel function (Holtzman et al., 2011).

Despite the emphasis on cognitive impairment in AD, there are also several non-cognitive symptoms. Behavioural and psychological symptoms have a prevalence rate of 60-92% in AD and can include apathy, anxiety, irritability, mild to moderate depression, sleep disturbances, disinhibition, hallucinations, and delusions (Apostolova, 2016; Fernández et al., 2010; Karantzoulis & Galvin, 2011; Li et al., 2014). The manifestation of these symptoms contribute to disease morbidity and have been associated with increased impairment in daily activities (Lyketsos et al., 1997), enhanced carer burden and stress (Shaji et al., 2009; Teri, 1997), decreased quality of life for the patient (Gonzalez-Salvador et al., 2000) and increased likelihood of earlier patient institutionalisation (Steele et al., 1990). Many of these non-cognitive symptoms are episodic, tend to worsen with time and can precede cognitive impairment or AD diagnosis (Wise et al., 2019).

#### *1.1.1.3 Neuropathological hallmarks of AD*

Alois Alzheimer defined two key neuropathological features of AD; extracellular amyloid plaques and intracellular neurofibrillary tangles (NFT) (Alzheimer, 1907). The presence of these features is still essential for the pathological diagnosis of AD.

Plaques are composed of aggregated amyloid beta ( $A\beta$ ) peptides.  $A\beta$ , which typically consists of 40-42 amino acid peptides, is generated as a result of amyloidogenic processing of amyloid precursor protein (APP) through sequential cleavages by  $\beta$  and  $\gamma$  secretases.  $A\beta$  production is precluded by nonamyloidogenic processing of APP in which  $\alpha$  secretase cleaves APP in the  $A\beta$  domain.  $A\beta$  overproduction and accumulation results from increased amyloidogenic processing of APP.  $A\beta$  peptides form synaptotoxic intermediate soluble oligomers and also fold into insoluble, highly fibrillogenic, beta-pleated amyloid fibrils that are the main component of dense core plaques (Glenner & Wong, 1984; Jarrett et al., 1993; Lambert et al., 1998). In addition to depositing as amyloid plaques in the brain parenchyma,  $A\beta$  peptides also deposit in cerebral blood vessels resulting in cerebral amyloid angiopathy (CAA) in approximately 85-95% of AD cases (Jellinger, 2002; Kalaria & Ballard, 1999). CAA amyloid deposits typically contain  $A\beta_{40}$  peptides whereas in the parenchyma  $A\beta_{42}$  peptides predominate and tend to be the major component of amyloid plaques (Serrano-Pozo, et al., 2011a). CAA can result in impaired blood flow, ischemic

lesions, infarcts or in worst cases, lobar haemorrhages (Deture & Dickson, 2019; Perl, 2010). Additionally, A $\beta$  targets mitochondria early on in the disease as A $\beta$  has been found in the mitochondria of post-mortem brains, brains of transgenic mice and brains of living AD patients (Ankarcrona et al., 2010). In mitochondria, A $\beta$  is thought to increase free radical generation and induce oxidative stress (Markesbery, 1997; Zhao & Zhao, 2013) which can result in tissue and cell damage.

NFTs are composed of aggregated, hyperphosphorylated, and misfolded tau (Brion et al., 1986). Tau is a microtubule-associated protein which is important for stabilising neuronal microtubules involved in axonal transport (Kadavath et al., 2015). Tau filaments in AD are also referred to as paired helical filaments (PHF) as they are composed of two smaller filaments that coil together (Kidd, 1963). The progression of NFTs in AD have been described in six stages. In stage one, NFTs appear in the entorhinal cortex and transentorhinal region, followed by the CA1 region of the hippocampus in stage two. NFTs then develop in the limbic structures in stage three and the amygdala, claustrum, and thalamus in stage four. In stage five, tangles develop in the isocortical areas and finally in the primary motor, sensory and visual areas in stage six (Arnold et al., 1991; Braak & Braak, 1991). The burden and distribution of NFTs correlates with the severity and duration of AD (Arriagada et al., 1992; Giannakopoulos et al., 2003).

Other neuropathological hallmarks include neuronal loss, reduction in synaptic connections and reactive gliosis. The oligomeric neurotoxic species of amyloid and tau are thought to drive neuronal and synaptic loss in early stages of AD (Forner et al., 2017; Overk & Masliah, 2014). Neuronal and synaptic loss parallel the distribution of NFTs in AD and begin in the hippocampus before spreading widely throughout the brain (Braak & Braak, 1991; Jahn, 2013). Synapse loss appears to precede neuronal loss and is the strongest correlate of cognitive decline surpassing correlations with tau burden and neuronal loss (Terry et al., 1991). Gliosis is also often observed in AD brains. Activated microglia, the resident phagocytes of the brain, tend to accumulate around and within dense-core amyloid plaques and in the vicinity of tangles (Itagaki et al., 1989; Serrano-Pozo et al., 2011b). Reactive astrocytes are also observed, although in lower abundance than microglia. Astrocytes react to cytokines released by active microglia and these changes are thought to be neurotoxic (Liddelow et al., 2017). Additionally, astrocytosis and microgliosis increase linearly throughout the disease unlike amyloid load which tends to plateau soon after symptom onset (Serrano-Pozo et al., 2011b). Both astrocytes and microglia are thought to play potentially causal roles in AD as genes associated with AD risk are enriched in these

cell types, in particular, microglia (Efthymiou & Goate, 2017; Skene & Grant, 2016). Recent work has also highlighted a role of both astrocytes and microglia in inflammation and pathological protein clearance in AD (Smith et al., 2022). Single-nuclei RNA-sequencing (snRNASeq) from post-mortem human brain tissue from AD and control brains with a variety of A $\beta$  and phospho-tau (pTau) pathology revealed significant changes in microglial and astrocyte gene expression between the two groups. Distinct sets of differentially expressed genes were delineated for each cell type and pathology. More specifically, in microglia with AD pathology, genes involved in autophagy, inflammation, phagocytosis and proteostasis were highly expressed. In astrocytes with AD pathology, enrichment was found in inflammatory, metal ion homeostasis and proteostasis pathways, highlighting an important role of these glial cells in AD pathology and a development of pathology-specific transcriptional responses. Specific transcription factors were also upregulated in each cell type highlighting distinct sets of factors involved in regulating responses of microglia and astrocytes to AD pathology.

Due to significant neuronal and synapse loss, several macroscopic features are also often present in AD brains. Typically, moderate cortical atrophy is observed which is most prominent in limbic lobe structures (e.g., hippocampus, amygdala) and multimodal association cortices (Deture & Dickson, 2019). Enlarged sulci and atrophied gyri are commonly seen in the frontal and temporal lobes whereas somatosensory and primary motor cortices are typically unaffected (Perl, 2010). However, macroscopic features are not specific to AD and these features are observed in clinically normal people and in other age-related disorders.

### 1.1.2 Early theories & treatments

#### 1.1.2.1 Amyloid Cascade Hypothesis

The identification of A $\beta$  in plaques led to the development of the “Amyloid Cascade Hypothesis” (ACH) which postulates that A $\beta$  deposition is the initial causative agent of AD pathology and ultimately results in NFT formation, neuronal death, and dementia (Hardy & Higgins, 1992; Hardy & Allsop, 1991). Several lines of evidence offer support for this hypothesis. For example, in the aggressive, typically early-onset familial form of AD (FAD), autosomal-dominant mutations in essential genes involved in APP processing and subsequent A $\beta$  production are present. Mutations in *APP* and presenilin 1/2 (*PSEN1/2*), which make up  $\gamma$  secretase, alter the proteolytic cleavage of APP resulting in increased production of A $\beta$ 42 peptides leading to AD pathology (Arber et al., 2019; Chévez-Gutiérrez



et al., 2012). Moreover, a considerable proportion of patients with Down's syndrome, who have an extra copy of chromosome 21 and thus overexpression of the *APP* gene, display a clinical manifestation of AD (Head et al., 2012; Wisniewski et al., 1985). Additionally, APP or APP/PS1 transgenic mouse models, in which FAD-associated mutant forms of human *APP* and or *PSEN1* are overexpressed, display some of the key features of AD including amyloid plaque formation, synaptic loss, and memory impairment (Puzzo et al., 2014). These findings initially offered convincing support for the validity of the ACH and led to the development of several potential amyloid-directed treatments for AD.

However, since its inception, the ACH has been widely contested by a large body of evidence. It has been consistently demonstrated that the accumulation and deposition of A $\beta$  only weakly correlates with disease severity or neuronal loss. Furthermore, some patients present with significant plaque burden but show no memory impairment symptoms (Aizenstein et al., 2008; Villemagne et al., 2011). Another issue with this hypothesis is the reliance on evidence generated from transgenic mouse models. These models arguably do not accurately represent human pathology as they carry FAD mutations which do not reflect 95% of cases which are sporadic (SAD) and polygenic. Additionally, although these models show evidence of A $\beta$  accumulation there is no evidence of tangle formation or neuronal death, two key features of human SAD pathology (Drummond & Wisniewski, 2017). Moreover, many clinical trials which focus on clearing and preventing A $\beta$  accumulation in the brain, have failed to demonstrate clinical efficacy as they are unable to prevent or slow the course of AD (Mehta et al., 2017). Currently, no disease-modifying therapies have been approved in the UK. This brings the ACH into question as A $\beta$  may not be the central pathogenic factor of AD. Thus, exploration of novel disease mechanisms and pathways is vital for the development of more fruitful drug targets.

#### 1.1.2.2 *Ca<sup>2+</sup> Hypothesis*

In cells, Ca<sup>2+</sup> is a ubiquitous second messenger involved in a range of physiological processes including cell proliferation, differentiation, gene transcription, and apoptosis (Berridge et al., 2000; Bootman et al., 2001). In neurons, the regulation of Ca<sup>2+</sup> homeostasis is vital for normal function, development, and health (Berridge et al., 1998; Emptage et al., 2001). Sustained elevated levels of [Ca<sup>2+</sup>] can trigger excessive cell proliferation, necrosis, and apoptosis (Calvo-Rodriguez et al., 2020). In 1987, it was postulated that persistent [Ca<sup>2+</sup>] imbalance can lead to the disruption of normal neuronal functioning and ultimately neurodegenerative diseases like AD (Khachaturian, 1987). This led to the development of

the “Ca<sup>2+</sup> hypothesis of Alzheimer’s Disease” which proposes that abnormal amyloid metabolism results in the alteration of normal neuronal Ca<sup>2+</sup> signalling pathways which affect Ca<sup>2+</sup> homeostasis and cause both a disruption of learning and memory processes and an increase in neuronal cell death (Khachaturian, 1989). This Ca<sup>2+</sup> dysregulation appears to occur early in the disease prior to the development of clinical symptoms or histopathological hallmarks (LaFerla, 2002). Ca<sup>2+</sup> dysregulation is characterised by both abnormal Ca<sup>2+</sup> homeostasis and exaggerated Ca<sup>2+</sup> responses to stimuli which may cause elevated resting [Ca<sup>2+</sup>] (McDaid et al., 2020). Support for the role of Ca<sup>2+</sup> dysregulation in AD is provided by a wealth of research that has shown that disturbances in Ca<sup>2+</sup> signalling have been reported in both familial (Zatti et al., 2004) and sporadic AD (Tolar et al., 1999), mouse models of the disease (Arbel-Ornath et al., 2017; Calvo-Rodriguez et al., 2020; Kuchibhotla et al., 2008) and in human-derived post-mortem brains and cells (Gibson et al., 1997; Gibson & Peterson, 1987; Mattson et al., 1992).

Ca<sup>2+</sup> ions are thought to contribute to the hyperphosphorylation of tau (Cao et al., 2019). Furthermore, Ca<sup>2+</sup>-dependent increases in APP processing have been reported, which result in the production of toxic A $\beta$  fragments and the activation of signalling cascades that ultimately lead to changes in synaptic plasticity and cognitive functioning (Chami & Checler, 2020). For example, the proteolytic activity of beta-secretase 1 (BACE1), which is involved in APP processing, is enhanced by Ca<sup>2+</sup> (Hayley et al., 2009). This evidence provides further support for the Ca<sup>2+</sup> hypothesis and suggests that Ca<sup>2+</sup> dysregulation is not only a consequence of AD but also contributes to disease progression and intensification. The role of Ca<sup>2+</sup> signalling in AD is discussed and explored in more detail in chapters 4, 5 and 6.

### *1.1.2.3 Current AD treatments*

Only symptom-modifying treatments are currently available for AD in the UK. Management of the disease is currently tailored to each individual patient and adapted as it progresses. Existing medications currently only have modest benefits, but evidence suggests that the appropriate treatment of cognitive symptoms can delay institutionalisation, prolong independence, and improve quality of life (Howard et al., 2015; Knapp et al., 2017; Laver et al., 2016).

There are currently only a small number of drugs approved by the FDA and licenced in the UK for AD treatment. Drugs include acetylcholinesterase inhibitors (AChEIs) and the NMDA receptor antagonist memantine which result in temporary symptom alleviation with varied effectiveness between patients. AChEIs, including donepezil, rivastigmine and galantamine,

increase levels of acetylcholine by preventing its breakdown at the synapse (Lane et al., 2018). Acetylcholine is a neurotransmitter involved in learning and memory which is reduced in AD brains (Jia et al., 2004). AChEIs lead to small improvements in cognitive function, daily living, and behaviour in mild and moderate AD (Birks, 2006; Knight et al., 2018). There is no evidence to suggest that one drug in this class is more efficacious than another (Birks, 2006). An alternative symptomatic treatment is memantine which is licensed for moderate and severe cases of AD. Memantine is a low affinity N-methyl-D-aspartate (NMDA) receptor antagonist which aims to reduce glutamate-induced excitotoxicity and subsequent neuronal dysfunction and death (Joe & Ringman, 2019). Memantine has been found have a small clinical benefit on cognition, daily living, clinical global rating, behaviour and mood in patients with moderate to severe AD, but no benefit in patients with mild AD (Mcshane et al., 2019). A meta-analysis of 11 trials has suggested that combination therapy using an AChEI and memantine can improve cognition, global function, and behavioural symptoms in moderate to severe AD more so than AChEIs alone (Chen et al., 2017).

These treatments can slow symptom progression and provide some symptomatic relief, but a number of patients who take these drugs do not respond (Farlow et al., 2008). Furthermore, these drugs are not disease-modifying as they cannot prevent onset or halt disease progression.

More recently, the US FDA approved the first disease-modifying treatment for AD. Aducanumab is a human IgG1 anti-A $\beta$  monoclonal antibody which targets A $\beta$  oligomers and fibrils (PCNS, 2020). Aducanumab has been approved, based on evidence that it can reduce A $\beta$  in the brain, under the accelerated approval pathway which means that further stage four clinical trials need to be completed (US Food and Drug Administration, 2021). Two phase three clinical trials were set up in 2015 by the sponsor Biogen to determine the efficacy of Aducanumab, however these studies were later terminated in 2019. Despite this, three months later Biogen concluded that there was sufficient clinical efficacy. One trial showed statistically significant effects in the high-dose group on several clinical outcome measures, but the other showed no benefits (Haeberlein et al., 2019; Kuller & Lopez, 2021). This has resulted in a lot of controversy surrounding the FDA's approval of Aducanumab (Alexander et al., 2021; Knopman et al., 2021; Knopman & Perlmutter, 2021) and it is still unclear when or whether it will be approved in the UK. However, Aducanumab is still the first drug to target one of the potential underlying causes of AD, this is a step in

the right direction and could result in a change to the level of priority and investment into AD drug development.

### 1.1.3 Aetiology of AD

#### *1.1.3.1 Non-genetic risk factors*

There are several non-genetic risk factors for AD which contribute to the complexity of AD causality. The strongest risk factor for AD is aging. With every 5-year increase in age, the prevalence of dementia doubles. In the US, prevalence steeply increases from 5.3% of 65-74 year olds to 13.8% of 75-84 year olds to 34.6% of people over 85 years old (Rajan et al., 2021). Other factors that have adverse effects on risk include type 2 diabetes, carotid atherosclerosis and hypertension (Xu et al., 2015). Moreover, gender is thought to modulate AD prevalence as approximately two-thirds of AD patients are women (Alzheimer's Association, 2020). Although the fact that women live longer than men will account for some of this discrepancy, it cannot completely explain it. Epidemiological evidence suggests that there are some protective factors against AD which include physical exercise, education, and social and cognitive engagement (Krueger et al., 2009; Sajeev et al., 2016; Sando et al., 2008). This large range of non-genetic risk factors that influence the development of AD suggest that AD is not mediated by genetics alone but by a combination of genetic and environmental risk factors.

#### *1.1.3.2 Genetic risk factors*

The vast majority of AD cases occur sporadically, however a rare (<0.5%) familial form (predominately early onset) is caused by mutations in one of three rare, highly penetrant mendelian genes involved in APP processing; amyloid precursor protein (*APP*), presenilin 1 (*PSEN1*) and presenilin 2 (*PSEN2*) which account for 14%, 80% and 5% of cases, respectively (Bateman et al., 2011; Bekris et al., 2010; Dai et al., 2018). *APP* and *PSEN1* mutations are associated with complete penetrance, meaning that inheriting a mutation in these genes guarantees AD development if the person lives a normal lifespan. Whereas *PSEN2* mutations have 95% penetrance meaning that not all people with this mutation develop AD (Goldman et al., 2011; Sherrington et al., 1996; Tedde et al., 2003). A $\beta$  overproduction and accumulation as a consequence of increased amyloidogenic processing of APP is thought to be the central cause of familial, early-onset AD.

Alternatively, typically late-onset sporadic AD has less familial aggregation and is described as a polygenic disease driven by a complex interplay between environmental and genetic

factors. Heritability estimates for AD are 58-79% (Gatz et al., 2006), suggesting that a significant component of risk for AD is driven by genetic factors. The strongest single genetic risk factor for AD is apolipoprotein E (*APOE*) located on chromosome 19, which was the first gene to be identified as a risk factor for SAD (Saunders et al., 1993). This gene has three disease-modifying coding variants,  $\epsilon 2$ ,  $\epsilon 3$ , and  $\epsilon 4$ . An increased AD-risk is observed in carriers of the  $\epsilon 4$  allele whereas a small protective effect is conferred by the  $\epsilon 2$  allele (Corder et al., 1994; Strittmatter et al., 1993).  $\epsilon 4$  heterozygotes have a 3-fold risk increase which rises to  $\sim 12$ -fold in homozygotes (Verghese et al., 2011). *APOE* participates in many pathways and the precise disease-relevant mechanisms are unknown, however, the presence of the  $\epsilon 4$  allele is thought to render the protein less efficient in its ability to clear  $A\beta$  from the brain across the blood-brain barrier (Deane et al., 2008). Unlike the *FAD*-associated causal genes, inheriting a genetic mutation in the *APOE*  $\epsilon 4$  gene does not guarantee that the individual will develop AD, it is a low penetrance allele.

Genome-wide association studies (GWAS) have identified several small effect size single nucleotide polymorphisms (SNPs) associated with AD. Combined with next generation sequencing, to detect AD-associated rare single nucleotide variants (SNVs), these genetic studies have identified more than 50 susceptibility loci for AD that reach genome-wide significance (Sims et al., 2020). GWAS is arguably the most successful approach to identify genetic risk factors for AD. In 2009, The Genetic and Environmental Risk in AD Consortium (GERAD) published two GWAS which demonstrated genome-wide statistically significant associations between AD and variants at phosphatidylinositol binding clathrin assembly protein (*PICALM*), clusterin (*CLU*), and complement receptor 1 (*CR1*) (Harold et al., 2009; Lambert et al., 2009). Several other studies quickly followed these initial GWAS, including Cohorts for Heart and Aging Research in Genomic Epidemiology (CHARGE) and AD Genetics Consortium (ADGC) which identified more novel genetic risk loci for AD including bridging integrator 1 (*BIN1*), exocyst complex component 3 like 2 (*EXOC3L2*), membrane spanning 4-domains A4A (*MS4A4*), CD2 associated protein (*CD2AP*), *CD33*, and EPH receptor A1 (*EPHA1*) (Naj et al., 2011; Seshadri et al., 2010). Subsequently, these independent consortia united to form the International Genomic and Alzheimer's Project (IGAP). IGAP discovered, through a large meta-analysis of previous GWAS, 20 loci that reached genome-wide significance consisting of *APOE* and 11 new susceptibility loci including myocyte enhancer factor 2C (*MEF2C*), protein tyrosine kinase 2 beta (*PTK2B*) and inositol polyphosphate-5-phosphatase D (*INPP5D*) (Lambert et al., 2013). In 2019, IGAP completed another meta-analysis which used data from a larger sample of cases (21,982) and cognitively normal

controls (41,944). They confirmed 20 previously identified risk loci and identified genome-wide significant associations between 5 novel loci; IQ motif containing K (*IQCK*), angiotensin I converting enzyme (*ACE*), ADAM metallopeptidase domain 10 (*ADAM10*), ADAM metallopeptidase with thrombospondin type 1 motif 1 (*ADAMTS1*) and WW domain containing oxidoreductase (*WWOX*), and AD (Kunkle et al., 2019). To identify rare genetic variation, next generation sequencing (NGS) in the form of whole-genome and whole-exome sequencing has been utilised. These techniques have identified several rare AD-associated SNVs including variants in the triggering receptor expressed on myeloid cells 2 (*TREM2*) gene that increase AD-risk 3-4.5-fold (Guerreiro et al., 2013; Jonsson et al., 2013).

More recently, to expand the analytical capability of GWAS, individuals with a family history of AD have been included in GWAS meta-analyses, an approach called genome-wide association by proxy (GWAX). One AD-by-proxy study identified a total of 37 loci including novel associations near coiled-coil domain containing 6 (*CCDC6*), tetraspanin 14 (*TSPAN14*), NCK adaptor protein 2 (*NCK2*) and sprouty related EVH1 domain containing 2 (*SPRED2*) (Schwartzentruber et al., 2021). This paper also used a variety of techniques including fine-mapping and colocalization analyses to predict likely causal genes which included *BIN1*, aph-1 homolog B (*APH1B*), *PTK2B*, paired immunoglobulin like type 2 receptor alpha (*PILRA*), cas scaffold protein family member 4 (*CASS4*), and the four aforementioned genes.

Human genetic studies serve as a platform for identifying risk genes, SNPs and pathways causally associated with AD and for developing novel therapeutic targets and treatments. However, despite the successes of GWAS, several challenges arise that make GWAS data interpretation and the exploitation of findings to treatment development difficult. Firstly, most detected SNPs are in strong linkage disequilibrium (LD) with other variants, making it hard to identify which SNPs are biologically linked to AD-risk. Secondly, many approaches used to identify causal variants have focused on coding SNPs, however, the majority of risk alleles associated with AD are located in non-coding regions of the genome, which makes functional interpretation problematic as it is not clear through which gene(s) or cell type(s) the risk variant is operating (Schaub et al., 2012). These non-coding regions may modify AD-risk via altering the function of DNA regulatory elements that in turn regulate gene expression.

Analytical approaches have gradually begun to tackle some of these challenges and decipher which cells and mechanisms are likely to be affected by AD risk alleles. Pathway

analysis is one analytical method that can determine which biological pathways may underly the genetic susceptibility to a disease. Risk loci that fall below the genome-wide significance threshold are often incorporated into these analyses to capture a larger range of genetic association information. Jones et al (2015) aimed to establish the causative pathways that may underpin LOAD by performing a pathway and integrated gene expression analysis on the 2013 IGAP GWAS (Jones et al., 2015; Lambert et al., 2013). Several disease-relevant processes were identified including protein ubiquitination, regulation of endocytosis, cholesterol transport, and the immune response. Pathway analysis has also been performed on the latest GWAS in which lipid metabolism, tau binding proteins, APP metabolism and immunity were implicated in AD (Kunkle et al., 2019). As both analyses identified immunity as a key biological pathway that may underpin the genetic susceptibility to AD, this provides compelling evidence for the implication of immune cells and pathways as probable effectors of genetic AD-risk. Thus, a fuller appreciation of the role of immune cells, including microglia as the principle immune cells of the brain, and networks in AD genetic risk is important.

AD is a complex polygenic disease which is driven by several environmental and genetic factors. Treatments that are currently administered in the UK only alleviate symptoms and do not prevent onset or halt disease progression. Due to the worldwide social and economic burden of AD, the need for a disease-modifying therapy is growing exponentially. Exploring novel disease mechanisms and pathways would facilitate the development of new treatments. As a large majority of GWAS-identified AD-risk is localised to non-coding regions which may modify risk via altering regulation of gene expression, and as analytical approaches have hinted at an important role for immune cells, including microglia, in AD, the regulation of gene expression in microglia cells stands out as an interesting and important area to explore.

## 1.2 Regulation of Gene Expression

Most cells in the human body contain the same genetic information encoded in their DNA. However, cells are phenotypically and morphologically different. This cellular diversity is achieved via DNA transcriptional regulatory elements and the molecular machinery such as transcription factors that interact to mediate specific gene expression patterns. The effective execution of biological processes depends on the precise temporal and spatial expression of genes. The dysregulation of gene expression can result in the development of disease (Maston et al., 2006).

Only approximately 1.5% of the human genome, which is comprised of around 3.2 billion nucleotides, is protein coding (Lander et al., 2001; Marian, 2014). Initially, the remaining non-coding regions were thought to be 'junk' DNA with no functionality. However, it is now known, due to projects such as the Encyclopedia of DNA Elements project (ENCODE), that a crucial function of the non-coding genome is regulation of gene expression (ENCODE, 2004; Harrow et al., 2012). Advancing our understanding the non-coding genome and its contribution to disease is important.

### 1.2.1 Chromatin

Chromatin is the complex of DNA, RNA, and proteins that form the chromosomes in eukaryotic cells. The basic structural and functional unit of chromatin is the nucleosome which contains around 146 bp of DNA coiled around eight histone proteins which help package DNA into a compact form (Luger et al., 1997). The core histones, H2A, H2B, H3 and H4, form each protein octamer. They are bound on the surface by a H1/H5 linker histone which adds an additional 20 bp of DNA to the nucleosome (Robinson & Rhodes, 2006; Thomas & Kornberg, 1975). Short linker DNA sequences connect nucleosomes together creating a structure that resembles beads on a string (Olins & Olins, 1974; Olins & Olins, 2003). To regulate gene expression, chromatin alters its physical state. Heterochromatin is a tightly packed state in which nucleosomes are closely packed making the DNA difficult to access. Conversely, euchromatin is a relaxed, loosely packed state in which nucleosomes are either spaced out or completely depleted. This makes the DNA more accessible, therefore exposing it to regulatory molecules such as transcription factors that facilitate gene expression (Allis & Jenuwein, 2016). Accessible DNA accounts for approximately 2-3% of the total genome (Thurman et al., 2012). The degree to which chromatin is exposed is known as chromatin accessibility which is a measure of the functional state of chromatin. Chromatin accessibility is regulated via several mechanisms including the alteration of transcription factor binding and chromatin remodelling proteins (Allis & Jenuwein, 2016; Klemm et al., 2019).

Chromatin remodellers, which are grouped into four families based on their structure: SWI/SNF (switch/sucrose-non-fermenting), ISWI (imitation switch), INO80 (inositol requiring 80) and CHD (chromodomain-helicase-DNA binding), play key roles in the regulation of chromatin accessibility. These enzymes are involved in a range of chromatin remodelling reactions including changing the conformation of histone octamers or nucleosome DNA, displacing octamers from DNA, and nucleosome sliding in which an octamer slides across the DNA exposing underlying sections of DNA to regulatory factors (Clapier & Cairns, 2009;



Rippe et al., 2007). The ability of these proteins to restructure nucleosomes is dependent on ATP. ATP hydrolysis provides chromatin remodellers with energy allowing them to disrupt contact between DNA and histones and in turn regulate chromatin accessibility (Tyagi et al., 2016). Remodellers are recruited to specific target sites via several elements including transcription factors, histone variants and modifications, DNA sequence and structure, and RNA molecules (Längst & Manelyte, 2015). Chromatin can also be remodelled by external stimuli and intracellular signalling including interleukin-33 (IL-33) and  $Ca^{2+}$ , this is discussed in more detail in Chapter 5 (section 5.1).

One recent method that is widely used to measure genome-wide chromatin accessibility is the assay for transposase-accessible chromatin using sequencing (ATAC-seq) (Buenrostro et al., 2013). This technique was first described in 2013 and since then has been used to tackle a wide range of disease-relevant biological questions including an evaluation of chromatin states in the prefrontal cortex of schizophrenia patients and investigating chromatin accessibility differences between leukaemia and normal haematopoiesis (Bryois et al., 2018; Corces et al., 2016; Rendeiro et al., 2016). This technique is outlined in more detail in Chapter 2 (section 2.7) and used to assess chromatin accessibility in Chapter 5.

### 1.2.2 Regulatory elements

Regulatory elements are important for the initiation and modulation of gene expression. They are non-coding sections of DNA that bind proteins such as transcription factors. Regulatory elements are motif-based but are only accessible when chromatin is open. The exposure of specific sets of regulatory elements allows for cell-specific gene expression. These elements are either situated proximally or distally to the genes they regulate and include promoters, and enhancers, silencers, and insulators.

#### 1.2.2.1 Promoters

Promoters are regulatory elements that promote the initiation of transcription via the binding of transcription factors. A typical promoter sequence comprises several sequence motifs, which include TATA box, B recognition element (BRE), Initiator element (INR) box, GC-box, and CCAAT-box. These motifs are positioned at specific locations relative to the transcription start site (TSS) (Bucher, 1990; Kanhere & Bansal, 2005). Promoters are typically located close to the genes they influence; at the 5' ends of genes immediately surrounding the TSS (Smale & Kadonaga, 2003). All genes have at least one promoter situated upstream, with around 52% of genes having several additional, alternative promoters (Kimura et al., 2006). The core promoter acts as the assembly point for the basic

transcriptional machinery and preinitiation complex (PIC), which is formed of general transcription factors and RNA polymerase II (Pol II) (Sainsbury et al., 2015). The PIC directs Pol II to the transcription start site which establishes the direction of transcription and initiates mRNA production. Binding of Pol II is sufficient to activate basal, low level RNA transcription. To modulate the rate of gene expression and regulate transcription initiation, additional activator proteins are required to bind to the proximal promoter which is situated upstream of the core promoter (Maston et al., 2006; Smale & Kadonaga, 2003).

#### *1.2.2.2 Enhancers*

Enhancers are cis-acting DNA sequences that facilitate the transcription of target gene(s) from locations upstream, downstream, or within a target or neighbouring gene (Blackwood & Kadonaga, 1998). They were first identified in the simian virus 40 genome as 72-bp repeat sequences that can increase gene transcription (Banerji et al., 1981; Moreau et al., 1981). Due to a lack of universal sequence characteristics, such as shared protein binding elements or CpG islands (Cowie et al., 2015; Maston et al., 2006), enhancers are typically harder to identify than promoters. Additionally, enhancers do not necessarily act on their closest promoter, they can regulate a gene, in some cases multiple genes, that are situated distally along a chromosome (Pennacchio et al., 2013). Enhancers have a dynamic nature, they regulate gene expression in a temporal-, spatial- and cell type-specific manner. To modulate expression of target genes, enhancers are brought into close spatial proximity of the core promoter via chromatin looping; a phenomenon in which sections of the genome fold into loops subsequently bringing the elements closer together in three-dimensional space (Kadauke & Blobel, 2009; Schoenfelder & Fraser, 2019). This allows DNA-binding transcription factors that are bound to promoters and enhancers to either interact or recruit other factors that mediate the long-range contact. Enhancer-promoter looping also delivers other factors like RNA polymerase and transactivators to the promoter in the right tissue and at the right time (Pennacchio et al., 2013). Some transcriptional activators bind both enhancers and proximal promoters in different genes making distinction between the two elements difficult (Maston et al., 2006).

#### *1.2.2.3 Silencers and insulators*

Two additional regulatory elements in the non-coding genome are silencers and insulators. Silencers repress promoter activity and subsequent target gene transcription via the binding of transcription factors known as repressors. Similarly to enhancers, they function independently of distance or orientation from the promoter (Ogbourne & Antalis, 1998).

Conversely, insulators, which are approximately 0.5-3 kb in length, prevent genes from being affected by neighbouring transcriptional activity. Insulators can both prevent the spread of heterochromatin and block communication between enhancers and promoters (Maston et al., 2006). For example, the zinc finger transcription factor, CCCTC-binding factor (CTCF), which can act as either an activator or a repressor of enhancers, can also function as an insulator protein. Upon binding to an insulator sequence, the communication between an enhancer and a gene promoter is blocked, thus preventing gene transcription. This mechanism allows for the blocking of inappropriate enhancer signals, stopping any spurious gene activation (Kim et al., 2015; Yusufzai et al., 2004).

#### *1.2.2.4 Histone modifications and regulatory elements*

Histone modifications are post-translational modifications which are covalently bound to histone proteins. There are around eight distinct histone modification types and these modifications have been detected in over 60 different residues (Kouzarides, 2007). Histone modifications can regulate gene expression by modifying the structure and function of chromatin via several mechanisms including the recruitment of chromatin remodellers and direct interaction with DNA. Active enhancers and promoters are associated with distinct histone modifications; thus the mapping of these modifications can be used to determine the activation status of proximal regulatory elements and to functionally annotate the genome (Tessarz & Kouzarides, 2014). Two common modifications that are used to mark proximal and distal regulatory elements are methylation and acetylation. Specifically, the methylation status (me1, me2 or me3) and the location of the modified lysine residue on histone tails are associated with specific gene expression states (Greer & Shi, 2014). For example, the trimethylation of lysine 4 of histone H3 (H3K4me3) and acetylation of lysine 9 and 14 of histone H3 (H3K9ac, H3K14ac) mark histones in promoter regions of actively transcribed genes (Bernstein et al., 2002; Guenther et al., 2007), whereas the monomethylation of lysine 4 of histone H3 (H3K4me1) and the acetylation of lysine 27 of histone H3 (H3K27ac) are associated with active enhancers (Creyghton et al., 2010; Heintzman et al., 2007). The high-resolution of these histone modification markers can help to define distinct chromatin states and allow for the identification of novel regulatory elements in the human genome.

#### 1.2.3 Transcription factors

Transcription factors represent approximately 8% of all human genes. Generally, these proteins bind DNA in a sequence-specific manner and regulate gene expression (Fulton et

al., 2009; Vaquerizas et al., 2009). Initial descriptions of the major transcription factor families, including basic helix-loop-helix (bHLH), C2H2-zinc finger, basic leucine zipper (bZIP), nuclear hormone receptor (NHR) and homeodomain, were made in the late 1980s (Johnson & McKnight, 1989). Transcription factors are grouped into families primarily based on the presence of distinct DNA binding domains (DBDs) which allow factors to bind to specific DNA sequences (Lambert et al., 2018).

Several transcription factors are generically expressed and serve the same function in all cell types. However, other transcription factors are expressed in a tissue- and cell-type specific manner. Lambert et al (2018) used RNA-seq to determine expression patterns of transcription factors and found that approximately one-third of human transcription factors are expressed in specific tissues. For example, GATA binding protein 4 (GATA4) and T-Box transcription factor 20 (TBX20), which are important for heart development and myocardial differentiation and function, were highly expressed in cardiac muscle whereas SRY-box transcription factor 2 (SOX2) and oligodendrocyte transcription factor 1 (OLIG1), which are required for stem-cell maintenance in the central nervous system (CNS) and the formation and maturation of oligodendrocytes, were expressed almost exclusively in the cerebral cortex.

#### *1.2.3.1 DNA binding and gene transcription*

To regulate transcription, transcription factors must be able to access nucleosome DNA. Transcription factors either bind directly, via direct interaction with short 6-12 bp sections of DNA known as motifs, or indirectly by binding to DNA as part of a larger protein complex. Transcription factors are known to cooperate with one another in a number of ways to activate transcription. These include altering transcription or chromatin state via synergistic regulation or by binding directly which each other as homodimers, trimers, or higher-order structures (Lambert et al., 2018).

Upon DNA-binding, the impact of different transcription factors on gene transcription varies. Some recruit accessory factors for the promotion of transcription, whilst others directly recruit RNA polymerase or block other proteins from binding to the same site (Akerblom et al., 1988; Frietze & Farnham, 2011). The primary action by most transcription factors is the recruitment of cofactors; coactivators and corepressors (Reiter et al., 2017). These cofactors tend to be multi-domain proteins or multi-subunit protein complexes which regulate gene expression via a number of mechanisms such as histone or transcription factor modification, chromatin and nucleosome remodelling and interaction

with the core transcriptional machinery (Frietze & Farnham, 2011; Vernimmen & Bickmore, 2015). Interferon-beta (*IFN-β*) gene expression requires the recruitment of multiple cofactors. The transcription factors interferon regulatory factor-3 (IRF-3), interferon regulatory factor-7 (IRF-7), activating transcription factor 2 (ATF-2)/c-Jun and nuclear factor kappa-light-chain-enhancer of activated B cells (NFκB) cooperatively bind as an enhancosome to the *IFN-β* promoter. This results in the recruitment of histone acetyltransferases including p300/CREB binding protein (CBP) and general control non-depressible 5 (GCN5), leading to nucleosome acetylation and changes to chromatin by remodellers (e.g. SWI/SNF complex) to initiate transcription (Panne, 2008). The recruitment of cofactors allows transcription factors to act as activators, repressors, or in cases where transcription factors can recruit several cofactors with opposing effects, both (Lambert et al., 2018). For example, when MYC associated factor X (MAX) is bound to DNA as a heterodimer with MYC proto-oncogene (MYC) it acts as an activator however, when bound as a heterodimer with MAX dimerization protein 1 (MXD1) it acts as a repressor (Amati & Land, 1994). The recruitment of specific cofactors by transcription factors is often regulated by effector domains such as the Krüppel associated box (KRAB) domain, present in approximately 350 human C2H2-zinc finger transcription factors. This domain recruits KRAB-associated protein 1 (KAP1) which acts as a platform for binding of a silencing complex composed of SET domain bifurcated histone lysine methyltransferase 1 (SETDB1), nucleosome remodelling and deacetylase (NuRD) and heterochromatin protein 1 (HP1). This results in the deposition of H3K9me3, a repressive histone modification, and the formation of heterochromatin (Ecco et al., 2017).

#### 1.2.3.2 Pioneer transcription factors

One class of transcription factors, known as master regulators or pioneer transcription factors, establish a heterochromatin state by directly binding to nucleosome DNA (Klemm et al., 2019). During remodelling of accessibility, these are the first transcription factors to bind to DNA (Sherwood et al., 2014; Zaret & Carroll, 2011). Once bound, these factors disrupt chromatin, and create nucleosome-free regions at regulatory elements, flagging parts of the genome for gene expression. Additional transcription factors are then recruited to the site to activate or prime enhancers and promoters and facilitate transcription (Zaret & Carroll, 2011). Purine rich box-1 (PU.1) and CCAAT-enhancer-binding protein (C/EBP) are two pioneer factors that bind and act in combination at specific enhancer sites to increase chromatin accessibility. For example, in macrophages the recruitment of p300 in response to Toll-like receptor 4 (TLR4) signalling primarily occurs at sites with combinatorial

interactions of PU.1 and C/EBP which result in a functionally active enhancer (Carotta et al., 2010; Ghisletti et al., 2010; Heinz et al., 2010). Additionally, the well documented 'Yamanaka' reprogramming transcription factors, octamer-binding transcription factor 3/4 (Oct3/4), Sox2, and Kruppel like factor 4 (Klf4), are also pioneer factors which can access closed chromatin. The fourth factor, MYC proto-oncogene (c-Myc) prefers to bind sites of open chromatin but can bind closed sites in conjunction with the other reprogramming factors (Iwafuchi-Doi & Zaret, 2014; Soufi et al., 2012). These proteins can convert fibroblasts into induced pluripotent stem cells (iPSCs) (Takahashi & Yamanaka, 2006). They initiate reprogramming by preferentially binding to closed distal enhancer target sites which subsequently activate genes that elicit both reprogramming and apoptosis (Soufi et al., 2012).

#### *1.2.3.3 Transcription factors and regulatory elements*

Promoters are typically occupied by transcription factors that are broadly expressed (e.g., GA-binding protein (GABP) and specificity protein 1 (SP1)) which are not sufficient to confer the regulatory control which is required for the generation of cell-type specific gene expression. The interaction of transcription factors and distal enhancers is needed for this. Enhancers, which are the main sites for signal integration, bind both lineage-determining transcription factors (LDTF) and signal-dependent transcription factors (SDTF). These transcription factors interact to select and activate enhancers. Initially, LDTFs and pioneer factors interact to create nucleosome-free regions and open chromatin (Holtman et al., 2017). This selection and exposure of enhancers by LDTFs allows for SDTFs, which are typically activated in response to stimulation from cell-signalling pathways, to bind enhancers and transition them from an inactive to an active state. This process is thought to be hierarchical; the binding of SDTF is dependent on LDTF binding but not vice versa (Heinz et al., 2013; Heinz et al., 2010). Examples of LDTFs include PU.1, a master regulator of myeloid lineages essential for microgliogenesis (Nerlov & Graf, 1998) and T cell factor 1 (TCF-1), which controls T cell fate and establishes the epigenetic identity of T cells (Johnson et al., 2018). SDTFs include NFκB, which is important for apoptosis and inflammation and translocates to the nucleus upon its activation by signal transduction pathways (Bhatt & Ghosh, 2014; Lanzillotta et al., 2015), and p53 tumour suppresser which integrates signals that mediate cell cycle progression, DNA damage repair and apoptosis (Kruiswijk et al., 2015).

#### 1.2.3.4 *Transcription factors and disease*

Transcription factors have many broad and diverse functions and their importance in human biology is highlighted by their association with a wide range of diseases. Approximately 19% of human transcription factors are currently associated with at least one disease phenotype, which is more than what has been documented for all other genes (16%). For example, in anterior pituitary hypoplasia, which occurs in conjunction with congenital growth-hormone deficiency, 12 of the 15 associated genes are transcription factors including several Sox and homeodomain family members (Lambert et al., 2018). Furthermore, associated SNPs for several polygenic diseases, identified by GWAS, are enriched for loci-encoding transcription factors. Some transcription factor loci harbour GWAS signals for several diseases, such as the Ikaros-family C2H2-zinc fingers, IKAROS family zinc finger 1 (IKZF1) and IKAROS family zinc finger 3 (IKZF3). These transcription factors are important for the adaptive immune response and reach genome-wide significance for several autoimmune diseases (Hu et al., 2011; John & Ward, 2011). The location of mutations in transcription factors can determine their impact on transcription factor function; mutations in the DBD lead to alterations in sequence specificity whereas mutations outside the DBD can alter protein interactions (Lambert et al., 2018; Muller & Vousden, 2013). The function of transcription factors can also uniquely be affected by variation or mutation in regulatory DNA. These variations may disrupt the binding of specific transcription factors and thus result in changes to gene expression.

As transcription factors are key players in disease, understanding how transcription factors regulate gene expression is important in assigning functionality to common disease-associated genetic variation that is likely to operate via gene regulation. As the interaction of transcription factors with other proteins is vital for the regulation of gene expression investigating protein-protein interactions of specific transcription factors is important. However, details of transcription factor interactions, particularly in specific cell-types, is generally lacking. Thus, investigating transcription factor interactomes in a cell-specific manner is important for understanding how they control gene regulation in different cell types. This is explored in more detail in Chapter's 3 and 4.

### 1.3 Microglia

Microglia are the resident phagocytes and principle immune cells of the brain, first described and characterised by Pio del Rio-Hortega (Rio-Hortega, 1919; Sierra et al., 2016). The proportion of microglia, compared to the total number of cells in the human CNS,

varies from 0.5% to 16.6% depending on location (Mittelbronn et al., 2001). Microglia have a complex and diverse range of functions in the brain. They are critical for processes such as immune surveillance, neuronal expansion, neurodevelopment and differentiation, and the establishment of synapses (Nayak et al., 2014). Microglia also respond to both environmental and internal stimuli and rapidly adapt their phenotype and function to suit the conditions of their local environment (Tay et al., 2017). Recently there has been an increasing interest in the role of aberrant microglia function in the neuropathology of neurodegenerative diseases like AD (Hansen et al., 2018).

### 1.3.1 Microglial ontogeny

Even though microglia were discovered over 100 years ago, their developmental origin has remained elusive and highly debated until relatively recently. Originally, several theories of microglial origin were put forward. Evidence that microglial progenitors emerge in the brain in the early stages of embryonic development suggests that microglia arise from embryonic progenitors. Conversely, morphological, phenotypic, and antigenic similarities between microglia and peripheral myeloid cells like macrophages, suggest a circulating blood monocyte origin (Ginhoux & Prinz, 2015). However, fate-mapping studies have established the current consensus that microglia are derived from a unique erythromyeloid progenitor (EMP) population which are generated in the embryonic yolk sac around embryonic day eight (E8) (Ginhoux et al., 2010; Kierdorf et al., 2013).

Upon the establishment of the circulatory system around E8.5, these cells begin to spread and infiltrate the neuroepithelium from E9/9.5. Here, microglial lineage-determining transcription factors, including PU.1 and interferon regulatory factor 8 (IRF8), are upregulated giving rise to embryonic microglia which ultimately proliferate and colonise the CNS parenchyma. This colonisation of the CNS is evolutionarily conserved across species and occurs prior to the formation of other glial cell types including astrocytes and oligodendrocytes which derive from the neuroectoderm (Swinnen et al., 2013; Tay et al., 2017; Verney et al., 2010). Microglia reside in the brain throughout life and maintain their population in both immune-activated and homeostatic conditions. Microglia are self-renewing and, in comparison to peripheral myeloid cells, have greater longevity (Ajami et al., 2007; Réu et al., 2017).

During different developmental stages, microglia express distinct sets of genes. These specific gene expression profiles divide microglia into three specific groups: early (E10.4 to E14), pre-microglia (E14 to postnatal day (P) 9) and adult microglia (P28 onwards).



Canonical microglia genes like Fc receptor-like molecule (*Fcrls*) and purinergic receptor P2Y<sub>12</sub> (*P2ry12*) are expressed in early microglia development whereas genes like MAF BZIP transcription factor B (*MafB*) are only expressed in adult microglia. Additionally, ATAC-seq has revealed the presence of distinct regulatory elements in each of these stages.

Researchers found that enhancer regions can be divided into two categories: enhancers accessible in only early and pre-microglia and enhancers prominent in adult microglia. No enhancers were only accessible in pre-microglia suggesting that this phase utilises the epigenetic landscape established in early development rather than experiencing unique chromatin remodelling (Bennett et al., 2016; Matcovitch-Natan et al., 2016). This demonstrates that specific expression programs are required for each phase of microglial development.

### 1.3.2 Microglial function

#### 1.3.2.1 Immune system and homeostasis

Immunological defence and homeostasis are two key functional features of microglia in the CNS. In the absence of any infections or immune insults, microglia maintain a constant homeostatic balance by sampling their local microenvironment. During this state microglia display a ramified morphology with long branching processes and a small cellular body. Microglia continuously extend and retract several processes and branches to cover long distances and survey large areas of the brain for both internal and external stimuli. Brain-derived signals alert microglia to damaged or dying cells marked for phagocytic removal or cellular waste, whereas signals from external sources notify microglia to invading pathogens (Davalos et al., 2005; Hanisch & Kettenmann, 2007; Nimmerjahn et al., 2005). Microglia are the macrophages of the CNS, acting as principal responders of the innate immune system. The detection of response-inducing stimuli initiates a change to the morphological state of microglia. Cell bodies enlarge whilst processes are retracted, and an amoeboid morphology is adopted (Colonna & Butovsky, 2017). This response aims to protect against inflammation, resolve injury and support remodelling and repair of tissue (Goldmann & Prinz, 2013; Minghetti & Levi, 1998).

To detect both pathogen-associated and tissue damage-associated molecular patterns (PAMPs and DAMPs) and act as a front-line defence for the innate immune system, microglia express an array of pattern-recognition receptors on their cell surfaces (Kigerl et al., 2014). These receptors include a family of transmembrane proteins known as toll-like receptors (TLRs). These receptors recognise a wide variety of pathogen-specific ligands like

viral RNA, lipoproteins from the cell walls of bacterial pathogens, and chemokines released from other immune cells (Lehnardt, 2010). Upon ligand binding, TLRs induce a cascade of signalling events that result in the activation of transcription factor NF $\kappa$ B. This activation leads to the upregulation of pro-inflammatory genes and subsequent increased production of chemokines including macrophage inflammatory protein-1 alpha (MIP-1 $\alpha$ ), monocyte chemoattractant protein-1 (MCP-1) and C-C motif chemokine ligand 5 (CCL4), pro-inflammatory cytokines such as interferon-alpha (IFN $\alpha$ ), interferon-beta (IFN $\beta$ ), interleukin-1 beta (IL-1 $\beta$ ), IL-6, IL-12 and tumour necrosis factor-alpha (TNF- $\alpha$ ), and free radicals like nitric oxide. These molecules recruit other immune cells to the site of damage and are essential for pathogen elimination (Olson & Miller, 2004; Takeuchi & Akira, 2001).

Microglia activation states have, for many years, been categorised as either M1 (classical) or M2 (alternative). This nomenclature is derived from the terms used to describe the pro- and anti-inflammatory activation states of peripheral macrophages (Sica & Mantovani, 2012). M1 activation can be described as a proinflammatory, neurotoxic state in which microglia produce proinflammatory chemokines and cytokines ultimately resulting in the initiation of inflammation and neurotoxicity. Conversely, M2 activation depicts an anti-inflammatory state in which arginase 1, growth factors like insulin-like growth factor 1 (IGF-1) and colony stimulating factor 1 (CSF1), neurotrophic factors like brain derived neurotrophic factor (BDNF) and nerve growth factor (NGF) and a range of anti-inflammatory cytokines such as IL-10 and transforming growth factor (TGF- $\beta$ ) are released. This state can induce phagocytosis to remove cellular debris, induce tissue repair and prevent cells from releasing pro-immune factors (Cherry et al., 2014; Franco & Fernández-Suárez, 2015; Kaoru & Christopher, 2011). Recently, the use of this terminology has been questioned and criticised for being too simplistic and not applicable to microglia activation *in vivo* (Morganti et al., 2016; Ransohoff, 2016). Much of the evidence that supports the use of these categories was determined in *in vitro* cell cultures which do not appropriately model the complex interactions of microglia *in vivo*. Furthermore, transcriptome studies reveal that the activation of microglia is variable, context dependent and cannot be restricted to these binary phenotypes (Wes et al., 2016). In neurodegeneration models in which microglia are exposed to competing stimuli, both neuroprotective and neurotoxic factors are co-expressed (Chiu et al., 2013). Thus, there is a requirement for a novel, unbiased categorisation of microglia activation which defines multiple microglia phenotypes associated with healthy, ageing and disease states.

*1.3.2.2 Neuronal development and synaptic pruning*

Microglia also have additional roles in the regulation of neuronal development via synaptic remodelling, neuronal-microglia interactions, and phagocytosis of cellular debris. Microglia are also critical for several neuronal processes including neurogenesis in the developing and adult brain and synaptic pruning.

Microglia, as the phagocytic cells of the brain, are involved in the removal of developing neurons. This process can either be passive, in which non-activated microglia engulf cellular debris, or active whereby microglia release TNF- $\alpha$ , the neurotrophin nerve growth factor or reactive oxygen species such as superoxide ions in order to facilitate neuronal apoptosis (Cherry et al., 2014; Frade & Barde, 1998; Marín-Teva et al., 2004; Sedel et al., 2004). The phagocytosis of neurons is particularly important in early development as, in rats and macaques, microglia phagocytosis controls levels of cortical neurons by eliminating neural precursors in proliferative regions of the developing cortex. Interventions that decrease microglia cell number in these areas increase the number of neural precursors. Conversely, increased activation of microglia results in decreased numbers of precursors (Cunningham et al., 2013). The impact of increasing the number of neuronal precursors in development on adult behaviour has yet to be determined but it does imply that microglia are important for regulating neuronal production in the developing brain. The role of microglia in neurogenesis also continues into adulthood. In mammals such as rodents and non-human primates, there are two well-defined, consensus brain areas in which adulthood neurogenesis occurs; the subventricular zone and the hippocampal subgranular zone (Alvarez-Buylla & Lim, 2004; Gage, 2002). In these areas, microglia continue to actively phagocytose the excess of new-born apoptotic neurons and this clearance is unaffected by inflammation or ageing (Sierra et al., 2010).

Microglia are also involved in synaptic pruning. They eliminate redundant neurons and dendritic spines that do not form functional circuits or receive inputs from synaptic connections (Tremblay et al., 2011). One mechanism employed to aid synaptic pruning is the complement system. One role of complement is to act as an innate immune surveillance system which is comprised of plasma proteins that tag apoptotic cells for engulfment and removal by microglia (Merle et al., 2015). In synaptic pruning, complement component 1q (C1q) and C3 tag redundant synapses for either recognition and elimination by microglia via complement receptor 3 (CR3) or for direct lysis through the complement cascade (Schafer et al., 2012; Stevens et al., 2007). Substantial deficits in retinogeniculate

synaptic refinement and elimination are seen in C1q and C3 knockout mice (Stevens et al., 2007). Complement also mediates synaptic pruning in other brain areas as C1q knockout mice have increased connectivity in the cortex (Chu et al., 2010). An additional mechanism used by microglia to mediate pruning is via the CX3C chemokine receptor 1 (CX3CR1). This receptor interacts with CX3C chemokine ligand 1 (CX3CL1) which is expressed by neurons. Disrupted CX3CR1- CX3CL1 interactions via CX3CR1 knockdown, result in reduced synaptic engulfment of excitatory synapses and increased dendritic spine densities on hippocampal neurons (Paolicelli et al., 2011). Thus, via several mechanisms, microglia are essential for effective synaptic pruning in the brain.

### 1.3.3 Microglia and AD

Microglia are involved in a wide range of biological processes in the brain. Dysregulation of these functions can disrupt CNS homeostasis and lead to the initiation or exacerbation of neurodegeneration. Interest in the role of microglia in neurodegeneration has increased dramatically over the past decade, there are several lines of evidence that point to an involvement of microglia in AD.

#### 1.3.3.1 Microglia in AD Brains

Even early descriptions of the neuropathological features of AD include gliosis and neuroinflammation (Alzheimer, 1907) suggesting early on that abnormal microglial histopathological hallmarks are present in AD brains. Later, in AD patients and animal models, microglia were found to engulf, proliferate, and converge around amyloid plaques at a density of 2-5-fold higher than in normal parenchyma (Bachiller et al., 2018; Frautschy et al., 1998). Furthermore, microglia activation increases with disease progression and severity and with A $\beta$  plaque progression (Griffin et al., 1995; Xiang et al., 2006). Some evidence, from AD mouse models, suggests that the accumulation of microglia around amyloid plaques has a protective function; microglia form a barrier around amyloid fibrils, compacting them into a less toxic form. This both prevents new A $\beta$  from joining existing plaques and decreases axonal dystrophy (Condello et al., 2015).

#### 1.3.3.2 Microglia and A $\beta$

In AD, microglia respond to harmful stimuli in the brain including A $\beta$ . Numerous receptors that bind A $\beta$  are expressed on microglia including TLR2, TLR4, TLR6, cluster of differentiation 36 (CD36), and NLR family pyrin domain containing 3 (NLRP3) (El Khoury et al., 2003; Heneka et al., 2015, 2013). A $\beta$  activates microglia via these receptors resulting in

the phagocytosis of A $\beta$ , cellular debris and dying cells to protect against neuroinflammation and injury. Moderate stimulation of microglia by low A $\beta$  levels allows microglia to effectively clear A $\beta$  via phagocytosis. However, high concentrations of A $\beta$  result in extensive activation of microglia and a chronic inflammatory response in which pro-inflammatory molecules including TNF- $\alpha$  and IL-1 $\beta$  are released. This in turn triggers neuronal damage along with a reduced ability of microglia to effectively clear A $\beta$  from the brain due to a large reduction in the expression of both A $\beta$ -targeting enzymes and receptors that bind A $\beta$  (Hickman et al., 2008; Johnston et al., 2011). Mouse models of AD, which lack TLR, NLRP3 and IL-1 $\beta$  signalling, have reduced A $\beta$  deposition and cognitive deficits (Heneka et al., 2015). Thus, the build-up of amyloid in the brain may be due, in part, to the chronic activation of microglia via receptors that bind A $\beta$  and the resulting inefficiency of microglia to clear A $\beta$ . The transition of microglia from the effective phagocytosis of A $\beta$  (at low A $\beta$  levels) to the triggering of a chronic inflammatory response in which pro-inflammatory factors are produced (at high A $\beta$  levels) may suggest that microglia, in the early stages, have a neuroprotective role but then begin to exacerbate AD pathology in the later stages of the disease. The findings presented so far implicate microglia in AD. However, they do not elucidate whether dysregulated microglial function, in response to A $\beta$  build-up, is a cause or consequence of AD pathology.

#### *1.3.3.3 Ca<sup>2+</sup> signalling and microglia*

As discussed in section 1.1.2.2, Ca<sup>2+</sup> dysregulation is thought to contribute to AD pathogenesis. In AD, Ca<sup>2+</sup> disruption is not only present in neurons but also other cells including microglia. AD patient-derived microglia have increased basal [Ca<sup>2+</sup>] levels but decreased amplitude and longer-lasting ATP-induced Ca<sup>2+</sup> response compared to controls (McLarnon et al., 2005). However, although Ca<sup>2+</sup> dysregulation has been widely studied in neurons, very little is known about the role of AD-related Ca<sup>2+</sup> alterations in microglia. Early work has shown that transient increases in [Ca<sup>2+</sup>] occur when microglia are stimulated with A $\beta$ <sup>25-35</sup>, a fragment of the A $\beta$  peptide. Increases in [Ca<sup>2+</sup>] subsequently lead to microglia activation and the production of neurotoxic factors (Combs et al., 1999). Many important microglial functions are mediated by Ca<sup>2+</sup> signalling including microglia activation (Färber & Kettenmann, 2006; Hoffmann et al., 2003), suggesting that disruptions in Ca<sup>2+</sup> in AD could disturb microglial functions.

#### 1.3.3.4 Genetic evidence

Recently, genetic studies have revealed a more direct, central role of microglial cells in AD-risk. A large proportion of genes associated to AD by GWAS are either selectively or preferentially expressed by microglia including *TREM2*, *CR1* and *CD33* (Bertram et al., 2008; Guerreiro et al., 2013; Jonsson et al., 2013; Lambert et al., 2009). Furthermore, Gosselin et al (2017) showed that expression for 28 out of 48 AD genes is higher in microglia than other brain cell types. Pathway analyses, which aim to assign functionality to AD genetic risk loci, also implicate microglia cells and pathways as probable effectors of AD-risk (Jones et al., 2015; Kunkle et al., 2019) (section 1.1.3.2).

Rare variants in *TREM2* have been associated with a 3-4.5-fold increase in AD-risk (Guerreiro et al., 2013; Jonsson et al., 2013). *TREM2* is a transmembrane glycoprotein, selectively and highly expressed by microglia, involved in cell proliferation, survival, and the phagocytosis of apoptotic cells (Takahashi et al., 2005,2007). The rare arginine 47 histidine (R47H) variant of *TREM2*, which is most robustly associated with AD, prevents the binding of *TREM2* to phospholipid ligands and impedes *TREM2*-mediated microglia activation (Hansen et al., 2018; Kober et al., 2016; Wang et al., 2015). Other *TREM2* variants impair the transport and expression of *TREM2* on the cell surface (Kleinberger et al., 2014). *TREM2* deficiency or haploinsufficiency in AD mouse models reduces microglia accumulation around A $\beta$  plaques which in turn promotes the spread and accumulation of A $\beta$  (Wang et al., 2015, 2016; Yuan et al., 2016). This suggests that loss of *TREM2* may disrupt the neuroprotective barrier formed by microglia that compacts A $\beta$  and prevents toxicity, thus exacerbating AD pathology.

The cell surface molecule, *CD33* is another microglia gene associated with AD (Bertram et al., 2008). *CD33* inhibits several downstream signalling pathways including phagocytosis (Linnartz-Gerlach et al., 2014). Increased expression of *CD33* is linked to more advanced cognitive decline (Karch et al., 2012). One *CD33* variant is associated with increased AD-risk and impairs the ability of microglia to phagocytose A $\beta$  by increasing *CD33* concentration and its subsequent inhibitory effects (Bradshaw et al., 2013). Finally, variants in *CR1* have also been associated with increased AD-risk (Lambert et al., 2009). *CR1* is part of the complement system which, in microglia, is important for synaptic pruning (section 1.3.2.2). Variants in complement genes suggest that the aberrant phagocytosis of synapses may contribute to AD pathogenesis (Crehan et al., 2012). The identification of these genes and others, including *HLA-DRB5-DRB1*, membrane spanning 4-domains A6A (*MS4A6A*), and

*BIN1* (Lambert et al., 2013) which are important for microglia function, as associated with AD-risk strongly suggests that microglia dysfunction may be a contributing factor underlying AD pathology.

Additional evidence for a role of microglia in AD comes from integrative epigenomic and GWAS studies. Tansey et al (2018) integrated AD GWAS results with sites of open chromatin in several cell-types and found that AD-risk SNPs were preferentially located in open chromatin regions in macrophages and microglia suggesting that AD-risk alleles are likely to operate in immune cells. This implicates microglia as a plausible mediator of common variant genetic risk for AD and supports a causal role of microglia in AD pathology.

Furthermore, the non-coding risk SNP of *BIN1*, a well-established AD-risk gene (Seshadri et al., 2010), also appears to operate in microglia. The AD association signal at *BIN1* has also been found to be cell-type specific. It is detected in microglia but not in any other cell-types or tissues tested (Young et al., 2021). Additionally, deletion of a microglia-specific enhancer that contained AD-risk variants using CRISPR-Cas9 resulted in reduced *BIN1* expression in microglia but not in neurons or astrocytes, highlighting that this microglial long-range enhancer links to *BIN1* (Nott et al., 2019). The synthesis of the two proceeding studies shows that *BIN1* is an expression quantitative trait loci (eQTL) that operates in microglia through a long-range enhancer, providing further evidence of a causal role of microglia in AD pathogenesis.

#### 1.3.4 Microglial gene *MEF2C*

Myocyte enhancer factor 2C (*MEF2C*) is a transcription factor expressed in microglia and is an interesting target for further investigation as it is both associated with AD and important for microglial function. A large meta-analysis confirmed that the SNP rs190982 within *MEF2C* acted as a protective factor for AD in the Caucasian population (Lambert et al., 2013). This association between rs190982 and AD has also been confirmed in a large Spanish sample (Ruiz et al., 2014).

##### 1.3.4.1 *MEF2C* in AD

The specific role of *MEF2C* and the underlying mechanisms of its protective allele in AD are yet to be determined. However, it has been postulated that as *MEF2C* is important for neuronal development, synapse formation and hippocampal-dependent learning and memory (Barbosa et al., 2008; Li et al., 2008), that it may be connected to synaptic dysfunction and cognitive deficits in AD. A large GWAS analysis found an association

between *MEF2C* AD-associated variants and general cognitive function (Davies et al., 2015). Furthermore, *MEF2C* is also expressed in brain regions that are both important for learning and memory and are affected early on in AD including the dentate gyrus and the entorhinal cortex (Leifer et al., 1994; Lyons et al., 1995).

On the other hand, *MEF2C* also regulates microglial function and may be involved in altered microglial inflammatory response in AD as *MEF2C* is important for restricting the response and activation of microglia to pro-inflammatory stimuli (Deczkowska et al., 2017; Lavin et al., 2014). In addition, 5xFAD mice, which express human APP (five AD-linked mutations) and *PSEN1* (two AD-linked mutations) transgenes, exhibit suppressed nuclear translocation of *Mef2c* as an early microglial phenotype. Additionally, in organotypic brain slices, A $\beta$  oligomers promote the deregulation of *Mef2c* in microglia resulting in abnormal microglial activation. This suggests that the deregulation of *Mef2c* may contribute to early microglia phenotypes in AD (Xue et al., 2021). Recent research has also suggested that the AD association signal at *BIN1*, rs6733839C>T confers AD-risk by elevating *MEF2C* binding which in turn increases *BIN1* expression (Young et al., 2021). Additionally, although both *BIN1* and *MEF2C* are expressed in many cells, they only appear to coexpress in primary microglia and induced pluripotent stem cell-derived macrophages. Thus, *BIN1*-associated increased *MEF2C* binding could be specific to these cell types.

#### 1.3.4.2 Microglia transcriptional networks

The transcriptional network of *MEF2C* appears to be central in AD-risk. In the Tansey et al (2018) paper, discussed above, AD-risk SNPs were found to be enriched in several microglial-macrophage open chromatin regions (OCR) for *MEF2* (which included motifs of *Mef2c*). Furthermore, genetic variants at these sites accounted for a substantial proportion of AD common variant SNP heritability. Disrupted DNA binding due to genetic variation at binding sites or altered gene expression in *cis* may lead to impaired transcriptional control by *MEF2C*. Thus, AD common-variant risk may operate through *MEF2C* transcriptional networks.

## 1.4 MEF2C

### 1.4.1 MEF2 transcription factor family

*MEF2C* is a member of the *MEF2* family of transcription factors which includes four human genes *MEF2A-D* (Breitbart et al., 1993; Martin et al., 1994; Martin et al., 1993; Yu et al., 1992). They are members of the larger MADS-box family of transcription factors (Black &



Olson, 1998; Naya & Olson, 1999). The name MADS-box was coined based on the first identified members: yeast mini chromosome maintenance 1 (MCM1) which is involved in mating-type selection (Passmore et al., 1988); *Arabidopsis thaliana* agamous (Yanofsky et al., 1990) and snapdragon *deficiens* (Sommer et al., 1990) which are both homeotic factors that regulate plant leaf identity; and human serum response factor (Norman et al., 1988) which controls muscle and growth-factor inducible genes (Shore & Sharrocks, 1995). The MADS-box is a conserved sequence, its N-terminal half is responsible for DNA-binding whereas the C-terminal half is required for dimerization (Shore & Sharrocks, 1995). Conserved residues in the MADS-box domain of the MEF2 family of transcription factors are required for DNA binding. However, MEF2 factors cannot form heterodimers with other MADS-box transcription factors suggesting that residues within the MADS-box that are required for dimerization are not conserved between MEF2 family members and other MADS-box transcription factors (Black & Olson, 1998).

MADS-box transcription factors bind similar A/T-rich DNA sequences. However, the MEF2 family consensus sequence is distinct from other MADS-box factors. Polymerase chain reaction-based binding site selection experiments have shown that MEF2 transcription factors regulate transcription by binding to DNA response elements with the CTA(A/T)<sub>4</sub>TAG consensus sequence (Andres et al., 1995; Olson et al., 1995). Recently, it has also been demonstrated that MEF2 family members can compensate for each other. The deletion of MEF2D in granule neurons of mouse-cerebellum resulted in an increase in the genomic occupancy of MEF2A at a distinct set of previously-bound MEF2D sites. Occupation of these sites by MEF2A also results in functional compensation for both genomic activation and gene expression (Majidi et al., 2019). This highlights an ability for members of this transcription factor family to carry out compensatory MEF2-dependent gene regulation.

#### 1.4.2 *MEF2C* gene

The human *MEF2C* gene is located on the long arm of chromosome 5 at position 14.3 (5q14.3). It spans approximately 187 kb with a total of 11 exons, 10 of which are coding. MEF2 was first documented and named in skeletal myotube nuclei in 1989 (Gossett et al., 1989). This study identified MEF2 as a DNA binding activity, essential for full enhancer activity, that recognises an A/T-rich element in the muscle creatine kinase (MCK) 5' enhancer. They determined that the MEF2 recognition sequence was distinct from the previously documented MEF1 (Buskin & Hauschka, 1989). Subsequently, several MEF2 binding sites were identified in enhancer and promoter regions for the majority of cardiac and skeletal muscle structural genes including the enzyme AMP deaminase 1 (Morisaki &

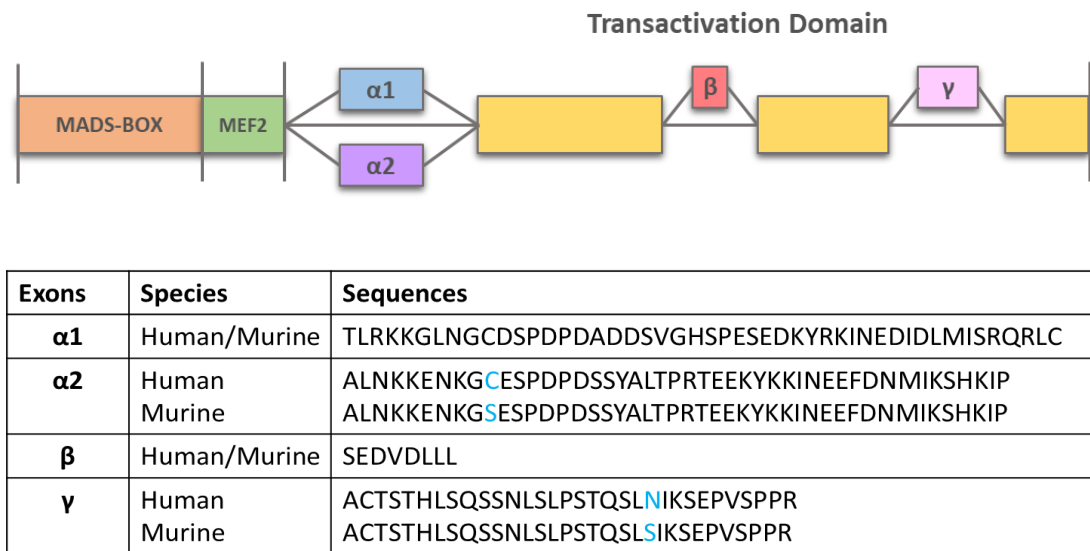
Holmes, 1993), the insulin-regulated glucose transporter GLUT4 (Liu et al., 1994), and the nuclear receptor Nur77 (Woronicz et al., 1995). Although MEF2 was primarily considered to be a muscle-specific transcription factor involved in muscle differentiation, MEF2 was later found to promote neuronal differentiation and development (Mao et al., 1999) suggesting that MEF2 has several functions in various cell types.

MEF2 mRNA is extensively alternatively spliced giving rise to multiple isoforms (Black & Olson, 1998; Zhu & Gulick, 2004). Alternative splicing is important for the regulation of gene expression and transcriptional diversity (Kelemen et al., 2013). Specifically, MEF2C contains three main alternative exons: mutually exclusive exon, skipping exon and 3' splice site selection. The mutually exclusive type of alternative splicing occurs in exon  $\alpha$ . It is located in a region adjacent to the MEF2 domain and either  $\alpha 1$ ,  $\alpha 2$ , or no  $\alpha$  exon is expressed. Alternatively spliced transcripts encoding exon  $\alpha 1$  are typically expressed in neurons and muscle cells whereas transcripts encoding  $\alpha 2$  are mainly expressed in muscle cells (Hakim et al., 2010; McDermott et al., 1993). Additionally, isoforms that lack the  $\alpha$  domain have increased MEF2C transcriptional activity (Infantino et al., 2013), whereas, the presence of the  $\alpha 2$  exon reduces the recruitment of repressive HDAC proteins to target promoters (Zhang et al., 2015).

The skipping type of alternative splicing occurs in exon  $\beta$ . This exon is located in the transcriptional activation domain and is either skipped or included in Mef2c isoforms. Typically in neurons, it is included (Hakim et al., 2010; McDermott et al., 1993) and isoforms that contain exon  $\beta$  more robustly activate MEF2-responsive reporters (Zhu et al., 2005). Finally, the 3' splice site selection type of alternative splicing occurs in the  $\gamma$  region, located in exon 10 of *MEF2C*. This region has been shown to encode a transcriptional repression domain. Isoforms that lack the  $\gamma$  domain cooperate better with myoblast determination protein 1 (MyoD) which interacts with MEF2C to facilitate skeletal muscle development (Zhu & Gulick, 2004). The locations of these spliced regions are depicted in Figure 1.1. The inclusion of these splice sites in microglia-like cells is discussed in more detail in Chapter 3 (sections 3.2.2 and 3.3.1).

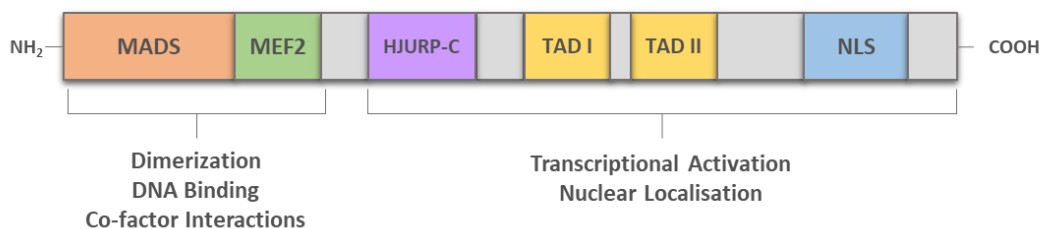
#### 1.4.3 MEF2C protein structure

The *MEF2C* gene encodes the protein MEF2C. The full length human MEF2C (NP\_001180279.1) protein sequence is 473 amino acids and is comprised of six domains including MADS, MEF2, HJURP-C, TAD1, TAD2 and NLS from N-terminus to C-terminus (Figure 1.2). At the extreme N-terminus, 56 amino acids make up the MADS domain. It is



**Figure 1.1. MEF2C alternative splicing sites.** A schematic of the MEF2C protein and its alternatively spliced exons ( $\alpha$ ,  $\beta$ , and  $\gamma$ ) that give rise to various MEF2C isoforms. The table details the sequences of the alternatively spliced exons in humans and rodents. Amino acids that vary between species are highlighted in blue. Diagram adapted and sequences extracted from Zhang et al (2015).

rich in A/T base pairs and plays a role in the mediation of dimerization of MADS-box proteins, DNA binding and providing areas for MEF2C co-factor interactions (Black & Olson, 1998). For high-affinity DNA binding and dimerization, this domain requires the immediate adjacent MEF2 domain extension (Molkentin et al., 1996a). The MEF2 domain consists of 29 highly conserved amino acids. This domain is unique to MEF2 family members and is also important for interactions with accessory factors (Black & Olson, 1998). Due to high



**Figure 1.2. MEF2C protein structure.** The schematic depicts the conceptual organisation and function of MEF2C's protein domains. The MADS-Box and MEF2 domains mediate dimerization of MADS-box proteins and DNA binding and facilitate MEF2C co-factor interactions. The C-terminal regions act as transcription activation domains (TAD I and TAD II) and contain signals necessary for nuclear localisation (NLS domain). Amongst MEF2 family members the MADS and MEF2 domains are highly conserved whereas there is large diversity in the C-terminal regions. *Abbreviations: MCM1 Agamous Deficiens Serum response factor (MADS), Myocyte enhancer factor-2 (MEF2), Holliday junction recognition protein C-terminal (HJURP-C), Transcription activation domain (TAD), Nuclear localisation signal (NLS).*

sequence conservation within this domain, all MEF2 family members can form homo- and heterodimeric structures (Molkentin et al., 1996a). Following the MEF2 domain lies the HJURP-C (Holliday junction recognition protein C-terminal) domain which is composed of 29 amino acids (Wu et al., 2011). The C-terminal regions of MEF2 family members act as transcription activation domains (TAD I and TAD II) and contain signals necessary for nuclear localisation (NLS domain) (Black & Olson, 1998). The NLS domain of the MEF2 proteins controls their translocation to the nucleus and has member-specific features (Borghi et al., 2001). MEF2 proteins overall share approximately 50% amino acid identity, with around 95% similarity in the MADS and MEF2 domains highlighting low conservation and large diversity in the structure of the C-terminal regions (Black & Olson, 1998).

#### 1.4.4 MEF2C function

MEF2 transcription factors are widely expressed in muscle and nervous tissues both in embryonic and adult cells (Edmondson et al., 1994; Potthoff & Olson, 2007; Uhlén et al., 2015, Human Protein Atlas available from <http://www.proteinatlas.org>). Of the MEF2 family, MEF2C is the most extensively expressed and is thought to play a role in a variety of biological processes including muscle formation (McGee et al., 2006), immune cell development (Wilker et al., 2008), the immune response (Deczkowska et al., 2017), and the development and function of neuronal cells (Shalizi & Bonni, 2005).

##### 1.4.4.1 Muscle cells

MEF2C has been most extensively studied in muscle cells and it has been implicated in the development of the three major muscle types: skeletal, cardiac, and smooth muscle. To activate skeletal muscle morphogenesis and differentiation, MEF2C binds directly to the regulatory regions of many muscle-specific genes (McKinsey et al., 2002). The deletion of *Mef2c* specifically in mouse skeletal muscles results in fragmented and disorganised sarcomeres, defects in the M line that lead to perinatal death, and incomplete development of myofibers (Potthoff et al., 2007).

MEF2C has also been implicated as an essential regulator for cardiac myogenesis. Targeted deletion of the region encoding the MADS-box and MEF2 domains to prevent DNA binding and dimerization and thus render the allele null was completed in the mouse *Mef2c* gene. As a result, in the cardiac muscle of the mutant mice, looped morphogenesis of the embryonic heart did not occur. Subsequently, the right ventricle of the heart did not form, and a range of cardiac muscle genes were not expressed (Lin et al., 1997). In endothelial cells and smooth muscle cells (SMCs), using a similar method as described above to mutate

the mouse *Mef2c* gene, Lin et al. documented severe vascular abnormalities, and by embryonic day 9.5, death in homozygotes. Endothelial cells could differentiate but could not organise into a vascular network. In addition, SMCs were unable to differentiate (Lin et al., 1998). These findings depict a role for MEF2C in the formation of the vascular system by controlling the differentiation and patterning of cells.

#### 1.4.4.2 Immune cells

MEF2C is also thought to play a role in B cell receptor signalling and the regulation of immune cell development. *In vitro*, stimulating B cell receptors in purified mouse B cells after *Mef2c* deletion results in dysfunctional B cell proliferation and reduced survival. *In vivo*, a marked reduction in T cell-dependent antibody responses and formation of germinal centres are also documented (Wilker et al., 2008).

MEF2 family members are also expressed in microglia, the immune cells of the brain (Speliotis et al., 1996). MEF2C is the most highly and differentially expressed MEF2 transcription factor in microglia and it has been implicated in the regulation of microglial enhancer landscapes as MEF2 binding motifs are overrepresented at enhancers of microglial-specific genes (Lavin et al., 2014). However, little is known about the specific role of MEF2C in microglial function. Recently, an inducible mouse model of microglia *Mef2c* deficiency showed that *Mef2c* loss is associated with a downregulation in CX<sub>3</sub>CR1, a molecule essential for restraining microglia responses to immune challenges. After delivery of a pro-inflammatory age-associated cytokine, TNF, into the cerebral spinal fluid of these mice, an exaggerated microglial response was observed. Further, primary microglia with siRNA-silenced *Mef2c* display downregulation of *Mef2c* and increased expression of C–C motif chemokine ligand 2 (*Ccl2*), *Ccl5*, *Il-1b* and *Tnf* which are proinflammatory chemokines and cytokines (Deczkowska et al., 2017). These data suggest that *Mef2c* is important for restricting the response and activation of microglia to pro-inflammatory stimuli.

#### 1.4.4.3 Neuronal cells

MEF2C is also highly expressed in neuronal cells (Leifer et al., 1993) and is necessary for development and function of the nervous system. In neural progenitor cells, a conditional knockout of *Mef2c* resulted in impaired neuronal differentiation. Additionally, *Mef2c*-null mice have reduced brain size, dysfunctional neuronal migration and disrupted layer formation in the neocortex (Li et al., 2008). This supports an essential role of MEF2C in early brain development. Further, MEF2 family members are crucial for learning and

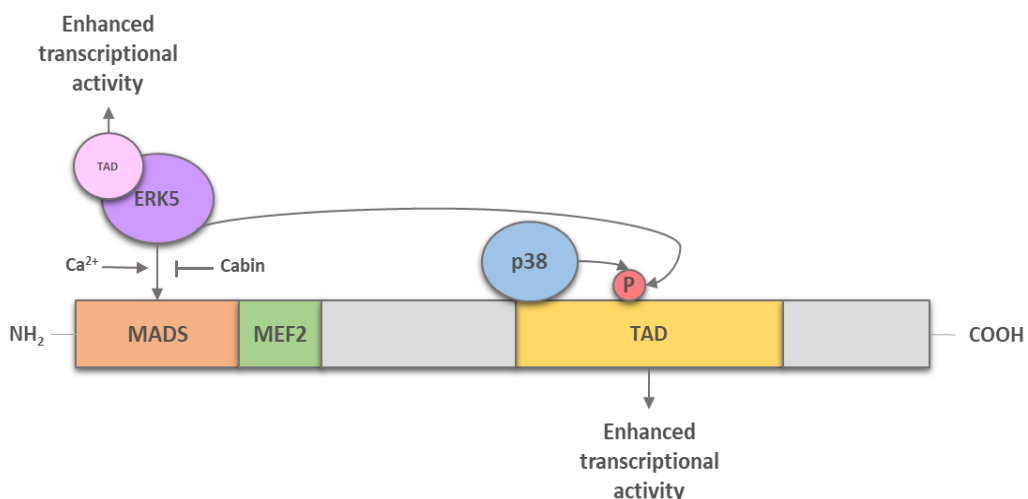
memory. *In vitro*, increasing MEF2 function results in a reduction in the number of hippocampal dendritic spines and excitatory synapses both of which are necessary for memory formation (Flavell et al., 2006; Rashid et al., 2014). More specifically, *Mef2c*-null mice demonstrate dysfunctional hippocampus-dependent learning and memory accompanied by an increase in excitatory synapses (Barbosa et al., 2008) suggesting a specific role of MEF2C in restricting the formation of excessive synapses in the hippocampus thus facilitating learning and memory. These findings provide evidence that MEF2C has both lineage-determining and signal-dependent activity.

#### 1.4.5 Regulation of MEF2C

MEF2C transactivation is regulated by a range of complex signalling pathways including phosphorylation by mitogen activated protein kinases (MAPK),  $\text{Ca}^{2+}$  signalling pathways and transcriptional repression by histone deacetylases.

##### 1.4.5.1 MAPK signalling

Several MAPK pathways converge on MEF2C and phosphorylate specific regions to confer changes to MEF2C transcriptional activity. MAPK are  $\text{Ca}^{2+}$ -responsive enzymes. p38 kinase and extracellular signal-regulated protein kinase (ERK) pathways have been shown to stimulate MEF2C activity (Figure 1.3). p38 is a direct interactor of MEF2C, it binds to the



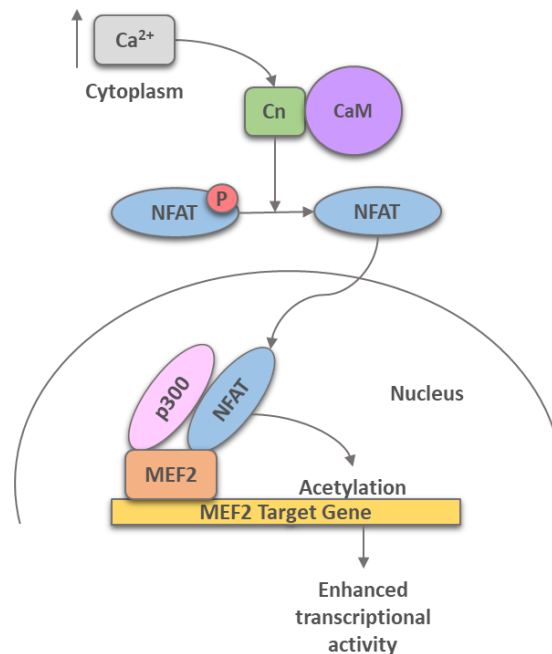
**Figure 1.3. MAPK regulation of MEF2C activity.** The MAP kinases p38 and ERK5 are known to regulate MEF2C activity. p38, a direct interactor of MEF2C, binds and phosphorylates MEF2C at specific residues in the transactivation domain, resulting in enhanced transcriptional activity. A second MAPK pathway involves the phosphorylation of the transactivation domain by ERK5 another direct interactor of MEF2C. ERK5 binds to the MADS domain and this interaction is either stimulated by  $\text{Ca}^{2+}$  or repressed by Cabin. ERK5 also acts as a coactivator of MEF2C as it possesses its own transcription activation domain which interacts at the MADS/MEF2 domain and enhances MEF2-dependent transcription. Figure adapted from Mckinsey et al 2002.

transcription activation domain of MEF2C and specifically phosphorylates threonine 293 and 300 and serine 387 and enhances the transcriptional activity of Mef2c (Han et al., 1997; Zhao et al., 1999). This p38-induced activation of MEF2C has been linked to the promotion of skeletal muscle differentiation (Zetser et al., 1999). Through yeast two-hybrid (Y2H) screens, ERK5 has also been shown to associate with MEF2C by binding to the MADS/MEF2 domains (Kato et al., 1997; Yang et al., 1998). Interactions between ERK5 and MEF2 family members are stimulated by  $\text{Ca}^{2+}$  and blocked by the co-repressor Cabin (Kasler et al., 2000). ERK5 can regulate MEF2C activity in two distinct ways. Similarly to p38, ERK5 phosphorylates MEF2C proteins in the transactivation domain leading to enhanced transcriptional activity (Yang et al., 1998). Phosphorylation of MEF2C by ERK5 stimulates the expression of c-jun which is essential for the regulation of cell-cycle progression (Marinissen et al., 1999; Wisdom et al., 1999). In addition, ERK5 possesses a unique transcriptional activation domain which interacts with MEF2C at the MADS/MEF2 domain and provides a coactivator function in MEF2C-dependent transcription (Kasler et al., 2000).

#### 1.4.5.2 $\text{Ca}^{2+}$ Signalling

$\text{Ca}^{2+}$  signalling pathways regulate MEF2 activity via several distinct mechanisms. Calcineurin is a serine/threonine phosphatase which is activated by  $\text{Ca}^{2+}$  and calmodulin binding (Rusnak & Mertz, 2000). It responds to continuous, low-amplitude  $\text{Ca}^{2+}$  transients (Li et al., 2012). One mechanism of calcineurin-dependent MEF2 activation involves the recruitment of nuclear factor of activated T-cells (NFAT) transcription factors (Figure 1.4). Calcineurin dephosphorylates NFAT which subsequently translocates to the nucleus. NFAT directly interacts with MEF2 (Blaeser et al., 2000; Kipanyula et al., 2016) and recruits the p300 coactivator to MEF2 target genes (Youn et al., 2000). Subsequently, p300 acetylates histones and “relaxes” chromatin around MEF2 target sites which allows for the expression of MEF2 target genes (Sun et al., 2010). These calcineurin-dependent MEF2-NFAT interactions are vital in skeletal muscle for the regulation of slow twitch fibre genes (Wu et al., 2000).

Similarly,  $\text{Ca}^{2+}$ /calmodulin-dependent protein kinase (CaMK) regulates MEF2 activity. CaMK is activated, in contrast to calcineurin, by transient, high-amplitude  $\text{Ca}^{2+}$  spikes (Li et al., 2012). The MEF2 domain of MEF2 factors is responsive to CaMK-mediated signals, however, CaMK is not thought to directly phosphorylate this region (Lu et al., 2000a). Thus, CaMK is likely to interact with MEF2 via an intermediary factor that associates directly with the MEF2 domain.

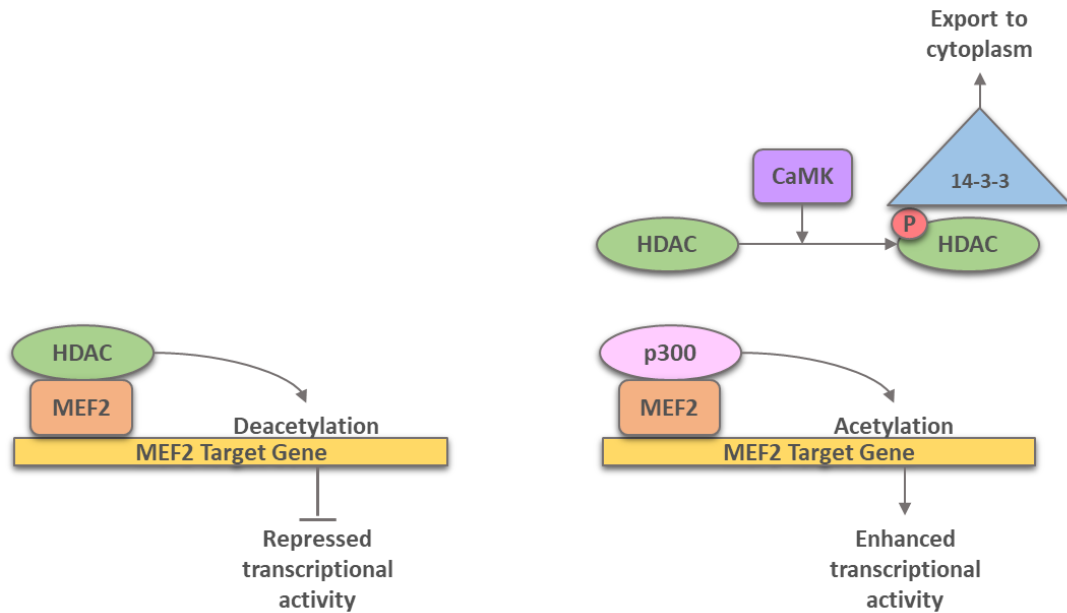


**Figure 1.4. Calcineurin regulation of MEF2 activity.** Increased intracellular  $[Ca^{2+}]$  facilitates the binding of calmodulin (CaM) to calcineurin (Cn), activating it. Activated calcineurin subsequently dephosphorylates the transcription factor NFAT. NFAT translocates to the nucleus where it directly interacts with MEF2. NFAT recruits the coactivator p300 which acetylates histones, relaxes chromatin, and facilitates expression of MEF2 target genes. Figure adapted from McKinsey et al 2002.

#### 1.4.5.3 Histone deacetylases and CaMK signalling

Histone deacetylases (HDACs) are thought to be the intermediary factors that confer the transcriptional activation activity of CaMK (Figure 1.5). In humans, there are approximately 17 HDACs which are divided into three classes. Class II HDACs 4,5,7, 9 regulate MEF2 activity by binding to the hydrophobic MEF2 domain of all MEF2 family members. Leucine 147, 151 and phenylalanine 150 are important sites for the association of these proteins (Han et al., 2005; Zhou et al., 2001). The N-terminal regions of these class II HDACs bind to MEF2 via a unique 18 amino acid sequence that is not seen in other HDAC proteins (Chan et al., 2003; McKinsey et al., 2001a). The association of HDAC and MEF2 proteins leads to the recruitment of HDACs to MEF2-dependent gene regulatory regions. Here, HDACs deacetylate core histones leading to the condensation of chromatin which represses transcription (Marks et al., 2003). CaMK phosphorylates the N-terminal regions of HDACs 4,5,7, and 9. This allows for the binding of the intracellular chaperone protein 14-3-3 to phosphorylated HDACs which subsequently disrupts HDAC-MEF2 complexes and facilitates cytoplasmic shuttling of HDACs by unmasking a nuclear export sequence (Grozing &





**Figure 1.5. CaMK regulation of MEF2 activity.** Histone deacetylases (HDACs 4,5,7 and 9) bind MEF2 and are recruited to MEF2-dependent gene regulatory regions where they deacetylate histones and condense chromatin repressing transcription.  $\text{Ca}^{2+}$ /calmodulin-dependent protein kinase (CaMK) phosphorylates HDACs in N-terminal regions creating docking sites for the binding of the chaperone protein 14-3-3. This protein then shuttles HDACs to the cytoplasm leaving MEF2 available for binding with histone acetyltransferases like p300 which enhance transcription via the acetylation of histones and chromatin relaxation. Figure adapted from McKinsey et al 2002.

Schreiber, 2000; McKinsey et al., 2000a; McKinsey et al., 2001b; Wang & Yang, 2001). MEF2 proteins are then free to interact with coactivator histone acetyltransferases (HATs) like p300 which bind to the MADS/MEF2 domains and relax chromatin by acetylating histones resulting in increased MEF2 transcriptional activity (McKinsey et al., 2001a; Sun et al., 2010).

Specific interactions between MEF2C and HDAC proteins are vital for several biological processes including myogenesis. Transient overexpression of HDAC4 and 5 in 10T1/2 cells results in blocked MyoD-dependent myogenesis. However, overexpressing HDAC5 mutants, which lack the MEF2 interaction domain, has no effect on the initiation of myogenesis. This suggests that HDACs suppress myoblast differentiation through their association with MEF2C. Additionally, the presence of CaMK signalling, which releases HDAC-induced repression of MEF2C, overcomes HDAC-mediated repression of myogenesis (Lu et al., 2000b). This highlights the essential role of HDAC-MEF2C interactions in the formation of muscle tissue.

#### 1.4.6 MEF2C and disease

Consistent with its widespread expression and importance in several biological functions, MEF2C has genetic links to a number of other disorders and diseases aside from AD. GWAS and genome sequencing studies have associated MEF2C as a candidate risk gene for several mental disorders including schizophrenia (Purcell et al., 2014; Ripke et al., 2014), attention deficit and hyperactivity disorder (ADHD) (Shadrin et al., 2018), bipolar disorder (Nurnberger et al., 2014; Xie et al., 2017) and major depressive disorder (Hyde et al., 2016). Mostly, the effect of the diseased-linked risk SNPs in these disorders on MEF2C function or expression is unknown. However, its role in schizophrenia is slightly more established. Schizophrenia is an adult-onset, highly heritable, psychiatric disorder characterised by distortions in perception, thinking, language, behaviour, and emotions. The dysregulation of neuronal gene expression in the prefrontal cortex (PFC) is an important feature of the neurobiology of schizophrenia suggesting that transcription factors that regulate gene expression may be important therapeutic targets. Mitchell et al. (2018) found that *Mef2c* overexpression in adult mouse PFC neurons, at baseline and after psychotogenic drug challenge, resulted in improved cognition and behaviour. This suggests that MEF2C may be a critical regulator of adult PFC function and if its expression or regulatory activity is altered in schizophrenia this may partially explain the cognitive dysfunction documented in patients. The potential involvement of MEF2C in these disorders highlights its importance in healthy human brain function.

MEF2C is also implicated in MEF2C haploinsufficiency syndrome. Coding-region nonsense or missense mutations and microdeletions in the *MEF2C* gene have been associated with this neurodevelopmental disorder. It is characterised by severe intellectual disability, seizures, autism-like symptoms, absence of speech and motor abnormalities (Engels et al., 2009; Le Meur et al., 2010; Vrečar et al., 2017). Moreover, MEF2C mutations have also been detected in patients with idiopathic intellectual disability (Zweier & Rauch, 2012). This suggests that altered or reduced MEF2C functions in humans have a profound impact on brain development and neurotypical behaviour, emphasising the importance of MEF2C in the brain and a requirement to understand more about the function of MEF2C.

#### 1.5 Protein-protein interactions

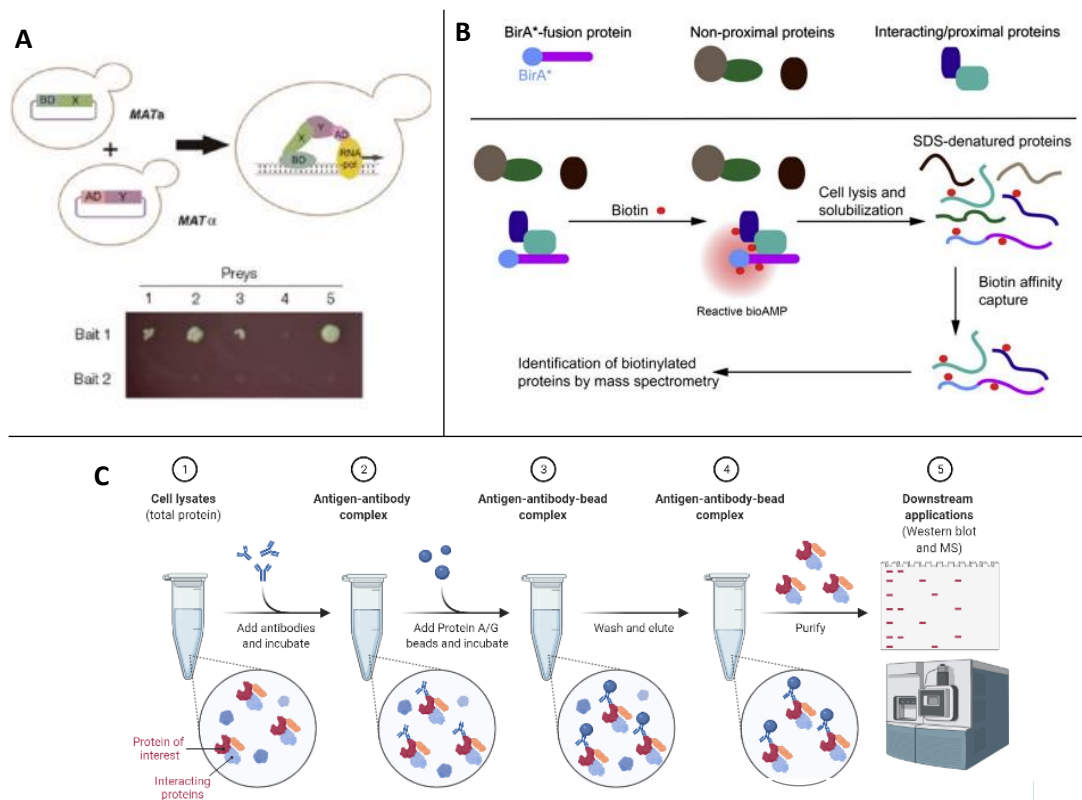
The function of MEF2C and its role in disease can be delineated by studying protein-protein interactions. Proteins are the building blocks of all the components of a cell and underly the functional diversity of different cell types. Protein-protein interactions are vital in the cell

for the coordination and shaping of the cellular response to endogenous and exogenous stimuli. Understanding the human proteome is important as it can inform structural and cellular mechanisms, aid the discovery of unknown isoforms, and elucidate how genome variation may contribute to disease (Havugimana et al., 2012; Menche et al., 2015).

### 1.5.1 Protein-protein interaction detection methods

There are a number of techniques that have been widely used to study protein-protein interactions including yeast two-hybrid (Y2H), co-immunoprecipitation mass spectrometry (co-IP-MS) and BioID (Figure 1.6).

Y2H (Figure 1.6, A) is a complementation assay in which two protein domains of a transcription factor are required: the DNA-binding domain (BD) and the DNA-activation domain (AD). These regions are fused to two proteins of interest the bait and the prey. If these two proteins of interest interact when expressed in a yeast cell, this reconstitutes the transcription machinery. The BD binds DNA and the AD activates RNA polymerase resulting in the transcription of a reporter gene (Fields & Song, 1989; Koh et al., 2012). This method allows for the identification of a direct interaction between protein pairs *in vivo*, it is fast,



**Figure 1.6. Protein-protein interaction detection methods.** (A) Yeast two-hybrid, image from Koh et al. (2012). (B) BioID, image from Roux et al. (2012). (C) Co-IP-MS, image created in BioRender.com.

inexpensive, and scalable. However, Y2H has a high false positive rate as yeast proteins can act as a bridge between the two proteins. Additionally, proteins may not behave or interact normally in these experiments due to a requirement for posttranslational modifications or protein folding which do not occur in yeast cells. Furthermore, in Y2H assays, interactions may occur between proteins that are not endogenously expressed in the same cell type or at the same time (Rao et al., 2014; Suter et al., 2008).

Conversely, the co-IP-MS technique (Figure 1.6, C) can be used to isolate endogenous protein interactomes from cell lysate using an antibody specific to the protein of interest. The antibody can be used to capture the protein of interest and any associated proteins. This antibody-protein complex is then captured by a solid support, which, in most cases, are magnetic agarose or sepharose beads. Complexes are subsequently washed to remove any non-specifically bound proteins and then eluted from the beads. Co-immunoprecipitated protein complexes are then analysed by mass spectrometry which rapidly identifies discrete members of the protein complex (Free et al., 2009). This method has several advantages over Y2H. Co-IP-MS can rapidly, sensitively, and reliably identify strong protein-protein interactions which are present in the native environment of the protein of interest. Additionally, these multi-protein complexes are isolated in a single experiment, capturing a large proportion of the protein interaction space, and making co-IP-MS a more efficient technique.

Another technique, that has been more recently developed, is BioID (Figure 1.6, B) (Roux et al., 2012, 2018). This is a proximity labelling technique which relies on the strong affinity between biotin and streptavidin. Proteins of interest are fused with the biotin ligase, BirA, and then transfected into the cell-type of interest. Once biotin is added to the cell, this stimulates BirA to biotinylate proteins in close proximity to the protein of interest. Streptavidin beads, which interact with biotin, are then used to isolate the protein complex. Similarly to co-IP-MS, biotinylated proteins are subsequently identified by MS. This technique has some advantages over co-IP-MS. Due to the strong affinity bond between biotin and streptavidin, harsher wash and lysis conditions can be used to remove more non-specific proteins. Additionally, it does not rely on an antibody which is one of the main limitations of the co-IP technique. In co-IP the epitope of the antibody may prevent some interacting proteins from binding, the antibody may also cross-react with proteins which are then falsely identified as interactors. Also, unlike co-IP, this technique can capture weak and transient protein interactions. However, a major disadvantage of this technique is the use of an exogenous fusion protein. This may influence the localisation and

functionally of the protein of interest (Weill et al., 2019) both of which would need to be verified prior to running the experiment. Additionally, for both co-IP and BioID, detected interactions are not necessarily direct associations, unlike interactions identified using Y2H, they may be indirect and associated via another protein. Thus, when using these techniques to screen for candidate interactors, additional, alternative validation experiments are required to confirm physical interactions.

It is important to consider the advantages and disadvantages of each technique before determining which protein-protein interaction method is most appropriate for a specific experiment. To identify MEF2C-associated proteins and understand more about the regulation and function of endogenous MEF2C, the co-IP-MS method was selected, this is discussed in more detail in Chapter 3 (section 3.1).

## 1.6 Thesis aims and structure

The importance of *MEF2C* in brain development and function is apparent from its genetic association to several mental and cognitive disorders including AD. However, the role of *MEF2C* in AD, specifically in microglia, remains under-investigated. AD common-variant risk is thought to operate through the MEF2C transcriptional network in microglia. Therefore, the overarching aim of this thesis was to elucidate how MEF2C is regulated by protein interactions and how MEF2C regulates gene expression and therefore AD-risk. Proteomic techniques have been used to determine what proteins are co-operating with and regulating this transcription factor. Whereas genomic techniques were used to investigate the effects of increased intracellular  $Ca^{2+}$  signalling on chromatin accessibility and to determine if these changes are mediated by  $Ca^{2+}$ -sensitive transcription factors, potentially including Mef2c. Accordingly, the experiments outlined in this thesis were used to:

- 1) Define the interactome of Mef2c in microglia-like cells (Chapter 3)
- 2) Investigate stimulus-dependent interactions of Mef2c (Chapter 4)
- 3) Investigate the effects of ionomycin treatment on chromatin accessibility (Chapter 5)

The novel findings presented in this thesis are summarised and discussed in Chapter 6.

## Chapter 2 Methods

### 2.1 Molecular Biology

#### 2.1.1 Plasmid vectors

Plasmid vectors used for plasmid construction are detailed in table 2.1 below.

**Table 2.1. Details of plasmid vectors used for plasmid construction.**

Vector	Description	Antibiotic Selection	Supplier
<b>pSF-EF1-Ub-Neo Vector</b>	Contains the Elongation Factor 1 alpha promoter upstream of the multiple cloning site and neomycin/G418 resistance driven by the ubiquitin promoter.	Kanamycin	Merck
<b>pcDNA3.1+/C-DYK</b>	Driven by a CMV promoter, pcDNA3.1+/C-(K)-DYK is equipped with a C-terminal DYKDDDDK (FLAG) tag for easy protein detection and purification.	Ampicillin	Genscript
<b>pcDNA3.1+/N-DYK</b>	Driven by a CMV promoter, pcDNA3.1+/N-(K)-DYK is equipped with a N-terminal DYKDDDDK (FLAG) tag for easy protein detection and purification.	Ampicillin	Genscript
<b>pcDNA3.1(+)</b>	This vector is designed for high-level, constitutive expression in a variety of mammalian cell lines. It contains a Geneticin <sup>®</sup> selectable marker and a forward-orientation multiple cloning site.	Ampicillin	Addgene

#### 2.1.2 Plasmid construction

Plasmids were constructed using complementary DNA (cDNA) synthesised from RNA from BV2 cells. TRI Reagent (Zymo Research) was used to lyse the cells which were subsequently stored at -80°C overnight to aid lysis. RNA was then extracted from the lysed cells using the Direct-zol<sup>™</sup> RNA miniprep kit (Zymo Research), following manufacturer's instructions. RNA was then incubated with random decamers (RETROscript), oligo(dT) (Invitrogen), 2.5mM dNTPs (ThermoFisher) and nuclease-free water for 5min at 65°C prior to incubating on ice for 1min. A reverse transcriptase reaction mix (5X SSIV buffer (Invitrogen), 0.1M DTT (Invitrogen), SuperScript IV RT (Invitrogen), nuclease-free water) was subsequently added to the annealed RNA and the combined reaction mixture was incubated for 5min at room temperature and then for 10min at 55°C. Finally the mixture was inactivated at 80°C for 10min. The resulting cDNA was diluted to a working concentration of 50ng/μl and stored at -20°C until needed for plasmid construction. All constructs were generated according to the

cloning methods in sections 2.1.3 to 2.2.6. The primers used for in-house construct generation are provided in table 2.2. For ease, some constructs were cloned by Genscript or purchased from Addgene (Kozhemyakina et al., 2009).

All plasmid constructs were created with full-length insert sequences asides from Cabin1. Due to the large sequence length of Cabin1 (6.5kb), it was both difficult and costly to clone the entire length of the sequence. A MEF2-binding motif of hCABIN1 has been identified in human MEF2 family members (Han et al., 2003). Therefore, a smaller fragment of mCabin1, that includes the proposed CABIN1-MEF2-binding site sequence, was generated. This fragment encompasses amino acids 1856-2187 (with the MEF2-binding region located at amino acids 2124-2157) and was cloned into pcDNA3.1(+)-N-DYK by Genscript.

### 2.1.3 Polymerase chain reaction

Oligonucleotide primers for polymerase chain reaction (PCR) were designed complementary to 18-24 bp of the target sequence. When required, appropriate restriction enzyme sites were added to the ends of the primer sequence. In addition, 3-5 random base pairs were added to the end of the restriction enzyme sequences to increase the efficiency of restriction enzyme cleavage. Primers were ordered from ThermoFisher and resuspended in nuclease-free water to a concentration of 100 $\mu$ M, working stocks were diluted to 10 $\mu$ M.

PCR was routinely performed using 2X Taq Polymerase Master Mix (Qiagen). When high fidelity PCR was needed, Q5<sup>®</sup> High Fidelity 2X Master Mix (NEB) was used. PCRs were run using C1000/S1000<sup>™</sup> Thermal Cyclers (BioRad). A typical PCR reaction with cycling parameters is provided in table 2.3. Annealing temperatures and extension times were adjusted to fit the estimated annealing temperatures of the primer pairs and length of PCR product to be amplified (1min per kb). PCR products were subsequently separated by gel electrophoresis using 1-2.5% (w/v) agarose gels (see section 2.1.4). After which products were cleaned and concentrated using a DNA Clean and Concentrator<sup>™</sup> (Zymo Research) kit, following manufacturer's instructions, then quantified using a Nanodrop spectrophotometer (DeNovix<sup>®</sup> DS-11 FX+).

### 2.1.4 Agarose gel electrophoresis

Typically, 1-2.5% (w/v) agarose (Fisher BioReagents) gels, for resolving DNA fragments, were made in 0.5x TBE buffer (45mM Tris base, 45mM boric acid, 1mM EDTA, pH 8.3). Agarose was dissolved in 0.5X TBE by heating in a microwave for two 1min cycles. After which, the nucleic acid gel stain, GelRed (Biotium), was added (5 $\mu$ l per 100ml). The gel

**Table 1.2. Details of plasmid vectors created in house or purchased.**

Construct	Species	Insert	Vector	Restriction Sites	Tag	Primers	Provided by
<b>Mef2c Isoform 1</b>	Mouse	Full-length Mef2c Isoform 1	pcDNA3.1	HindIII/ BamHI	C-terminal HA	N/A	pcDNA3.1-MEF2C-HA was a gift from Andrew Lassar (Addgene plasmid # 32515 ; <a href="http://n2t.net/addgene:32515">http://n2t.net/addgene:32515</a> ; RRID:Addgene_32515)
<b>Mef2c Isoform X4</b>	Mouse	Full-length Mef2c Isoform X4	pcDNA3.1(+)-C-HA	HindIII/ApaI	C-terminal HA	N/A	Genscript
<b>Hdac4</b>	Mouse	Full-length Hdac4	pcDNA3.1(+)-N-DYK	KpnI/EcoRI	N-terminal Flag	N/A	Genscript
<b>Hira</b>	Mouse	Full-length Hira	pcDNA3.1(+)-N-DYK	NotI/XhoI	N-terminal Flag	N/A	Genscript
<b>Cabin1</b>	Mouse	Cabin1 Fragment	pcDNA3.1(+)-N-DYK	BamHI/XhoI	N-terminal Flag	N/A	Genscript
<b>Oasl1</b>	Mouse	Full-length Oasl1	pcDNA3.1(+)-N-DYK	BamHI/ EcoRI	N-terminal Flag	N/A	Genscript
<b>Ncoa5</b>	Mouse	Full-length Ncoa5	pSF-EF1-Ub-Neo	NotI/Clal	N-terminal Flag	PF 5' GCTAGCGGCCGCGCCATGGAT TACAAGGATGACGACGATAAG ATGAATACGGCTCCATCAAGA PR 5' GCTAATCGATTGAGTAATGCCT CTGGTAAGATCC	In-house



Chapter 2 Methods

<b>Thoc6</b>	Mouse	Full-length Thoc6	pSF-EF1-Ub-Neo	NotI/ClaI	N-terminal Flag	PF 5' GCTAGCGGCCGCGCCATGGAT TACAAGGATGACGACGATAAG ATGGAGCATGCCGACCG PR 5' GCTAATCGATTCAAAGGACA AAGAGAAGGCTCG	In-house
--------------	-------	-------------------	----------------	-----------	-----------------	--	----------

**Table 2.3. PCR reaction protocol.** Annealing temperatures and extension times were adjusted to fit the estimated annealing temperatures of the primer pairs and length of PCR product to be amplified (1min per kb).

50 $\mu$ l PCR Reaction		Cycling Conditions	
PCR Amplification	Volume ( $\mu$ l)	Temp ( $^{\circ}$ C)	Time
PCR Master Mix	25	95	3min
10 $\mu$ M Forward primer	1	95	30sec
10 $\mu$ M Reverse primer	1	<b>Then 30 cycles of:</b>	
Template cDNA	1-6	55-60	30sec
Nuclease-free water	Up to 50	72	1min per kb
		<b>Final extension:</b>	
		72	5min
<b>Hold at 12<math>^{\circ}</math>C</b>			

solution was poured into a gel cast with a comb inserted. Once set, the gel was transferred to an electrophoresis tank and covered in 0.5X TBE buffer. Loading dye (6X Orange G) was added to each sample before loading into wells along with a Quick Loading<sup>®</sup> 2-Log DNA Ladder (NEB) to use as a size standard. Gels were typically run for 30min-1h at 100V. DNA bands, stained with GelRed, were visualised by performing UV transillumination of the gel (Molecular Imager<sup>®</sup> Gel Doc<sup>™</sup> XR+ Imaging System, BioRad).

#### 2.1.5 DNA extraction from gels

If required, desired DNA bands, stained with GelGreen<sup>®</sup> Nucleic Acid Gel Stain (Biotium) were extracted from gels using a sterile razor blade on a Safe Imager<sup>™</sup> 2.0 Blue-Light Transilluminator (Invitrogen). Extracted fragments were recovered using Zymoclean<sup>™</sup> Gel DNA Recovery Kit (Zymo Research), following manufacturer's instructions.

## 2.2 DNA Cloning

### 2.2.1 Restriction digestion of DNA

All restriction enzymes were purchased from NEB. Vector (1 $\mu$ g) and insert DNA (varied concentrations) were prepared for cloning by cutting with the appropriate restriction enzymes and 10X Cut Smart Buffer (NEB) in a final volume of 20 $\mu$ l. For vector digests, 1 $\mu$ l fast alkaline phosphatase (Thermo Scientific) was also added to minimise re-circularisation of the vector DNA. The reactions were incubated for 1h at 37 $^{\circ}$ C then for 20min at 85 $^{\circ}$ C to inactivate the restriction enzymes.

### 2.2.2 Ligation of DNA sequences into expression vectors

Digested insert and vector DNA were either ligated in a quick reaction or overnight. For a quick ligation, Quick Ligase Reaction Buffer (2X) and Quick Ligase (NEB) were used, and the reaction was incubated for 10min at room temperature. For overnight ligation, T4 DNA

Ligase Buffer (10X, with 10mM ATP) and T4 DNA ligase (NEB) were used followed by overnight incubation at 4°C. A standard 20µl reaction consisted of a 3:1 molar ratio of insert to vector DNA. Vector-only control reactions were also included to confirm successful linearization and dephosphorylation of the vector.

### 2.2.3 Transformation of bacteria

Chemically competent cells (*E. coli*), typically DH5α (NEB), were thawed on ice prior to use. Between 1-2.5µl of the ligation reactions were used to transform 10-25µl of competent cells in pre-chilled 1.5ml microcentrifuge tubes (Thermo Scientific). Reactions were incubated on ice for 30min, after which cells were heat shocked for 30sec at 42°C and then chilled on ice for 2min. To aid recovery, 250µl of warm LB Broth media (Sigma-Aldrich®) was added to the cells which were subsequently incubated at 37°C for 1h. Transformation reactions were then centrifuged for 1min at 8,000rpm. Most of the media was then removed, and the pellet resuspended in the remaining 20-40µl. The reactions were then plated onto LB agar (Sigma-Aldrich®) plates supplemented with the appropriate antibiotic, either kanamycin (50µg/ml) or ampicillin (100µg/ml), and incubated overnight at 37 °C.

### 2.2.4 PCR colony screen

Colonies selected for screening were tested using a standard PCR reaction using 2X Taq Polymerase Master Mix. Pipette tips were used to pick colonies into an empty PCR tubes (StarLab). Individual tips were then placed in 1ml LB medium with the appropriate antibiotic for later use. 5µl of nuclease free water was added to the PCR tubes which were subsequently incubated at 95°C for 5min, whilst the LB tubes were stored at 37°C. 1µl of this heated product was used as a template in a 10µl PCR reaction (see section 2.1.3), alongside the appropriate primers (0.5µl of 10µM stock) to screen for the presence of the insert. PCR products were resolved on agarose gels (section 2.1.4) and positive clones were identified by the presence of a band at the correct size on an agarose gel. 20µl of the LB media (stored earlier) containing the positive colony or colonies was used to inoculate individual 15ml Falcon tubes of 5ml LB media along with the appropriate antibiotic then incubated overnight (12-16h) at 37°C, 200rpm.

### 2.2.5 Plasmid DNA isolation

Plasmid DNA was isolated from the 5ml overnight cultures using a Monarch® Plasmid Miniprep Kit (NEB), following manufacturer's instructions. DNA was subsequently quantified using a Nanodrop spectrophotometer (DeNovix® DS-11 FX+). Prior to isolation,

glycerol stocks, for long-term storage, were created by adding 500µl of grown bacteria to 500µl 50% glycerol (Sigma-Aldrich®) and then stored at -80 °C.

Miniprep constructs (500ng) were digested by restriction digest (section 2.2.1) and separated by gel electrophoresis (section 2.1.4) to confirm the presence of the insert.

#### 2.2.6 DNA sequencing

Positive constructs, confirmed to contain the insert and vector DNA, were sent off for Sanger Sequencing by Source Bioscience, Cambridge. Sequencing chromatogram traces were verified using Chromas version 2.6.6 (Technelysium Pty Ltd).

### 2.3 Cell Biology

#### 2.3.1 Mammalian cell culture

HEK293T (human embryonic kidney 293T) and BV2 (mouse microglia cell line) cells were typically cultured in Thermo Scientific 25cm<sup>2</sup> (T25) flasks containing 5ml medium and maintained in an incubator in a humidified atmosphere of 5% CO<sub>2</sub> and 95% air at 37°C.

HEK293T cells were cultured in Dulbecco's Modified Eagle Medium/Nutrient Mixture F-12 (DMEM/F-12, GIBCO) supplemented with 4% (v/v) Foetal Bovine Serum (FBS). BV2 cells were cultured in Roswell Park Memorial Institute (RPMI) 1640 medium (GIBCO)

supplemented with 10% (v/v) FBS. Media was stored at 4°C and warmed to 37°C prior to use. At approximately 80% confluence, cells were passaged to maintain healthy and viable cultures. Media was first removed from the flasks. As BV2 cells are both adherent and suspension, the media was centrifuged for 3min at 1000rpm to pellet the cells in suspension. To passage adherent cells, 3ml of Accutase (Invitrogen™) was added and the flask and the cells were incubated at 37°C for 5min to detach the cells. After detachment verification via microscope, the Accutase was inactivated by the addition of 3ml media.

Cells were pelleted by centrifugation at 1000rpm for 3min at room temperature. Cell pellets were then resuspended in 10ml of fresh media and reseeded at an appropriate

density. To seed a specific number of cells, cells resuspended in 10ml of fresh media were counted using a haemocytometer (Bright-Line) while trypan blue stain (GIBCO) was used to

assess cell viability. For long-term storage of cells, the cell pellet was resuspended in the appropriate media supplemented with 7.5% (v/v) dimethyl sulfoxide (DMSO, Sigma-Aldrich®), aliquoted in cryovials and stored in liquid nitrogen.

### 2.3.2 Immunocytochemistry

BV2 cells ( $0.5 \times 10^6$ ) were seeded onto sterile glass coverslips (22mm x 22mm) in 35mm TC-treated culture dishes (Corning) and allowed to grow for 24h. Cells were washed twice with serum-free RPMI and then left to incubate for 1h in serum-free RPMI. After which, cells were treated with either 1 $\mu$ M ionomycin (Biotechne, Tocris) (dissolved in DMSO) or DMSO as a vehicle control for 1h. Cells were subsequently washed twice in PBS (GIBCO) and then fixed for 10min in 2ml 3.7% formal saline (150mM NaCl, 90% H<sub>2</sub>O, 3.7% (v/v) formaldehyde). After fixing, cells were washed again in PBS for 5min then incubated in 2ml 100% ethanol for another 5min to aid fixation. PBS was used again to wash the cells for 5min. Cells were then either stored in 2ml sucrose storage medium (125mM sucrose, 1.62mM MgCl<sub>2</sub>, 25% (v/v) PBS, 25% (v/v) glycerol) for later use or permeabilised with 0.2% (v/v) Triton X-100 in PBS for 15min at 4°C. Following permeabilisation, cells were washed three times with PBS for 5min. Cells were subsequently blocked with 200 $\mu$ l 10% (w/v) BSA in PBS for 30min at room temperature. Coverslips were then dipped in PBS tween (0.02% v/v) to help the primary antibody flood the surface of the cover slip and removed to a humidifying chamber. 100 $\mu$ l of primary antibody, Mef2c (D80C1) XP<sup>®</sup> Rabbit mAb (Cell Signalling Technology), at 1:400 dilution in PBS was added to each coverslip and incubated overnight at room temperature. The next day, cells were washed in PBS for 5min and then incubated with 1ml of secondary antibody, goat anti-rabbit IgG 568 (Alexa Fluor), at 1:5000 dilution in PBS for 1h at room temperature. Following a final wash in PBS for 5min, coverslips were carefully rinsed in dH<sub>2</sub>O then mounted onto glass slides with VECTASHIELD<sup>®</sup> (Vector Laboratories). Cells were visualised using the CCD Microscope Camera Leica DFC3000 G. Images were then assembled using ImageJ in which images were cropped and adjusted for brightness and contrast but otherwise not manipulated.

### 2.3.3 Dual-luciferase reporter assays

For dual-luciferase reporter assays, cells were seeded at approximately  $2 \times 10^6$  cells per plate into 96-well plates and incubated overnight until a confluence of 60-80% was reached (approximately 24h). DNA constructs (300ng per 4-well condition) were transfected into cells using Lipofectamine<sup>®</sup> 2000 (Lipo2000) Transfection Reagent (Invitrogen) added in the ratio of 3 $\mu$ l Lipofectamine to every 1 $\mu$ g DNA. Lipo2000 was first incubated in Opti-MEM<sup>®</sup> Reduced Serum Medium (GIBCO) for a few minutes before the addition of DNA constructs. To test Mef2c interactors, cells were either transfected with an inducible luciferase reporter vector, pGL4.27 luc, containing a Mef2c transcription response element (TRE) motif to which Mef2c is expected to bind and release luciferase, or an empty pGL4.27 luc

vector to act as a control. The Mef2c TRE reporter construct was made by Mr. Chris Smith. A range of interactor DNA constructs were transfected alongside each vector to investigate how they affect Mef2c reporter activity. GFP was transfected alongside both Mef2c TRE and the empty backbone in each experiment to act as a control and to ensure each condition was transfected with the same total amount of DNA. *Renilla* luciferase (1ng per 4-well condition) was also added to each well to control for background luminance. Transfection mixes were incubated for 20min at room temperature before adding directly to the cells at 10% of the medium volume (e.g., 7.5µl into 75µl cells). Approximately 24-48h post-transfection, the Dual-Glo® Luciferase Assay System (Promega) was used to measure luciferase activity. Dual-Glo® Reagent, equal to the volume of medium, was added to the cells, then left to rotate gently at room temperature for 10min to allow for cell lysis. Firefly luciferase activity, a measure of the transcriptional activity of the promoter driving the reporter gene, was then determined using a Berthold LB 96 V plate-reader. Dual Glo® Stop & Glo® Reagent, equal to the original culture medium volume, was added to each well to quench the firefly signal and release the *Renilla* signal. The plate was then incubated for 10min at room temperature, after which *Renilla* luciferase activity was measured.

The experiment was repeated in triplicate. In individual reporter assays, Firefly luciferase activity was normalised against background *Renilla* activity prior to interpretation. To allow for comparison across repeats, luciferase activity from the TRE reporter vector was also normalised against the luciferase activity from the empty background vector for each condition. Results from each repeat were then combined and the presented results represent the mean and standard deviation calculated across the three normalised repeats.

## 2.4 Protein Analysis

### 2.4.1 Sample preparation

To detect endogenous proteins, BV2 cells were seeded, at approximately  $3 \times 10^6$  cells per plate, in 6-well plates and left to grow to a confluence of 60-80% (approximately 24h) before cell lysis. After removal of media, cells were washed with 1ml PBS and subsequently lysed directly in 100µl of lysis buffer (125mM Tris pH 6.8, 4% (w/v) sodium dodecyl sulphate (SDS), 20% (v/v) glycerol, 5% (v/v) β-mercaptoethanol, 0.01% (w/v) bromophenol blue). Cells were scraped into 1.5 microcentrifuge tubes, sonicated briefly (four 2sec bursts) using a UP50H Ultrasonic Processor (Hielscher) and then heated to 95°C for 5min. Samples were then separated by SDS-PAGE (section 2.4.2). Samples were placed at -20°C for long-term storage.

#### 2.4.2 Sodium dodecyl sulphate-polyacrylamide gel electrophoresis

Protein samples were separated on 10-12% (v/v) acrylamide gels by sodium dodecyl sulphate-polyacrylamide gel electrophoresis (SDS-PAGE) using a Mini-PROTEAN® Tetra System (Bio-Rad). The resolving gel was prepared first and typically contained 12% (v/v) acrylamide (30% (w/v) acrylamide, 0.8% (w/v) bis-acrylamide stock solution (37.5:1)), 1.5M Tris pH 8.8, 0.1% (w/v) SDS, 0.075% (w/v) ammonium persulphate (APS) and 0.06% (v/v) N,N,N',N'-tetramethylethylenediamine (TEMED). Whilst polymerising, the resolving gel was layered with dH<sub>2</sub>O to exclude air from the gel and give it a smooth surface. Once set, the stacking gel was prepared and consisted of 1.5M Tris pH 6.8, 5% (v/v) acrylamide (30% (w/v) acrylamide, 0.8% (w/v) bis-acrylamide stock solution (37.5:1)), 0.1% (w/v) SDS, 0.1% (w/v) APS, 0.1% (v/v) TEMED. The stacking gel was then layered onto the resolving gel following removal of the distilled water, directly after which a comb was inserted. Once polymerised, the gels were secured into a tetra cell which was placed in a tank and submerged in 1X SDS-PAGE running buffer (10X: 0.25M Tris base, 1.92M glycine, 0.1% (w/v) SDS, pH 8.3). Prepared samples were then loaded into the wells along with a Precision Plus Protein™ All Blue Standards (BioRad) protein ladder as a protein standard. Gels were run at 150V for approximately 75min.

#### 2.4.3 Western blotting

Following SDS-PAGE, gels were transferred to 0.2µm pore size nitrocellulose membrane (Amersham™ Protran™) for 1h at 100V in transfer buffer (25mM Tris-base, 192mM glycine, 20% (v/v) methanol) using the Mini Trans-Blot® Electrophoretic Transfer Cell (Bio-Rad). Membranes were subsequently blocked for 1h, with constant, gentle rotation, in 1X TBS Tween (10X TBST; 100mM Tris-base, 1M NaCl, 0.5% (v/v) Tween 20, pH 7.6) with 5% (w/v) dried skimmed milk powder (Marvel). This prevents non-specific binding and reduces background signal by blocking any unoccupied sites on the membrane prior to primary antibody incubation. Membranes were then washed briefly with 1X TBST and subsequently incubated for 1h, with constant rotation, at room temperature and then overnight at 4°C in primary antibody. Primary antibodies were prepared, at the required concentration, in 5ml 1X TBST with 5% (v/v) western blocking reagent (WBR) and 0.5% (w/v) sodium azide. The next day, membranes were briefly washed with 1X TBST before incubation with secondary antibody, diluted in 1X TBST with 1% (w/v) milk powder for 1h at constant rotation protected from light. Membranes were then washed in 1X TBST for 30min before detection using the two-colour Odyssey® Infrared Imaging System (LI-COR Biosciences).

### 2.4.4 Antibodies

Table 2.4 lists the antibodies used in this thesis, along with their individual uses and required dilutions. Abbreviations: WB; western blot, ICC; immunocytochemistry, IP; immunoprecipitation.

## 2.5 Proteomics

### 2.5.1 Crosslinking antibodies to protein G Dynabeads

Prior to immunoprecipitation, Mef2c (D80C1) XP® Rabbit mAb and Rabbit (DA1E) mAb IgG XP® isotype control antibodies (Cell Signalling Technology) were crosslinked to protein G Dynabeads™ (Invitrogen™). Prior to crosslinking, the antibodies were coupled (4µg per IP) to 50µl of Dynabeads™, previously washed and equilibrated in 500µl PBS, by incubating at 4°C for 1h with rotation (22rpm). The beads were recovered from the solution using a DynaMag™-2 magnetic rack (Invitrogen) and washed three times in PBS. The antibody-coupled beads were then washed twice in 200µl conjugation buffer (20mM sodium phosphate, 0.15M NaCl, pH 7-9). The bound antibody was crosslinked to the beads through

**Table 2.4. Antibodies used in this thesis for protein analysis.**

Name	Source	Primary/ Secondary	Type	Use and dilution
<b>Mef2c XP®</b>	Cell Signalling Technology	Primary	Rabbit mAb	ICC (1:400) WB (1:1000) IP (20 µl)
<b>Rabbit IgG XP® Isotype Control</b>	Cell Signalling Technology	Primary	Rabbit mAb	IP (4 µg)
<b>ANTI-FLAG® M2</b>	Sigma-Aldrich®	Primary	Mouse mAb	WB (1:1000)
<b>Anti-HDAC4</b>	abcam	Primary	Mouse mAb	WB (1:500)
<b>Anti-NFATc2</b>	Santa Cruz Biotechnology	Primary	Mouse mAb	WB (1:200)
<b>Recombinant Anti-HDAC5 (phospho S498)</b>	abcam	Primary	Rabbit mAb	WB (1:1000)
<b>Alexa Fluor™ Plus 800</b>	Invitrogen	Secondary	Goat anti-mouse	WB (1:15000)
<b>Alexa Fluor™ Plus 800</b>	Invitrogen	Secondary	Goat anti-rabbit	WB (1:15000)
<b>Alexa Fluor™ 680</b>	Invitrogen	Secondary	Goat anti-mouse	WB (1:15000)
<b>Alexa Fluor™ 680</b>	Invitrogen	Secondary	Goat anti-rabbit	WB (1:15000)
<b>Alexa Fluor™ 568</b>	ThermoFisher	Secondary	Goat anti-rabbit	ICC (1:5000)



incubation with 5mM bis(sulfosuccinimidyl)suberate (BS<sup>3</sup>, Thermo Scientific™) in 250µl of conjugation buffer (per sample) by rotating for 30min at room temperature. The crosslinking reaction was subsequently quenched by the addition of 12.5µl (per sample) quenching buffer (1M Tris HCl, pH 7.5) and incubation for 15min at room temperature with rotation. Crosslinked beads were then washed three times with 200µl PBST (0.02% Tween) and stored in 50µl of conjugation buffer at 4°C.

### 2.5.2 Co-immunoprecipitation

BV2 cells were seeded in six Thermo Scientific 175cm<sup>2</sup> (T175) flasks (three flasks per IP condition ~ 90 x10<sup>6</sup> cells) and grown to confluency (approximately 48-72h). Suspension cells in the media were removed and centrifuged for 3min at 1000rpm at room temperature. Meanwhile the remaining adherent cells were washed twice with PBS and 7.5ml of Accutase® (Sigma-Aldrich®) was added to each flask and incubated at 37°C for 5min to detach the adherent cells. Accutase® was inactivated by the addition of 7.5ml media and cells were pelleted by centrifugation at 1000rpm for 3min at room temperature. Cell pellets were then resuspended and combined in 12ml of PBS (2ml per flask). Cells were subsequently split into aliquots and centrifuged for 5min at 1200rpm and 4°C. After removal of PBS, cells were lysed in ice-cold RIPA buffer (500µl per flask; 150mM NaCl, 50mM Tris pH 8.0, 1% (v/v) Triton X-100, 0.5% (w/v) sodium deoxycholate, 1mM EGTA) supplemented with Pierce™ Protease Inhibitor Tablets, EDTA-free (500µl of x25 stock dissolved in 10ml) and Pierce™ Phosphatase Inhibitor Tablets (1 tablet in 10ml buffer), to preserve phosphorylation sites, for 30min at 4°C. Cell lysates were then homogenised for two, 5sec bursts using a POLYTRON® PT3100 (Kinematica) then via passage through a 21G-26G needle six times. Lysis was confirmed via microscopy and homogenisation was repeated if required. The lysate was then divided into 1.5ml Eppendorfs and clarified by centrifugation for 5min at 13,000rpm and 4°C. Samples were then combined and 50µl was removed for the 'Input Sample'. The cell lysate was then precleared with 50µl protein G Dynabeads™, previously equilibrated in RIPA buffer for 1h at 4°C with constant rotation (10rpm). The beads were then recovered using a DynaMag™-2 magnetic rack (Invitrogen) and the precleared lysate split into two (one co-IP, one control). The precleared lysate was pelleted by centrifugation to remove insoluble material for 10min at 13,000rpm and 4°C. The resulting supernatant was then added directly to 25µl of antibody crosslinked protein G Dynabeads™. Samples were then incubated overnight at 4°C with rotation (10rpm). The next day, the beads were recovered using the magnetic rack and a 50µl sample was taken from the remaining supernatant for the 'Unbound Sample'. The beads were subsequently

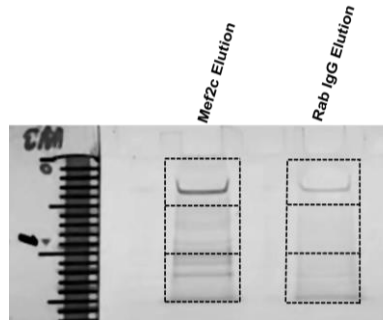
washed four times in 1ml RIPA buffer. After the final wash, RIPA buffer was removed and 70µl reducing buffer (NuPAGE™ LDS Sample Buffer (4X), 50mM TCEP) was added to the beads. 50µl of reducing buffer was also added to the 'Input' and 'Unbound' samples. All samples were subsequently incubated at 95°C for 5min. Beads were then removed, via the magnetic rack, from the 'Elution samples' before resolution and detection by SDS-PAGE and Western Blot (sections 2.4.2 and 2.4.3).

### 2.5.3 Ionomycin stimulation

To investigate the effect of increased  $[Ca^{2+}]$  on the Mef2c interactome, BV2 cells were treated with the antibiotic ionomycin (Biotechne, Tocris), which increases intracellular  $[Ca^{2+}]$ , prior to co-IP. BV2 cells were seeded into T175 flasks as described above. To avoid using suspension cells, which need additional centrifugation which may activate the cells, eight confluent T175 flasks were used (four flasks per IP condition). Suspension cells were discarded, and only adherent cells were used. These cells were washed twice with serum-free RPMI and then left for 1h in serum-free RPMI. After which, cells were treated with 1µM ionomycin (dissolved in DMSO) for 1h. Cells were subsequently subjected to the co-IP protocol detailed above.

### 2.5.4 Co-IP sample preparation for mass spectrometry

For mass spectrometry (MS) analysis, 40µl aliquots of the immunoprecipitated protein complexes and control samples were resolved by electrophoresis on a pre-cast 4-12% gradient NuPAGE™ Bis-Tris gel (Invitrogen). Samples were run in 1X MOPS SDS Running Buffer (Life Technologies) for approximately 15min (about 2cm into the gel) using the XCell Surelock™ Mini-Cell system (Invitrogen). After electrophoresis, gels were fixed in 50% (v/v) methanol and 7% (v/v) acetic acid for 15min at room temperature with rotation. Gels were subsequently washed twice for 5min in molecular biology-grade water. Gels were then stained with GelCode™ Blue Stain Reagent (ThermoFisher) at room temperature for 1h with rotation to visualise protein bands. Gels were then de-stained in molecular biology-grade water for 1-2h at room temperature then overnight at 4°C. This method of staining is compatible with MS as the protein is not fixed in the de-staining process. Images of stained gels were taken using the Odyssey® Infrared Imaging System (LI-COR Biosciences). Clean scalpel blades were then used to excise three equally sized bands from both the Mef2c antibody and IgG control antibody lanes (Figure 2.1). These bands were placed into sterile 1.5ml Eppendorf tubes, sealed with parafilm, and sent for MS analysis.



**Figure 2.1. Band excision of Mef2c IP elutions for analysis by MS.** Aliquots of the immunoprecipitated protein complexes and control samples were resolved on a 4-12% polyacrylamide gradient gel by electrophoresis. Three equally sized gel slices from each elution were excised for MS as indicated on the image. A ruler is pictured on the image to detail how far the samples were run into the gel and at what lengths the cuts were made.

### 2.5.5 Protein identification by mass spectrometry

Excised gel plugs were sent to the Functional Genomics and Proteomics Laboratories at the University of Birmingham to be processed for MS. Up to 10 $\mu$ g of protein is digested using trypsin gold (Promega). The UltiMate<sup>®</sup> 3000 HPLC series (Dionex) was used for peptide concentration and separation. Peptides were eluted using a Triversa Nanomate nanospray source (Advion Biosciences) into a QExactive HF Orbitrap mass spectrometer (ThermoFisher Scientific). Peptide data were matched against the Uniprot database using Protein Discovery 2.2 software and the Sequest HT algorithm (ThermoFisher). The Sequest HT search engine calculates cross-correlation (XCorr) scores, the number of fragment ions that are common for two different peptides with the same precursor mass, for peptide matches. It presents peptide matches that have the best XCorr score for each spectrum and calculates a preliminary SpScore score which it uses to filter peptide candidates. XCorr scores are calculated for peptide spectrum matches (PSMs) if they pass the SpScore filter. Variable modifications were deamidation (N and Q), oxidation (M) and phosphorylation (S, T and Y). Two missed cleavage were allowed, and data were filtered with a false discovery rate (FDR) of 0.01. Proteins with at least two high confidence peptides are accepted as real hit.

### 2.5.6 HEK293T co-immunoprecipitation

To validate interactions, HEK293T cells were seeded, at approximately 0.5x10<sup>6</sup> cells per well, into in 35mm TC-treated culture dishes (Corning) and left to grow to a confluence of 60-80% (approximately 24h). Each well was then transfected with 2 $\mu$ g of the appropriate DNA construct(s). Constructs transfected for HEK293T co-IP are listed in table 2.5. DNA was transfected into cells using Lipofectamine<sup>®</sup> 2000 (Lipo2000) Transfection Reagent (Invitrogen) added in the ratio of 3 $\mu$ l Lipo2000 to every 1 $\mu$ g DNA. Lipo2000 was first

**Table 2.5. DNA constructs transfected for co-IPs from HEK293T cells.**

Construct	Species	Tag	Source
<b>Mef2c Isoform 1</b>	Mouse	C-terminal HA	pcDNA3.1-MEF2C-HA was a gift from Andrew Lassar
<b>Mef2c Isoform X4</b>	Mouse	C-terminal HA	Genscript
<b>Hdac4</b>	Mouse	N-terminal FLAG	Genscript
<b>Hira</b>	Mouse	N-terminal FLAG	Genscript
<b>Cabin1</b>	Mouse	N-terminal FLAG	Genscript
<b>Oasl1</b>	Mouse	N-terminal FLAG	Genscript
<b>Ncoa5</b>	Mouse	N-terminal FLAG	In-house
<b>Thoc6</b>	Mouse	N-terminal FLAG	In-house

incubated in Opti-MEM® Reduced Serum Medium (GIBCO) for a few minutes before the addition of the appropriate DNA constructs. Transfection mixes were incubated for 20min at room temperature before adding directly to the cells at 10% of the medium volume (e.g., 100µl into 1ml cells). Dishes were incubated for a further 24h before cell lysis.

For the co-IP, cells were carefully washed with 1ml PBS before the addition of 500µl of ice-cold RIPA buffer supplemented with protease and phosphatase inhibitors. Cells were scraped into 1.5ml Eppendorf tubes and left to incubate on ice for 30min. Cell lysates were then homogenised via passage through a 21G-26G needle six times. Lysis was confirmed via microscopy and homogenisation was repeated if required. The lysates were clarified by centrifugation for 5min at 13,000rpm and 4°C and the supernatant was transferred to new tubes. A 50µl aliquot was taken from each sample for the 'Input Sample'. Anti-FLAG® M2 magnetic beads (Sigma-Aldrich®), prewashed in RIPA buffer, were used for antibody capture. 20µl of beads were added to each sample and left to incubate overnight at 4°C with rotation (10rpm). The next day, the beads were recovered using the DynaMag™-2 magnetic rack (Invitrogen) and a 50 µl sample was removed from the remaining supernatant for the 'Unbound Sample'. The beads were subsequently washed four times in 300µl RIPA buffer. After the final wash, RIPA buffer was removed and 70µl reducing buffer (NuPAGE™ LDS Sample Buffer (4X), 50mM TCEP) was added to the beads. 50µl of reducing buffer was also added to the 'Input' and 'Unbound' samples. All samples were subsequently incubated at 95°C for 5min. Beads were then removed, via the magnetic rack, from the 'Elution samples' before resolution and detection by SDS-PAGE and Western Blot (sections 2.4.2 and 2.4.3).

## 2.6 Bioinformatics

### 2.6.1 General

DNA and protein sequence homology searches were performed using the BLAST (Basic Local Alignment Search Tool) program. Gene and protein sequences were obtained using the National Center for Biotechnology Information (NCBI) databases. Alignment of nucleotide and protein sequences were performed with Clustal Omega (Madeira et al., 2019). DNA to protein translation and molecular weight prediction was carried out using the Expasy (Expert Protein Analysis System) proteomics server from the Swiss Institute of Bioinformatics (<http://www.expasy.org/>). Statistical analysis and graphical representation of reporter assay and spectral count data was carried out using GraphPad Prism v7.04. For all experiments, a p-value of  $<0.05$  was deemed statistically significant.

### 2.6.2 Mass spectrometry data analysis

Several bioinformatics tools were used to analyse the MS data. DOG 2.0 (Ren et al., 2009) was used to align peptide sequences and phosphorylation sites to the full protein sequence. Prediction of phosphorylation sites was performed with PhosphoMotif Finder from the Human Protein Reference Database (Amanchy et al., 2007). NCBI was used to identify previously known interactors. NCBI sources its interaction data from other databases including the Biological General Repository for Interaction Datasets (BioGRID), the Biomolecular Interaction Network Database (BIND), and the Human Protein Reference Database (HPRD). RStudio (R Core Team, 2020) was used to filter the data, using the `dplyr` package and create Venn diagrams, using the `VennDiagram` package to visualise overlaps between the datasets.

#### 2.6.2.1 Filtering methods

For each biological replicate, peptide counts across the three excised bands were combined and any contaminants or protein entries supported by fewer than two peptides were excluded. Both true Mef2c-associated proteins and contaminants are pulled down in co-IP-MS experiments, therefore scoring each putative interacting protein against proteins that are recovered in the IgG control purification is very important. Thus, using the unstimulated dataset, two alternative filtering methods were explored as modes of sorting the MS data.

The IgG hard filter method involved filtering the proteins identified in each Mef2c IP against a list of proteins detected across all three IgG IP replicates to remove any proteins that had immunoprecipitated non-specifically. Subsequently the resulting lists from each replicate

were combined to generate a list of 66 potential Mef2c-interacting proteins. These proteins were filtered further using the Contaminant Repository for Affinity Purification (CRAPome) database ([www.crapome.org](http://www.crapome.org), accessed June 2021) (Mellacheruvu et al., 2013). This database contains human proteins that have been identified in negative control affinity purification followed by MS experiments. Each protein is scored based on the number of experiments (out of 716) that the protein is identified in, and a percentage is calculated. The identified Mef2c-interacting proteins were converted to their human orthologs and subsequently ranked based on their CRAPome percentage to enable the identification of high confidence interactors. There is no gold standard for the CRAPome percentage cut off for a protein to be deemed high confidence. Papers that report using the CRAPome use a large range of percentage cut offs, from 5% to 80% (De Munter et al., 2017; Kuenzi et al., 2016; Morgan et al., 2019; Pedley et al., 2020). Here, a conservative CRAPome cut off has been used. Proteins with a percentage less than 10% were defined as high confidence interactors. This resulted in a list of 12 high confidence interactors for the unstimulated dataset.

The second method applied to the dataset was Significance Analysis of INteractome (SAINTexpress v3.4) (Teo et al., 2014). SAINTexpress is a statistical method for probabilistically scoring protein-protein interaction data from affinity purification MS experiments. It determines, based on the data, whether prey proteins identified in an affinity-purified sample are either a true interactor of the bait protein or a non-specific binder or contaminant. To be classified as a true interaction the prey must be observed in high abundance, at a level significantly higher than in the negative control purification. Ultimately, the probability score generated by SAINT represents the confidence level of putative interactions. For this quantitative analysis, the total number of spectral counts (PSMs-peptide spectrum matches) for each protein from each replicate were used. 110 prey proteins with a Bayesian false discovery rate (BFDR) of less than 0.05 or a SAINT score of 0.7 or greater were defined as significant putative interactors of Mef2c.

The overlap between the significant interactors identified by the IgG filter and by SAINTexpress were assessed. SAINTexpress identified more significant interactors (110) compared to the hard-filtered method (66). 100% of the interactors identified by the IgG filter were also identified by SAINTexpress. Both methods identify similar proteins of interest, the high confidence proteins identified by the IgG filter and further ranking by the CRAPome were very similar to the most significant SAINTexpress interactors. The SAINTexpress method has a slight advantage to the IgG (hard-filtered list) filter as it allows

proteins that appear at a very low abundance in the IgG control to be considered as potential interactors. This method has also been used recently to analyse protein interaction data generated by BioID (Go et al., 2021). Therefore, SAINTexpress was used as the final filtering method for the aforementioned unstimulated MS data (see Chapter 3, section 3.2.4.1) and for the stimulated dataset (see Chapter 4, section 4.2.5.1). The CRAPome database was also used to help identify proteins of interest for further investigation by ranking proteins based on their CRAPome percentage score.

#### 2.6.2.2 STRING and Metascape

To investigate known functional relationships between identified Mef2c-associated proteins, the STRING database (<https://string-db.org/>) was used to view interactions (Szklarczyk et al., 2019). This database contains known and predicted protein-protein interactions and can be used to summarise the network of putative interactions for a specific set of proteins. STRING derives its interactions from five main sources: genomic context predictions, high-throughput lab experiments, (conserved) co-expression, automated text mining, and previous knowledge in databases. High-throughput lab experiments and previous knowledge in databases were used as prediction methods with a medium confidence threshold (0.4). Proteins were converted to their human identifiers for this analysis as the available data is more complete and protein-protein interactions are relatively conserved between species (Pérez-Bercoff et al., 2013; Qian et al., 2011; Sharan et al., 2005).

The biological functions of genes were annotated using Metascape's gene ontology enrichment analysis (Zhou et al., 2019). This tool looks at what gene ontology terms are over-represented within a gene set to determine what biological processes these genes are involved in. All genes in the genome were used as the enrichment background. The tool collects terms with a p-value <0.01, a minimum count of three, and an enrichment factor >1.5 (the ratio between the observed counts and the counts expected by chance) and groups them into clusters based on their membership similarities. The most statistically significant term within a cluster was chosen to represent the cluster.

#### 2.6.3 MAGMA

Multi-marker Analysis of Genomic Annotation (MAGMA v1.10) (de Leeuw et al., 2015) was used to assess the relevance of identified Mef2c interactors and Ca<sup>2+</sup>-associated genes to AD-risk. MAGMA is a tool for gene-set enrichment analysis of GWAS genotype data. MAGMA generates single p-values of protein coding genes by combining SNPs and linkage

disequilibrium (LD) structure. It uses these genes with associated p-values to run an enrichment analysis which looks for excess significance in the supplied gene set. It tests whether the genes in the supplied gene set are jointly associated with the phenotype of interest. For use in the analysis, GWAS data for AD was extracted from the Kunkle et al. (2019) paper by Dr. Matt Hill. The MHC region, which is known to be problematic due to extensive LD, high gene density and extreme polymorphism (Trowsdale & Knight, 2013), was removed along with the *APOE* gene as the association signal is so strong here that it increases the signal strength of other genes in the region which is again, problematic. Three gene sets were created; Mef2c unstimulated interactions, Mef2c stimulated interactions and genes assigned to differentially accessible regions. For each of these sets the human Entrez IDs were used. A p-value of <0.05 for the enrichment test was deemed statistically significant.

## 2.7 ATAC-seq

### 2.7.1 Library preparation

For ATAC-seq, eight T25 flasks of BV2 cells were seeded as described in section 2.3.1. After growth to 70-80% confluence, cells were washed twice with serum-free RPMI and then left to incubate for 1h in serum-free RPMI. After which, cells were treated with either 1 $\mu$ M ionomycin (dissolved in DMSO) or DMSO as a vehicle control (four flasks per condition) for 1h. Cells were then passaged and counted as described in section 2.3.1. Subsequently, 250,000 cells, from each flask, were pelleted for 5min at 3000rpm at 4°C. The ATAC-seq preparation process followed the OMNI-ATAC protocol (Corces et al., 2017) and all steps were performed on ice or at 4°C unless otherwise specified. Cell pellets were first resuspended in 250 $\mu$ l cold cell lysis buffer (0.1% (v/v) IGEPAL (Sigma-Aldrich®), 0.1% (v/v) Tween-20 (Sigma-Aldrich®), and 0.01% (w/v) digitonin (Sigma-Aldrich®) in ATAC resuspension buffer (RSB; 10mM Tris-HCL pH 7.4, 10mM NaCl, 3mM MgCl<sub>2</sub>)) to isolate nuclei. Nuclei were subsequently incubated on ice for 3min, then 50 $\mu$ l (50,000 cells) from each sample were removed to new Eppendorfs prior to being washed by the addition wash buffer (0.1% (v/v) Tween-20 in RSB) and inversion three times to mix. Successful lysis was confirmed under a microscope. After washing, nuclei were centrifuged for 10min at 3000rpm. Pellets were resuspended in 50 $\mu$ l transposition mix (25 $\mu$ l 2X Tagmentation Buffer (Diagenode), 2.5 $\mu$ l Tagmentase (Tn5 transposase)-loaded (Diagenode), 16.5 $\mu$ l PBS, 0.5 $\mu$ l 1% (w/v) digitonin, 0.5 $\mu$ l 10% (v/v) Tween-20, 5 $\mu$ l nuclease-free water) by pipetting up and down six times and incubated at 37°C for 30min. A DNA Clean and Concentrator-5 Kit (Zymo Research) was used to isolate and clean the DNA library. Samples were stored at -

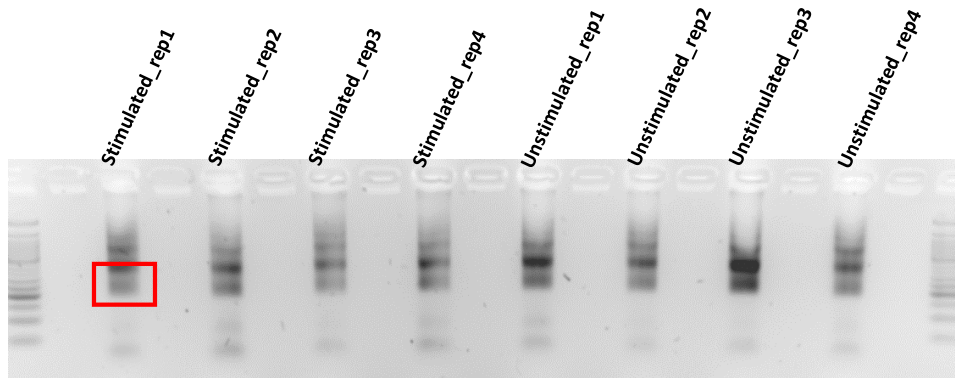


20°C overnight in 20µl of elution buffer (Zymo Research). To reduce the amount of technical variation, flasks were processed in batches of four (two treated with ionomycin and two treated with DMSO) and both batches were processed on the same day.

Samples were defrosted on the bench and then amplified for a total of 12 PCR cycles (C1000/S1000™ Thermal Cyclers BioRad) following the parameters outlined in table 2.6. Primers used for each sample included a generic forward primer (Ad1) and a unique reverse primer (Ad2). After amplification, DNA fragments were isolated and cleaned again as described previously using the DNA Clean and Concentrator-5 Kit (Zymo Research). DNA was subsequently size separated by gel electrophoresis (described in section 2.1.4) using a 2.5% gel supplemented with 10µl SafeView Nucleic Acid Stain (NBS Biologicals), so DNA fragments that represent the insertion of sequencing adapters in either one or two nucleosomes by transposase can be extracted. PCR products (20µl) were pre-mixed with 6X loading dye (OrangeG) prior to loading onto the gel, leaving a one well gap between each sample to prevent cross-contamination. A 50bp DNA ladder (NEB) was also loaded to determine the size of the DNA fragments. The gel was run at 100V for 45min to allow the DNA to separate sufficiently for the extraction of DNA between the range of 175-400bp (Figure 2.2). A sterile scalpel was used to cut amplicons of this size range out of the gel which was viewed using a SafelImager™ 2.0 Blue-Light Transilluminator (Invitrogen). DNA was subsequently extracted from the gel slices using the Zymoclean™ Gel DNA Recovery Kit (Zymo Research). Samples were then prepared for sequencing. First, the ATAC-seq library was quantified using the Qubit® 4 Fluorometer (range 10pg/µl-100ng/µl) and the Qubit™ dsDNA HS Assay Kit (ThermoFisher). The Fragment Analyzer™ system was used to determine the average fragment length of DNA in each sample (range 290-334bp). DNA was then pooled to a final molarity of 10nM in 40µl of elution buffer and sequenced using

**Table 2.6. ATAC-seq PCR reaction protocol**

50 µl PCR Reaction		Cycling Conditions	
PCR Amplification	Volume (µl)	Temp (°C)	Time
25µM Primer Ad1 (Nextera)	2.5	72	5min
25µM Primer Ad2 (Nextera)	2.5	98	30sec
Master mix (2x NEBNext)	25	<b>Then 12 cycles of:</b>	
Transposed DNA	20	98	10sec
		63	30sec
		72	1min
<b>Hold at 4°C</b>			



**Figure 2.2. Size separation of ATAC-Seq DNA samples by gel electrophoresis.** ATAC-seq PCR samples were size separated by gel electrophoresis using a 2.5% gel so DNA fragments between 175-400bp could be extracted. These fragments represent the insertion of sequencing adapters in either one or two nucleosomes by transposase. A one well gap was left between each sample to prevent cross-contamination. The area excised from the gel is highlighted in lane one by a red box.

an in-house Illumina NovaSeq 6000 system (preparation and sequencing performed by Dr. Joanne Morgan).

### 2.7.2 Sequencing, QC, and bed file preparation

Paired-end sequencing was carried out on the ionomycin stimulated and unstimulated BV2 cell line ATAC-seq libraries using the Illumina NovaSeq 6000 system. A total of 32 sequencing files were produced; four FASTQ files were present for each of the eight samples. Forward and reverse read files (R1/2) were run on both lanes (L001/2) to avoid bias, half on each lane. Adapter sequences were pre-trimmed by Dr. Joanne Morgan. Reads from each lane were first combined prior to any downstream processing. For quality control, FastQC (Andrews, 2010) was run on each concatenated FASTQ file (R1/2). All files passed the quality control measures and were included in the analysis. Subsequently, the forward and reverse FASTQ files for each sample were aligned to the mouse genome (mm10) using BWA and the `bwa mem` command and a thread count of 20 to speed up mapping (Li & Durbin, 2009). After alignment, subsequent analysis followed the workflow set out by Reske et al (2020). The aligned `.sam` files were converted to `.bam` files, sorted and indexed prior to the removal of mitochondrial reads using Samtools (Li et al., 2009). Mitochondrial reads are removed due to a lack of chromatin packaging which makes the mitochondrial genome more accessible (Bogenhagen, 2012). Samtools was then used to restrict files to properly-paired reads, count the number of reads per file and subsample each file. Files were subsampled to the same read count as the 3\_DMSO sample as this file had the lowest read count. PCR duplicates were subsequently removed from the samples using Picard (*Picard Tools*, 2009). Using Samtools, files were finally sorted by read name

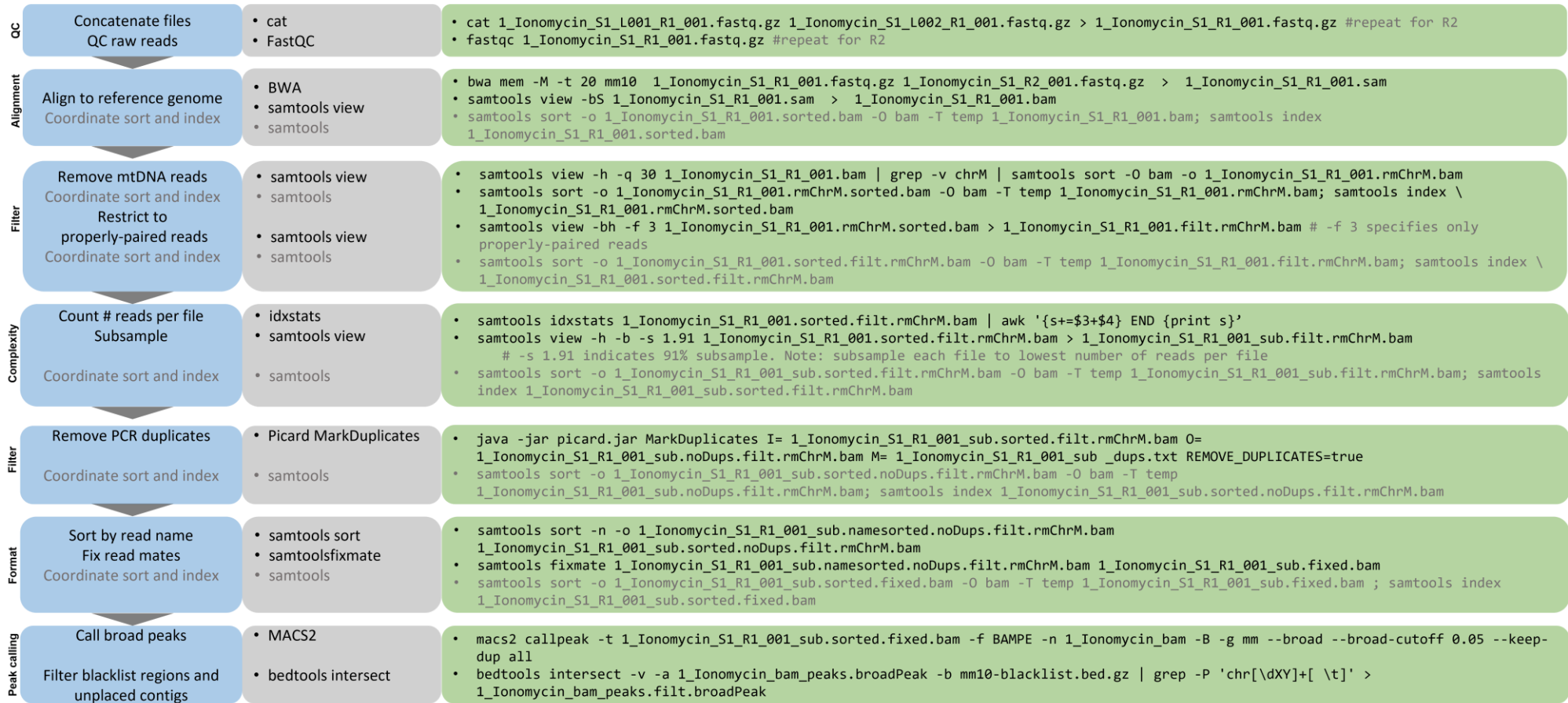
and then read mates were fixed to correct any flaws in read-pairing that occurred during alignment. MACS2 (Zhang et al., 2008) was used to call peaks using the `BAMPE` parameter to process paired-end reads. An FDR of  $<0.05$  was set as the peak significance threshold. `Bedtools intersect` was then used to filter blacklist regions. A summary of this analysis and the code used is presented in Figure 2.3.

### 2.7.3 Differential accessibility analysis

The R Bioconductor package `DiffBind` (Stark & Brown, 2011) was used to identify sites that are differentially bound between conditions. Peaksets for each sample were read into R using the `dba` command and a sample sheet. The `dba.blacklist` function was then used to remove blacklisted regions of the mm10 reference genome that are known to be problematic (`blacklist=DBA_BLACKLIST_MM10`). These regions include ones with unusual base concentration or a high number of repeats. The blacklists available under this function have been identified as part of the ENCODE project (Amemiya et al., 2019) and the application of these lists prevents problematic regions in the mm10 genome from being identified as differentially bound. After blacklist removal, a binding matrix was calculated using the `dba.count` function using affinity scores which are scores based on read counts for each sample.

Next the data was normalised using the `dba.normalize` function. `Diffbind` has several options for normalising data. Library-size based normalisation is one option which either calculates the library size based on the sequencing depth (total number of aligned reads for each sample) which is known as the Full library size (`DBA_LIBSIZE_FULL`) or based on Reads in Peaks (RiP) which are the sum of reads that overlap consensus peaks in each sample (`DBA_LIBSIZE_PEAKREADS`). This way of calculating library sizes accounts for both sequencing depth and the efficiency of the experiment. Another normalisation option uses native normalisation methods supplied with `DESeq2` and `edgeR`. The `DESeq2` method (`DBA_NORM_RLE`) calculates the geometric mean for each gene across samples (Love et al., 2014) whereas the `edgeR` method (`DBA_NORM_TMM`) uses the trimmed mean of M-values approach (Robinson & Oshlack, 2010). Background normalisation can also be performed in `Diffbind`. This method involves dividing the genome into large bins and counting overlapping reads (Lun & Smyth, 2016). In `Diffbind` `background=TRUE` needs to be specified and the native normalisation methods can be applied to these background bins. The final normalisation method, `loess` fit, is based on calculating normalisation factors for each read count in the consensus count matrix. This method can help correct

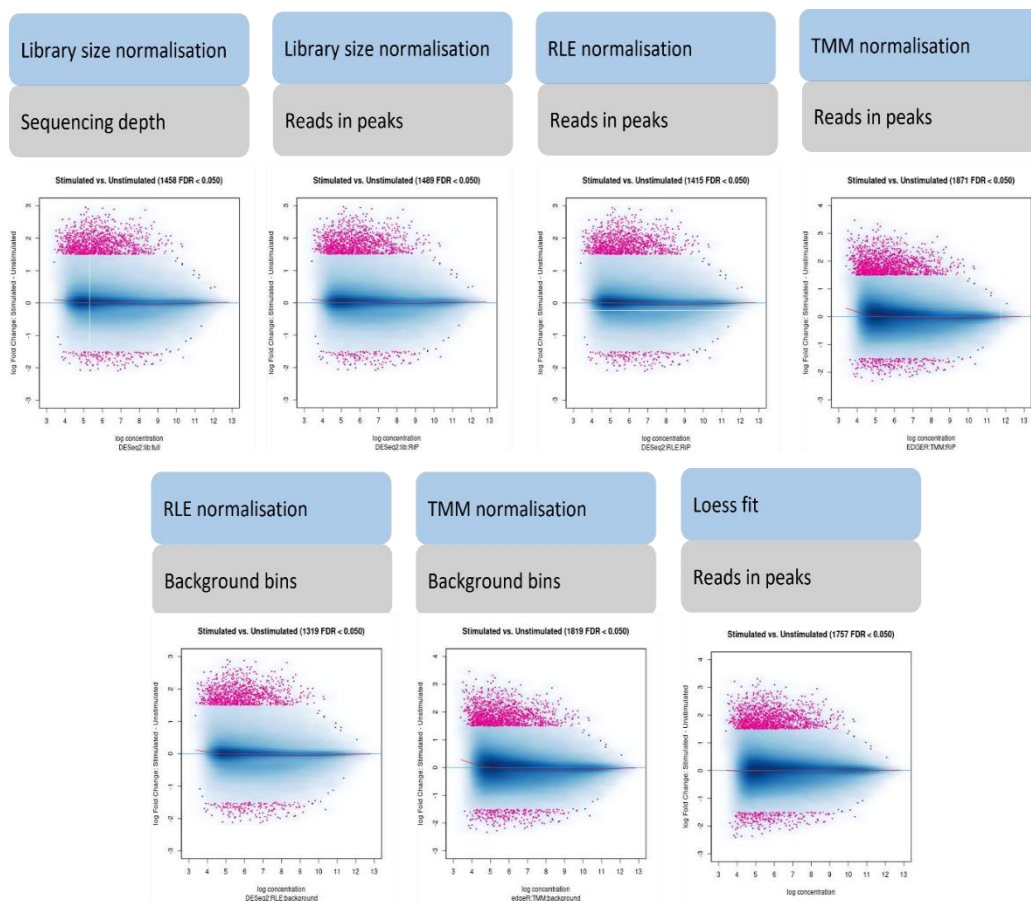
## Chapter 2 Methods



**Figure 2.3. ATAC-seq data processing workflow.** This schematic covers the steps taken, with example commands, to process the ATAC-seq data from raw reads to calling peaks for downstream differential accessibility analysis. Each line of code was run for each sample (1-8) and 'Ionomycin' was replaced by 'DMSO' for the control samples.

biases in the data including trended biases (Lun & Smyth, 2016). Reske et al (2020) recommends that multiple normalisation methods should be systematically compared prior to continuing with the differential accessibility analysis. Therefore, all seven methods were run on the dataset to deem which was most appropriate.

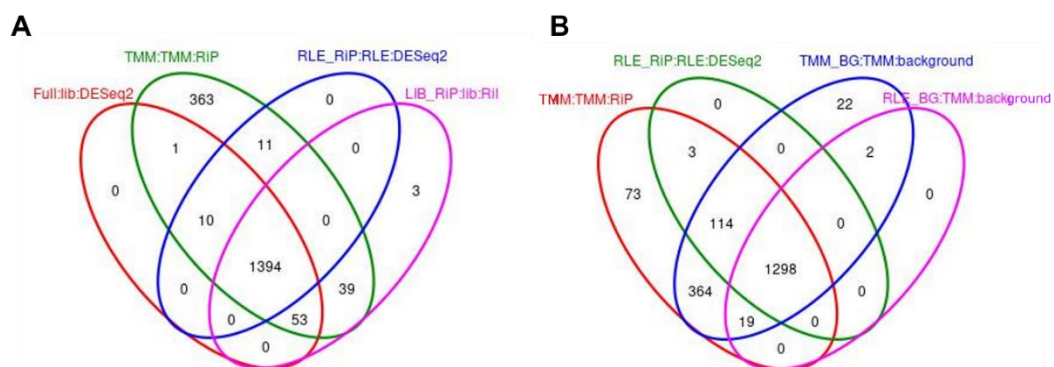
After normalisation with each method, the differential analysis function, `dba.analyze`, was invoked to assess the effect of normalisation on differential accessibility. Differentially bound sites were retrieved using the `dba.report` function, restricting to sites with a fold change of  $\geq 1.5$  (`fold=1.5`). This fold change cut off was applied to reduce noise as, under ionomycin stimulation, it is expected that only a subset of sites, rather than the whole chromatin landscape, will change. To visualise the effect of normalisation on the data, MA plots from each analysis were generated using the `dba.plotMA` function, restricting to sites with a fold change of  $\geq 1.5$  (`fold=1.5`) (Figure 2.4). The plots reveal that the different



**Figure 2.4. MA plots of differentially accessible peaks after applying the seven different normalisation methods to the dataset.** The data was normalised using seven different methods: full library-size, reads in peaks (RiP) library-size, RLE RiP, TMM RiP, RLE background, TMM background, or loess fit. After normalisation with each method, differential accessibility was measured and visualised in MA plots, restricting to sites with a fold change of  $\geq 1.5$ . Comparing the plots reveals that the different normalisation methods do not really alter the global properties of the data.

normalisation methods do not drastically change the global properties of the data which reflects the controlled experimental design. This differs from other examples in the literature which report distinct differences in chromatin accessibility patterns depending on the normalisation method used (Reske et al., 2020; Wilson et al., 2019). In this current analysis, the only difference is a slight alteration in the absolute fold change between methods. However, some of the methods are not appropriate due to the nature of the dataset. The full-library size method is not suitable as the samples have already been down sampled to the same read depth. There is also no trended bias in between the sample groups so the loess fit normalisation is also not appropriate. This leaves the RiP based methods and the background methods. As there appears to be little technical variation in the data, normalising to RiP is likely to be a better option. When comparing the RiP methods (Figure 2.5) it seems that the RLE (DESeq2) overlaps best with the other methods showing the least variation of differentially accessible sites. The other methods alter the data distribution to a greater extent. Therefore, the RLE\_RiP\_DESeq2 method was chosen as the most appropriate normalisation method and the differential accessibility data generated from this was used in downstream analyses.

To visualize normalised differentially accessible peaks, *BedGraph* files, extracted from the MACS2 peak calling analysis, were normalised using the size factors for each sample. Size factors were calculated by multiplying the normalisation factor for each sample by the sample library size then dividing by  $1 \times 10^6$ . A reciprocal of the size factor was then



**Figure 2.5. Comparison of normalisation methods.** The number of differential peaks with a fold change  $\geq 1.5$  after each normalisation method were compared using Venn Diagrams. There is a large degree of overlap between each method highlighting little variation between each normalisation method. The RLE method seems to overlap best with the other methods showing the least variation of differentially accessible sites. **(A)** Library-size normalisation (full and RiP) methods compared to the RLE RiP and TMM RiP methods. **(B)** Background normalisation methods (RLE and TMM) compared to the RLE RiP and TMM RiP methods.

generated by dividing 1 by each size factor. This number was then used to scale the *BedGraph* files by multiplying it with the score for each peak position. This normalised *BedGraph* file was then converted to a binary *BigWig* file using the `fetchChromSizes mm10` command to create the *chrom.sizes* file for the mm10 UCSC database and then running the `bedGraphToBigWig` command to convert the file. Normalised peaks in these files were visualised using the integrative genomics viewer (IGV; Robinson et al., 2011).

#### 2.7.4 Principal components analysis

Prior to further analysis, the data was analysed using a principal components analysis (PCA). PCA is an unsupervised statistical method which can be used to summarise large and complex datasets. It can increase the interpretability of data as it can be used to identify relationships between samples or any patterns in the data that may exist but be difficult to identify (Groth et al., 2013). To summarise the variation across the samples, Diffbind was used again to run the PCA, using the `dba.plot` function, on all peaks in the normalised dataset.

#### 2.7.5 *De novo* motif enrichment analysis

Hypergeometric Optimization of Motif EnRichment (HOMER) v4.11 (Benner et al., 2017; Heinz et al., 2010), which is a tool for analysing NGS data and motif discovery, was used to test the enrichment of transcription factor binding motifs in the mouse BV2 open chromatin peak set. Prior to the motif analysis, peak files were annotated using the `annotatePeaks.pl` command. This associates peaks with nearby genes by determining the closest transcription start site (TSS). It also provides additional information about important genomic features by calling another program, `assignGenomeAnnotation`. This includes information about whether a peak is in the TSS, transcription termination site, exon, 5' UTR exon, 3' UTR exon, intronic or intergenic regions.

To find enriched motifs in genomic regions the `findMotifsGenome.pl` command was run. The size of the region for motif finding was set to a fixed size of 200 bp using the `-size 200` command. Since HOMER motif analysis is a differential motif discovery algorithm, it must first create a set of background sequences to use as a control. By default, HOMER randomly selects a sufficient number of background regions from the specified genome (mm10) so that the total number of regions is either twice the total number of peaks or 50000, whichever is larger. HOMER will choose background regions that match the GC content distribution of the input sequences. HOMER then screens the input and background sequences against its library of known transcription factor motifs, reporting

enriched motifs with a p-value of  $<0.05$ . Then, the *de novo* motif finding is performed in which the input and background open chromatin regions are queried for sequences of specific lengths (-len 8,10,12). Sequences enriched in open chromatin regions are then compared to a database of known transcription factor motifs, returning motifs with a p-value of  $<0.05$ . Ultimately HOMER produces files containing enrichment scores for either known or *de novo* transcription factor motif locations. The *de novo* motif file is a more concise output that matches enriched motifs to transcription factors so only the *de novo* results are reported here. For the motif analysis on the differential peaks, a custom background was created from the consensus peaks (all BV2 peaks) data file.

#### 2.7.6 Functional enrichment analysis

The online tool Genomic Regions Enrichment of Annotations (GREAT; McLean et al., 2010) was used to test whether genes associated with increased or decreased chromatin accessibility or genes linked to Mef2c motifs are enriched within particular biological categories. GREAT associates genomic regions with nearby genes which are then assigned a basal regulatory domain that consists of a proximal domain, 5kb upstream and 1kb downstream of the gene TSS, and a distal domain, 1Mb upstream or downstream of the gene TSS. GREAT then calculates the enrichment of regulatory regions, provided by the user, within these domains. It uses a binomial test that corrects for variability in gene regulatory domain size. GREAT (<http://great.stanford.edu/public/html/>) was accessed and run in November 2021, using the whole mouse genome (mm10) as a background.



## Chapter 3 Investigating the protein interactome of Mef2c in unstimulated BV2 cells

### 3.1 Introduction

In sporadic cases of AD, there is a large polygenic contribution as over 50 susceptibility loci with genome-wide significance have now been identified (Sims et al., 2020). Recently, immune cells have been implicated as probable effectors of AD-risk as genetic studies have shown that many AD-risk genes are also preferentially or selectively expressed by microglia (Jonsson et al., 2013; Lambert et al., 2013). *MEF2C*, which is an AD-risk gene, is expressed in microglia where it regulates target gene expression (Escott-Price et al., 2015; Lambert et al., 2013). *MEF2C* encodes the transcription factor myocyte enhancer factor 2C, hereafter referred to as MEF2C. The transcriptional network of MEF2C is thought to be an important underlying AD-risk mechanism. In microglia and macrophages, AD-risk single nucleotide polymorphisms (SNPs) are enriched in open chromatin regions that contain DNA binding motifs for MEF2C (Tansey et al., 2018). Disrupted DNA binding due to genetic variation at these sites leading to altered gene expression in *cis* may result in impaired transcriptional control by MEF2C. Thus, MEF2C-dependent gene regulation in microglia may confer, in part, AD-risk.

To understand how MEF2C regulates expression of AD-risk genes it is important to investigate its interactome. As discussed in the General Introduction (section 1.5), understanding protein-protein interactions can help to elucidate how genome variation may contribute to disease (Havugimana et al., 2012; Menche et al., 2015). More specifically, protein-protein interaction studies have successfully identified new interactors of a range of proteins, elucidating mechanisms of disease pathology, common molecular risk pathways and potential therapeutic targets (Goehler et al., 2004; Liu et al., 2018; Pedley et al., 2020). For example, co-immunoprecipitation-mass spectrometry (co-IP-MS) has shown that post-translational control of microglial transcription factors by interacting proteins can impact AD-like pathology. The ubiquitin ligase, constitutive photomorphogenic 1 (COP1), has been shown to interact with the transcription factor CCAAT/enhancer binding protein beta (c/EBP $\beta$ ) which is upregulated in AD and regulates pro-inflammatory genes in microglia. COP1 regulates the expression of this transcription factor and its absence results in the initiation of pro-inflammatory and neurodegeneration-related gene programs (Ndoja et al., 2020). This suggests that COP1 is a key suppressor of

c/EBP $\beta$ -induced pathogenic gene expression. Therefore, using this technique to study MEF2C could reveal potential interactors that regulate MEF2C-dependent AD-risk gene regulation.

The vast majority of MEF2C interacting partners have been identified in muscle cells (Dong et al., 2017). Some of these muscle-related interacting partners include MyoD, Myogenin and ERK5. Both MyoD and Myogenin are myogenic regulatory factors and are important for myoblast specification and differentiation, respectively (Dodou et al., 2003). Both factors directly interact with MEF2C to activate transcription and promote myogenesis (Black et al., 1998; Molkenin et al., 1995). The mitogen-activated kinase ERK5 is vital for cardiac muscle cell development (Hayashi et al., 2004). ERK5 phosphorylates MEF2C resulting in increased transactivation activity (Kato et al., 1997; Yang et al., 1998).

Conversely, only a small number of known MEF2C interactors have been identified in immune cells (Dong et al., 2017) highlighting a requirement to study the MEF2C interactome in other cell types such as microglia. One of these immune cell-related interactors is p38, a mitogen-activated protein kinase. In monocytes activated by LPS, increased transactivation activity of MEF2C is achieved via p38-mediated phosphorylation, suggesting that p38 activates MEF2C in response to infection in peripheral immune cells (Han et al., 1997). Additionally, it is speculated that MEF2C may interact with the microglial master regulator PU.1 as these factors work in unison to exert control (Adcock & Caramori, 2009; Martin, 1991). Furthermore, in microglia, enhancers bound by PU.1 are also enriched for MEF2 binding motifs, implying that these two factors are potential collaborative partners (Gosselin et al., 2014). However, this enrichment does not explicitly establish that these proteins interact, they may simply co-bind enhancers.

Direct exploration of the MEF2C interactome in a microglia cell model is required to understand more about how MEF2C is regulated. Investigating protein partners of MEF2C in microglia may also lead to the identification of modifiable interactors that may manipulate MEF2C activity and act as novel therapeutic targets for AD. For example, HDAC4 is known to interact with and repress MEF2C (Wang et al., 1999). Abnormal expression of HDAC4 via inhibitors or overexpression may allow for the manipulation of MEF2C transcriptional activity (Mielcarek et al., 2015).

As discussed in the General Introduction (section 1.5.1), several techniques for detecting protein-protein interactions are available. After examination of the literature and

consideration of the advantages and disadvantages of each technique, the co-IP-MS method was identified as the most appropriate technique to isolate the Mef2c protein interactome. It is a fast and reliable method that captures a large proportion of the protein interaction space in one experiment, unlike Y2H. It also does not rely on an exogenous fusion protein, as in BioID, which may affect the functionality and localisation of Mef2c. Additionally, interactions are confirmed between proteins that exist in their native state. To address the major limitations of co-IP-MS, validation experiments were also completed.

This chapter details the first interactome of Mef2c in microglia-like cells. The microglial interactome of Mef2c has been defined in a physiologically relevant system using co-IP-MS to isolate Mef2c from BV2 cells. MS data was used to identify potentially novel Mef2c-associated proteins to understand more about the regulation and function of Mef2c. For the sake of clarity, all proteins will be referred to as their unitalicized gene names throughout this chapter.

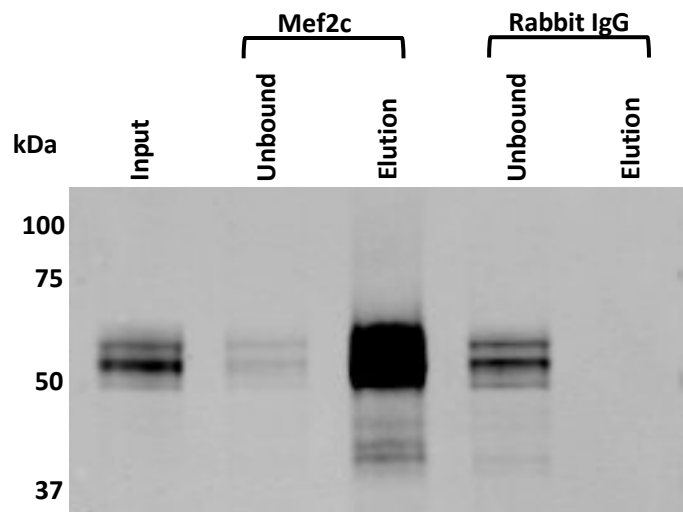
## 3.2 Results

### 3.2.1 Co-immunoprecipitation of Mef2c in BV2 cells

Co-immunoprecipitation combined with mass spectrometry (co-IP-MS) in BV2 cells was used to confirm the presence of Mef2c isoforms, identify phosphorylation sites and characterise the Mef2c interactome. Proteins were extracted from BV2 cells, and the Mef2c-interacting complex was isolated using an anti-Mef2c antibody (as described in section 2.5.2). Proteins were resolved by SDS-PAGE and detected by western blotting (Figure 3.1). This demonstrated that Mef2c can be successfully co-immunoprecipitated from BV2 cells. The co-IP protocol efficiently depleted Mef2c from the whole cell extracts (lane 2 - unbound) and the Mef2c antibody complex was enriched on the protein G Dynabeads (lane 3 - elution). Significantly, Mef2c did not immunoprecipitate with an unrelated rabbit IgG, as Mef2c was not detected in the control elution (lane 5).

### 3.2.2 MS analysis of Mef2c

Three potential Mef2c isoforms; isoforms 1 (Q3V1B5), X4 (A0A0H2UKB6) and X9 (A0A0H2UH28), were identified in BV2 cells by MS. Across all identified isoforms and all three experiment replicates a total of 29 Mef2c peptides were detected (Table 3.1). Peptides assigned to isoform 1 spanned 46% of the protein; peptides identifying isoform X4



**Figure 3.1. Mef2c co-IP.** Western blotting was used to show that the Mef2c antibody could immunoprecipitate Mef2c from BV2 cells. Whole cell extracts were incubated overnight with a Mef2c antibody crosslinked to protein G Dynabeads. The eluted Mef2c complex was resolved by SDS-PAGE and detected by western blotting (lane 3). A negative control IP with a monoclonal rabbit IgG was also performed to ensure Mef2c did not precipitate non-specifically (lane 5). Whole cell extracts were also sampled before (Input, lane 1) and after IP (unbound, lanes 2 and 4) to demonstrate the depletion of Mef2c.

**Table 3.1. Identification of Mef2c peptides in unstimulated BV2 cells.** The Mef2c peptides identified by MS for all isoforms are presented. Three Mef2c isoforms were identified; isoforms 1, X4 and X9. Peptides are grouped by the isoform(s) they identified.

Mef2c Isoform	Peptide Sequence
All	NSMSPGVTHRPPSAGNTGGLMGGDLTSGAGTSAGNGYGNPR NSPGLLVSPGNLNK LFQYASTDMDK YTEYNEPHER NTMPSVNQR VLIPPGSK
Mef2c Isoform 1 Only	KGLNGCDSPDPDADDSVGHSPESDKYR GLNGCDSPDPDADDSVGHSPESDKYR GLNGCDSPDPDADDSVGHSPESDK KINEDIDLMISR INEDIDLMISR TNSDIVETLRK
Mef2c Isoform X4 Only	ENKGSESPDPDSSYALTPR TNSDIVEALNKK TNSDIVEALNK KINEEFDNMIK INEEFDNMIK
Mef2c Isoforms 1 and X4	SPVDSLSSCSSYDGSREDHRNEFHSPIGLTRPSPDER SPVDSLSSCSSYDGSREDHR SPVDSLSSCSSYDGSDR HEAGRSPVDSLSSCSSYDGSREDHR HEAGRSPVDSLSSCSSYDGSDR EDHRNEFHSPIGLTRPSPDER NEFHSPIGLTRPSPDER NIQAKSPPPMNLGMNMR SPPPMNLGMNMR SEPVSPPR
Mef2c Isoforms 1 and X9	TNSDIVETLR
Mef2c Isoforms X4 and X9	GSESPDPDSSYALTPR

spanned 44% of the protein; and peptides identifying isoform X9 spanned 25% of the protein. No peptides were uniquely assigned to isoform X9; therefore, its identification is not of high confidence, and it is not likely to be one of the predominant isoforms expressed by BV2 cells.

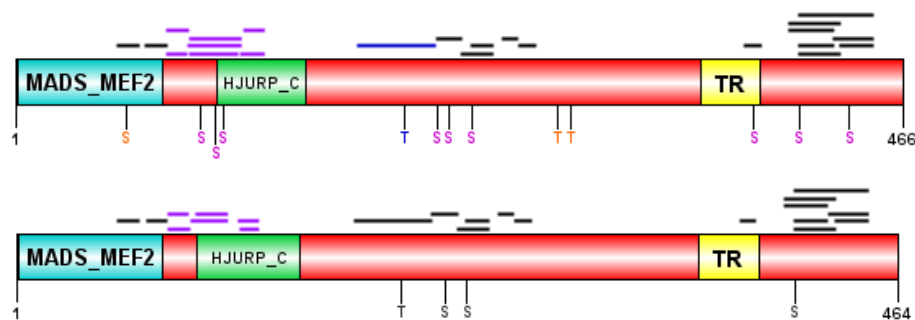
To determine which splice variants were present in the two predominant immunoprecipitated isoforms, 1 and X4, their sequences were directly compared to the splice site sequences presented in the General Introduction (Figure 1.1). Isoform 1

contained the  $\alpha 1$  exon whereas isoform X4 contained  $\alpha 2$ . Neither of the isoforms included the  $\beta$  exon, whereas both contained the  $\gamma$  exon. All isoform 1 and isoform X4 identifying peptides were aligned to the appropriate Mef2c protein sequence to visually establish their positioning (Figure 3.2).

### 3.2.3 Phosphoproteomic analysis of Mef2c

MS data also provides information regarding amino acid modifications such as phosphorylation. Phosphorylated peptides are initially identified by an approximate 80 Da mass increase (Larsen et al., 2001). Phosphorylation is an especially interesting post-translational modification to investigate because it can modulate the DNA binding activity of transcription factors either positively or negatively (Hunter & Karin, 1992). As phosphorylation data is more readily available for isoform 1 peptide information for this isoform was filtered to determine a list of phosphorylated peptides. In total, seven phosphopeptides were observed (Table 3.2). The potential phosphorylated residues in each peptide were compared to known phosphorylation sites to determine the most likely phosphorylated residue(s). One novel phosphopeptide was identified, MS nominated T205 as the likely phosphorylated residue. Additionally, three sites were previously documented in the literature but not identified by this MS data (see Figure 3.2).

The full length Mef2c isoform 1 sequence was screened for known kinase phosphorylation motifs using PhosphoMotif Finder from the Human Protein Reference Database (Table 3.3).



**Figure 3.2. Mef2c phosphorylation sites and peptides in BV2 cells.** This figure depicts the protein sequences of Mef2c isoform 1 (top) and isoform X4 (bottom). Both diagrams show the location of identified peptide sequences (black lines). Sequences unique to each isoform are depicted in purple. Phosphorylation sites identified by MS for each isoform are also shown. More is known about the phosphorylation of isoform 1, so only these sites are categorised by colour: known Serine (S), and threonine (T) phosphorylation sites (orange) and common phosphorylation sites between this MS data and previously known data (pink). The novel phosphopeptide and nominated phosphorylation site are in blue. Domains and their approximate amino acid positions (extracted from NCBI) are also indicated for both isoforms. Figures created in DOG 2.0.

**Table 3.2. Mef2c phosphopeptides identified by MS.** Mef2c isoform 1 peptides identified by co-IP-MS were filtered to obtain a list of phosphopeptides. The potentially phosphorylated residues (serine/threonine) within each peptide sequence are highlighted in blue. The most likely phosphorylated residue in each phosphopeptide is also nominated based on previous findings in the literature.

Peptide Sequence	Potential Phosphorylation Sites	Sites Identified by MS	Nominated Phosphorylation Site(s)	Evidence
KGLNGCDSPDPDA DDSVGHSPESDK YR	S98, S106, S110	S98 S106 S110	S98, S106, S110	Huttlin et al (2010)
NSPGLLVSPGNLN K	S222, S228	S222 S228	S222, S228	Huttlin et al (2010) Zhou et al (2013)
SPPPMNLGMNRR SEPVSPPR	S240 S384, S388	S240 S388	S240 S388	Huttlin et al (2010) Zhu & Gulick (2004)
SPVDSLSSCSSYD GSDR	S412, S416, S418, S419, S421, S422, S423, S427	S412 S422	S412	Lynch et al (2005)
EDHRNEFHSPIGLT RSPDER	S438, T443, S446	S438 S446	S438	Zhou et al (2013)
NMSPGVTHRPPS AGNTGGLMGGDL TSGAGTSAGNGYG NPR	S181, S183, T187, S192, T196, T205, S206, T210, S211	T205	T205	No previous evidence for phosphorylation at these sites, likely to be a novel phosphopeptide

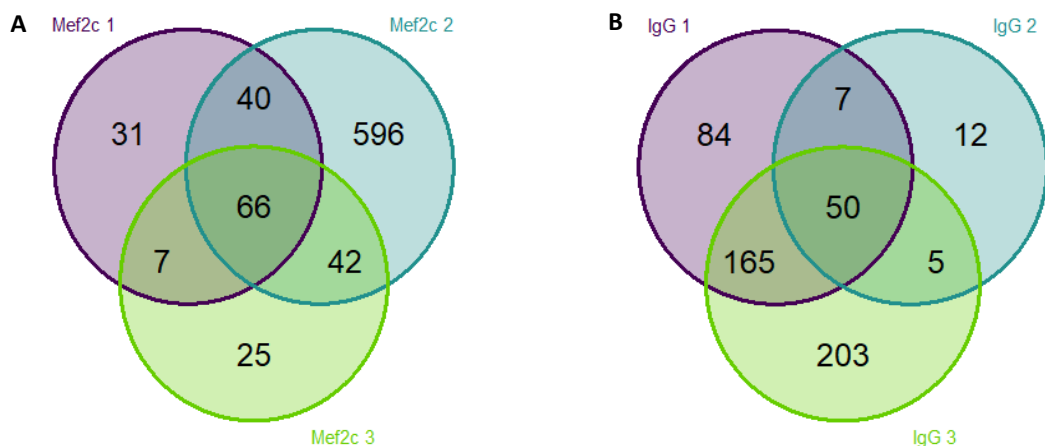
**Table 3.3. Mef2c phosphorylated residues and their predicted kinases.** The location of the nominated phosphorylated residues in the Mef2c amino acid sequence are listed. PhosphoMotif Finder was used to predict which kinases or phosphatase substrates may phosphorylate the specific residues.

Phosphorylated Residue	Predicted Phosphorylating Kinase/Phosphatase Substrate
<b>S98</b>	GSK-3, ERK1, ERK2, CDK5, b-Adrenergic Receptor
<b>S106</b>	b-Adrenergic Receptor, G protein-coupled receptor kinase 1, MAPKAPK2, GSK-3
<b>S110</b>	MAPKAPK2, GSK-3, ERK1, ERK2, CDK5, Casein Kinase II
<b>T205</b>	Casein Kinase I, G protein-coupled receptor kinase 1
<b>S222</b>	PKA, PKC, GSK-3, ERK1, ERK2, CDK5
<b>S228</b>	GSK-3, ERK1, ERK2, CDK5
<b>S240</b>	GSK-3, ERK1, ERK2, CDK5, SAPK, Growth associated histone H1
<b>S388</b>	G protein-coupled receptor kinase 1, MAPKAPK2, GSK-3, Casein Kinase I, ERK1, ERK2, CDK1, CDK2, CDK4, CDK5, CDK6, Growth associated histone H1, Cdc2
<b>S412</b>	GSK-3, ERK1, ERK2, CDK5, Growth associated histone H1, G protein-coupled receptor kinase 1, Pyruvate dehydrogenase, Casein Kinase I, Casein Kinase II, MAPKAPK2
<b>S438</b>	Casein Kinase I, GSK-3, ERK1, ERK2, CDK5

This database contains known kinase and phosphatase substrates in addition to binding motifs for kinase and phosphatases curated from published experimental data and reports the presence of putative kinases that are capable of phosphorylating a given residue within the Mef2c sequence. Predicted phosphorylation residues in the Mef2c amino acid sequence may be phosphorylated by a variety of kinases or phosphatase substrates involved in regulating a wide range of processes including cell growth, differentiation, survival and adhesion, the cell cycle, synaptic function and cytoskeleton regulation (Buscà et al., 2016; Dhavan & Tsai, 2001; Schitteck & Sinnberg, 2014).

### 3.2.4 Proteomic analysis of Mef2c binding proteins

Aside from providing important information regarding post-translational modifications, co-IP-MS can also identify physically associated proteins (interactors). Mef2c and IgG control experiments were carried out in triplicate to increase the confidence of the identified Mef2c-interacting proteins. To assess the variability between the three replicates, a hard filter using the list of IgG background proteins was applied (see section 2.6.2.1 for more detail). The Venn diagrams highlight variability between the IgG-filtered proteins present in the three separate Mef2c experiments and between the proteins identified in the IgG replicates (Figure 3.3 A, B). This highlights the requirement of multiple repeats to filter out contaminants and non-specific interactions.



**Figure 3.3. Venn diagrams depicting the overlap between biological replicates.** Three biological replicates of the Mef2c and Rabbit IgG co-IP-MS were completed. These diagrams display the number of overlapping proteins (based on accession number) between each replicate and highlight the variability between experiments. **(A) Mef2c replicates.** Prior to visualisation, a hard filter was applied to each Mef2c replicate; any proteins that were present in the IgG lists were removed from the dataset. This clearly highlights that there are 66 Mef2c-associated proteins that do not appear in the IgG control but are present in all three Mef2c experiments. **(B) Rabbit IgG replicates.** Several proteins (50) are present in all three IgG experiments, but a large amount of variability is obvious across the three replicates.



#### 3.2.4.1 SAINTexpress

SAINTexpress (see section 2.6.2.1) was used to identify 110 significant Mef2c-interactors (Table 3.4). The SAINT score output, which determines the probability that a protein is a true interactor of Mef2c, was plotted against  $\log_2$  fold change to visually represent the SAINTexpress data (Figure 3.4). Proteins are coloured by CRAPome score with proteins that are not present in the CRAPome database assigned a score of 100%. Cut offs for SAINT score ( $>0.7$ ) and fold change ( $>3$ ) were applied to the dataset and highlight a clear group of high confidence Mef2c-associated proteins. To narrow down proteins of interest, 13 high confidence interactors were identified using a CRAPome threshold score of less than 10%. Both the full list and the CRAPome filtered list were then subject to further investigation; identification of proteins of interest, gene ontology analysis (GOA) and STRING annotation.

#### 3.2.4.2 STRING

The STRING database was used to investigate known functional relationships between the identified Mef2c-associated proteins. Interactions in both the CRAPome filtered and full lists were viewed in STRING. In the high confidence list ( $n=13$ ), one distinct network was identified: MEF2/HDAC/HIRA complex. The six remaining proteins are not known to interact with the other proteins in this list (Figure 3.5). These protein sets can be identified in the STRING network of the full protein list ( $n=110$ ) (Figure 3.6). Here, these proteins have additional connections to proteins that did not surpass the CRAPome threshold. Additional identified networks include the THO complex and the spliceosome. The THO complex is required for transcription elongation and is part of the TREX complex which is involved in exporting mRNA into the cytoplasm (Chavez, 2000; Stäßer et al., 2002). The spliceosome is a large and complex macromolecular machine (Nilsen, 2003) formed of approximately 200 proteins, found primarily in the nucleus it is responsible for pre-mRNA splicing (Jurica & Moore, 2003).

#### 3.2.4.3 Known Interactors

Known interactors of Mef2c were extracted from the National Center for Biotechnology Information (NCBI) entry for Mef2c (Human Mef2c NCBI) (Table 3.5, Appendix 1). NCBI sources its interactions from other databases including the Biological General Repository for Interaction Datasets (BioGRID), the Biomolecular Interaction Network Database (BIND), and the Human Protein Reference Database (HPRD). Listed interactions are identified using techniques like the yeast two-hybrid (Y2H) system that detects direct, binary interactions.

**Table 3.4. Mef2c-associated proteins prioritised by SAINTexpress.** The Mef2c-interacting proteins depicted here were detected by MS in the unstimulated Mef2c or IgG control co-IP experiments and surpass the significance threshold  $<0.05$  BFDR. SAINTexpress, which is a statistical method for probabilistically scoring protein-protein interactions from affinity purification MS experiments, was used to statistically score the data set. The significant interacting proteins have also been ranked based on their CRAPome percentage. This allows for easier identification of interacting proteins of high confidence and therefore, of interest. *Title annotations: MW (kDa): molecular weight. Total Score (Sequest HT): total protein score calculated by the summation of the individual scores of each peptide, higher scores reflect better identification. Spec: spectral counts for the bait-prey pair. ctrlCounts: spectral counts in the negative controls. SaintScore: main probability score. FoldChange: average spectral count in test interaction divided by the average in controls, zero counts are replaced by 0.1. BFDR: Bayesian false discovery rate.*

#	Accession Number	Gene Name	MW (kDa)	Total Score (Sequest HT)	Spec	ctrlCounts	SaintScore	FoldChange	BFDR	CRAPome Score (%)
1	B9EKC5	Cabin1	243.1	59.67	23 43 3	0 0 0	1	230	0	0.14
2	Q8VI94	Oasl1	59.1	4.84	2 4 2	0 0 0	0.98	26.67	0	1.12
4	A0A087WQ92	Hdac4 Iso2	34.3	13.1	6 7 6	0 0 0	1	63.33	0	1.96
3	Q60929	Mef2a	53.5	31.43	17 12 14	0 0 0	1	143.33	0	1.96
5	Q6NZM9	Hdac4	118.5	40.6	28 31 26	0 0 0	1	283.33	0	1.96
6	Q61666	Hira	111.7	55.24	36 28 12	0 0 0	1	253.33	0	2.37
7	A0A0H2UH28	Mef2c IsoX9	52.3	19.07	2 4 10	0 0 0	0.99	53.33	0	2.51
8	A0A0H2UKB6	Mef2c IsoX4	50.3	151.31	79 85 78	0 0 0	1	806.67	0	2.51
9	Q3V1B5	Mef2c	50.4	184.48	88 96 69	0 0 0	1	843.33	0	2.51
10	Q80WC1	Ubn2	141.7	36.03	12 26 2	0 0 0	0.99	133.33	0	2.51
11	E9Q5K9	Ythdc1	85.6	5.17	4 6 5	0 0 0	1	50	0	5.87
12	Q91W39	Ncoa5	65.3	199.92	88 85 67	3 0 13	1	15	0	6.15
13	B7ZDF5	Hdac5	121.9	35.84	22 28 26	0 0 0	1	253.33	0	7.68
14	A0A0R4J0J6	Thoc5	78.7	18.42	6 12 5	0 0 0	1	76.67	0	7.82
15	G3UWQ7	Prc1	72	14.04	8 10 2	0 0 0	0.99	66.67	0	9.64

Chapter 3 Investigating the protein interactome of Mef2c in unstimulated BV2 cells

16	Q3TFQ8	Pygb	96.6	10.43	5 5 9	0 0 0	1	63.33	0	9.92
17	Q8R3N6	Thoc1	75.4	15.39	14 12 5	0 0 0	1	103.33	0	10.61
18	E0CYH0	Wtap	44.2	8.41	2 5 4	0 0 0	0.99	36.67	0	10.75
19	Q5U4D9	Thoc6	37.3	10.23	5 6 4	0 0 0	1	50	0	11.03
20	Q8CH25	Sltm	116.9	15.31	5 11 7	0 0 0	1	76.67	0	11.45
21	A0A023T778	Magohb	17.3	25.26	7 9 3	0 0 0	1	63.33	0	11.59
22	Q8BP60	Nxf1	70.3	21.46	13 7 6	0 0 0	1	86.67	0	15.50
23	E9QP00	Tra2a	32.6	8.94	5 8 3	0 0 0	1	53.33	0	16.20
24	Q64012	Raly	33.2	22.05	4 12 7	0 0 0	1	76.67	0	16.20
25	Q3UYV9	Ncbp1	91.9	7.56	6 8 6	0 0 0	1	66.67	0	17.32
26	Q9Z1A1	Tfg	43	35.87	17 13 18	0 0 0	1	160	0	17.60
27	Q0VBL3	Rbm15	105.7	22.96	12 4 14	0 0 0	1	100	0	17.74
28	Q00PI9	Hnrnpul2	84.9	7.68	3 4 11	0 0 0	1	60	0	18.85
29	A0A2R8VK76	Cpsf1	161.7	11.84	2 12 15	0 0 0	0.99	96.67	0	19.41
30	Q3UYX6	Srsf10	33.1	20.56	8 6 4	0 0 0	1	60	0	20.95
31	Q6PE01	Snrnp40	39.3	23.25	3 13 2	0 0 0	0.99	60	0	20.95
32	A0A0N4SV80	Zfp638	214.3	18.65	12 19 20	0 0 0	1	170	0	21.23
33	D3YWX2	Ylpm1	240.9	83.99	45 56 50	0 0 0	1	503.33	0	22.63
34	P62996	Tra2b	33.6	26.93	14 15 5	0 0 2	0.98	17	0	22.77
35	Q3TUQ5	Pnn	82.5	15.73	2 10 7	0 0 0	0.99	63.33	0	23.18
36	A0A1S6GWJ4	Ddx41	71.1	23.04	3 11 3	0 0 0	1	56.67	0	23.88
37	Q99MR6	Srrt	100.4	10.57	4 11 10	0 0 0	1	83.33	0	23.88
38	Q80YR5	Safb2	111.8	62.96	37 39 37	0 0 0	1	376.67	0	25.84

Chapter 3 Investigating the protein interactome of Mef2c in unstimulated BV2 cells

39	A0A0B4J1E2	Snw1	61.4	9.88	3 5 3	0 0 0	1	36.67	0	26.68
40	Q62189	Snrpa	31.8	25.03	5 12 6	2 0 4	0.67	3.83	0.04	27.09
41	G3UY42	Pabpn1	34	11.93	3 7 5	0 0 0	1	50	0	28.77
42	Q9JIX9	Acin1	150.6	34.39	7 16 13	0 0 0	1	120	0	28.77
43	S4R1M2	Safb	105.3	34.6	18 15 18	0 0 0	1	170	0	28.77
44	Q6A068	Cdc5l	92.1	5.49	3 3 5	0 0 0	1	36.67	0	29.19
45	H9KV00	Son	268.7	5.49	3 7 2	0 0 0	0.99	40	0	30.59
46	B1AZI6	Thoc2	182.7	34.62	5 30 8	0 0 0	1	143.33	0	31.01
47	A1A4A7	Pgam5	32.3	16.08	6 12 3	0 0 0	1	70	0	31.15
48	Q9D554	Sf3a3	58.8	14.27	3 8 7	0 0 0	1	60	0	31.98
49	P26369	U2af2	53.5	62.91	3 27 13	0 0 3	0.88	14.33	0.01	32.26
50	Q52KI8	Srrm1	106.8	0	2 5 2	0 0 0	0.98	30	0	33.52
51	Q8VDM6	Hnrnpul1	95.9	11.73	4 2 9	0 0 2	0.83	7.5	0.03	35.47
52	Q99KP6	Prpf19	55.2	31.61	9 20 10	0 0 2	1	19.5	0	36.59
53	Q3UIJ2	Eif2s3x	51.1	23.8	4 16 6	2 0 2	0.88	6.5	0.01	37.71
54	H7BX95	Srsf1	28.3	36.44	10 22 10	0 0 5	0.95	8.4	0	39.11
55	Q9CQF3	Nudt21	26.2	17.58	7 12 3	0 0 3	0.86	7.33	0.02	41.20
56	H3BJW3	Cpsf6	63.4	16.77	6 9 2	0 0 2	0.86	8.5	0.02	41.76
57	Q5SUS9	Ewsr1	69	6.57	3 3 2	0 0 0	0.99	26.67	0	42.04
58	P63163	Snrpn	24.6	19.2	5 11 5	0 0 4	0.85	5.25	0.02	43.02
59	Q3UXI9	Ilf2	43	21.17	5 11 5	0 0 2	0.96	10.5	0	43.72
60	P57784	Snrpa1	28.3	21.35	5 12 5	0 0 2	0.96	11	0	43.85
61	Q3UA14	Sf3b2	98.1	28.66	7 20 17	0 0 0	1	146.67	0	44.27

Chapter 3 Investigating the protein interactome of Mef2c in unstimulated BV2 cells

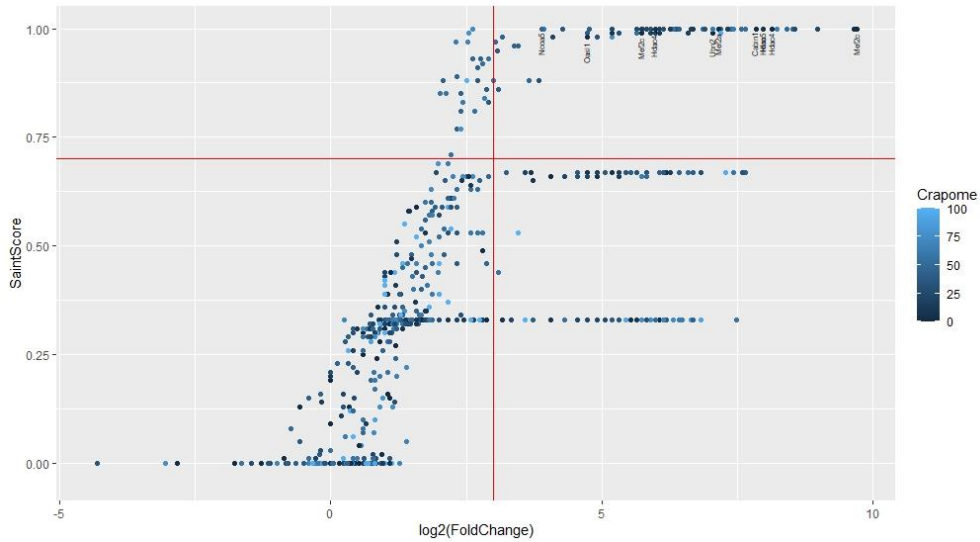
62	K3W4R2	Myh14	228.4	68.13	34 11 14	0 0 9	0.91	6.56	0.01	44.41
63	B2RSV4	Sf3b3	135.5	83.24	11 47 24	3 0 0	1	27.33	0	44.97
64	P70372	Elavl1	36.1	33.93	5 18 3	0 0 0	1	86.67	0	44.97
65	Q3UI57	Mcm3	91.5	3.91	2 5 3	2 0 0	0.77	5	0.03	44.97
66	P62141	Ppp1cb	37.2	26.99	12 15 7	0 0 5	0.93	6.8	0.01	45.11
67	Q8BTI8	Srrm2	294.7	28.48	4 18 21	0 0 0	1	143.33	0	45.25
68	P62137	Ppp1ca	37.5	29.16	13 15 10	3 0 6	0.88	4.22	0.01	45.39
69	Q3TWW8	Srsf6	39	15.49	6 10 8	0 0 0	1	80	0	45.53
70	Q91VR5	Ddx1	82.4	36.35	20 13 21	6 0 0	0.98	9	0	46.23
71	H3BL37	Tcof1	138.5	21.9	3 14 2	0 0 0	0.99	63.33	0	46.37
72	Q6P4T2	Snrnp200	244.4	95.15	17 62 29	0 0 2	1	54	0	46.51
73	Q8BK67	Rcc2	55.9	26.9	7 22 8	3 0 3	0.93	6.17	0.01	46.93
74	Q99PV0	Prpf8	273.4	84.03	20 65 26	0 0 0	1	370	0	47.35
75	P62317	Snrpd2	13.5	16.41	4 12 5	0 0 4	0.81	5.25	0.03	47.49
76	Q3THB0	Eif4b	68.8	12.17	8 8 4	2 0 2	0.89	5	0.01	48.04
77	Q60749	Khdrbs1	48.3	79.9	41 47 31	3 0 5	1	14.88	0	48.60
78	Q14C24	U2af1	27.8	42.36	3 23 12	0 0 3	0.88	12.67	0.02	49.02
79	AOA2I3BRL8	Rbmxl1	42.2	46.61	20 33 21	0 0 9	0.97	8.22	0	49.72
80	G5E866	Sf3b1	145.7	106.17	15 59 28	0 0 0	1	340	0	50.42
81	Q6PHQ9	Pabpc4	72.2	51.3	20 24 16	0 0 0	1	200	0	52.51
82	P62320	Snrpd3	13.9	14.13	4 6 4	0 0 2	0.92	7	0.01	52.65
83	Q3U1C2	Ruvbl1	50.2	14.32	5 8 2	0 0 0	0.99	50	0	52.79
84	AOA1L1STE4	Ilf3	97.4	27.94	12 12 20	0 0 0	1	146.67	0	52.93

Chapter 3 Investigating the protein interactome of Mef2c in unstimulated BV2 cells

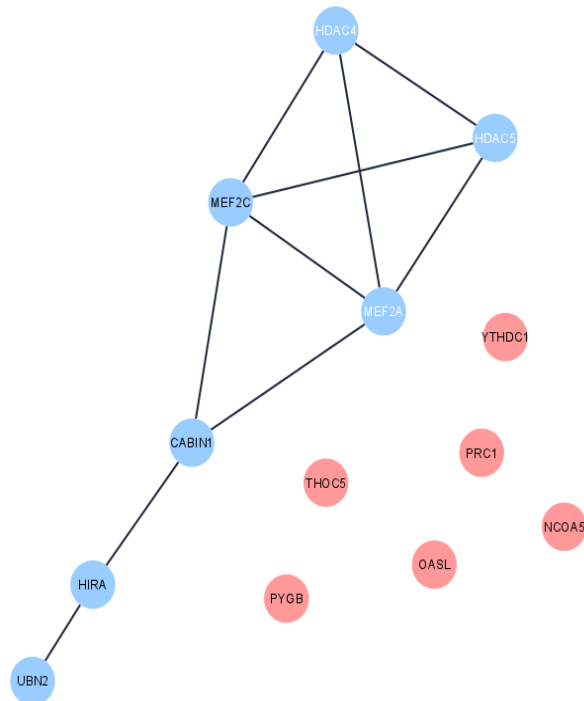
85	Q6A0E3	Eftud2	109.7	28.25	14 27 16	0 0 0	1	190	0	53.21
86	Q569Z6	Thrap3	108.1	13.33	7 11 17	0 0 0	1	116.67	0	53.35
87	Q6ZWN5	Rps9	22.6	16.34	4 12 3	0 0 3	0.81	6.33	0.03	54.19
88	Q8K019	Bclaf1	105.9	15.43	11 18 20	0 0 0	1	163.33	0	54.47
89	P84104	Srsf3	19.3	26.81	13 15 4	0 0 4	0.88	8	0.02	54.75
90	P35979	Rpl12	17.8	19.7	4 8 2	0 0 3	0.71	4.67	0.04	55.45
91	Q3T9L0	DdX49	49.1	21.4	8 16 6	0 0 4	0.93	7.5	0.01	56.42
92	P29341	Pabpc1	70.6	80.81	54 43 34	13 0 17	0.85	4.37	0.02	56.98
93	Q91VC3	Eif4a3	46.8	69.24	19 33 25	5 3 11	0.85	4.05	0.02	58.38
94	Q3U8W9	Hnrnpr	70.8	11.54	3 17 4	0 0 0	1	80	0	58.94
95	O35286	Dhx15	90.9	51.18	18 33 25	2 0 3	1	15.2	0	60.34
96	Q6ZQ61	Matr3	95.2	12.15	16 10 14	0 0 0	1	133.33	0	61.59
97	Q3U6P5	Hnrnpc	36.9	46.63	11 24 8	2 0 6	0.83	5.38	0.03	62.01
98	Q3UZG3	Hnrnpa3	39.7	70.12	18 35 16	4 2 8	0.97	4.93	0	62.43
99	Q7TMK9	Syncrip	69.6	48.63	6 30 7	3 0 3	0.84	7.17	0.02	64.11
100	G5E924	Hnrnpl	66.9	44.35	8 29 15	0 0 0	1	173.33	0	64.25
101	Q5BLK1	Rps6	28.7	14.96	4 11 3	0 0 4	0.69	4.5	0.04	65.08
102	E9QNN1	Dhx9	149.6	70.47	19 42 29	0 0 0	1	300	0	65.64
103	Q3TQX5	DdX4x	73.1	152.25	66 49 34	12 0 14	0.97	5.73	0	69.55
104	Q9Z2X1	Hnrnpf	45.7	62.4	15 27 19	2 2 6	1	6.1	0	73.74
105	Q3UK83	Hnrnpa1	38.8	66.67	12 35 11	4 0 7	0.77	5.27	0.03	77.09
106	Q3U536	Npm1	32.5	9	2 7 2	0 0 0	0.98	36.67	0	77.37
107	Q8C2Q7	Hnrnph1	51.2	59.28	17 29 18	2 2 7	0.99	5.82	0	77.93

Chapter 3 Investigating the protein interactome of Mef2c in unstimulated BV2 cells

<b>108</b>	Q3TVV6	Hnrnpu	87.9	67.95	26 43 29	16 0 9	0.69	3.92	0.04	80.73
<b>109</b>	A0A0A0MQA5	Tuba4a	52.9	53.26	18 24 2	0 0 0	0.99	146.67	0	94.83
<b>110</b>	Q9CQE8	RTRAF	28.1	10.3	6 7 4	0 0 3	0.88	5.67	0.01	N/A

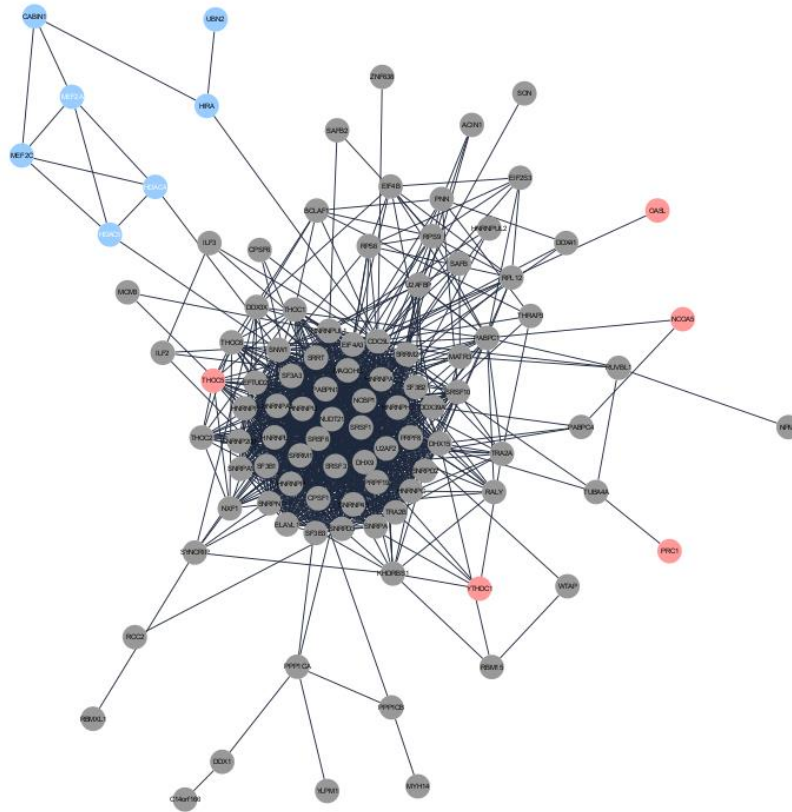


**Figure 3.4. Fold change and SAINT score output from SAINTexpress.** Visualisation of output from SAINTexpress on proteins identified by MS. Log<sub>2</sub> fold change is plotted against SAINT score, the probability that a protein is an interactor of Mef2c. The red lines represent cut offs set at  $\geq 0.7$  for SAINT score and  $\geq 3$  for fold change. This leaves a clear group of high confidence interacting proteins in the top right corner. These proteins include Hdac4, Hdac5, Oasl1, Mef2a, Cabin1, Ubn2, Hira, and Ncoa5. Proteins are coloured according to their CRAPome score (%). Proteins not in the CRAPome database are assigned a score of 100%.



**Figure 3.5. Protein-protein interaction network of high confidence Mef2c-associated proteins.** Interactions between high confidence Mef2c-associated proteins extracted from the STRING v11.5 database. One distinct network has been identified (blue). Proteins with no known interactions with the other proteins are shown in pink. Known Mef2c interacting proteins are represented by white writing. All interactors are shown.





**Figure 3.6. Protein-protein interaction network of Mef2c-associated proteins.** Interactions between all Mef2c-associated proteins extracted from the STRING v11.5 database. The colour categorisation from the high confidence STRING diagram has been carried over to this interactome. Known Mef2c interacting proteins are represented by white writing. Only interactors that are connected within a network are shown.

Most known interacting proteins are primarily found in cardiac and skeletal muscle cells rather than immune cells. Exploring these interactions in a more physiologically relevant system, to determine if these interactions also occur in immune cells, will further understanding of how Mef2c is regulated and how it functions in microglia cells. Currently, no Mef2c co-IP-MS studies have been completed in a microglia cell line highlighting the novelty of this work.

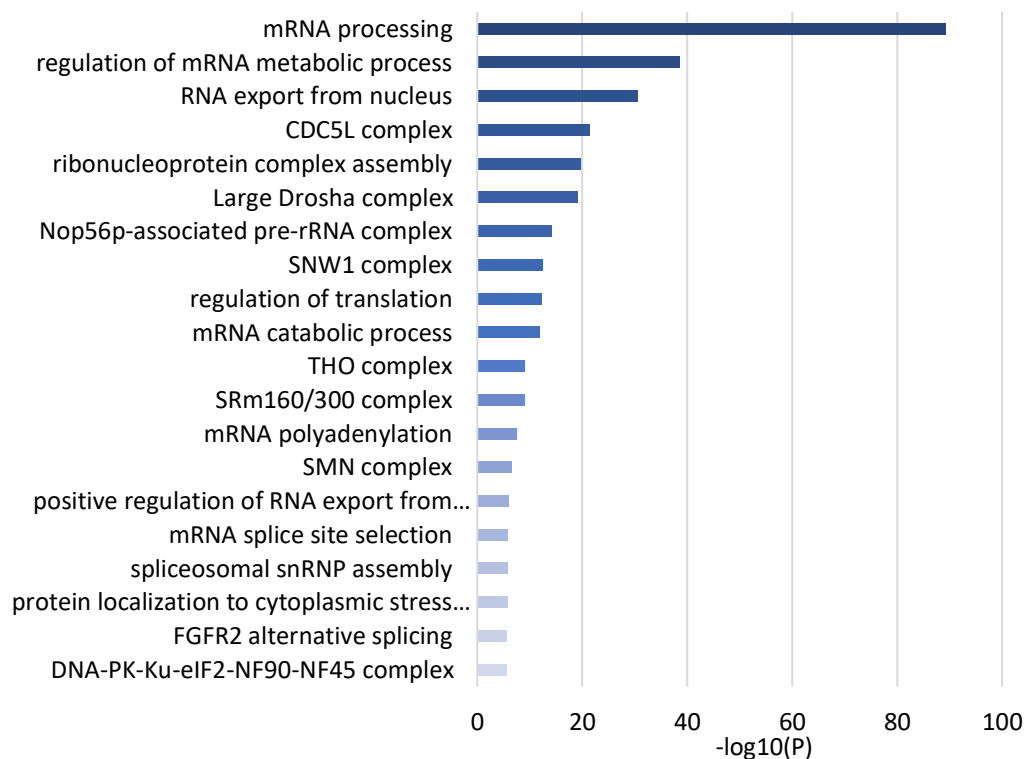
All 110 identified Mef2c interacting proteins were compared to the list of known interactors. Among the identified Mef2c interacting proteins were several previously characterised interactors; two members of the histone deacetylase family HDAC4 and HDAC5 and another member of the MEF2 family MEF2A. HDACs -4 and -5 are class II HDACs that interact with the MADS domains of all MEF2 family members, they act as transcriptional repressors (McKinsey et al., 2002; Miska et al., 1999). The identification of known interactors in this current dataset increases the confidence of the other novel interacting proteins.

**Table 3.5. Known MEF2C interactors.** Known interactors of human MEF2C downloaded from the National Center for Biotechnology Information (NCBI), that have also been identified in the current dataset (additional interactors listed in Appendix 1). Descriptions of each interactor have been extracted from their corresponding NCBI entry.

Interactor	Description	Source	Experimental Evidence	Cell/Tissue Type	Publication
<b>HDAC4</b>	Class II member of histone deacetylase family. Possesses histone deacetylase activity and represses transcription when tethered to a promoter.	BioGRID HPRD	Affinity Capture-Western; Reconstituted Complex; Y2H	C2.7 myoblasts, HEK293T, COS fibroblasts, Yeast, C2C7 myoblasts, C2C12 myoblasts	Backs et al (2008); Borghi et al (2001); Chan et al (2003); Dressel et al (2001); Micheli et al (2005); Miska et al (2001); Wang & Yang (2001); Wang et al (1999); Wang et al (2005)
<b>HDAC5</b>	Class II member of histone deacetylase family. Possesses histone deacetylase activity and represses transcription when tethered to a promoter.	BioGRID HPRD	Reconstituted Complex	Yeast, HEK293T	Dressel et al (2001); Lu et al (2000a)
<b>MEF2A</b>	Member of the MADS box transcription enhancer factor 2 (MEF2) family of proteins, which play a role in myogenesis.	BioGRID	Affinity Capture-MS	HEK293T (stable OE)	Li et al (2015)
<b>MEF2C</b>	Member of the MADS box transcription enhancer factor 2 (MEF2) family of proteins, which play a role in myogenesis.	BioGRID HPRD	Reconstituted Complex	C2C12 myoblasts, C3H-10T1/2 fibroblasts, COS7 fibroblasts	Janson et al (2001); Lazaro et al (2002)

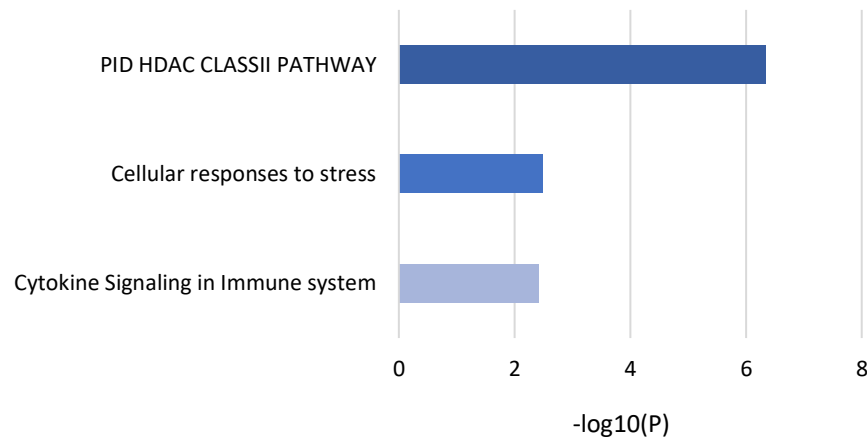
## 3.2.5 Functional annotation of Mef2c interactors

All identified Mef2c-interacting proteins (n=110) were annotated using Metascape's gene ontology enrichment analysis. This tool looks at what gene ontology terms are over-represented within a gene set to determine what biological processes they are involved in (Zhou et al., 2019). Several, primarily nuclear, biological processes were identified for the full list of proteins with the top four processes including mRNA processing, regulation of mRNA metabolic process, RNA export from the nucleus and the CDC5L complex (Figure 3.7). The high confidence list (n=13) was also functionally annotated (Figure 3.8). Three main processes were identified: HDAC Class II pathway; cellular response to stress; and cytokine signalling in the immune system. The identified biological processes do differ between the two lists most interestingly with the addition of cytokine signalling in the immune system: a cell-type specific process highlighting the importance of studying interactions in specific cell lines.



**Figure 3.7. Biological process annotations for Mef2c-associated proteins identified by MS.**

Metascape's enrichment analysis was used to determine which biological processes are enriched in the full list of Mef2c-interactors. The data are presented in a heatmap, coloured by p-value, of enriched terms linked to the two lists of proteins. The  $-\log_{10}(P)$  score of each process is graphed whereby larger values indicate a more significant association.



**Figure 3.8. Biological process annotations for high confidence Mef2c-associated proteins identified by MS.**

Metascape's enrichment analysis was used to determine which biological processes are enriched in the high confidence list of Mef2c-interactors. The data are presented in a heatmap, coloured by p-value, of enriched terms linked to the two lists of proteins. The  $-\log_{10}(P)$  score of each process is graphed whereby larger values indicate a more significant association.

The data analyses described in this section highlight a number of interesting Mef2c-interacting proteins to investigate. Several proteins identified in the HIRA complex, also known as the histone chaperone complex, are histone cell cycle regulator (Hira), calcineurin binding protein 1 (Cabin1) and ubinuclein 2 (Ubn2). HIRA has been previously shown to interact with other MEF2 family members but not directly with MEF2C. Cabin1, which has also been previously linked to other MEF2 members but not MEF2C, is known to suppress MEF2/HIRA-mediated transcription (Yang et al., 2011). The association with Hira and Cabin1, along with the identification of the transcriptional repressors Hdac4 and Hdac5, suggests that Mef2c is being held in a partially repressed state. Another known member of the HIRA complex that was immunoprecipitated alongside Mef2c is Ubn2 which is primarily responsible for specific recognition and direct binding of H3.3, a canonical histone variant whose distribution by the complex is vital during development (Xiong et al., 2018).

2'-5'-oligoadenylate synthetase-like 1 (Oasl1) was identified as a high confidence interactor with a CRAPome score of 1.7%. It is an interesting protein to investigate further as no previous associations between Oasl1 and Mef2 family members have been reported in the literature. Oasl1 is an important immune gene; it can enhance innate immunity (Zhu et al., 2015a). Oasl1 also inhibits the translation of another immune response-related transcription factor IRF7 (Lee et al., 2013). Thus, Oasl1 may be a regulator of Mef2c,

involved in Mef2c-regulated microglia function and an interesting protein to investigate further.

Another protein of interest marked for further investigation is nuclear receptor coactivator 5 (Ncoa5). Ncoa5 has a CRAPome score of 6.15% making it a high confidence interactor. Ncoa5 is a transcriptional coregulator which has both coactivator and corepressor functions (Sauvé et al., 2001). No previous associations between Ncoa5 and any members of the Mef2 family have been reported. The peptide data for these proteins of interest, along with Hdac4 and Hdac5 are provided in Table 3.6.

**Table 3.6. MS data for the Mef2c-associated proteins Ncoa5, Oasl1, Cabin1, Hira, Ubn2, Hdac4 and Hdac5.** The table shows the peptide sequences of the Hira complex members Cabin1, Hira and Ubn2, the novel protein interactors Ncoa5 and Oasl1 and the known interactors Hdac4 and Hdac5. Peptide sequences identified by MS are presented for each interactor together with the peptide count and percentage coverage values generated from each biological replicate.

Protein of Interest	Peptide Sequences	Mass Spectrometry Data
<p><b>Ncoa5</b></p> <p>579 amino acids 65.3 kDa</p> <p>CRAPome Score: 6.15%</p>	<p>SSADSLPGPISR GGHPPAIQSLINLLADNR QPLGAASGSSLK SQPSSQPLQSGQVLP SATPTPAAPPTSQQELQAK LAPASTMASQRPV SSTGINFDNPSVQK GGSPFAIVITQQHQIHR ALDTLIQSGPALSHLVSQTAAQVGRPQAPMGSYQR NMGPRPGAPSQGLFGQPSSR YLTAETDKIINYLR FDAERPVDCSVIVV NK RFDAERPVDCSVIVV NK LLRSSADSLPGPISR SCTVNIMFGTPQEHR MANDAILQER RDPYSGDSR DLGMVVDLIFLNTEVSL SQALEDVSR NMPQADAMVVLVAR RYFEEIQR YLTAETDK DYAESVGR DDSYFDR DPYSGDSR GPPGPESQSR KDDSYFDR YFEEIQR VDDYCR DHRDPVYDR RKDDSYFDR</p>	<p><b>MEF2C 1</b> Coverage: 55% Peptide Count: 45</p> <p><b>MEF2C 2</b> Coverage: 51% Peptide Count: 43</p> <p><b>MEF2C 3</b> Coverage: 49% Peptide Count: 33</p>

<p><b>Oasl1</b></p> <p>511 amino acids 59kDa</p> <p>CRAPome Score: 1.7%</p>	<p>GQRPIILDPADPTNNVAEGYR ISFQEPGGER ALGPSCPSSEVYANLIK VGCFGNGTVLR IQLSQGYLGLQR</p>	<p><b>MEF2C 1</b> Coverage: 6% Peptide Count: 2</p> <p><b>MEF2C 2</b> Coverage: 12% Peptide Count: 4</p> <p><b>MEF2C 3</b> Coverage: 6% Peptide Count: 2</p>
<p><b>Cabin1</b></p> <p>2187 amino acids 243kDa</p> <p>CRAPome Score: 0.24%</p>	<p>HAFEEGLR IAALNASSTIEDDHEGSFK LSGLSAQAGPSGK QQQPPTVYLLHYR KLDPEEEDDPFNNEYVQAEAK TSTVSADLANLLK EAQEAEAFALYHK AYHELLEAR RGDSLGEVAFPPQGLPAGAEER QAGHYLHEEAAR SWCCNSDGALLR VDFQGLLVK LAFLYTYSK GKTEESLESTEAFR QVDEETALEQAVK ASPEDGQESPQHPK LPNLHNDVSVSLEEIDK TLLLDAYR FYVQVLQK SAILSAQSAANVR AVVHLLRPTLCTSGFDR DKESPQVGPTEPMDTSEAAGR KLPLADGSGPGPEPGGR QQPAPLAPSPAAPTTTAAPTMAAR MGPLNQLPVVTDIR VLEDTLSELAEGSEHPGSK HSTSLPNLLR GMAYDLSR NCPAGVVTGR LEFSNVGPHR LSFDSATFMESEK HATPVLNCFR TLPEFDSYK LVQPIPFFTWK FDSWAGMALAR VVEQSVQKPVADSSASAYIPSKPPASTPPLWDGK IPVDEIDRPGSFAWHMNR LFEAGDYK FCQVHLGAATQR</p>	<p><b>MEF2C 1</b> Coverage: 11% Peptide Count: 22</p> <p><b>MEF2C 2</b> Coverage: 23% Peptide Count: 40</p> <p><b>MEF2C 3</b> Coverage: 2% Peptide Count: 3</p>

	TNFFNGIWR IFEEQPCLR	
<b>Hira</b>  1015 amino acids 112kDa  CRAPome Score: 1.22%	LFTECQEQLDILR ELLPVIGQNLK YLVNEGFEYR RPLVVIHELFDK TLDWQLETSITKPFDECGGTHVLR ETSSASSVTGVVNGESLEDIRK KLELEVETVEK ATYIGPSTVFGSSGK ATPGAPSLTSVIPTAVER QDSLALQCADFR LLPMSLSVQSPAALSTEK HWLLLYAR LANVEQWR LPIPGPQR FPEILATLR GLTWDPVGK TNMDFVGHR SLSVWLTCLK LSWSPDGHYLVSAHAMNNSGPTAQIER LIMVWK DSMNATSTPAASSPSVLTPSK LLKPTWVNHNGKPIFSVDIHPDGTK SLAIMTEAQLSTAVIENPEMLK DLLGPVHCSTGSQWESTVVGLR VLTAAGSCDVVCVACEK VVIWNMSPVLQEDDEKDENIPK EAMCLSAPALAK	<b>MEF2C 1</b> Coverage: 33% Peptide Count: 29  <b>MEF2C 2</b> Coverage: 21% Peptide Count: 27  <b>MEF2C 3</b> Coverage: 15% Peptide Count: 12
<b>Ubn2</b>  1314 amino acids 142kDa  CRAPome Score: 0.73%	LVHTEDPFTDEHKER EPPRPEPPPPPLPLQTPPPR YGGFYINTGTLQFR LLQQGLQR VSLEPLPAR LPLATPK LPLSTSPGNGSQGPHPLVSR QLGVVALNSHK IKEDDIEVK KLHLNVQDDR KPQDLAHTGISSGLIAGSSIQNP RVAFISLSPVR LHLNVQDDR KLDSTQTAHSSSLIAGHTGPVPK SPFSMAASPK QSPTLNLLPSNR	<b>MEF2C 1</b> Coverage: 11% Peptide Count: 12  <b>MEF2C 2</b> Coverage: 21% Peptide Count: 21  <b>MEF2C 3</b> Coverage: 2% Peptide Count: 2

	<p>           VAFISLSPVR            LFDEEGR            TLLCNLVEIK            LGCYELEPNK            SLQPGAQHAAALPHSPLPAHLQQAFNDGGQSK            QEVEMLAK            VVPTLPEGLPVLLEK            VHQSAAVQQNYVSPLOATISK         </p>	
<p> <b>Hdac4</b>            1076 amino acids            119kDa            CRAPome Score: 0%         </p>	<p>           LQEFVLNK            LSSTVGHSLIEAQK            EGSVAPLPLYTSPSLPNITLGLPATGPAAGAAGQQD            AER            LDHQFSLPLEPALR            EQQLQQELLALK            ATLEELQTVHSEAHTLLYGTNPLNR            VNHMPSTVDVATALPLQVAPTAVPMDLR            LPCGGVGVSDTIWNEVHSSGAAR            DQPVELLNPAR            EHQALLDEPYLDR            QQFQQQLHLSK            QILIAEFQR            ETEPGQRPATEQELLFR            DGPVATALK            LALPALQQR            FTTGLVYDTLMLK            MSSQSHPDGLSGR            EPSLAGVQVK            IISKPSEPPR            TQSAPLPQNAQALQHLVIQQHQHFLEK            ILFPGTHLTPYLSTSPLE            NYQASMEAAGIPVSGSHRPLSR            AQSSPASATFPMSVQEPPTKPR            IISKPSEPPRQPESHPEETEEELREHQALLDEPYLDR            LPGQKEPSLAGVQVK            QEPIESEEEEEAEATR            QKLDSSLTSVFVR            QQALLLEQQR            LQETGLR         </p>	<p> <b>MEF2C 1</b>            Coverage: 30%            Peptide Count: 26         </p> <p> <b>MEF2C 2</b>            Coverage: 36%            Peptide Count: 29         </p> <p> <b>MEF2C 3</b>            Coverage: 20%            Peptide Count: 26         </p>
<p> <b>Hdac5</b>            1113 amino acids            121kDa            CRAPome Score:            2.43%         </p>	<p>           TPLHSIPVAVEVKPVLPGAMPSSMGGGGGGSPSPV            ELR            QPTTHPEETEEELTEQQEALLGEGALTIPR            QQSTLIAVPLHGQSPLVTGER            ESAIASTEVK            QALQSLR            EQQLQQELLVLK            LEQQLLILR            LLGPISQK            EPSLEILPR            ATLDEIQT VHSEYHTLLYGTSPLE            LFADAQQQLQPLQVYQAPLSLATVPHQALGR         </p>	<p> <b>MEF2C 1</b>            Coverage: 24%            Peptide Count: 21         </p> <p> <b>MEF2C 2</b>            Coverage: 20%            Peptide Count: 26         </p> <p> <b>MEF2C 3</b>            Coverage: 18%            Peptide Count: 26         </p>



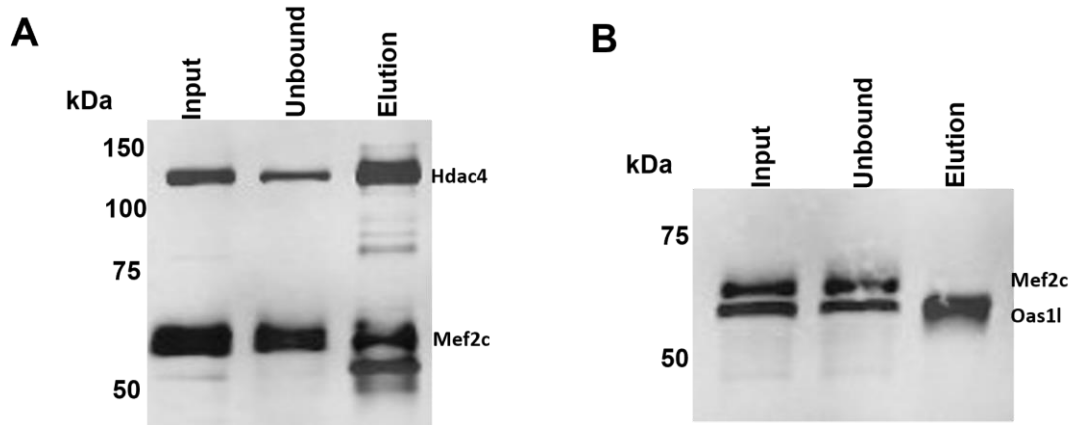
GALAGPMDPALR
TQSSPLPQSPQALQQLVMQQQHQQFLEK
SKEPTPGGLNHSLPQHPK
QLLFAEFQK
VIEIQSK
MAVGCLVELAFK
KATLDEIQT VHSEYHTLLYGT SPLNR
SPTDQPTVVK
QRLEQQLLILR
KLLGPISQK
FAAGLGCSLR
LQEFLLSK
LPLLG PYDSR
DGTVISTFK

### 3.2.6 Validating putative interactors of Mef2c

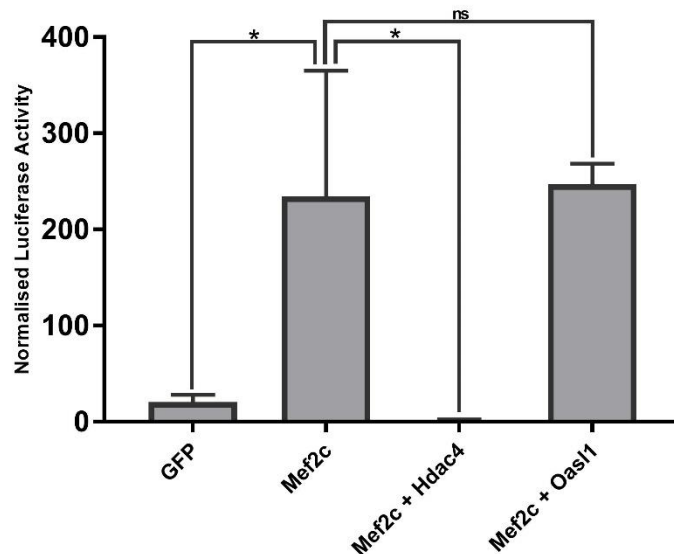
The main limitation with co-IP-MS experiments is that the detected interactors may not necessarily directly interact with the protein of interest, they may indirectly interact via another protein. The majority of interactors are likely to be tertiary, only a few proteins will directly interact with Mef2c. Additionally, some identified proteins may have cross-reacted with the antibody and thus not be true interactors. Therefore, prior to any further analysis, putative interactors of Mef2c must be validated. To do this, HEK293T cells were co-transfected with Mef2c and the interactors of interest which had been previously synthesised with an N-terminal flag tag (sections 2.1 and 2.2). A flag co-IP (section 3.5.6) was used to pull down the interactors and potentially Mef2c if a direct interaction exists between the proteins. The direct interaction between Hdac4 and Mef2c was successfully validated, HA-tagged Mef2c was pulled down alongside flag-tagged Hdac4 (Figure 3.9 A). However, Mef2c-HA was not eluted alongside flag-tagged Oasl1 suggesting that these two proteins do not directly interact (Figure 3.9 B).

To test the functional consequences of the Hdac4/Mef2c interaction a reporter assay system was used in which the transcriptional activity of a Mef2c TRE reporter gene was measured (Figure 3.10). Mef2c was overexpressed individually and in conjunction with Hdac4 or Oasl1 and a one-way analysis of variance (ANOVA) was used to test significance. A significant difference in Mef2c TRE binding was observed between conditions [F (3, 8) =12.02, p=0.0025]. Tukey's multiple comparisons test revealed that overexpressing Mef2c alone (M= 234.3, SD= 130.8) significantly increased TRE binding and subsequent reporter gene expression in comparison to the GFP only control (M= 20.5, SD= 7.7, p=0.0179). However, overexpressing both Mef2c and Hdac4 (M= 1.8, SD= 0.6) together resulted in a

reduction in luciferase activity compared to the overexpression of Mef2c alone ( $p=0.0113$ ). The overexpression of Oasl1 alongside Mef2c ( $M=247.1$ ,  $SD=21.3$ ) had no significant impact on transcriptional activity compared to Mef2c alone ( $p=0.9950$ ). This corroborates the HEK293T co-IP data and suggests that Hdac4, but not Oasl1, is a direct interactor of Mef2c and that it represses Mef2c transcriptional activity.



**Figure 3.9. Validation of the putative interactors Hdac4 and Oasl1.** Flag IP-WB was used to confirm that Hdac4 does directly interact with Mef2c, but Oasl1 may not. **(A)** Using Flag antibody beads Hdac4 was immunoprecipitated from transfected HEK293T cells along with Mef2c suggesting that the two proteins directly interact. **(B)** Using Flag antibody beads Oasl1 was immunoprecipitated from transfected HEK293T cells, but Mef2c was not pulled down alongside suggesting that Mef2c and Oasl1 do not directly interact. This highlights the requirement to validate interactors identified by co-IP-MS.



**Figure 3.10. Hdac4 represses Mef2c activity in a reporter assay system.** Overexpressing Mef2c in HEK293T cells alongside an inducible luciferase reporter vector containing a Mef2c TRE motif, results in increased reporter gene and luciferase expression. Overexpressing Mef2c and Hdac4 together results in a significant decrease in this activity confirming the repression of Mef2c activity by Hdac4. Overexpressing Oasl1 alongside Mef2c has no effect on Mef2c activity which corroborates the finding that these two proteins do not directly interact ( $p \leq 0.05 = *$ ) ( $n=3$ ).

### 3.3 Discussion

AD common-variant risk is thought to operate through the MEF2C transcriptional network in microglia. Therefore, elucidating how MEF2C is regulated is particularly important as it may provide a means of manipulating Mef2c activity and altering Mef2c-dependent regulation of AD-risk genes. In this chapter, co-IP-MS delineated the first interactome of endogenous Mef2c in microglia-like cells. The data revealed that Mef2c exists as two main isoforms in BV2 cells. Additionally, 110 putative interactors of Mef2c were identified. These included Cabin1 and two repressive Hdac proteins. It was predicted that these proteins are holding Mef2c in a partially repressed state in basal BV2 cells.

#### 3.3.1 Distinct Mef2c isoforms in BV2 cells are detected by MS

The presence of peptides mapping to different Mef2c isoforms suggests that BV2 cells express several Mef2c isoforms. These isoforms are also evidenced in the additional bands present in the western blot (Figure 3.1). Peptides corresponding to three Mef2c isoforms, 1, X4 and X9, were identified (Table 3.1) and spanned 46%, 44% and 25% of the protein, respectively. With six peptides unique to isoform 1, five peptides unique to isoform X4 but no peptides unique to isoform X9 it is likely that Mef2c exists as two predominant isoforms in BV2 cells: 1 and X4. The protein sequences of these two isoforms differ very close to the MEF2 binding site (Figure 3.11) so it is possible that these isoforms have different binding partners. Additionally, transcription factor splice variants can also have different functions. The E47 splice variant of the transcription factor E2A is important for controlling the number of deep and upper layer neurons whereas the E12 variant has no impact on layer-specific neurogenesis (Pfurr et al., 2017). Thus, these identified Mef2c isoforms may play different roles in BV2 cells.

As discussed in the General Introduction (section 1.4.2), MEF2C is extensively alternatively spliced generating multiple protein isoforms (Black & Olson, 1998; Zhu & Gulick, 2004). MEF2C contains three main alternative exons; mutually exclusive exon ( $\alpha$ ), skipping exon ( $\beta$ ) and 3' splice site selection ( $\gamma$ ). The inclusion or exclusion of these splice sites is cell-type specific and can affect the function of the MEF2C protein. The inclusion of these alternative exons in BV2 cells was examined by direct comparison of the isoform and exon sequences. Isoform 1 contained the  $\alpha$ 1 exon whereas isoform X4 contained  $\alpha$ 2. Neither of the isoforms included the  $\beta$  exon, whereas both contained the  $\gamma$  exon (Figure 3.12). Thus, the main difference between the two primary isoforms expressed by BV2 cells is the  $\alpha$  exon. Previous work has shown that transcripts encoding  $\alpha$ 2 are primarily expressed in muscle

```

Isoform_1      1 MGRKKIQITRIMDERNRQVTFTRKRFGLMKKAYELSVLCDCEIALIIFNSTNKLQYAST
Isoform_X4     1 MGRKKIQITRIMDERNRQVTFTRKRFGLMKKAYELSVLCDCEIALIIFNSTNKLQYAST

Isoform_1     61 DMDKVLLKYTEYNPHEPESRTNSDIVETLRKKGLNGCDSPPDPADDSVGHSPEDKYRKI
Isoform_X4     61 DMDKVLLKYTEYNPHEPESRTNSDIVEALNKKENKGSESPPDPS--SYALTPRTEEKYKKI

Isoform_1    121 NEDIDLMISRQRLCAVPPPSFEMPVTIPVSSHNSLVYSNPVSTLGPNLLPLAHPSLQRN
Isoform_X4    119 NEEFDNMIKSHKIPAVPPPSFEMPVTIPVSSHNSLVYSNPVSTLGPNLLPLAHPSLQRN

Isoform_1    181 SMSPGVTHRPPSAGNTGGLMGDDLTSAGAGTSAGNGYGNPRNSPGLLVSPGNLNKNIQAKS
Isoform_X4    179 SMSPGVTHRPPSAGNTGGLMGDDLTSAGAGTSAGNGYGNPRNSPGLLVSPGNLNKNIQAKS

Isoform_1    241 PPPMNLGMNRRKPDRLRVLIIPGSKNTMPSVNQRINNSQSAQSLATPVVSVATPTLPGQGM
Isoform_X4    239 PPPMNLGMNRRKPDRLRVLIIPGSKNTMPSVNQRINNSQSAQSLATPVVSVATPTLPGQGM

Isoform_1    301 GGYPSAISTTYGTEYSLSSADLSSLSGFNTASALHLGSVTGWQQQHLHNMPPSALSQ LGA
Isoform_X4    299 GGYPSAISTTYGTEYSLSSADLSSLSGFNTASALHLGSVTGWQQQHLHNMPPSALSQ LGA

Isoform_1    361 CTSTHLSQSSNLSLPSTQSLSIKSEPVSPPRDRTTTPSRYPQHTRHEAGRSPVDSLSSC
Isoform_X4    359 CTSTHLSQSSNLSLPSTQSLSIKSEPVSPPRDRTTTPSRYPQHTRHEAGRSPVDSLSSC

Isoform_1    421 SSSYDGS DREDHRNEFHSPIGLTRPSPDERESPSVKRMRLSEGWAT
Isoform_X4    419 SSSYDGS DREDHRNEFHSPIGLTRPSPDERESPSVKRMRLSEGWAT

```

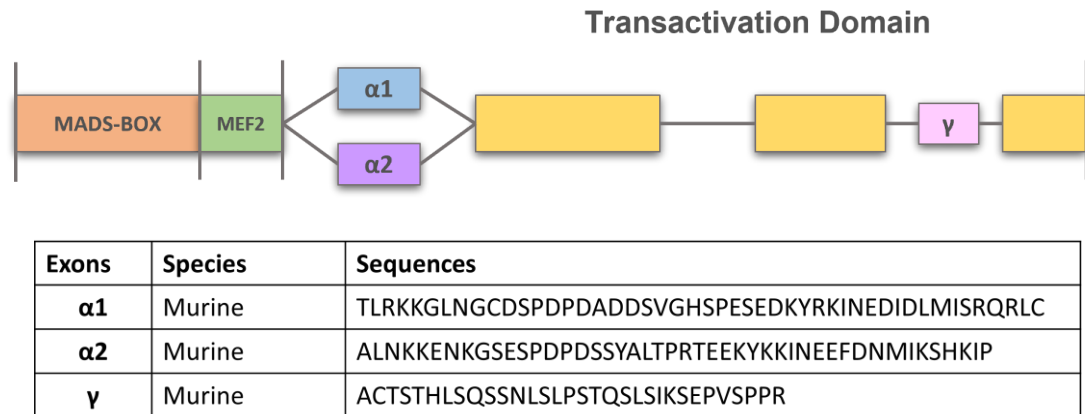
**Figure 3.11. Sequence alignment of the two predominant Mef2c isoforms expressed in BV2 cells.** Sequences of Mef2c isoform 1 and isoform X4 were aligned to illustrate the sequence differences which are highlighted in blue. These differences may mean that these isoforms have different functions and interacting partners.

cells whereas the  $\alpha 1$  exon is expressed in both muscle and neuronal cells (Hakim et al., 2010). This new data suggests that BV2 cells express both  $\alpha$  exons. Microglia-like cells may selectively express certain Mef2c isoforms to aid transcriptional regulation and function.

The inclusion of different  $\alpha$  exons in the Mef2c isoforms may partially explain the presence of two repressive complexes, the Hira complex and the Hdac complex. The presence of the  $\alpha 2$  exon is thought to reduce HDAC recruitment to target promoters (Zhang et al., 2015). Thus, as the  $\alpha 2$  isoform is more resistant to Hdac-induced repression the Hdac proteins may primarily repress the  $\alpha 1$  isoform, the Hira/Cabin1 complex may be required to repress the  $\alpha 2$  isoform. However, confirmation of this would require further investigation.

### 3.3.2 Co-immunoprecipitation of known Mef2c interactors

Three known interacting proteins, Hdac4, Hdac5, and Mef2a, were identified in the co-IP-MS experiments. This strengthens the validity of the data and means that any identified



**Figure 3.12. The inclusion of alternative exons in the Mef2c protein in microglia-like cells.** The alternative exons that are included in the identified isoforms are depicted here. Isoform 1 contains the  $\alpha 1$  exon whereas isoform X4 contains  $\alpha 2$ . Neither of the isoforms included the  $\beta$  exon, whereas both contained the  $\gamma$  exon. The table details the sequences of the alternatively spliced exons in rodents. Diagram adapted from Figure 1.4.1 (General Introduction). This diagram is simplified and does not show the domains HJURP\_C and TR as depicted in Figure 3.2 as they cover the alternative exon regions.

novel interactors are therefore of high confidence. Mef2a, as a Mef2 family member, has high sequence homology with Mef2c and confirmation of their interaction supports the concept that Mef2 family members can form heterodimers with each other (Molkentin et al., 1996a). Further, unique Mef2a peptides were identified confirming that the identification of Mef2a is not a cross-mapping issue. The interaction between these transcription factors has also been demonstrated by tandem affinity purification followed by MS with MEF2A as the bait protein (Li et al., 2015). However, in this experiment, HEK293T cells were stably transfected with tagged MEF2A cDNA. The use of tags may affect protein-protein interactions and over-expression of the bait protein may result in misfolding and mislocalisation. The data presented in this thesis confirms Mef2a as an interactor of Mef2c in a more relevant and appropriate system; an endogenously expressing microglia-like cell line.

HDAC4 and HDAC5 are two enzymes that have also previously been shown to interact with MEF2C. The interaction of MEF2C and HDAC4 has been demonstrated by both affinity capture western (Wang et al., 1999) and Y2H screens (Wang et al., 2005) suggesting that HDAC4 binds directly to MEF2C. However, similarly to above, in the affinity capture HDAC4 and MEF2C were tagged and overexpressed in HEK293T cells, and the interaction was only confirmed by western blot not by MS. HDAC5 has also been directly associated with MEF2C in anti-tag co-IP (Joshi et al., 2013). However, only a weak, low confidence interaction was detected in CEM T-lymphoblast cells between HDAC5 and MEF2C. The interaction between

these class II HDACs and MEF2C has thus been confirmed in cell-type specific model which is a more physiologically-relevant cell model in which the interactions form between endogenous proteins.

It was expected that more transcription factors would co-IP with Mef2c as transcription factors exist in multi-protein complexes and collaborate to regulate target gene expression (Adcock & Caramori, 2009; Martin, 1991). Many transcription factors have been previously identified as interactors of MEF2C including SOX18, SPI, ASCLI, GATA4 and TWIST2. However, none of these proteins were identified in these experiments, consistent with the idea that Mef2c is in a partially repressed state. Additionally, in section 3.1, it was speculated that Mef2c may interact with the microglial master regulator PU.1 as these transcription factors are known to work together to exert control and enhancers bound by PU.1 in microglia are also enriched for MEF2 binding motifs (Adcock & Caramori, 2009; Gosselin et al., 2014; Martin, 1991). However, this data suggests that these proteins do not interact in unstimulated microglia-like cells.

### 3.3.3 Gene ontology analysis reveals involvement of Mef2c in several biological processes

Gene ontology analysis revealed that Mef2c is involved, through its interactions with other proteins, in several processes including mRNA processing, regulation and export and the spliceosome. The export of mRNA from the nucleus primarily involves members of TREX complex, of which, four proteins were identified in this dataset: THO complex (Thoc) 1, 2, 5 and 6 (Chavez, 2000; Stäßer et al., 2002). The TREX complex is recruited to mRNA via interactions with transcription factors (Katahira, 2015). Thus, the putative interaction between Mef2c and these complex members is unsurprising; it is facilitating the essential transport of mRNA to the nucleus for efficacious gene expression.

The spliceosome is a ribonucleoprotein complex that catalyses nuclear pre-mRNA splicing. The spliceosome consists of many proteins, several of which were identified in this dataset. Potentially, Mef2c could interact with splicing factors in microglia-like cells, however interactions between splicing factors and Mef2 family members have not been previously demonstrated. Caution in the interpretation of these interactions must be taken due to the lack of evidence for the involvement of Mef2 factors in splicing. Additionally, most of these proteins have high CRAPome scores which increases the likelihood that these are contaminants rather than true interactions.

Interestingly, the gene ontology analysis also revealed cytokine signalling in the immune system as being enriched in the high confidence list of proteins. A number of identified proteins were related to this process including *Oasl1*, *Mef2a* and *Mef2c*, all of which are thought to be involved in the immune response (Deczkowska et al., 2017; Zhu et al., 2015a). The co-IP-MS of Mef2c in microglia-like cells has identified processes specific to immune cells which are unlikely to be identified in other cell types. This highlights the importance of studying protein interactomes in cell-specific models.

#### 3.3.4 Co-IP suggests Mef2c is being held in a partially repressed state in BV2 cells

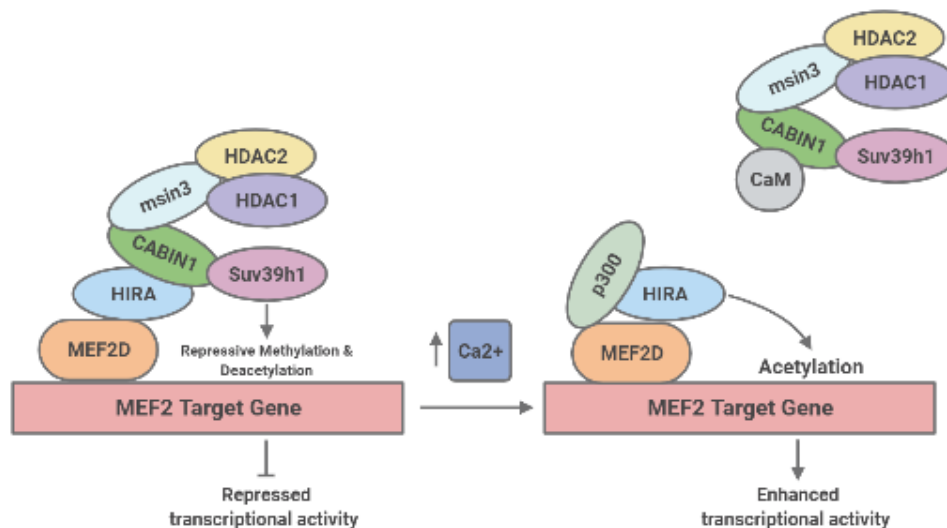
A subset of the co-immunoprecipitated proteins were identified as members of the HIRA complex; Hira, Cabin1 and Ubn2. The HIRA complex is an evolutionally conserved histone chaperone complex which deposits the histone variant H3.3 into chromatin (Tagami et al., 2004). This deposition has been associated with actively transcribed genes and plays a role in the activation and maintenance of gene expression patterns (Filipescu et al., 2014; Shi et al., 2017). Specifically, within the complex, HIRA acts as a scaffold protein which unites the other subunits; binding UBN2 through its N-terminal WD repeat region and CABIN1 via its C-terminal C domain (Banumathy et al., 2009; Rai et al., 2011). UBN2 is primarily responsible for specific recognition and direct binding of H3.3 (Xiong et al., 2018). The explicit role of CABIN1 within the complex remains unknown, however, it is thought to negatively regulate interactor activity (Sun et al., 1998).

Asides from its role in the HIRA complex, HIRA has been shown to interact with MEF2D, another MEF2 family member. This results in an increase in MEF2D transcriptional activity (Yang et al., 2011). The interaction between Hira and Mef2c in BV2 cells may result in a similar outcome; Hira may interact with Mef2c to facilitate transcription. CABIN1 is also known to interact with other MEF2 family members. It represses the activity of these proteins in three main ways: CABIN1 recruits HDACs to target genes via the mSin3 co-repressor, it blocks Ca<sup>2+</sup>-dependent association of MEF2 with ERK5 which enhances MEF2 transcriptional activity, and it represses calcineurin; an upstream regulator of MEF2 activity (McKinsey et al., 2002). Additionally, CABIN1 suppresses MEF2D/HIRA mediated transcription (Yang et al., 2011). In muscle cells, HIRA interacts directly with MEF2D, and it moves to MEF2D target sites where it recruits CABIN1, mSin3, HDAC1, HDAC2 and Suv39h1 which leads to the repression of chromatin. Increases in Ca<sup>2+</sup> result in the binding of calmodulin to CABIN1 which leads to the release of the repressive machinery and leaves the MEF2D/HIRA complex available for p300 binding, subsequent histone acetylation,

relaxation of chromatin and enhanced transcriptional activity (Jang et al., 2007; Robinson & Dilworth, 2018; Youn & Liu, 2000) (Figure 3.13). CABIN1 also directly interacts with MEF2B and holds MEF2B in a transcriptionally inactive state. Increases in  $Ca^{2+}$  also dissociate CABIN1 from MEF2B via the competitive binding of calmodulin to CABIN1 (Youn et al., 1999).

Collectively, the evidence presented above suggests that Mef2c may be partially held in a transcriptionally inactive state in unstimulated BV2 cells by Cabin1 and the known Mef2c interactors Hdac4 and Hdac5. These proteins may be repressing Mef2c transcriptional activity, preventing Hira-mediated transcription and holding Mef2c in a silenced state. This provides further explanation for the lack of transcription factors, coactivators and other known interactors identified.  $Ca^{2+}$  can release the repression of CABIN1 and the HDACs on other MEF2 family members (Mckinsey et al., 2000b; Robinson & Dilworth, 2018).

Therefore, it would be interesting to investigate the influence of stimulating BV2 cells with ionomycin to increase intracellular  $[Ca^{2+}]$  prior to co-IP-MS (see Chapter 4). This may release Mef2c from its repressed state and result in a remodelling of the Mef2c interactome.



**Figure 3.13. Regulation of MEF2D activity by HIRA and CABIN1.** The interaction between HIRA and MEF2D recruits HIRA to MEF2D target sites. Here, HIRA recruits CABIN1, mSin3, HDAC1, HDAC2 and Suv39h1. Repressive methylation and deacetylation of histones by Suv39h1 and HDACs respectively, subsequently represses chromatin around the MEF2D target gene inhibiting transcription. Increases in intracellular  $[Ca^{2+}]$  allow for the binding of calmodulin (CaM) to CABIN1, releasing the CABIN1, mSin3, HDAC1, HDAC2 and Suv39h1 complex from HIRA. The HIRA-MEF2D complex is then left open for p300 binding which acetylates histones and forms permissive chromatin available for transcription. Figure adapted from Robinson and Dilworth (2018). Created in BioRender.com.



As mentioned in the General Introduction (section 1.4.1), MEF2 factors have shown a compensatory ability. MEF2A functionally compensated for MEF2D after its deletion in granule neurons. MEF2A only occupied a subset of previously-bound MEF2D sites but this resulted in similar gene expression (Majidi et al., 2019). Although this experiment was carried out in granule neurons and a compensatory mechanism was identified specifically between MEF2A and MEF2D, there remains a possibility that this phenomenon occurs in other cell types and between other family members. In microglia-like cells, where Mef2c is held in a transcriptionally inactive state, other Mef2 family members expressed in microglia, including Mef2a and Mef2d, may be able to functionally compensate for a portion of Mef2c-dependent gene regulation. It would be important to establish the compensatory mechanisms of MEF2 factors in microglial cells and whether other family members can occupy MEF2C sites whilst MEF2C is either depleted or repressed by HDAC proteins.

### 3.3.5 Co-IP identifies potential novel Mef2c interactors

Two novel interactors, Oasl1 and Ncoa5, were identified and may warrant further investigation. No previous association between Oasl1 or Ncoa5 and any of the Mef2 family members has been reported in the literature. Oasl1 deficiency in mice has been found to promote antiviral immunity and increase resistance to implanted tumours suggesting that Oasl1 is important for regulating the immune response (Lee & Oh, 2016; Sim et al., 2019). Mef2c is also thought to play a role in the immune response; it regulates the reaction of microglia to immune challenges (Deczkowska et al., 2017). Therefore, these proteins could be working in conjunction to regulate this response in microglia-like cells. On the other hand, Ncoa5 is a transcriptional coregulator and another high confidence interactor which may be a coactivator or corepressor of Mef2c activity. Mef2c is known to interact with another nuclear receptor coactivator, Ncoa2 which coactivates Mef2c to enhance and stabilise transcription (Canté-Barrett et al., 2014; Chen et al., 2000). However, Ncoa5 and Ncoa2 are not part of the same family and there is very little similarity between their protein sequences so it is not clear whether Ncoa5 would interact with Mef2c in a similar way to Ncoa2. Validating and exploring these interactions further would provide evidence on the potential function and regulation of Mef2c in BV2 cells.

### 3.3.6 Mef2c directly interacts with Hdac4 but not Oasl1

The direct interaction between Mef2c and its associated proteins requires validation prior to any follow-up analysis. HEK293T co-IP western blots were used to confirm the direct interaction between Hdac4 and Mef2c suggesting that these two proteins interact in

microglia-like cells. This is in conjunction with previous research which has reported this interaction in yeast and HEK293T cells (Wang et al., 1999, 2005). This interaction was also validated functionally with a reporter system confirming the repression of Mef2c activity by Hdac4. This is also in line with previous work which suggests that Hdac4 is a transcriptional repressor of Mef2 family members (McKinsey et al., 2002; Miska et al., 1999). However, Oasl1 was not found to interact directly with Mef2c which highlights the limitation of co-IP-MS experiments and the requirement to run validation experiments. The lack of a direct interaction between Mef2c and Oasl1 could mean that these two proteins interact indirectly through another protein in a protein complex or that Oasl1 has cross-reacted with the antibody or is a contaminant. As it is expected that most identified interactions will be tertiary rather than binary this is most likely to be the case for Oasl1.

Time constraints and practical limitations meant that validation experiments could only be run on these two putative interactors. Future work should focus on completing these validation experiments and determining if any of these interactions are isoform specific. Due to the location of the sequence difference between isoform 1 and isoform X4 they could have different binding partners. Only Mef2c isoform 1 was used to validate interactions so an interaction between Oasl1 and Mef2c isoform X4 cannot be ruled out.

### 3.3.7 Limitations

Whilst being an effective tool for identifying protein-protein interactions, co-IP-MS may not be able to capture low affinity, weak and transient protein interactions that depend on the cellular environment. Co-IP is also limited by the antibody used. The epitope may be in the same location as a binding site for an interacting protein meaning that the antibody disrupts the ability of the protein to bind. Thus, some interactions may be lost. Additionally, some identified interactors may have just cross-reacted with the antibody. If this is the case, they will always be identified as a true interactor. Further, detected interactions are not necessarily direct associations, unlike interactions identified using Y2H, they may be indirect and associated via another protein. Therefore, validation experiments, as carried out on Hdac4 and Oasl1 (section 3.2.6), are required prior to any further analysis.

### 3.3.8 Conclusions

This work has delineated the first interactome for endogenous Mef2c in microglia-like cells. It has revealed that two Mef2c isoforms, with specific alternatively spliced exons, may be selectively expressed in BV2 cells. Additionally, 110 putative Mef2c interactors have been identified and could ultimately be used as a means of manipulating Mef2c activity and

altering the Mef2c-dependent regulation of AD-risk genes. These interacting proteins include Cabin1, Hdac4 and Hdac5. Based on the literature, it was predicted that these proteins are predominantly holding Mef2c in a partially transcriptionally inactive state in unstimulated BV2 cells. For other MEF2 family members, the repression of HDAC4, HDAC5 and CABIN1 can be relieved by  $Ca^{2+}$ . Therefore, investigating the impact of ionomycin-treatment, to elevate intracellular  $[Ca^{2+}]$  levels, on Mef2c repression and its ability to form interactions is particularly important and will be explored in the next chapter.

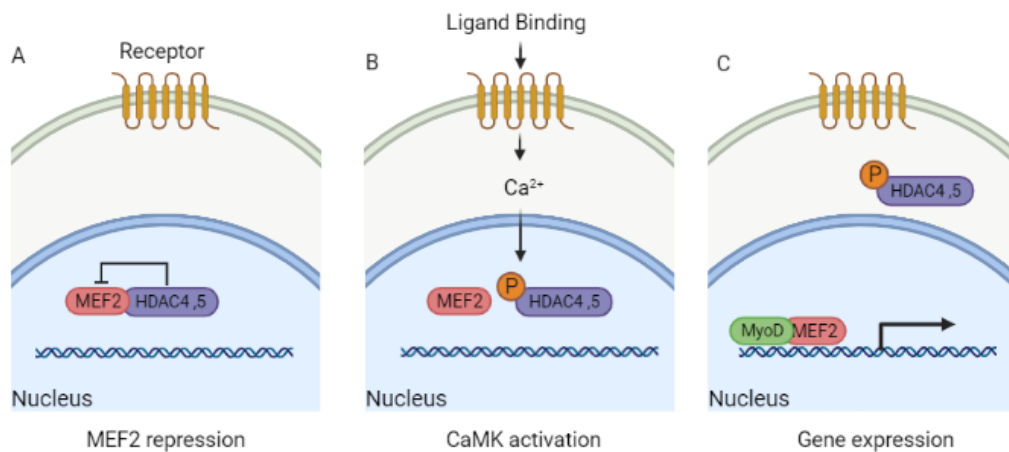
## Chapter 4 Investigating the effect of ionomycin treatment on the Mef2c interactome

### 4.1 Introduction

The Mef2c interactome described in the preceding chapter (section 3.2.4) contains several proteins such as Hdac4, Hdac5, and Cabin1 that are predicted to repress the transcriptional activity of Mef2c essentially restraining the activity of Mef2c in BV2 cells. Releasing Mef2c from this repressed state may result in changes to the Mef2c interactome, augmenting transcriptional activity. Furthermore, additional microglia-relevant proteins may be recruited to the de-repressed Mef2c complex, modulating transcriptional activity and the regulation of AD-risk genes in BV2 cells.

As mentioned above, the main repressors of Mef2c activity in BV2 cells are likely to be Hdac4, Hdac5 and Cabin1. These proteins are all regulated by  $Ca^{2+}$  signalling. HDAC4 and HDAC5 are known repressors of MEF2 function that bind to MEF2 and inhibit transcription as follows (McKinsey et al., 2002; Miska et al., 1999). In muscle cells, the initiation of  $Ca^{2+}$  signalling within the cell activates  $Ca^{2+}$ /calmodulin-dependent protein kinases I and IV (CaMKI/IV). Subsequently, these enzymes phosphorylate HDAC4 and HDAC5 resulting in their dissociation from MEF2 and exposure of their nuclear export signals. This initiates the translocation of the HDACs from the nucleus into the cytoplasm, allowing MEF2 to bind to transcriptional co-activators such as MyoD to regulate myogenesis (McKinsey et al., 2000b; Stewart & Crabtree, 2000) (Figure 4.1). While this process has been shown to be important in muscle cells, a similar mechanism may operate in other cell types such as microglia. As microglial cells and BV2 cells can be activated by a range of exogenous stimuli including LPS, serum deprivation and viral infection (Rock et al., 2004; Yao & Fu, 2020), stimulating BV2 cells with ionomycin to raise intracellular  $[Ca^{2+}]$  may also activate these cells resulting in Hdac4 and Hdac5 dissociating from Mef2c, allowing this transcription factor to potentially form new interactions.

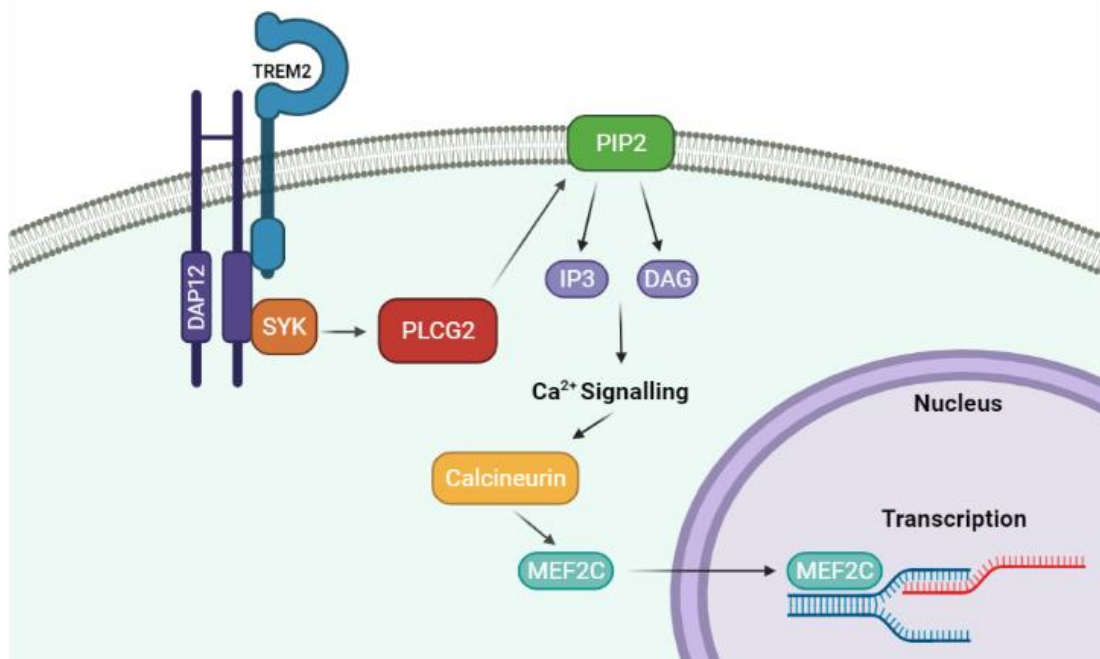
CABIN1 is also known to inhibit members of the MEF2 family. As described in Chapter 3 (Figure 3.13), CABIN1 suppresses MEF2D/HIRA mediated transcription. However, increases in  $[Ca^{2+}]$  result in the release of the CABIN1 repressive complex from HIRA which leads to enhanced transcriptional activity of MEF2D (Jang et al., 2007; Robinson & Dilworth, 2018;



**Figure 4.1. Regulation of gene transcription by HDAC4 and HDAC5. (A)** In muscle cells, histone deacetylase 4 and 5 (HDAC4,5) bind to the transcription factor MEF2 and inhibit the expression of muscle-specific genes. **(B)** Ca<sup>2+</sup>/calmodulin-dependent protein kinases I and IV (CaMKI/IV) are activated by Ca<sup>2+</sup> signalling upon removal of serum from the cell culture medium. These kinases subsequently phosphorylate HDAC4 and HDAC5 causing their dissociation from MEF2. **(C)** Post phosphorylation, HDAC4 and HDAC5 translocate to the cytoplasm leaving MEF2 free to promote the expression of muscle-specific genes by interacting with other transcription factors like MyoD. Figure adapted from Stewart and Crabtree (2000). Created with BioRender.com.

Youn & Liu, 2000). In BV2 cells, Mef2c is likely to be held in a similar repressed state by Cabin1 (section 3.3.4). This raises the possibility that ionomycin treatment may modulate this interaction.

MEF2C itself is also activated by Ca<sup>2+</sup>-dependent mechanisms. Translocation of MEF2C to the nucleus requires activation of calcineurin by calreticulin, a Ca<sup>2+</sup> binding chaperone essential for Ca<sup>2+</sup> homeostasis and storage (Michalak et al., 2002). Additionally, MEF2C activates transcription of the *calreticulin* gene, thereby creating a positive feedback loop (Lynch et al., 2005). As MEF2C can be activated in a Ca<sup>2+</sup>-dependent manner, it has been postulated that MEF2C may play a role downstream of other AD-risk genes including TREM2 and phospholipase C gamma 2 (PLC $\gamma$ 2) in microglia (Hansen et al., 2018) (Figure 4.2). Activation of the cell surface receptor TREM2 initiates a range of signal transduction pathways important for phagocytosis, proliferation, and survival (Hansen et al., 2018; Poliani et al., 2015; Takahashi et al., 2005; Zheng et al., 2017). Briefly, TREM2 directly interacts with DNAX activation protein of 12kDa (DAP12), an adapter protein which contains an immunoreceptor tyrosine-based activation motif (ITAM). This interaction recruits spleen tyrosine kinase (SYK) (Andreone et al., 2020). SYK can also activate PLC $\gamma$ 2, an enzyme that has also been associated with AD (Sims et al., 2017). This phospholipase cleaves phosphatidylinositol(4,5)-bisphosphate (PIP2) into two secondary messengers;



**Figure 4.2. A role for MEF2C downstream of AD-risk genes TREM2 and PLCγ2.** Interaction of TREM2 and the cell-surface adapter protein DAP12, recruits the tyrosine kinase SYK. SYK activates PLCγ2 which cleaves PIP2 into two secondary messengers; IP3 and DAG which activate Ca<sup>2+</sup> signalling. This, and the subsequent activation of calcineurin may result in the translocation of MEF2C to the nucleus and the initiation of gene transcription. Figure adapted from Hansen et al., (2018). Created with BioRender.com.

inositol 1,4,5-trisphosphate (IP3) and diacylglycerol (DAG) which further propagate Ca<sup>2+</sup> signalling (Berridge, 2009; Putney & Tomita, 2012; Song et al., 2019). The activation of Ca<sup>2+</sup> signalling and calcineurin may subsequently lead to the translocation of MEF2C to the nucleus and the initiation of gene transcription. As AD-risk SNPs have been found to be enriched in several microglial open chromatin regions that contain DNA binding motifs for MEF2C, the activation of Ca<sup>2+</sup> signalling may result in impaired transcriptional control of MEF2C due to genetic variation at binding sites (Tansey et al., 2018). Therefore, exploring the interactome of Mef2c after elevating [Ca<sup>2+</sup>] levels is both important and relevant to AD as the investigation of its Ca<sup>2+</sup>-dependent interacting partners may shed light on its potential role as a downstream signal integrator of this AD genetic risk pathway. To address this hypothesis, co-IP-MS (sections 2.5 and 3.2.1) was used to delineate the Mef2c interactome in ionomycin-treated BV2 cells. For the sake of clarity, all proteins will be referred to as their unitalicized gene names throughout this chapter.

## 4.2 Results

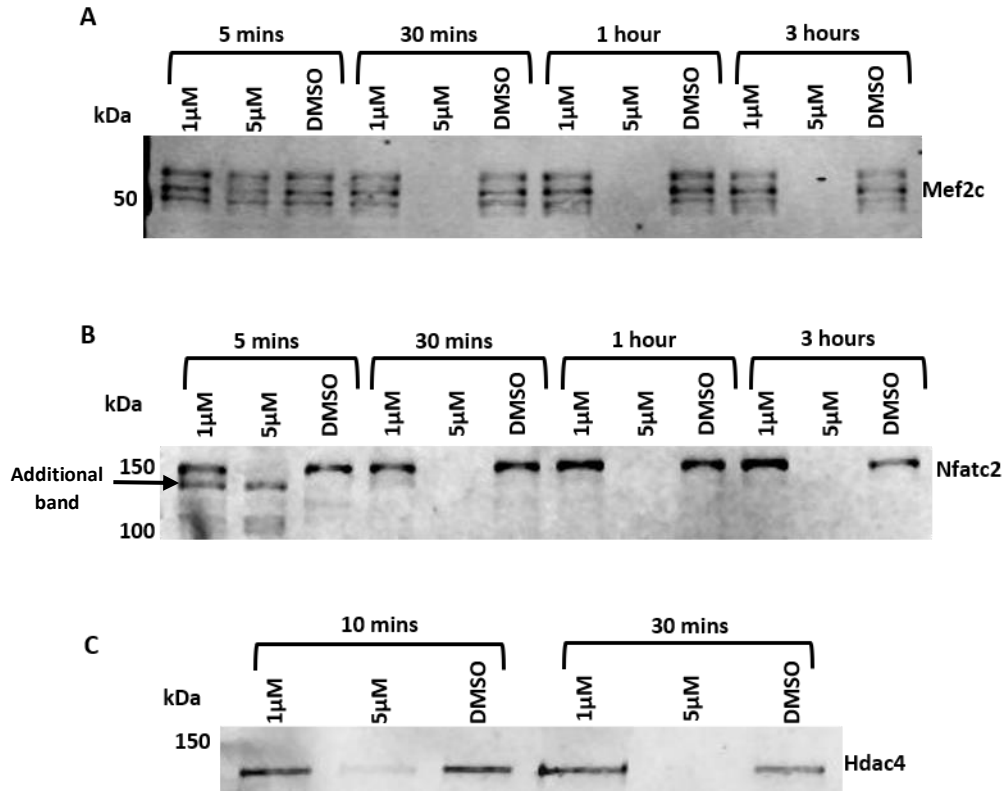
### 4.2.1 Ionomycin stimulation optimisation

Prior to using ionomycin to increase  $[Ca^{2+}]$  levels in BV2 cells for co-IP, optimisation was required to determine the concentration and exposure time needed to induce changes to the Mef2c interactome. Western blots were used to investigate whether ionomycin exposure (1 $\mu$ M or 5 $\mu$ M) at varying time intervals could induce phosphorylation changes in proteins relevant to the Mef2c repression complex (Figure 4.3). No noticeable phosphorylation changes, for example changes in molecular weight or additional bands, were observed in ionomycin-treated cells with an anti-Mef2c antibody (Figure 4.3 A). To determine if ionomycin was having any effect on the cells, a positive control was tested; Nuclear factor of activated T cells 2 (Nfatc2) (Figure 4.3 B). An additional, lower molecular weight band was visible in the 1 $\mu$ M condition after 5min. This additional band is likely to be dephosphorylated Nfatc2 as members of the NFAT family become dephosphorylated by the  $Ca^{2+}$ -dependent phosphatase, calcineurin, upon ionomycin stimulation. Dephosphorylation of NFAT proteins results in the exposure of a nuclear localisation signal, translocation to the nucleus and a stimulation of transcriptional activity (Hogan et al., 2003; Okamura et al., 2000). However, this band was not visible after 30min suggesting the initial changes in phosphorylation occur rapidly after the addition of ionomycin. These data can cautiously be interpreted as evidence that ionomycin treatment is raising intracellular  $[Ca^{2+}]$  in BV2 cells leading to dephosphorylation and activation of the  $Ca^{2+}$ -responsive transcription factor Nfatc2.

As described in Figure 4.1, the phosphorylation of Hdac4 and Hdac5 by CaMK1/IV is required for their dissociation from Mef2c and a relief of inhibition. Therefore, evidence of phosphorylation of these proteins would suggest that ionomycin was inducing their dissociation from Mef2c so Hdac4 and phospho-Hdac5 antibodies were tested. No noticeable differences between conditions in terms of phosphorylation were observable for the Hdac4 antibody (Figure 4.3 C). For the phospho-Hdac5 antibody, despite optimisation, the resulting blots were not successful so no conclusions regarding the effect of ionomycin on the phosphorylation of Hdac5 could be made (images not shown).

### 4.2.2 Mef2c co-immunoprecipitation in ionomycin-treated BV2 cells

While the Nfatc2 western blots provide evidence that ionomycin is influencing the activation status of  $Ca^{2+}$ -responsive proteins in BV2 cells, they do not provide any direct evidence of a change to the Mef2c/Hdac complex. Having found some evidence that



**Figure 4.3. Ionomycin optimisation.** BV2 cells were incubated with either 1 μM or 5 μM ionomycin for varying time intervals prior to western blot analysis. **(A) Mef2c Antibody.** A rabbit monoclonal anti-Mef2c antibody was used to detect Mef2c in lysates incubated with ionomycin for 5mins, 30mins, 1h and 3h. No discernible change in the phosphorylation of Mef2c was observed between ionomycin-treated and control DMSO-only conditions. **(B) Nfatc2 Antibody.** A mouse monoclonal anti-Nfatc2 antibody was used, as a positive control, to detect Nfatc2, a  $Ca^{2+}$ -sensitive transcription factor in lysates incubated with ionomycin for 5mins, 30mins, 1h and 3h. Additional bands were observed in the 1 μM condition after 5mins suggesting that ionomycin induces dephosphorylation of Nfatc2 in BV2 cells. **(C) Hdac4 Antibody.** A mouse monoclonal anti-Hdac4 antibody was used to detect Hdac4 in lysates incubated with ionomycin for 10 or 30mins as this was determined, from the Nfatc2 antibody, to be the optimum time for phosphorylation changes. No changes to the phosphorylation of Hdac4 were observed between ionomycin-treated and control DMSO-only conditions. 5 μM ionomycin was toxic to BV2 cells after just 10mins of ionomycin exposure.

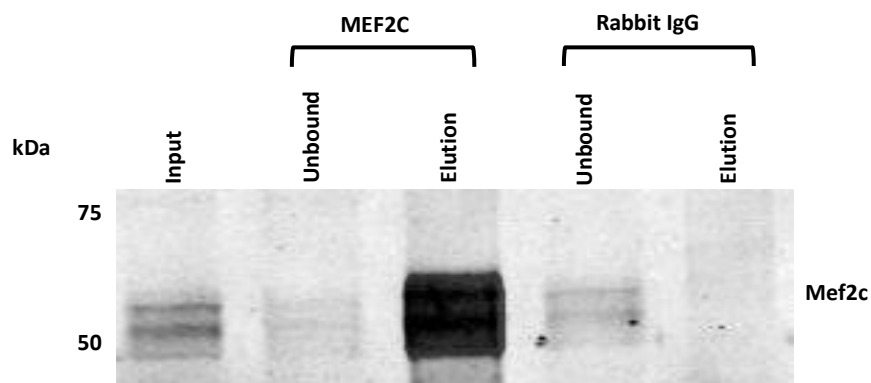
ionomycin treatment was having the desired biological effect, co-IP-MS was used to purify the Mef2c complex from ionomycin-treated BV2 cells. As a longer stimulation time is required to allow downstream interaction changes to occur, a 1h stimulation with 1 μM ionomycin, as stimulation with 5 μM ionomycin for up to 30mins was clearly toxic to the cells, was deemed to be appropriate for use in co-IP experiments. Adherent BV2 cells were incubated with 1 μM ionomycin for 1h prior to co-IP (Figure 4.4). The Mef2c antibody complex was enriched on the protein G Dynabeads (lane 3- elution) demonstrating that Mef2c can be successfully immunoprecipitated from ionomycin-stimulated BV2 cells.



## 4.2.3 MS analysis of Mef2c in ionomycin-treated cells

From the MS data, two distinct isoforms were identified; isoforms 1 (Q3V1B5/Q8CFN5) and X4 (A0A0H2UKB6), again supporting the notion that Mef2c exists as two main isoforms in BV2 cells (section 3.2.2). Similar numbers of unique and shared peptides were found for each isoform suggesting that ionomycin stimulation is not likely to affect Mef2c splicing or the relative abundance of each isoform. Across all identified isoforms and all three experiment replicates a total of 30 Mef2c peptides were identified by MS (Table 4.1). Peptides assigned to isoform 1 spanned 51% of the protein whereas peptides corresponding to isoform X4 spanned 59% of the protein.

A change to the accession number assigned to Mef2c isoform 1 was noted on UniProt (Bateman et al., 2021) upon analysis of the third replicate. Prior to this change, Q3V1B5 referred to isoform 1. However, as of April 2021, Q8CFN5 is now isoform 1 as this is the longest isoform. Q3V1B5 is now referred to as Mef2c isoform 2 (Q8CFN5-2). As this change occurred during data acquisition, in the first two replicates Mef2c isoform 1 is Q3V1B5 whereas in the third it is Q8CFN5, leading to Mef2c isoform 1 being filtered out of the dataset. All peptides detected by MS for Mef2c isoform 1 (Q3V1B5/Q8CFN5) map to the sequence for Q3V1B5; none are unique to either accession number. Therefore, for simplicity, ease of analysis, and comparison to the unstimulated dataset, all peptides associated with either accession number were classed as Mef2c isoform 1 under the Q3V1B5 accession number.



**Figure 4.4. Mef2c co-IP post ionomycin treatment.** Western blotting was used to show that the Mef2c antibody could immunoprecipitate Mef2c from BV2 cells treated with ionomycin. Whole cell extracts were incubated overnight with Mef2c antibody crosslinked to protein G Dynabeads. The eluted Mef2c complex was resolved by SDS-PAGE and detected by western blotting (lane 3). A negative control IP with a monoclonal rabbit IgG was also performed to ensure Mef2c did not precipitate non-specifically (lane 5). Whole cell extracts were also sampled before (input, lane 1) and after IP (unbound, lanes 2 and 4) to demonstrate the depletion of Mef2c.

**Table 4.1. Identification of Mef2c peptides in stimulated BV2 cells.** Two isoforms of Mef2c were characterised: isoforms 1 and X4. The Mef2c peptides identified by MS for all isoforms are presented. Peptides are grouped by the isoform(s) they identified. Isoforms not previously identified in Chapter 3 are highlighted in blue.

Mef2c Isoform	Peptide Sequence
<b>Both</b>	<p>KAYELSVLCDCEIALIIFNSTNK  AYELSVLCDCEIALIIFNSTNK  HEAGRSPVDSLSSCSSSYDGSDREDHR  HEAGRSPVDSLSSCSSSYDGSDR  SPVDSLSSCSSSYDGSDR  SPVDSLSSCSSSYDGSDREDHR  LFQYASTDMDK  EDHRNEFHSPIGLTRPSPDER  NEFHSPIGLTRPSPDER  NIQAKSPPPMNLGMNNR  NSMSPGVTHRPPSAGNTGGLMGGDLTSGAGTSAGNGYGNPR  NSPGLLVSPGNLNK  NTMPSVNQR  SEPVSPPR  SPPPMNLGMNNR  VLIPPGSK  YTEYNEPHESR</p>
<b>Mef2c Isoform 1 Only</b>	<p>GLNGCDSPDPDADDSVGHSPESDK  GLNGCDSPDPDADDSVGHSPESDKYR  INEDIDLISR  KGLNGCDSPDPDADDSVGHSPESDKYR  KINEDIDLISR  TNSDIVETLR  TNSDIVETLRK</p>
<b>Mef2c Isoform X4 Only</b>	<p>GSESPDPDSSYALTPR  INEEFDNMIK  IPAVPPPSFEMPVTIPVSSHNSLVSNPVSTLGNPNLLPLAHPQLR  KINEEFDNMIK  TNSDIVEALNK  TNSDIVEALNKK</p>

#### 4.2.4 Phosphoproteomic analysis of Mef2c in ionomycin-treated cells

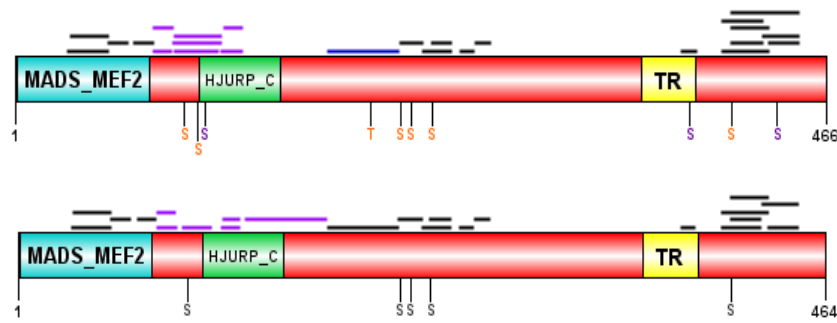
As discussed in Chapter 3 (section 3.2.3), MS data also gives information regarding amino acid modifications such as phosphorylation. Mef2c isoform 1 peptide information was searched to find phosphorylated peptides and to determine whether these phosphopeptides differed from those observed in the unstimulated Mef2c data. In total, five phosphopeptides were identified (Table 4.2). The potential phosphorylated residues in each peptide were compared to known phosphorylation sites to determine the most likely phosphorylated residue(s). No new phosphorylation sites or phosphopeptides were observed whilst putative phosphorylation sites S110, S388 (SEPVSPPR), S422, and S438

**Table 4.2. Mef2c phosphopeptides identified by MS.** Mef2c isoform 1 peptides identified by co-IP-MS were filtered to obtain a list of phosphopeptides. The potentially phosphorylated residues (serine/threonine) within each peptide sequence are highlighted in blue. The most likely phosphorylated residue in each phosphopeptide is also nominated based on previous findings in the literature.

Peptide Sequence	Potential Phosphorylation Sites	Sites Identified by MS	Nominated Phosphorylation Site(s)	Evidence
KGLNGCDS <b>S</b> PDPDAD DSVGH <b>S</b> PE <b>S</b> EDKYR GLNGCDS <b>S</b> PDPDADD SVGH <b>S</b> PE <b>S</b> EDKYR	S98, S106, S110	S98 S106	S98, S106	Huttlin et al (2010)
NSPGLLV <b>S</b> PGNLNK	S222, S228	S222 S228	S222, S228	Huttlin et al (2010) Zhou et al (2013)
SPPPMNLGMN <b>N</b> R NIQAK <b>S</b> PPPMNLGM NNR	S240	S240	S240	Huttlin et al (2010)
HEAG <b>R</b> SPVDS <b>L</b> SSCS SSYDG <b>S</b> DR	S412, S416, S418, S419, S421, S422, S423, S427	S412	S412	Lynch et al (2005)
NSM <b>S</b> PGV <b>T</b> HRPPSA GNTGGLMG <b>G</b> DL <b>T</b> S GAG <b>T</b> SAGNGYGN <b>R</b>	S181, S183, T187, S192, T196, T205, S206, T210, S211	S/T no specific site identified	T205- due to findings in previous MS analysis	No previous evidence for phosphorylation at these sites, likely to be a novel phosphopeptide

(EDHRNEFHSPIGLTRPSPDER) were not detected. The novel phosphopeptide identified in the unstimulated dataset was also observed here which increases its validity as a phosphopeptide. However, this time, the MS analysis did not nominate a likely phosphorylated residue.

All isoform 1 and isoform X4 associated peptides from all six MS experiments were aligned to the appropriate Mef2c protein sequence to visually establish their positioning (Figure 4.5). Nominated phosphorylation sites were also added. For isoform 1, as phosphorylation data is more readily available, sites identified in all six experiments are shown in orange whereas sites identified only in the unstimulated dataset are shown in purple. As no new putative Mef2c phosphorylation sites were identified in the stimulated data set, there was no requirement to run the sites through PhosphoMotif Finder to identify potential phosphorylating kinases or phosphatase substrates as this was previously done in Chapter 3 (section 3.2.3).



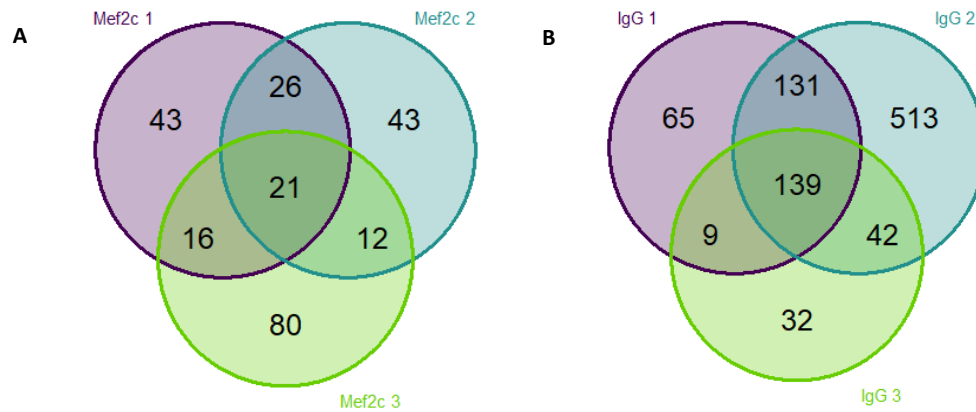
**Figure 4.5. Mef2c phosphorylation sites and peptide sequences in BV2 cells (stimulated and unstimulated).** This figure depicts the protein sequences of both Mef2c isoform 1 (top) and isoform X4 (bottom). Both diagrams show the location of the identified peptide sequences (black lines) identified by all six MS experiments with both stimulated and unstimulated cells. Sequences unique to each isoform are depicted in purple. Phosphorylation sites identified by MS for each isoform are shown. For isoform 1, as phosphorylation data is more readily available, only these sites are categorised by colour: serine (S), and threonine (T) sites identified in stimulated and unstimulated datasets (orange) and sites identified in unstimulated datasets only (purple). The novel peptide for Mef2c isoform 1, identified in both datasets, is depicted by a dark blue line. Functional domains and their approximate amino acid positions (extracted from NCBI) are also indicated for both isoforms. Figures created in DOG 2.0.

#### 4.2.5 Proteomic analysis of Mef2c binding proteins in ionomycin-treated cells

Following the workflow described in Chapter 3 (section 3.2.4), Mef2c and IgG control immunoprecipitations were carried out in triplicate to increase the confidence of the identified Mef2c-interacting proteins. To assess the variability between the three replicates, a hard filter using the list of IgG background proteins was applied (see section 2.6.2.1 for more detail). The Venn diagrams highlight variability between the IgG-filtered proteins present in the three separate Mef2c experiments and between the proteins identified in the IgG replicates (Figure 4.6 A, B). Again, highlighting the requirement of multiple repeats to filter out contaminants and non-specific interactions.

##### 4.2.5.1 SAINTexpress

SAINTexpress (see section 2.6.2.1) was used to identify 30 significant Mef2c-interactors (Table 4.3). The SAINT score output, which determines the probability that a protein is a true interactor of Mef2c, was plotted against  $\log_2$  fold change to visually represent the SAINTexpress data (Figure 4.7). Proteins are coloured by CRAPome score with proteins that are not present in the CRAPome database assigned a score of 100%. Cut offs for SAINT score ( $>0.7$ ) and fold change ( $>3$ ) were applied to the dataset and highlight a clear group of high confidence Mef2c-associated proteins. These interactors were then subject to further investigation; identification of proteins of interest (POI), gene ontology analysis (GOA) and



**Figure 4.6. Venn diagrams depicting the overlap between biological replicates.** Three biological replicates of the Mef2c and Rabbit IgG co-IP-MS were completed. These diagrams display the number of overlapping proteins (based on accession number) between each replicate and highlights the variability between experiments. **(A) Mef2c replicates.** Prior to visualisation, a hard filter was applied to each Mef2c replicate; any proteins that were present in the IgG lists were removed from the dataset. This clearly highlights that there are 21 Mef2c-associated proteins that do not appear in the IgG control but do appear in all three Mef2c experiments. **(B) Rabbit IgG replicates.** Several proteins (139) are present in all three IgG experiments, but a large amount of variability is obvious across the three replicates.

STRING annotation. Initial inspection and comparison of the SAINT outputs (Table 4.4) showed that similar spec scores for both Mef2c isoforms were recovered from the unstimulated and stimulated datasets which highlights the reproducibility of these data. It also revealed a dramatic reduction in the abundance of Hdac4, Hdac5 and Cabin1 compared to the unstimulated dataset. Consequently, Hdac4, Hdac5 and Cabin1 are no longer high confidence interactors of Mef2c, suggesting that ionomycin treatment is successfully dissociating these repressor proteins as hypothesised.

#### 4.2.5.2 STRING

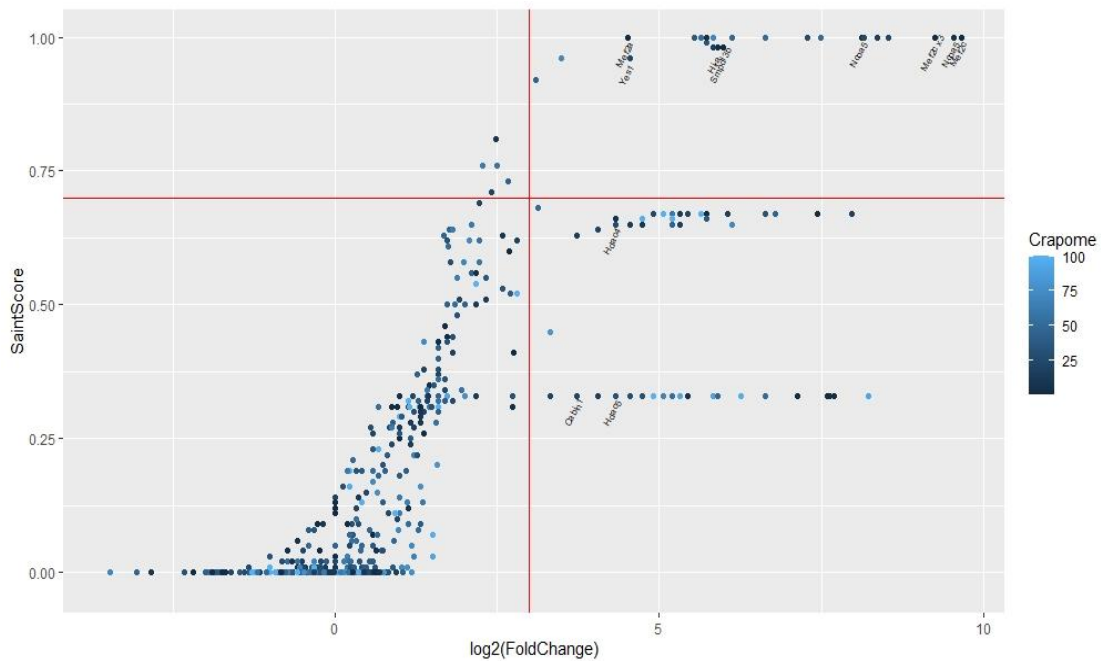
The STRING database was used to investigate known functional relationships between the 30 putative Mef2c-associated proteins (Figure 4.8). Relatively few interactions were detected between the interacting proteins. Applying the medium confidence (0.400) level revealed four distinct networks: Mef2a/Mef2c, Safb/Safb2, Ncoa5/Pabpc4 and a larger complex including Yes1/Khdrbs1/Hnrnpr/Hnrnpl/Tra2b/Ythdc1/Ddx17. More than half of the interacting proteins, shown in pink, are not known to interact with any of the other proteins in this list. The large number of proteins with no known interactions highlights a general absence of interaction data and a requirement for more protein-protein interaction experiments. This situation is particularly acute for microglia where, other than the data presented in this thesis, no interactome data is available.

**Table 4.3. Mef2c-associated proteins prioritised by SAINTexpress.** The Mef2c-interacting proteins depicted here were detected by MS in either the ionomycin-stimulated Mef2c or IgG control co-IP experiments and surpass the significance threshold  $<0.05$  BFDR. SAINTexpress, which is a statistical method for probabilistically scoring protein-protein interactions from affinity purification MS experiments, was used to statistically score the dataset. The significant interacting proteins have also been ranked based on their CRAPome percentage; the number of negative control experiments (collected using affinity purification followed by MS) that the specific protein is found in (out of 716 experiments). This allows for an easier identification of interacting proteins of high confidence and therefore, of interest. *Title annotations: MW (kDa): molecular weight. Total Score (Sequest HT): total protein score calculated by the summation of the individual scores of each peptide, higher scores reflect better identification. Spec: spectral counts for the bait-prey pair. ctrlCounts: spectral counts in the negative controls. SaintScore: main probability score. FoldChange: average spectral count in test interaction divided by the average in controls, zero counts are replaced by 0.1. BFDR: Bayesian false discovery rate.*

#	Accession	Gene Name	MW (kDa)	Total Score (Sequest HT)	Spec	ctrlCounts	SaintScore	FoldChange	BFDR	CRAPome Score (%)
1	Q3TLX9	Smpd13b	51.6	34.43	14 3 2	0 0 0	0.98	63.33	0	0.84
2	Q60929	Mef2a	53.5	55.63	23 14 9	0 2 0	1	23	0	1.96
4	Q61666	Hira	111.7	24.37	12 2 4	0 0 0	0.98	60	0	2.37
3	Q3V1B5	Mef2c	50.4	249.31	112 92 40	0 0 0	1	813.33	0	2.51
5	A0A0H2UKB6	Mef2c IsoX4	50.3	151.87	60 87 36	0 0 0	1	610	0	2.51
6	E9Q5K9	Ythdc1	85.6	9.05	3 4 9	0 0 0	1	53.33	0	5.87
7	Q91W39	Ncoa5	65.3	242.77	80 89 54	0 0 0	1	743.33	0	6.15
8	B7ZC24	Ncoa5 IsoX1	48	95.73	24 30 30	0 0 0	1	280	0	6.15
9	Q8BH59	Slc25a12	74.5	24.36	17 13 9	0 7 0	0.81	5.57	0.01	9.22
10	Q3TNL1	G6pdx	59.2	16.25	9 3 9	0 0 0	1	70	0	12.43
11	Q8BP60	Nxf1	70.3	14	5 10 2	0 0 0	0.98	56.67	0	15.5
12	Q9Z1A1	Tfg	43	159.95	16 53 30	0 0 0	1	330	0	17.60
13	P62996	Tra2b	33.6	15.72	4 7 5	0 3 0	0.71	5.33	0.04	22.77
14	O88990	Actn3	103	136.41	51 44 16	0 0 0	1	370	0	23.74

Chapter 4 Investigating the effect of ionomycin treatment on the Mef2c interactome

<b>15</b>	Q3TJI7	Yes1	60.6	5.86	3 2 2	0 0 0	0.96	23.33	0.01	25.00
<b>16</b>	Q80YR5	Safb2	111.8	111.35	18 20 48	0 0 0	1	286.67	0	25.84
<b>17</b>	S4R1M2	Safb	105.3	53.49	10 13 24	0 0 0	1	156.67	0	28.77
<b>18</b>	Q9Z0X1	Aifm1	66.7	4.23	2 3 2	0 0 0	0.96	23.33	0.01	31.56
<b>19</b>	Q3TK27	Gnl3	60.7	17.09	3 10 3	0 0 0	0.99	53.33	0	35.75
<b>20</b>	Q3TI61	Psm2	100.2	8.79	3 4 7	0 0 0	1	46.67	0	37.85
<b>21</b>	Q91VR5	Ddx1	82.4	62.1	29 13 18	0 7 0	0.92	8.57	0.01	46.23
<b>22</b>	Q9D0I9	Rars	75.6	12.52	7 9 3	0 3 0	0.73	6.33	0.03	46.51
<b>23</b>	Q60749	Khdrbs1	48.3	128.25	46 51 42	0 2 0	1	69.5	0	48.6
<b>24</b>	A0A2I3BRL8	Rbmxl1	42.2	48.11	16 18 20	0 0 0	1	180	0	49.72
<b>25</b>	Q6PHQ9	Pabpc4	72.2	30.22	13 12 5	0 0 0	1	100	0	52.51
<b>26</b>	A0A1L1STE4	Ilf3	97.4	10.43	4 4 7	0 0 0	1	50	0	52.93
<b>27</b>	Q3U8W9	Hnrnpr	70.8	10.75	6 5 6	0 3 0	0.76	5.67	0.03	58.94
<b>28</b>	G5E924	Hnrnpl	66.9	20.56	8 10 11	0 6 0	0.76	4.83	0.02	64.25
<b>29</b>	Q3TF40	Nono	60.4	11.5	8 3 6	0 0 0	1	56.67	0	70.53
<b>30</b>	Q3U741	Ddx17	72.5	45.81	19 15 11	0 4 0	0.96	11.25	0	73.04

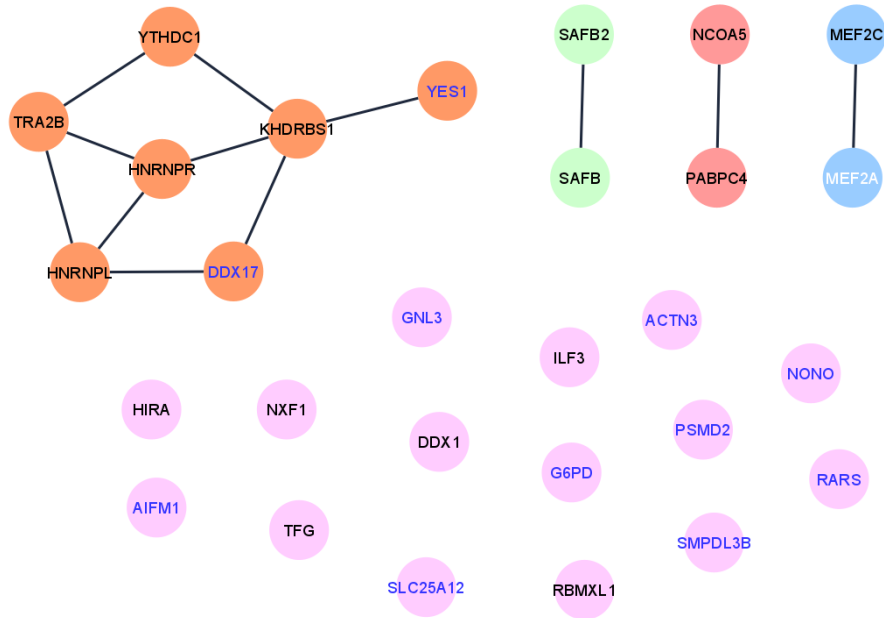


**Figure 4.7. Fold change and SAINT score output from SAINTexpress.** Visualisation of output from SAINTexpress on proteins identified by MS after ionomycin treatment. Log<sub>2</sub> fold change is plotted against SAINT score, the probability that a protein is an interactor of Mef2c. The red lines represent cut offs set at  $\geq 0.7$  for SAINT score and  $\geq 3$  for fold change. This leaves a clear group of high confidence interacting proteins in the top right corner. These proteins include Mef2a, Ncoa5, Hira, Smpd3b, and Yes1. Proteins are coloured according to their CRAPome score (%). Proteins not in the CRAPome database are assigned a score of 100%.

**Table 4.4. Spectral counts for Mef2c, Hdac4, Hdac5, and Cabin1 in unstimulated and stimulated datasets.** Accession numbers, gene names, spectral counts, SAINT scores and BFDR scores from each dataset (unstimulated vs. stimulated) are presented in the table below. This shows that similar spec counts for both isoforms of Mef2c were detected in the unstimulated and stimulated datasets. The table also shows that Hdac4, Hdac5 and Cabin1 are no longer significant high confidence interactors of Mef2c.

Accession Number	Gene Name	Unstimulated			Stimulated		
		Spec Counts	SAINT Score	BFDR	Spec Counts	SAINT Score	BFDR
Q6NZM9	Hdac4	28 31 26	1	0	4 2 0	0.65	0.2
B7ZDF5	Hdac5	22 28 26	1	0	6 0 0	0.33	0.4
B9EKC5	Cabin1	23 43 3	1	0	4 0 0	0.33	0.42
Q3V1B5	Mef2c Isoform 1	88 96 69	1	0	112 92 40	1	0
A0A0H2UKB6	Mef2c Isoform X4	79 85 78	1	0	60 87 36	1	0





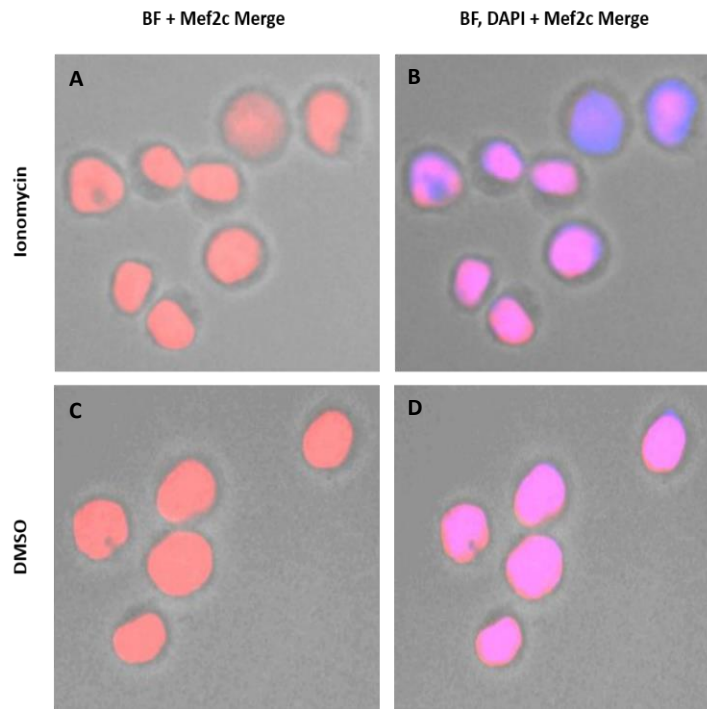
**Figure 4.8. Protein-protein interaction networks of Mef2c-associated proteins.** Interactions between all Mef2c-associated proteins extracted from the STRING v11.5 database. Four distinct networks have been identified which are represented by different colours. Half of the Mef2c-associated proteins were found to have no known interactions with the other proteins (pink). Known interacting proteins are represented by white text and proteins unique to the stimulated dataset are represented by dark blue text.

#### 4.2.5.3 Known interactors

All 30 identified Mef2c interacting proteins were compared to a list of known interactors obtained from NCBI (section 3.2.4.3, Table 3.5, Appendix 1). Mef2a, another member of the MEF2 family and a previously characterised interactor, was again identified as a significant Mef2c-associated protein. The presence of Mef2a in this dataset increases the confidence of the other novel interacting proteins.

#### 4.2.5.4 Subcellular location of Mef2c interactors

Interestingly, the subcellular location of several of the identified interactors is in the cytoplasm. To clarify whether ionomycin stimulation is resulting in the translocation of Mef2c out of the nucleus and into the cytoplasm, BV2 cells were stimulated with either 1  $\mu$ M ionomycin or DMSO for 1h prior to immunocytochemistry using a monoclonal anti-Mef2c antibody to visualise the localisation of Mef2c in BV2 cells (Figure 4.9). Merging images of Mef2c staining with brightfield, to show the whole cell, and DAPI stain, to visualise the location of the nucleus, it was determined that Mef2c was present in the

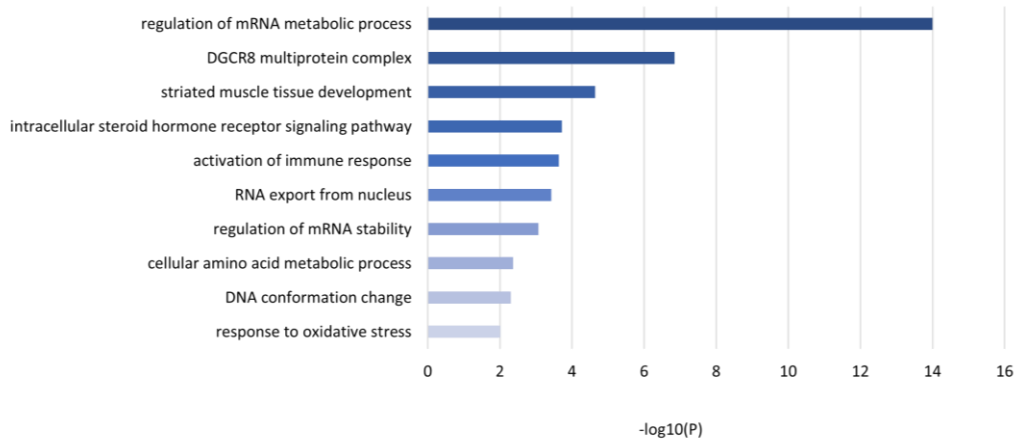


**Figure 4.9. Subcellular location of Mef2c after ionomycin stimulation.** BV2 cells were stimulated with either 1 $\mu$ M ionomycin or DMSO for 1h prior to fixation and analysis by immunocytochemistry using a monoclonal anti-Mef2c antibody. No differences in the subcellular location of Mef2c were observed between conditions. Mef2c and DAPI stains overlap to show that Mef2c is localised in the nucleus in both ionomycin- and DMSO-treated cells. **(A)** Merged image of ionomycin-treated cells under brightfield (BF) and Mef2c (RFC). **(B)** Merged image of ionomycin-treated cells under brightfield (BF), DAPI to visualise the nucleus and Mef2c (RFC). **(C)** Merged image of DMSO-treated cells under brightfield (BF) and Mef2c (RFC). **(D)** Merged image of DMSO-treated cells under brightfield (BF), DAPI and Mef2c (RF).

nucleus of BV2 cells after treatment with both DMSO and ionomycin. This confirms that Mef2c is not translocating to the cytoplasm after ionomycin treatment.

#### 4.2.6 Functional annotation of Mef2c interactors in ionomycin-treated cells

All identified Mef2c-interacting proteins (n=30) were annotated using Metascape's gene ontology enrichment analysis. Several biological processes were identified with the top five processes including regulation of mRNA metabolic process, DGCR8 multiprotein complex, striated muscle tissue development, intracellular steroid hormone receptor signalling pathway and activation of the immune response (Figure 4.10). The activation of the immune response is a cell-type specific process which highlights the importance of studying protein-protein interactions in specific and disease-relevant cell types. Sphingomyelin phosphodiesterase acid like 3B (Smpd13b) and YES proto-oncogene 1 (Yes1) are two



**Figure 4.10. Biological process annotations for Mef2c-associated proteins identified by co-IP-MS in ionomycin-treated BV2 cells.** Metascape's enrichment analysis was used to determine which biological process were enriched in the list of Mef2c-interactors. The data are presented in a heatmap, coloured by p-value, of enriched terms linked to the list of proteins. The  $-\log_{10}(P)$  score of each process is graphed whereby larger values indicate a more significant association.

identified Mef2c-associated proteins which have been assigned to this biological process annotation and are of particular interest.

Smpdl3b is a GPI-anchored, lipid-modulating phosphodiesterase with a CRAPome score of 0.84% making it a high confidence interactor. This protein plays a role in membrane fluidity and lipid composition and is active on the surface of dendritic cells and macrophages (Heinz et al., 2015; Mitrofanova et al., 2019; Yoo et al., 2015). Yes1 is a protein tyrosine kinase involved in range of biological processes including cell survival, cell growth and apoptosis (Jung et al., 2011; Tausin et al., 2011). No previous associations between Smpdl3b or Yes1 and Mef2 family members have been reported in the literature. Both proteins do not appear in the unstimulated data set so may rely on the dissociation of Hdac4/5 and Cabin to interact with Mef2c. The peptide data for these interactors of interest are provided in Table 4.5.

#### 4.2.7 Comparison of unstimulated and stimulated datasets

To determine the similarities and differences between the unstimulated and stimulated datasets, significant interacting proteins ( $<0.05$  BFDR) from each set of experiments were directly compared. Figure 4.11 depicts the overlap between the two datasets showing that 18 proteins (including Mef2c isoforms 1 and X4) are shared between the two datasets. 12 proteins are unique to the stimulated dataset whereas 92 proteins are found only in the

**Table 4.5 MS data for the Mef2c-associated proteins of interest; Smpdl3b and Yes1.** The table shows the peptide sequences of the putative novel interactors Smpdl3b and Yes1. Peptide sequences identified by MS are presented for each interactor together with the peptide count and percentage coverage values generated from each biological replicate.

Protein of Interest	Peptide Sequences	Mass Spectrometry Data
<b>Yes1</b>  541 amino acids 60.6 kDa  CRAPome Score: 25%	WTAPEAALYGR  EVLEQVER  IADFLGAR  GSLDLFLK	<b>MEF2C 1</b>  Coverage: 5% Peptide Count: 3  <b>MEF2C 2</b>  Coverage: 3% Peptide Count: 2  <b>MEF2C 3</b>  Coverage: 3% Peptide Count: 2
<b>Smpdl3b</b>  456 amino acids 51.6 kDa  CRAPome Score: 0.84%	ATLNLKDLVTYFLNLR  DLVTYFLNLR  EIEPKPDFILWTGDDTPHVPNESLGAAVLAIVER  ESFNEEYLK  IASEPHILQR  LTEAYQVPDASVSSMHTALTR  TTLPGVVDGANNPGIR  VIAGQFFGHHHTDSFR  VYAALGNHDFHPK  YYVYNSVSYNHLTCEDSCR	<b>MEF2C 1</b>  Coverage: 33% Peptide Count: 10  <b>MEF2C 2</b>  Coverage: 9% Peptide Count: 3  <b>MEF2C 3</b>  Coverage: 4% Peptide Count: 2

unstimulated samples. The proteins assigned to each of these categories are presented in Table 4.6. The overlap between the two datasets increases confidence in the 18 shared interactors as they have reached significance in six separate experiments.

#### 4.2.7.1 STRING

Known functional relationships between the significant Mef2c interactors from both datasets were viewed in STRING (Szklarczyk et al., 2019) (Figure 4.12). Six out of 11 stimulated only interactors and 17 out of 18 shared interactors are found in the main STRING complex. However, 11 Mef2c-associated proteins (five stimulated only and one shared) did not interact with any other proteins in either dataset. This highlights that most

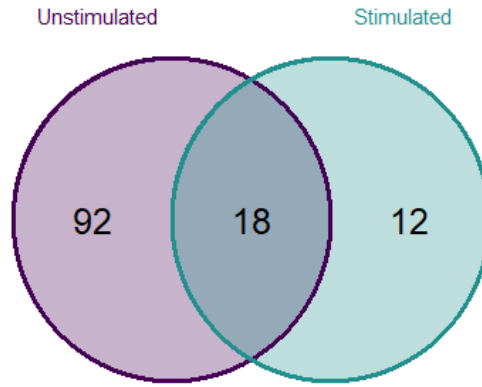
Chapter 4 Investigating the effect of ionomycin treatment on the Mef2c interactome

**Table 4.6 Mef2c-associated proteins from unstimulated and stimulated datasets.** Proteins identified by MS and prioritised by SAINT as putative interactors of Mef2c (<0.05 BFDR) in both unstimulated and stimulated BV2 cells. Each interactor is identified by its Uniprot accession number and gene name. Proteins are organised based on their occurrence in the datasets; common between both or unique to either stimulated or unstimulated.

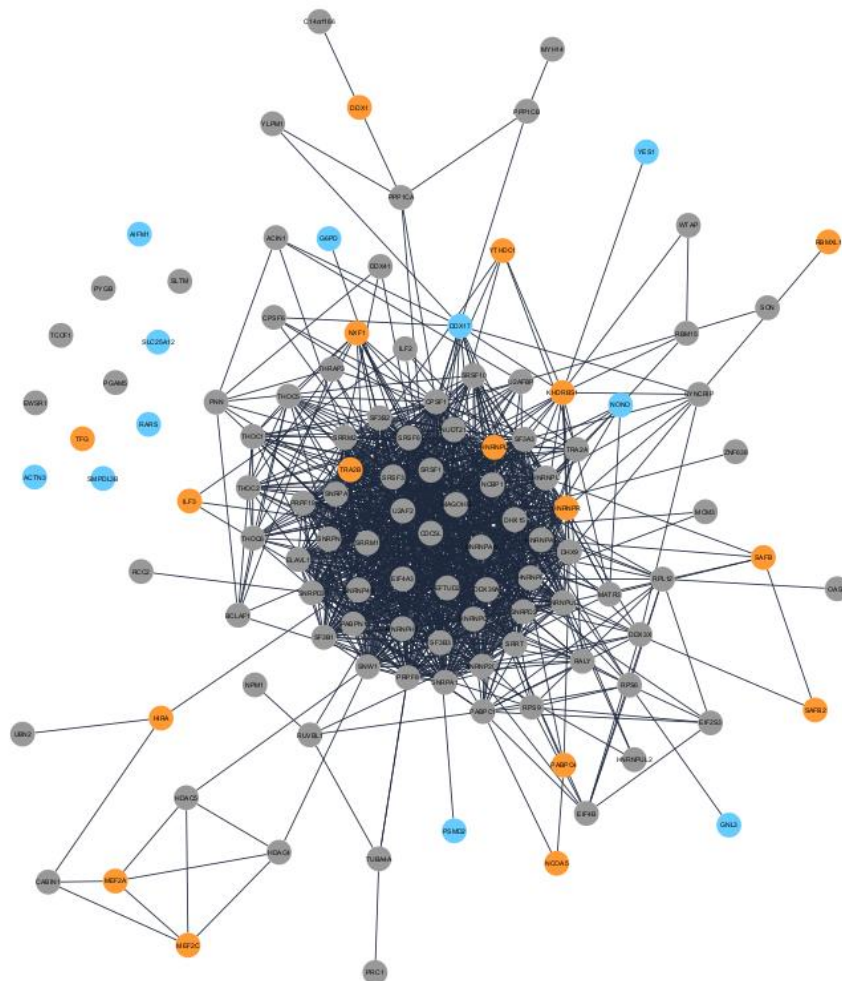
Common Interactors	Stimulated Only	Unstimulated Only				
A0A0H2UKB6 Mef2c Isoform X4	B7ZC24 Ncoa5 Isoform X1	A0A023T778 Magohb	G3UY42 Pabpn1	Q00PI9 Hnrnpul2	Q3UYX6 Srsf10	Q8BT18 Srrm2
A0A1L1STE4 Ilf3	Q88990 Actn3	A0A087WQ92 Hdac4 Isoform 2	G5E866 Sf3b1	Q0VBL3 Rbm15	Q3UZG3 Hnrnpa3	Q8C2Q7 Hnrnp1
A0A2I3BRL8 Rbmx1l	Q3TF40 Nono	A0A0A0MQA5 Tuba4a	H3BJW3 Cpsf6	Q14C24 U2af1	Q52K18 Srrm1	Q8CH25 Sltm
E9Q5K9 Ythdc1	Q3TI61 Psmc2	A0A0B4J1E2 Snw1	H3BL37 Tcof1	Q3T9L0 Ddx49	Q569Z6 Thrap3	Q8K019 Bclaf1
G5E924 Hnrnp1	Q3TJI7 Yes1	A0A0H2UH28 Mef2c Isoform X9	H7BX95 Srsf1	Q3TFQ8 Pygb	Q5BLK1 Rps6	Q8R3N6 Thoc1
P62996 Tra2b	Q3TK27 Gnl3	A0A0N4SV80 Zfp638	H9KV00 Son	Q3THB0 Eif4b	Q5SUS9 Ewsr1	Q8VDM6 Hnrnpul1
Q3U8W9 Hnrnpr	Q3TLX9 Smpdl3b	A0A0R4J0J6 Thoc5	K3W4R2 Myh14	Q3TQX5 Ddx4x	Q5U4D9 Thoc6	Q8VI94 Oas1
Q3V1B5 Mef2c Isoform 1	Q3TNL1 G6pdx	A0A1S6GWJ4 Ddx41	Q3S286 Dhx15	Q3TUQ5 Pnn	Q62189 Snrpa	Q91VC3 Eif4a3
Q60749 Khdrbs1	Q3U741 Ddx17	A0A2R8VK76 Cpsf1	P26369 U2af2	Q3TVV6 Hnrnpu	Q64012 Raly	Q99KP6 Prpf19
Q60929 Mef2a	Q8BH59 Slc25a12	A1A4A7 Pgam5	P29341 Pabpc1	Q3TWW8 Srsf6	Q6A06 Cdc5l	Q99MR6 Srrt
Q61666 Hira	Q9D019 Rars	B1AZI6 Thoc2	P35979 Rpl12	Q3U1C2 Ruvbl1	Q6A0E3 Eftud2	Q99PV0 Prpf8
Q6PHQ9 Pabpc4	Q9Z0X1 Aifm1	B2RSV4 Sf3b3	P57784 Snrpa1	Q3U536 Npm1	Q6N2M9 Hdac4	Q9CQE8 RTRAF
Q80YR5 Safb2		B7ZDF5 Hdac5	P62137 Ppp1ca	Q3U6P5 Hnrnpc	Q6P4T2 Snrnp200	Q9CQF3 Nudt21
Q8BP60 Nxf1		B9EKC5 Cabin1	P62141 Ppp1cb	Q3UAI4 Sf3b2	Q6PE01 Snrnp40	Q9D554 Sf3a3
Q91VR5		D3YWX2	P62317	Q3UI57	Q6ZQ61	Q9JIX9

Chapter 4 Investigating the effect of ionomycin treatment on the Mef2c interactome

<b>Ddx1</b>		<b>Ylpm1</b>	<b>Snrpd2</b>	<b>Mcm3</b>	<b>Matr3</b>	<b>Acin1</b>
<b>Q91W39</b> <b>Ncoa5 Isoform 1</b>		E0CYH0 <b>Wtap</b>	P62320 <b>Snrpd3</b>	Q3UIJ2 <b>Eif2s3x</b>	Q6ZWN5 <b>Rps9</b>	Q9Z2X1 <b>Hnrnpf</b>
<b>Q9Z1A1</b> <b>Tfg</b>		E9QNN1 <b>Dhx9</b>	P63163 <b>Snrpn</b>	Q3UK83 <b>Hnrnpa1</b>	Q7TMK9 <b>Syncrip</b>	
<b>S4R1M2</b> <b>Safb</b>		E9QP00 <b>Tra2a</b>	P70372 <b>Elavl1</b>	Q3UXI9 <b>Ilf2</b>	Q80WC1 <b>Ubn2</b>	
		G3UWQ7 <b>Prc1</b>	P84104 <b>Srsf3</b>	Q3UYV9 <b>Ncbp1</b>	Q8BK67 <b>Rcc2</b>	



**Figure 4.11. Venn diagram to depict the overlap between stimulated and unstimulated datasets.** After filtering using SAINT (<0.05 BFDR) 110 proteins were classed as significant in the unstimulated dataset and 30 proteins were deemed significant in the stimulated. This diagram depicts the number of common proteins shared between the two datasets (18). This leaves 12 proteins unique to the stimulated dataset and 92 proteins unique to the unstimulated.

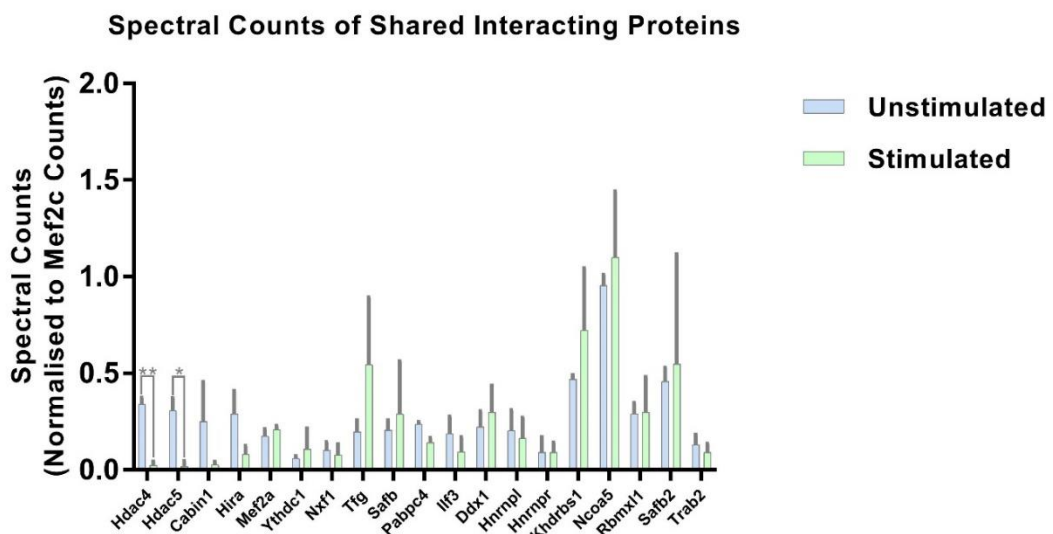


**Figure 4.12. Protein-protein interaction network of all Mef2c interacting proteins.** Interactions between all Mef2c-associated proteins from both unstimulated and stimulated datasets extracted from the STRING v11.5 database. Proteins are colour coded according to the experiments they were identified in; interactors identified in stimulated only (blue), interactors identified in unstimulated only (grey) and interactors identified in both (orange).

of the interactors identified in the stimulated dataset are found in similar networks to the proteins identified in the unstimulated dataset. This suggests that Mef2c interactors may work in similar networks and be involved in similar biological functions.

#### 4.2.7.2 Spectral counts

Spectral counts for the 16 proteins that were detected in both datasets, asides from Mef2c, and the counts of the three repressors (Hdac4, Hdac5 and Cabin1) were directly compared and statistically analysed (Figure 4.13). Spectral counts from each biological replicate were first normalised to the spectral counts of the bait protein Mef2c. This accounts for the variation in the number of Mef2c peptides immunoprecipitated across each repeat and allows for ease of comparison and downstream analysis between stimulated and unstimulated datasets in case ionomycin changes the affinity of the antibody to Mef2c. Multiple T-tests were used to test for significant differences between the average spectral count of each protein in the unstimulated and stimulated datasets. Statistical significance was determined using the Holm-Sidak method as recommend by Prism, with a p-value of <0.05 deemed statistically significant. Treating BV2 cells with ionomycin significantly reduced the spectral count of both Hdac4 (M1= 0.34, M2= 0.023, t(4)=13.57, p=0.003) and Hdac5 (M1= 0.31, M2= 0.016, t(4)=6.921 p=0.04) compared to unstimulated cells. No other significant differences between interactors were noted however a non-significant reduction



**Figure 4.13. Spectral counts of shared interacting proteins and key Mef2c repressors.** Treating BV2 cells with ionomycin reduces the abundance, as measured by spectral counts, of both Hdac4, Hdac5, and, to a lesser extent, Cabin1 compared to unstimulated cells confirming the dissociation of these primary repressors from Mef2c (p≤.05 = \*, p≤.01 = \*\*).



in spectral count was also detected in Cabin1 ( $M1= 0.25$ ,  $M2= 0.027$ ,  $t(4)=1.88$ ,  $p=0.883$ ). These data confirm that Hdacs 4 and 5 and, to a lesser extent, Cabin1 dissociate from the Mef2c complex following ionomycin treatment.

#### 4.2.7.3 MAGMA

Finally, MAGMA (de Leeuw et al., 2015) was used to investigate the relevance of identified Mef2c interactors to AD-risk. The overall enrichment of AD-risk within the unstimulated and stimulated Mef2c interactor sets was tested. For both gene sets, unstimulated ( $p=0.17156$ ) and stimulated ( $p=0.37242$ ), there was no significant enrichment of AD association signals. This suggests that the identified Mef2c interactors are not significantly associated with AD-risk.

### 4.3 Discussion

In unstimulated BV2 cells, Mef2c is predominately being held in a repressed state by Hdac4, Hdac5, and Cabin1. The experiments described in this chapter revealed that ionomycin treatment, that is known to increase intracellular  $[Ca^{2+}]$ , results in the dissociation of the main repressive proteins from Mef2c. This allows Mef2c to form some new interactions. However, no additional transcription factors were identified suggesting that there is no Mef2c activating complex that binds to Mef2c and enhances its transcriptional activity following the dissociation of Hdac4, Hdac5, and Cabin1.

#### 4.3.1 Further validation of distinct Mef2c isoforms in BV2 cells

The presence of peptides mapping to different Mef2c isoforms in these ionomycin-treated experiments suggests that BV2 cells express several Mef2c isoforms. As isoforms 1 and X4 were identified again, this offers further support for their expression in BV2 cells. The abundance of the isoforms in each dataset do not drastically differ so it is not likely that ionomycin treatment is affecting the splicing of Mef2c and subsequent expression of each isoform. Stimulating BV2 cells with ionomycin also does not appear to induce phosphorylation of Mef2c at different sites as no new phosphorylation sites were identified.

#### 4.3.2 Co-immunoprecipitation of the known interactor Mef2a

Due to the dissociation of known interactors Hdac4 and Hdac5, only one known interacting protein, Mef2a, was identified in the stimulated co-IP-MS experiments. The identification of Mef2a strengthens the validity of the data; any identified novel interactors are therefore of high confidence. Other high confidence interactors from the unstimulated dataset including Hira and Ncoa5 were also identified. These data show that ionomycin has not destroyed all interactions or had a detrimental impact on cell viability. Thus, the method of increasing intracellular  $[Ca^{2+}]$  using ionomycin to release Mef2c from its repression was successful and appropriate.

#### 4.3.3 Gene ontology analysis reveals involvement of Mef2c in several biological processes

Gene ontology analysis showed that several biological processes, similar to those identified in the unstimulated dataset, were enriched in the dataset. This suggests that Mef2c is involved, through its interactions with other proteins, in several processes including regulation of mRNA metabolic process, striated muscle tissue development and activation

of the immune response. mRNA metabolic process includes chemical reactions or pathways that are involved in carrying mRNA to ribosomes for protein assembly. Therefore, the proteins identified for this GO term are involved in the modulation of these mechanisms. These proteins include YTH domain containing 1 (Ythdc1) which regulates alternative splicing; a process important for protein diversity, nuclear RNA export factor 1 (Nxf1) which is involved in the export of mRNA from the nucleus, and transformer 2 beta homolog (Tra2b) which helps to control pre-mRNA splicing (Grüter et al., 1998; Roundtree et al., 2017; Tacke et al., 1998). As discussed in Chapter 3 (section 3.3.3), it is possible that Mef2c is involved in the export of mRNA from the nucleus since proteins that aid this process are recruited to mRNA via interactions with transcription factors (Katahira, 2015). Thus, an interaction with Nxf1 could not be excluded. However, interactions between splicing factors and Mef2 family members have not been previously demonstrated. Caution in the interpretation of these interactions must be taken due to the lack of evidence for the involvement of MEF2 factors in splicing.

Striated muscle tissue development is another biological process enriched in the dataset. This term includes proteins that play a role in the progression of striated muscle from formation to mature structure. Proteins assigned to this group include alpha-actinin-3 (Actn3), which is a component of the sarcomeric Z line in skeletal muscle (Mills et al., 2001). In addition, Mef2c and Mef2a have been assigned to this group as they play vital roles in the development and function of skeletal muscle (Anderson et al., 2015; Black & Olson, 1998). Thus, the interaction between Mef2c and other proteins in muscle development is unsurprising given the well-documented role of Mef2c in this process. The fact that this biological process has been flagged in the GOA reflects the canonical role of the MEF2 protein family in muscle development. Thus, research into Mef2c in other cell types is needed to expand the understanding of the function of Mef2c outside of muscle cells.

Interestingly, the GOA also revealed activation of the immune response as another process enriched in the dataset. Several identified proteins were related to this process, two of which, Yes1 and Smpd13b, have low CRAPome scores and are of particular interest (see section 4.3.5). The identification of an immune-specific process, which is unlikely to be identified in cell types such as muscle, highlights the importance of studying protein:protein interactions in specific cellular models.

#### 4.3.4 Ionomycin-treatment releases Mef2c from its repressed state

Ca<sup>2+</sup> signalling has been shown to dissociate HDAC4 and HDAC5 from MEF2 which allows MEF2 to bind to other cofactors to promote the expression of genes important for the regulation of myogenesis (Mckinsey et al., 2000b; Stewart & Crabtree, 2000) (Figure 4.1). Similarly, increases in [Ca<sup>2+</sup>] result in the release of the CABIN1 repressive complex from HIRA which leads to enhanced transcriptional activity of MEF2D (Jang et al., 2007; Robinson & Dilworth, 2018; Youn & Liu, 2000). Based upon these studies, it was hypothesised that stimulating BV2 cells with ionomycin to increase intracellular [Ca<sup>2+</sup>] prior to co-IP-MS may alleviate the repression of Mef2c by both Cabin1 and Hdac4/5 in BV2 cells.

This phenomenon has been verified in microglia-like cells with endogenously-expressed proteins and without recourse to reconstituted protein complexes. Comparison of the stimulated and unstimulated datasets reveals a dramatic reduction in the abundance of Hdac4, Hdac5, and Cabin1 following ionomycin treatment. These data suggest that Hdac4, Hdac5, and Cabin1 have dissociated from Mef2c resulting in a partial relief of repression. Release of Mef2c from its repressed state might be expected to result in new interactions between Mef2c and other transcriptional activators. For example, Mef2c would be expected to interact with other transcription factors as these proteins exist in multi-protein complexes that regulate target gene expression (Adcock & Caramori, 2009; Martin, 1991). However, after the apparent release of Mef2c from its repression, no new transcription factors were identified. These data suggest that in the absence of additional co-activators, Mef2c would still be unable to form transcriptional active complexes that facilitate gene expression. However, the histone regulator Hira is still identified as an interactor after ionomycin treatment. In the absence of CABIN1, HIRA has been previously shown to interact with MEF2D and enhance transcriptional activity (Yang et al., 2011). Thus, as the abundance of Cabin1 has been reduced, this could allow Hira to enhance the transcriptional activity of Mef2c and contribute to the activation of Mef2c target genes.

One explanation for the lack of a Mef2c activation complex, if one exists in BV2 cells, is that another signal may be required to form a transcriptionally active complex. Ca<sup>2+</sup> alone may only be sufficient to dissociate the repressor proteins from Mef2c, allowing Hira to potentially promote transcriptional activity. The binding of additional cofactors, formation of a new complex and the further promotion of Mef2c transcriptional activation may rely on another, as yet unidentified, stimulus. It is also possible that some of the novel proteins recruited to the Mef2c complex after ionomycin treatment can function as co-activators.

#### 4.3.5 Co-IP identifies two potential novel interacting proteins

It was hypothesised that stimulating BV2 cells with ionomycin to increase intracellular  $[Ca^{2+}]$  would release Mef2c from its repressed state and allow it to form new interactions. After comparison of the unstimulated and stimulated datasets, 12 proteins were identified as new interactors. Of the 12 new proteins in the Mef2c interactome in ionomycin-treated cells, *Yes1* and *Smpdl3b* may be of particular interest because they are microglial A $\beta$  response proteins (MARPs) (Monasor et al., 2020). MARPs are microglial proteins that progressively change in response to the accumulation of A $\beta$ . More specifically, *Smpdl3b* was found to be downregulated in middle stages of A $\beta$  deposition whereas *Yes1* was found to be downregulated in advanced stages suggesting a role for both proteins in the microglial response to A $\beta$  accumulation. Additionally, *Smpdl3b* has been found to be upregulated by inflammatory stimuli and identified as a negative regulator of Toll-like receptor signalling suggesting an involvement in the modulation of pro-inflammatory mechanisms (Heinz et al., 2015). As Mef2c is also involved in the response of microglia to immune challenges (Deczkowska et al., 2017), it is not surprising that these proteins may interact with each other to regulate the immune response. Both *Yes1* and *Smpdl3b* only appear in the ionomycin-treated data set so may rely on the dissociation of Hdac4/5 and Cabin1 to interact with Mef2c.

#### 4.3.6 Limitations

Due to the nature of the experimental design, care must be taken when comparing the unstimulated and stimulated datasets. The stimulation of BV2 cells prior to co-IP-MS was designed as a follow-on experiment so both experiments were not run concurrently. If the experiment was to be re-run, stimulated and unstimulated co-IPs should be compared at the same time using quantitative MS. An additional limitation was highlighted by the identification of several cytoplasmic interactors. The subcellular location of Mef2c after ionomycin treatment was investigated, and it was confirmed that Mef2c was not translocating to the cytoplasm. Thus, it is likely that some of the cytoplasmic interactors in the list are false positives that may have cross-reacted with the Mef2c antibody, a common problem when immunoprecipitating endogenous proteins from cells and tissue. Antibody availability and specificity are arguably the major limitations of the co-IP-MS technique. There are several ways reduce the number of false positives including the use of multiple independent antibodies to replicate interactors (Benson et al., 2017), using proximity labelling methods such as BioID to identify proteins that co-purify with bait protein

attached to biotin ligase negating the requirements for a specific antibody (Roux et al., 2018) or by using Mef2c-knockout cells as a control to further filter out contaminants.

#### 4.3.7 Conclusions

Co-IP-MS of Mef2c in ionomycin-stimulated BV2 cells has been useful for understanding how this transcription factor may operate in response to increased  $[Ca^{2+}]$ . Additionally, the presented interactome is one of very few mapped, dynamic interactomes. Stimulation of BV2 cells with ionomycin to increase intracellular  $[Ca^{2+}]$  prior to co-IP-MS depleted the Mef2c interactome of the three transcriptional repressors, Hdac4, Hdac5, and Cabin1. Although several new proteins such as Yes1 and Smpd13b were identified in the Mef2c interactome after ionomycin treatment, no well characterised transcriptional co-activators appeared to be recruited to the remodelled Mef2c complex. Having shown that ionomycin treatment alters the Mef2c interactome I aimed to determine what effect this treatment may have on chromatin accessibility. Analysis of differentially accessible peaks is likely to shed light on  $Ca^{2+}$ -regulated transcriptional processes in BV2 cells (Chapter 5).

## Chapter 5 Assessing the effect of ionomycin treatment on the chromatin landscape

### 5.1 Introduction

The results from the previous chapter reveal that the repression of Mef2c by Hdac4, Hdac5 and Cabin1 in unstimulated BV2 cells can be partially alleviated by ionomycin stimulation to increase intracellular  $[Ca^{2+}]$ . Having demonstrated that ionomycin treatment results in changes to the Mef2c interactome, the effect of this treatment on chromatin accessibility was investigated. Analysing differential accessibility may illuminate transcriptional processes in BV2 cells that are potentially regulated by  $Ca^{2+}$ .

As discussed in the General Introduction (section 1.2.1), the biophysical state of chromatin partly determines the gene regulatory profile of a cell. In regions of open chromatin where DNA is exposed, transcription factors can interact with regulatory elements to control gene expression. Different cell-types have unique sets of accessible regions containing regulatory elements which dictate cellular function and identity, creating diversity between cell types. For example, changes to chromatin accessibility can be induced by interleukin-33 (IL-33) in microglia. Injection of IL-33 into APP/PS1 mice induces remodelling of chromatin accessibility and transcription factor binding resulting in enhanced phagocytic activity and the amelioration of A $\beta$  pathology (Lau et al., 2020). This study not only shows that external stimuli can induce alterations in chromatin accessibility but that there is a therapeutic potential of reprogramming chromatin profiles of microglia to treat AD. The chromatin state of cells can also change in response to the activation of specific signalling pathways including  $Ca^{2+}$ . Changes in  $[Ca^{2+}]$  can alter chromatin accessibility and result in the opening of chromatin and activation of transcription in peripheral immune cells (Brignall et al., 2017; Zhu et al., 2021). Therefore, it may have similar effects in microglia-like cells.

Chromatin accessibility is regulated via several mechanisms and involves the dynamic interplay between transcription factors, histones, and active chromatin remodellers. Klemm et al (2019) presents four mechanisms that point to an involvement of transcription factors in initiating chromatin remodelling. The first two mechanisms involve interactions between transcription factors, which compete with histones or internucleosomal architectural proteins for DNA access, and chromatin. The other mechanisms involve direct binding of transcription factors to nucleosome DNA or trans interactions with accessible enhancer elements. These models highlight the ability of transcription factors to directly

remodel chromatin. Therefore, determining what transcription factor binding motifs, potentially including motifs for Mef2c, are overrepresented in differentially accessible sites may point to what transcription factors are capable of binding to these sites and potentially, based on the evidence presented above, be involved in initiating Ca<sup>2+</sup>-induced changes to chromatin accessibility.

MEF2C and other Ca<sup>2+</sup>-related transcription factors like NFAT, are thought to play a role downstream of AD-risk genes including *TREM2* and *PLCY2* (Hansen et al., 2018). Other models of Ca<sup>2+</sup>-activated gene expression reveal that the activation of *TREM2* results in the initiation of Ca<sup>2+</sup> signalling which may result in the translocation of MEF2C and NFAT to the nucleus leading to changes in gene transcription (Hogan et al., 2003; Lynch et al., 2005). These Ca<sup>2+</sup>-dependent accessible regions may contain AD-risk SNPs and result in impaired transcriptional control of MEF2C as AD-risk SNPs have been found to be enriched in several microglial open chromatin regions that contain DNA binding motifs for MEF2C (Tansey et al., 2018). This is also relevant for AD generally as the dysregulation of Ca<sup>2+</sup> signalling has been identified as a key AD pathogenic pathway (section 1.1.2.2). Ca<sup>2+</sup> signalling dysregulation in AD has been extensively studied in neurons but little is known about Ca<sup>2+</sup> signalling in microglia (Hemonnot et al., 2019; Tong et al., 2018). Therefore, understanding how Ca<sup>2+</sup> signalling is affecting chromatin accessibility in microglia-like cells and what transcription factors, potentially including Mef2c, are capable of binding these ionomycin-responsive sites is of particular importance and may shed light onto how increases in [Ca<sup>2+</sup>] in AD affect chromatin status in microglia.

To assess the effect of increases in intracellular [Ca<sup>2+</sup>] on chromatin accessibility in microglia-like cells, the assay of transposase accessible chromatin sequencing (ATAC-seq) was used. ATAC-seq is a relatively new technique that has been widely used in the study of chromatin biology. This technique has already been used to elucidate enhancer landscapes in healthy tissue and cells (Fullard et al., 2018), identify changes in accessibility between leukaemia and normal haematopoiesis (Corces et al., 2016; Rendeiro et al., 2016) and evaluate the chromatin states in the prefrontal cortex of schizophrenic patients (Bryois et al., 2018).

In this chapter, ATAC-seq was used to determine the effects of ionomycin treatment on chromatin accessibility in BV2 cells. Chromatin accessibility was compared between ionomycin-stimulated and unstimulated BV2 cells. Differentially accessible regions were annotated to individual genes and motif enrichment analysis was used to determine which



transcription factors are capable of binding to these ionomycin-responsive sites. As Mef2c is a  $\text{Ca}^{2+}$ -sensitive transcription factor (see sections 1.4.5.2 and 4.1), the Mef2c motif is likely to be recovered from differentially accessible peaks after increases in intracellular  $[\text{Ca}^{2+}]$ .

The aims of this chapter were as follows: To identify the transcription factor motifs enriched at ionomycin-responsive differentially accessible sites in BV2 cells, to identify potential genes and processes regulated by  $\text{Ca}^{2+}$ , and to assess the relevance of genes associated with  $\text{Ca}^{2+}$ -regulated microglial peaks to AD-risk using MAGMA. For the sake of clarity, all proteins will be referred to as their unitalicized gene names throughout this chapter.

## 5.2 Results

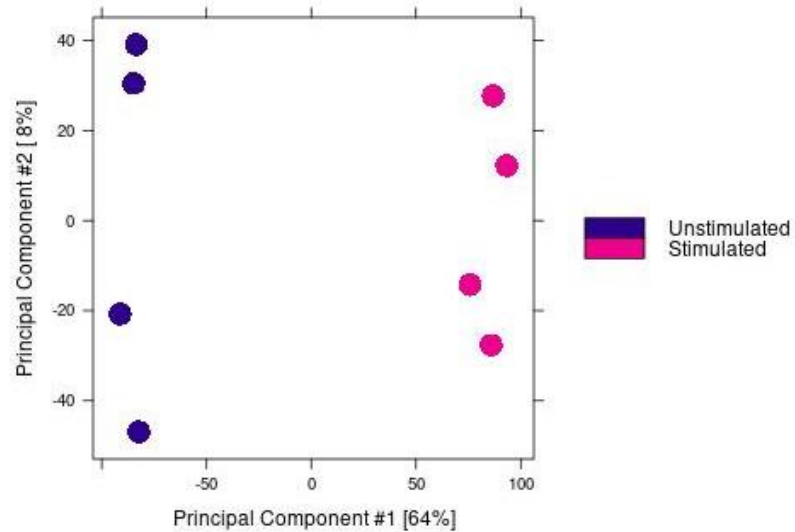
As described in Chapter 2 (section 2.7), BV2 nuclei, either ionomycin-treated or untreated, were incubated with a hyperactive Tn5 transposase enzyme which binds to and selectively excises DNA from open chromatin regions of the genome. The DNA fragments were simultaneously tagged with adapter sequences carried by Tn5 to allow for identification after sequencing. After purification and PCR amplification, DNA fragments were sequenced. Sequencing files were aligned to the mm10 reference genome and processed to remove mitochondrial reads and PCR duplicates (as described in section 2.7.2). The final number of reads per file were counted and peaks were subsequently called from these files. The resulting run metrics are presented in Table 5.1. These data show that a large number of reads and peaks have been recovered from each sample.

### 5.2.1 Principal components analysis

To estimate the variance between the chromatin accessibility of the stimulated and unstimulated cells a principal components analysis (PCA) was run through Diffbind (Stark & Brown, 2011). Figure 5.1 depicts a plot of the first two principal components of the PCA undertaken on all peaks in the normalised dataset. The first two principal components explain 72% of the total variance in the data. The first principal component, which captures 64% of the variance, separates the eight samples based on experimental condition, either ionomycin-stimulated (pink) on the right-hand side of the plot or unstimulated (purple) on the left-hand side of the plot. The second principal component captures 8% of the variance in the data and horizontally separates samples on the y-axis. This separation is likely based on harvest batch. Whilst running the ATAC-seq experiment, cells were harvested and processed in two batches for ease, each with two samples from each condition. This has added variation, but it is much smaller than the experimental variation. Most of the

**Table 5.1. Run metrics for ATAC-seq files.** Shown are the number of reads, peaks, and filtered peaks (after blacklist removal) for each sequencing sample post alignment and processing.

Sample	#Reads	#Peaks	#Filtered Peaks
1_Ionomycin	113340167	113337	113137
2_Ionomycin	114904022	119397	119197
3_DMSO	112014959	111108	110923
4_DMSO	115963854	114013	113826
5_Ionomycin	117331847	118113	117925
6_Ionomycin	121095680	111977	111787
7_DMSO	120517081	108428	108244
8_DMSO	115975032	110870	110671



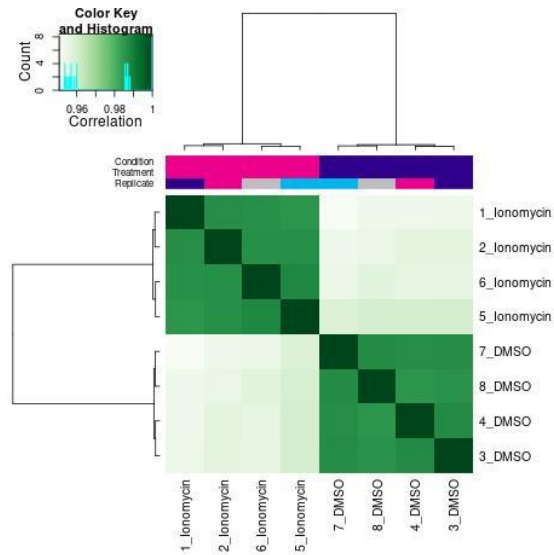
**Figure 5.1. PCA plot of open chromatin site read counts derived from unstimulated and ionomycin-treated BV2 cells.** PCA undertaken on all peaks (stimulated and unstimulated cells) in the normalised dataset. The first principal component explains 64% of the variance in the data and is separating the samples based on experimental condition. The second principal component explains 8% of the variance and separates samples on the y-axis likely by harvest batch. In total, the first two principal components explain 72% of the total variance.

variation in the samples is driven by the experimental condition rather than harvest batch or any other variable.

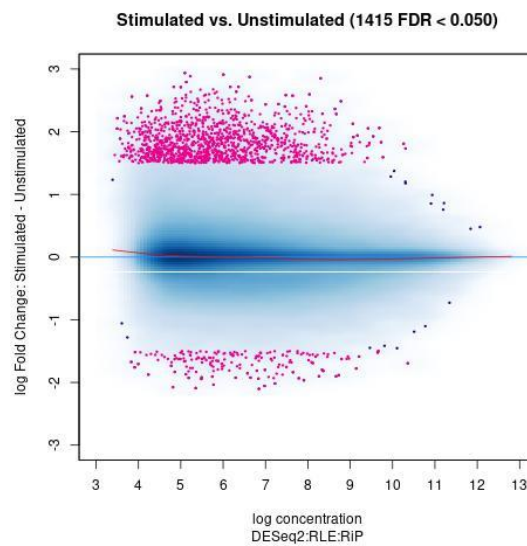
### 5.2.2 Differential accessibility analysis

Prior to running the differential accessibility analysis, a correlation heatmap was plotted based on read counts for each sample (affinity scores) to visualise the correlation between samples (Figure 5.2). All samples appear to be highly correlated, however, the sample groups do separate completely and are more similar within groups than between, highlighting a discernible difference between conditions. Diffbind was then used to identify differentially bound sites between the unstimulated and stimulated conditions after data normalisation (see section 2.7.3). This revealed 41,735 differentially accessible sites. The relationship between the overall Tn5 transposase binding level at each site and the magnitude of change in binding enrichment between conditions is visualised in Figure 5.3. This MA-plot, which is a type of Bland-Altman plot (difference plot) applied to genomic data, shows that there are 1415 differentially accessible sites with a fold change of greater than or equal to 1.5 (fold change applied to reduce noise, see section 2.7.3). 1241 of these sites have increased accessibility after ionomycin treatment whereas 174 have decreased accessibility. To highlight the differential accessibility of the identified peaks, normalised peak files were visualised using IGV. Figure 5.4 shows a general picture of the chromatin

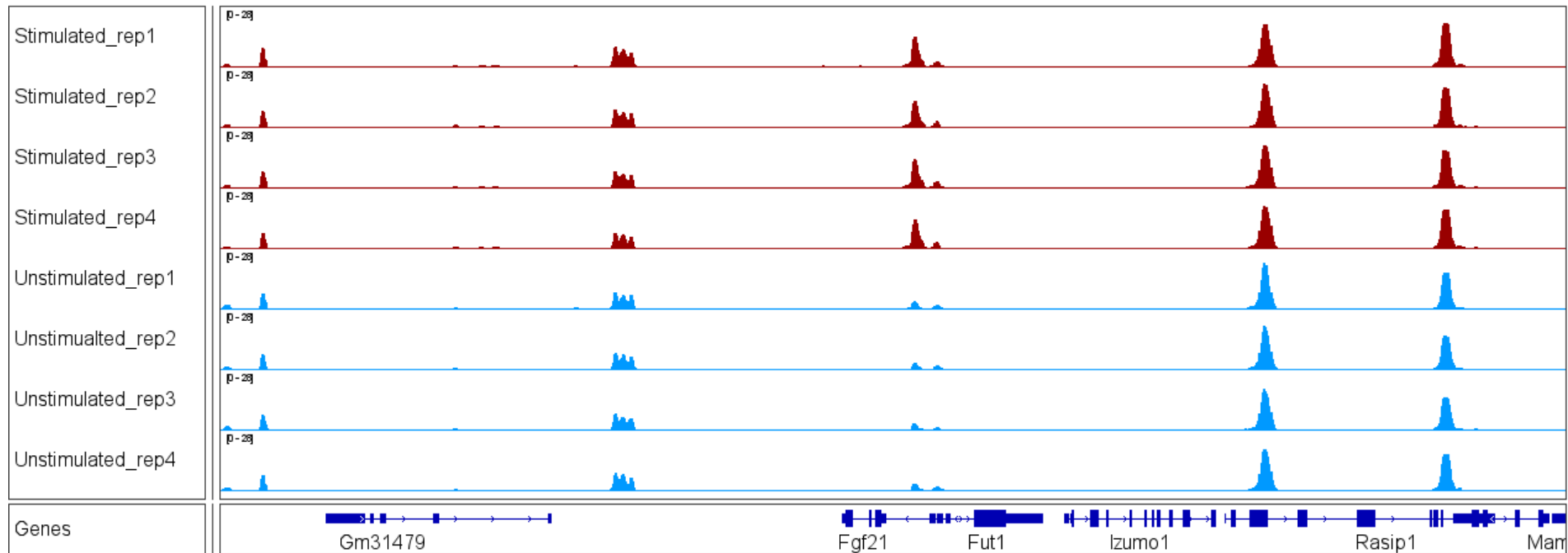
landscape around one differential peak. This demonstrates that there are invariant peaks in the dataset; the majority of accessible sites are apparently unresponsive to increases in intracellular [Ca<sup>2+</sup>]. These data also show that ATAC-seq profiles are highly reproducible when comparing technical replicates.



**Figure 5.2. Correlation heatmap to visualise the relationship between unstimulated and stimulated BV2 cells.** Read counts for each sample (affinity scores) were used to plot this heatmap which shows that there is a high level of correlation between samples. The samples do separate completely based on their condition and samples in each group are more similar to each other than to the samples in the other condition.



**Figure 5.3. MA plot of differentially accessible sites between unstimulated and stimulated BV2 cells.** This plot shows that there are 1415 differentially accessible sites with a fold change of  $\geq 1.5$  in the two conditions. 1241 of these sites have increased accessibility after ionomycin treatment whereas 174 have decreased accessibility.










**Figure 5.4. General picture of the chromatin landscape in stimulated and unstimulated BV2 cells.** Peak files for each replicate were visualised in IGV. This image shows the chromatin landscape surrounding one differential peak. It highlights that there are invariant peaks in the dataset. Ionomycin treatment has not resulted in changes to all chromatin regions, the change in accessibility is specific to certain regions. Peaks are scaled to the highest peak in the display by manually setting the data range for each track to 0-28 (Y-axis).


















5.2.3 *De novo* motif enrichment analysis

HOMER was used for *de novo* motif enrichment analysis to identify potential transcription factor binding sites. Prior to searching differential peaks for enriched motifs, the consensus peaks set, which contains all BV2 peaks, was searched to determine what transcription factor motifs are overrepresented in open chromatin in BV2 cells generally. This will provide a good indication of what the open chromatin landscape looks like in BV2 cells and allow for comparison with the motifs associated with differentially accessible peaks. BV2 open chromatin regions were significantly enriched for 24 transcription factor motifs (Table 5.2). Enriched motifs were matched to several microglial-related transcription factors including the microglia master regulator PU.1 (*Sfpi1*) and CCAAT/enhancer binding protein delta (C/EBPD) which is important for regulating proinflammatory gene expression in microglial activation (Ejarque-Ortiz et al., 2010). Another member of the MEF2 family, Mef2d, which has a very similar motif to Mef2c, was also detected. In fact, Mef2c was the second-best match for this motif. Collectively, these motifs validate the microglial-like chromatin profile of BV2 cells.

**Table 5.2. Enriched motifs in BV2 open chromatin.**

% Targets (proportion of differentially accessible sites containing specified motif); % Background (proportion of background regions (generated by HOMER) containing specified motif).

Rank	Motif	Best Match	% Targets	% Background	p-value
1		Fra1	21.45	3.62	1.00E-12304
2		BORIS	15.43	1.90	1.00E-11024
3		PB0058.1_Sfpi1_1	27.18	8.20	1.00E-8746
4		RUNX(Runt)	13.35	5.99	1.00E-2022
5		Atf2	12.74	6.18	1.00E-1610
6		KLF1	12.15	6.07	1.00E-1425
7		Usf2	9.62	5.66	1.00E-688

8		PB0113.1_E2F3_2	8.10	4.54	1.00E-666
9		Mef2d	2.73	1.04	1.00E-541
10		HAND2	1.89	0.70	1.00E-393
11		ZBTB32	16.16	12.43	1.00E-332
12		CEBPD	3.23	1.71	1.00E-307
13		Stat5a	1.43	0.54	1.00E-290
14		PB0146.1_Mafk_2	0.19	0.01	1.00E-258
15		SIX1	0.15	0.00	1.00E-226
16		NFY	4.36	2080	1.00E-214
17		Unknown-ESC-element(?)	0.25	0.02	1.00E-203
18		TAL1::TCF3	2.29	1.27	1.00E-188
19		Hoxc9	0.13	0.00	1.00E-184
20		Hand1::Tcf3	3.46	2.24	1.00E-164
21		Znf281	0.22	0.03	1.00E-151
22		PB0182.1_Srf_2	2.89	1.86	1.00E-140
23		PB0111.1_Bhlhb2_2	0.13	0.01	1.00E-115
24		POL009.1_DCE_S_II	4.03	3.10	1.00E-74

Interestingly, one of the top motifs matched to brother of regulator of imprinted sites (BORIS), a transcription factor involved in chromatin reorganisation that is not expressed in microglia. However this protein also has an oncogenic role (Janssen et al., 2020). In the immortalisation process of BV2 cells, oncogenes are introduced to the microglial genome. This could explain the presence of this transcription factor in BV2s and in the motif enrichment analysis.

Subsequently, *de novo* motif enrichment analysis was used to identify the potential transcription factor binding sites located in differentially accessible peaks. The consensus peak set, which contains all BV2 peaks, was used as a background. Differentially accessible regions were significantly enriched for ten transcription factor motifs (Table 5.3). The top three motifs were binding sites for Atf4 (target = 35.34%, background = 2.69%, p-value =  $1 \times 10^{-398}$ ), NFATC3 (target = 27.21%, background = 5.91%, p-value =  $1 \times 10^{-141}$ ) and p53 (target = 4.52%, background = 0.84%, p-value =  $1 \times 10^{-25}$ ). These motifs differ from the BV2 enriched motifs which highlights that specific transcription factor motifs are overrepresented in sites associated with ionomycin-induced changes in chromatin accessibility in BV2 cells. The top motifs were aligned to a differential accessible peak to illustrate the presence of these transcription factor binding sites within differentially accessible regions of the genome (Figure 5.5).











Activating transcription factor 4 (*Atf4*) encodes a cAMP-response element binding protein of the same name, which is a master regulator of several signalling pathways including oxidative stress, inflammation, autophagy and protein translation (Pitale et al., 2017). Atf4 belongs to the activating transcription factor/cyclic AMP response element binding protein (ATF/CREB) family of basic region-leucine zipper (bZIP) transcription factors. Protein levels of Atf4 are also significantly upregulated in the brains of AD patients and the abnormal regulation of gene expression by Atf4 has been implicated in AD (Lewerenz & Maher, 2009; Ohno, 2014).

Nuclear factor of activated T-cells 3 (NFATC3) is a known regulator of transcriptional activation. This protein is also known to be activated by  $\text{Ca}^{2+}$ . Calcineurin, a  $\text{Ca}^{2+}$ /calmodulin-dependent protein phosphatase, dephosphorylates and activates NFAT family members (c1-c4) resulting in their nuclear import (Hogan et al., 2003). This leads to the regulation of cytokine expression and alterations to immune cell behaviour (Crabtree & Olson, 2002). Levels of NFAT proteins have been found to be altered in in patients with mild cognitive impairment and AD. Additionally, NFATs have been linked to



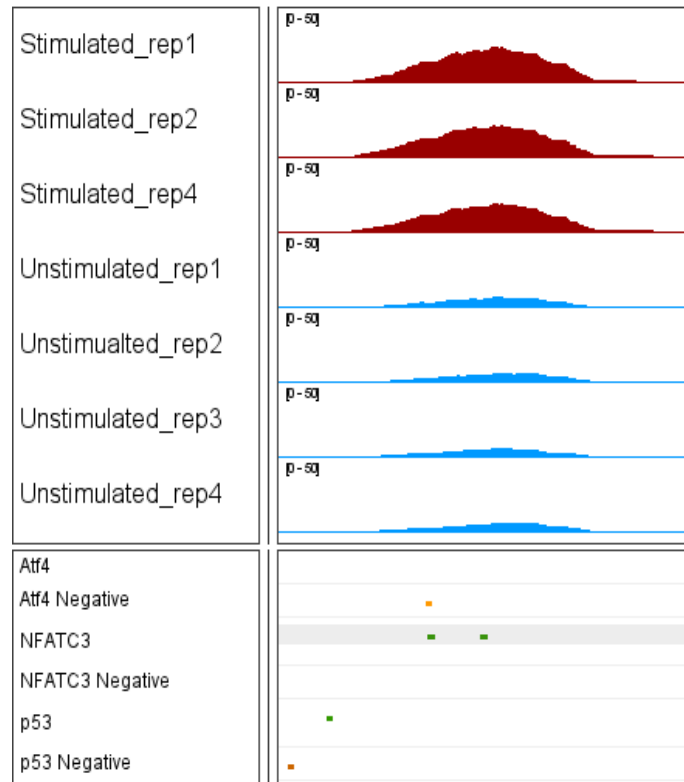
**Table 5.3. Enriched motifs in differentially accessible peaks.**

% Targets (proportion of differentially accessible sites containing specified motif); % Background (proportion of consensus peak regions containing specified motif).

Rank	Motif	Best Match	% Targets	% Background	p-value
1		Atf4	35.34	2.69	1.00E-398
2		NFATC3	27.21	5.91	1.00E-141
3		p53	4.52	0.84	1.00E-25
4		SD0002.1_at_AC_acceptor	7.28	3.01	1.00E-15
5		Bhlha15	2.4	0.42	1.00E-14
6		CHR(?)	2.76	0.57	1.00E-14
7		POU5F1	15.34	8.99	1.00E-13
8		MEIS2	1.13	0.08	1.00E-13
9		Prdm15	1.98	0.34	1.00E-12
10		IRF4	4.17	1.41	1.00E-12

neuroinflammation in early stages of AD and neuronal cell death (Abdul et al., 2009; Luoma & Zirpel, 2008; Shioda et al., 2007). The identification of NFAT acts as a positive control as it is a well-known  $\text{Ca}^{2+}$ -responsive protein suggesting that increases in intracellular  $[\text{Ca}^{2+}]$  are changing the state of chromatin in BV2 cells.

p53 is a tumour-suppressor protein that has well documented roles in many cancers. p53 causes cell cycle arrest in response to DNA damage and can activate apoptosis if the damaged cell cannot re-enter the cell cycle (Vousden & Lane, 2007). Additionally, p53 has










**Figure 5.5. Top motif hits aligned to a differentially accessible region.** Motif sequences, both forward and reverse, were aligned to a differentially accessible region to illustrate the presence of these motifs within differentially accessible areas. Peaks are scaled to the highest peak in the display by manually setting the data range for each track to 0-50 (Y-axis).

been implicated in neurodegenerative diseases. In AD brains p53 expression is significantly increased, predominantly in glial cells, and may play a role in apoptosis (Kitamura et al., 1997). Furthermore, the upregulation of p53 can induce tau phosphorylation (Hooper et al., 2007). The activation of p53 also induces the expression of microRNAs that are important for pro-inflammatory functions and suppress tissue repair and anti-inflammatory mechanisms in microglia (Aloia et al., 2015).

To determine if sites of increased and decreased accessibility are enriched for specific transcription factor motifs, HOMER's *de novo* motif enrichment analysis was also performed on the increased and decreased accessibility peaks individually. In the increased accessibility peaks, seven motifs were found to be significantly enriched in the accessible regions (Table 5.4). The top motif hits included Atf4 (target = 40.13%, background = 2.82%, p-value =  $1 \times 10^{-419}$ ) and NFATC3 (target = 30.62%, background = 5.96%, p-value =  $1 \times 10^{-157}$ ). These two motifs capture a large proportion of peaks with the Atf4 motif covering 498 of 1241 increased accessibility peaks and NFATC3 covering 380 of 1241. In the decreased accessibility peaks, 16 motifs were found to be significantly enriched in the accessible regions (Table 5.5). p53 was found to be the most enriched motif (target = 37.36%,

**Table 5.4. Enriched motifs in increased accessibility peaks.**

% Targets (proportion of differentially accessible sites containing specified motif); % Background (proportion of consensus peak regions containing specified motif).














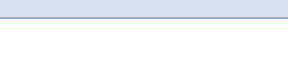
Rank	Motif	Best Match	% Targets	% Background	p-value
1		Atf4	40.13	2.82	1.00E-419
2		NFATC3	30.62	5.96	1.00E-157
3		ALX3	20.31	10.89	1.00E-21
4		POL002.1_INR	4.92	1.26	1.00E-17
5		POL009.1_DCE_S_II	1.77	0.18	1.00E-14
6		SD0002.1_at_AC_acceptor	3.3	0.79	1.00E-13
7		RORA	2.58	0.49	1.00E-13



background = 2.49%, p-value =  $1 \times 10^{-56}$ ). The p53 motif also captures a large proportion of decreased accessibility peaks, 66 of 174. This suggests that different motifs are associated with ionomycin-induced increases and decreases in chromatin accessibility.

In the *de novo* enrichment analysis, sequences enriched in OCRs are compared to a database of known transcription factor motifs. HOMER reports both the transcription factor with the closest match to the motif and also similar transcription factor motifs found. Other transcription factors, besides from Atf4, NFATC3 and p53, could be capable of binding the enriched motifs in differentially accessible regions. Therefore, the motifs of the top three transcription factors were checked against the other similar matches in the HOMER output. For NFATC3 the top motif matches included NFATC3, NFAT, NFATC1 and NFATC2. It is unsurprising that these factors target very similar motifs as they are all members of the same NFAT transcription factor family. Interestingly, Nfatc2 was used in Chapter 4 (section 4.2.1) to test the effect of ionomycin treatment on BV2 cells. Dephosphorylation of Nfatc2 was detected after ionomycin stimulation suggesting that it is

**Table 5.5. Enriched motifs in decreased accessibility peaks.**

% Targets (proportion of differentially accessible sites containing specified motif); % Background (proportion of consensus peak regions containing specified motif).

Rank	Motif	Best Match	% Targets	% Background	p-value
1		p53	37.36	2.49	1.00E-56
2		ZNF416	21.84	2.27	1.00E-25
3		GATA4	9.2	0.24	1.00E-19
4		NFYB	52.3	22.35	1.00E-17
5		ZNF341	8.05	0.22	1.00E-17
6		Prdm15	7.47	0.19	1.00E-16
7		NEUROD1	9.2	0.54	1.00E-14
8		Tcf7	9.77	0.65	1.00E-14
9		NFIA	5.75	0.11	1.00E-14
10		Hnf1	5.75	0.11	1.00E-13
11		FOXB1	8.62	0.48	1.00E-13
12		Sox5	5.75	0.13	1.00E-13
13		PB0208.1_Zscan4_2	6.32	0.2	1.00E-12
14		SOX10	5.75	0.16	1.00E-12

15		PB0090.1_Zbtb12_1	16.67	3.27	1.00E-12
16		Sox6	12.64	1.76	1.00E-12

being translocated to the nucleus in response to increases in  $[Ca^{2+}]$ . In the nucleus, Nfact2 is capable of binding to the NFATC3 motif associated with ionomycin-induced changes in chromatin accessibility. However, it is unclear, without directly testing transcription factor binding, which of these family members, if any, bind to this overrepresented motif.

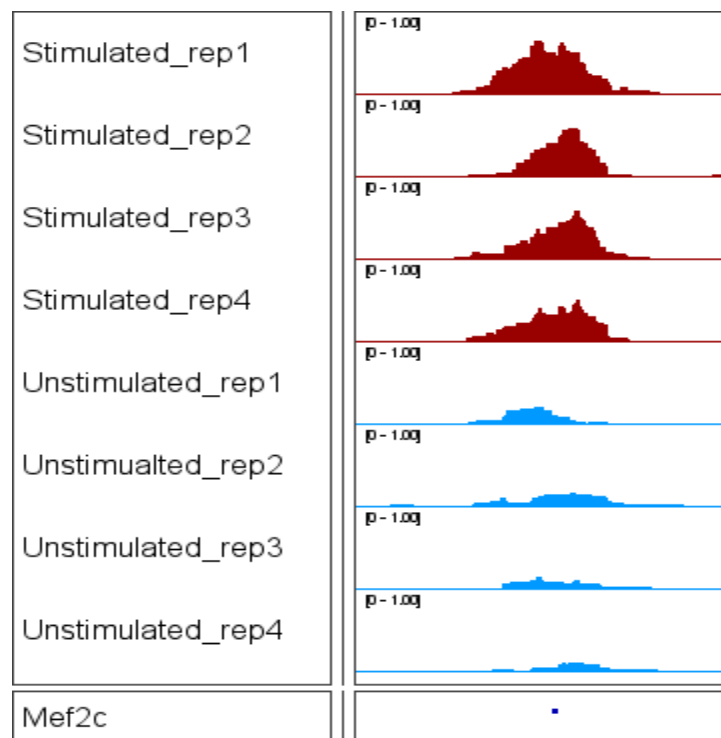
The top three motifs matched to the assigned Atf4 motif region were Atf4, C/EBP homologous protein (Chop), and ATF4. Chop is also known as growth arrest and DNA damage-inducible protein 153 (GADD153) and belongs to another subgroup of the bZIP family; the CCAAT/enhancer-binding protein (C/EBP) family. It is a nuclear transcription regulator which controls genes involved in a wide range of cellular processes including differentiation, apoptosis, autophagy and inflammation (Yang et al., 2017). As Atf4 and Chop are both bZIP transcription factors these two proteins can form heterodimers which induce the expression of genes important for protein synthesis and the unfolded protein response (Han et al., 2013). The identification of Chop as a similar motif suggests that Atf4 may not be the sole transcription factor that is capable of binding to this OCR. In fact, an interaction between these factors could be necessary for binding to occur. For p53, the top three similar motifs were all linked p53. This suggests that the motifs at these differentially accessible regions are likely to be targeted by p53 rather than by another transcription factor.

Changes in chromatin accessibility were not found to be enriched for the Mef2c motif which suggests that this motif is not one of the major motifs associated with ionomycin-induced changes in chromatin accessibility. However, Mef2c is a  $Ca^{2+}$ -sensitive protein and may still contribute in some way to  $Ca^{2+}$ -dependent accessibility changes. Therefore, differentially accessible peaks were directly searched for instances of the Mef2c motif to identify at which sites the Mef2c motif is enriched. 202 Mef2c motif-containing differentially accessible regions (MDARs) were identified showing that some Mef2c-motif containing regions do become differentially accessible after ionomycin-treatment. The majority (179) of MDARs were associated with increased accessibility. A full table of the chromosome positions and genes associated with these regions of open chromatin is

presented in Appendix 2. This list of potential gene targets was compared to the list of Mef2c interactors identified in Chapters 3 and 4. There was no overlap between the two lists suggesting that the Mef2c motif is not overrepresented in sites associated with its putative interactors after ionomycin treatment. However, the Mef2c motif (GATATTTTAGC) was found in the regulatory region of the *App* gene (chr16\_85247285\_85247685) (Figure 5.6). This suggests that Mef2c may contribute to the regulation of *App* in a  $\text{Ca}^{2+}$ -dependent manner.

#### 5.2.4 Peak annotation

To identify potential genes regulated by  $\text{Ca}^{2+}$ , peaks were annotated to genes using HOMER (section 2.7.5). The top five most significant peaks were associated with CBFA2/RUNX1 partner transcriptional co-repressor 3 (*Cbfa2t3*), a member of the myeloid translocation gene family; BCAR1 scaffold protein (*Bcar1*), a member of the crk-associated substrate family of scaffold proteins; TBC1 domain family member 16 (*Tbc1d16*), a Rab4A GTPase activating protein; stanniocalcin 2 (*Stc2*), a homodimeric glycoprotein and fibroblast growth factor 21 (*Fgf21*), a member of the fibroblast growth factor family. Several additional genes of interest were identified including three AD-risk genes KAT8 regulatory NSL complex

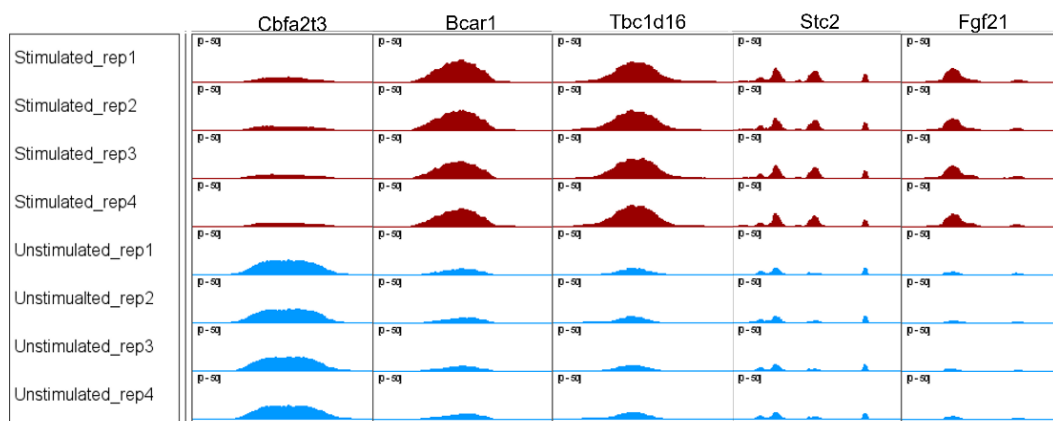


**Figure 5.6. Mef2c motif identified in the regulatory region of the *App* gene.** The Mef2c binding motif (GATATTTTAGC) found in the differentially accessible region assigned to the *App* gene was aligned in IGV to visually illustrate its presence in this region. This highlights that Mef2c may contribute to the regulation of *App* in a  $\text{Ca}^{2+}$ -dependent manner. Peaks are scaled to the highest peak in the display by manually setting the data range for each track to 0-1 (Y-axis).

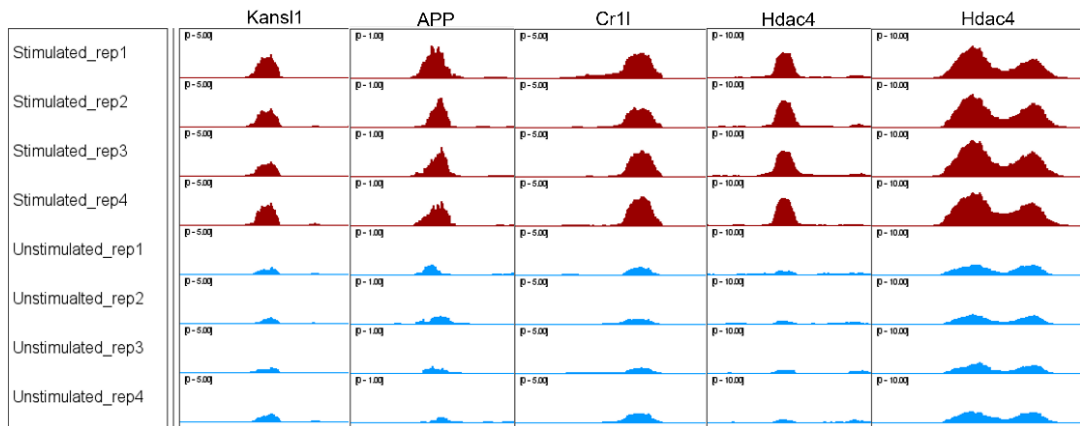
subunit 1 (*Kansl1*), *App*, and complement receptor 1 like (*Cr1l*), the mouse ortholog of human *CR1*, and the known Mef2c interactor *Hdac4* (Table 5.6). Each of the identified genomic regions were visualised in IGV. Figure 5.7 depicts the top five most significant peaks whereas Figure 5.8 depicts the additional genes of interest. Both figures show peak data for each replicate within the two conditions. For all genes, there is a noticeable difference in the size of the differential peak between conditions and this is consistent across all replicates.

**Table 5.6. Gene annotations of the top five most significant peaks and four additional genes of interest.** Shown are gene names, chromosome locations, fold change (stimulated vs. unstimulated) and p-values of the gene's association with the most significant peaks and genes of interest.

Gene Name	Chromosome	Start	End	Fold Change	p-value
<i>Cbfa2t3</i>	chr8	122699076	122699476	-1.694939363	0
<i>Bcar1</i>	chr8	111720182	111720582	1.731692284	6.49E-282
<i>Tbc1d16</i>	chr11	119191725	119192125	1.807911669	9.06E-269
<i>Stc2</i>	chr11	31371485	31371885	2.059755542	8.81E-262
<i>Fgf21</i>	chr7	45616291	45616691	2.052878876	5.43E-228
<i>Kansl1</i>	chr11	104439654	104440054	1.543242402	1.28E-22
<i>App</i>	chr16	85247285	85247685	1.721051223	7.20E-10
<i>Cr1l</i>	chr1	195129856	195130256	1.711687308	1.23E-26
<i>Hdac4</i>	chr1	92074655	92075055	2.574901076	9.79E-101
		92183125	92183525	1.513214705	7.86E-66



**Figure 5.7. Top five most significant peaks and their associated gene names.** IGV was used to visualise the top five most significant differentially accessible peaks in the dataset. All four replicates from each condition are included to highlight the small degree of variability within conditions. The associated gene names are also included. For each gene there is a discernible difference between stimulated and unstimulated BV2 cells. Peaks are scaled to the highest peak in the display by manually setting the data range for each track to 0-50 (Y-axis).



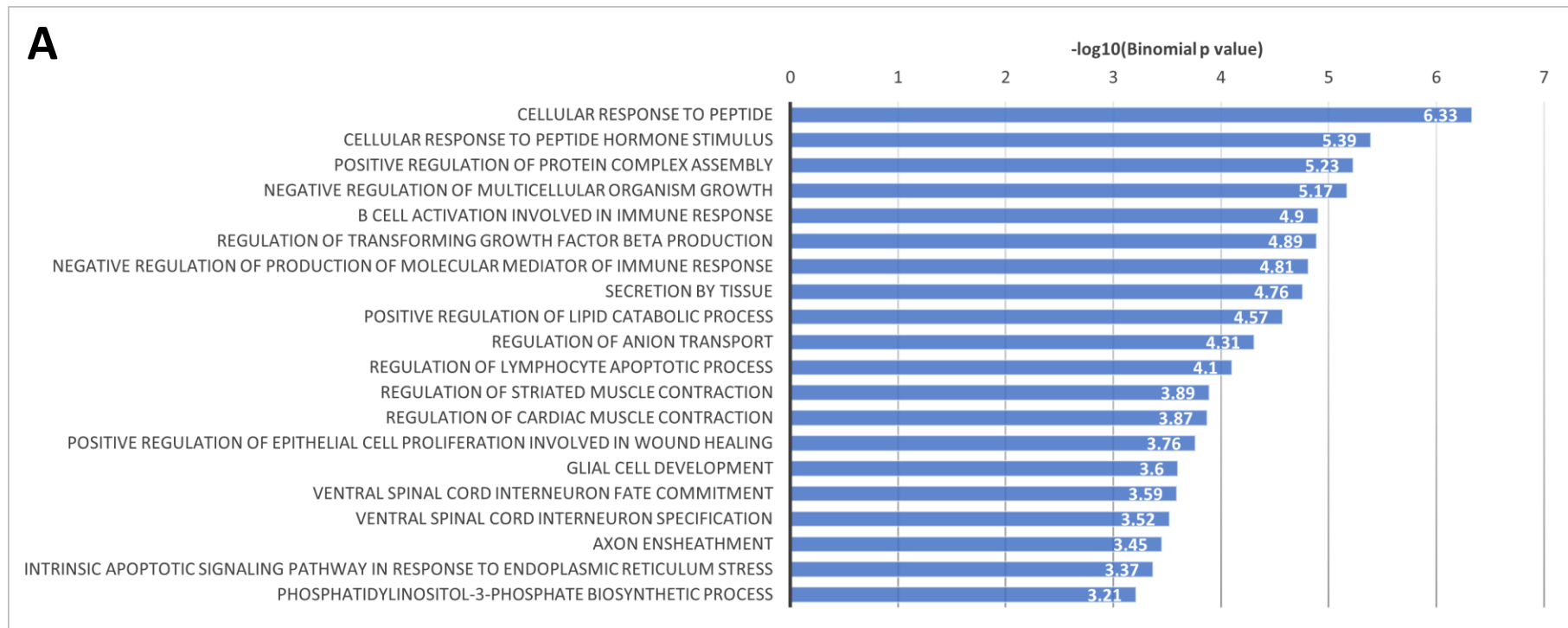
**Figure 5.8. Differentially accessible regions of the additional genes of interest.** IGV was used to visualise differentially accessible peaks of the AD-risk genes *Kansl1*, *APP* and *Cr1l* and the Mef2c interactor *Hdac4*. All four replicates from each condition are included to highlight the small degree of variability within conditions. The associated gene names are also included. For each gene there is a discernible difference between stimulated and unstimulated BV2 cells. Peaks are scaled to the highest peak in the display by manually setting the data range for each track to 0-5 (Y-axis).

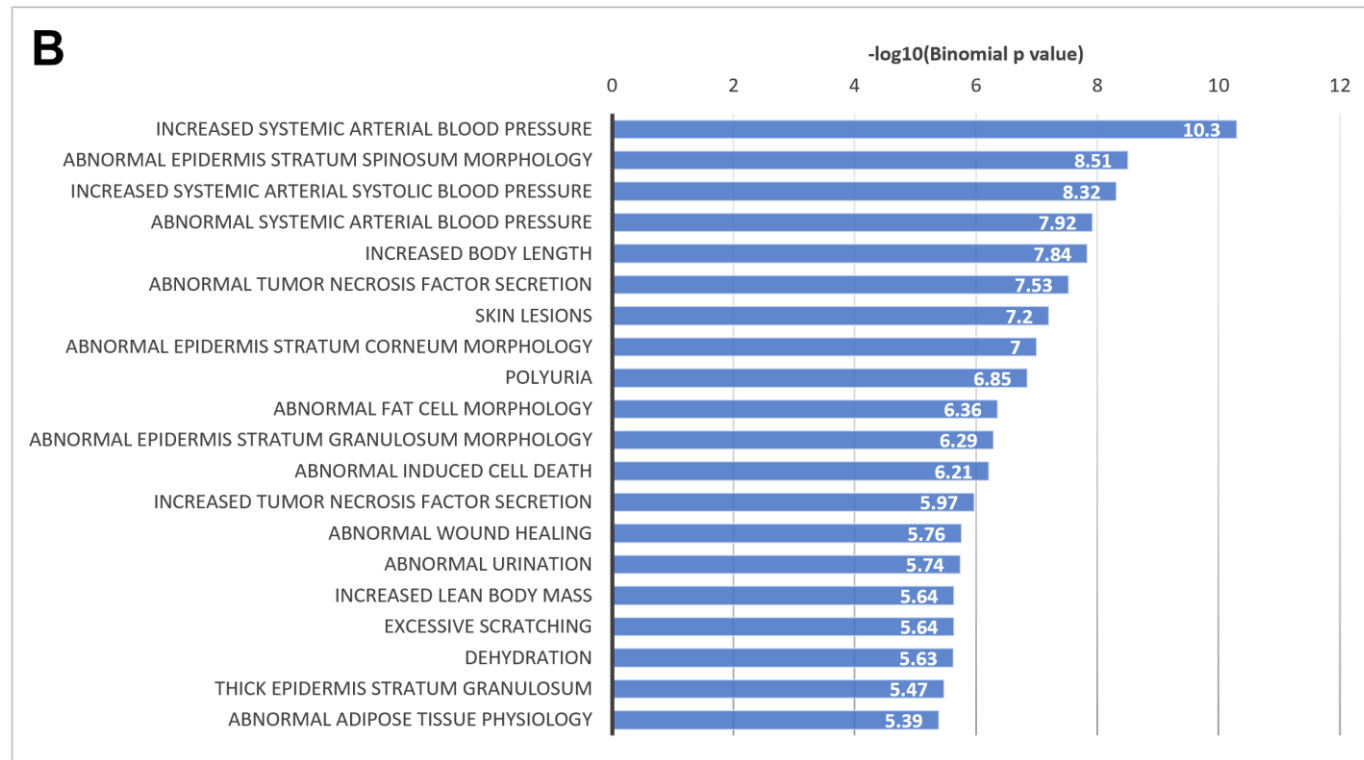
### 5.2.5 Functional enrichment analysis

The online tool Genomic Regions Enrichment of Annotations (GREAT) was used to test whether the assigned genes are enriched for specific biological processes. As the motif analysis revealed that sites associated with increased and decreased accessibility after ionomycin treatment contain binding motifs for different sets of transcription factors, the genes associated with these regions were assessed separately to determine if they are involved in different biological processes. Figure 5.9 shows the most significantly enriched biological processes and mouse phenotype terms from GREAT that were associated with genes mapping to the increased accessibility peaks. In the GO biological processes terms (Figure 5.9 A), four of the 20 most significantly enriched terms describe immune-related processes, including glial cell development and B cell activation involved in immune response. Looking at the mouse phenotype terms (Figure 5.9 B), the identified terms were not as immune-cell specific but did include some interesting phenotypes including abnormal induced cell death.

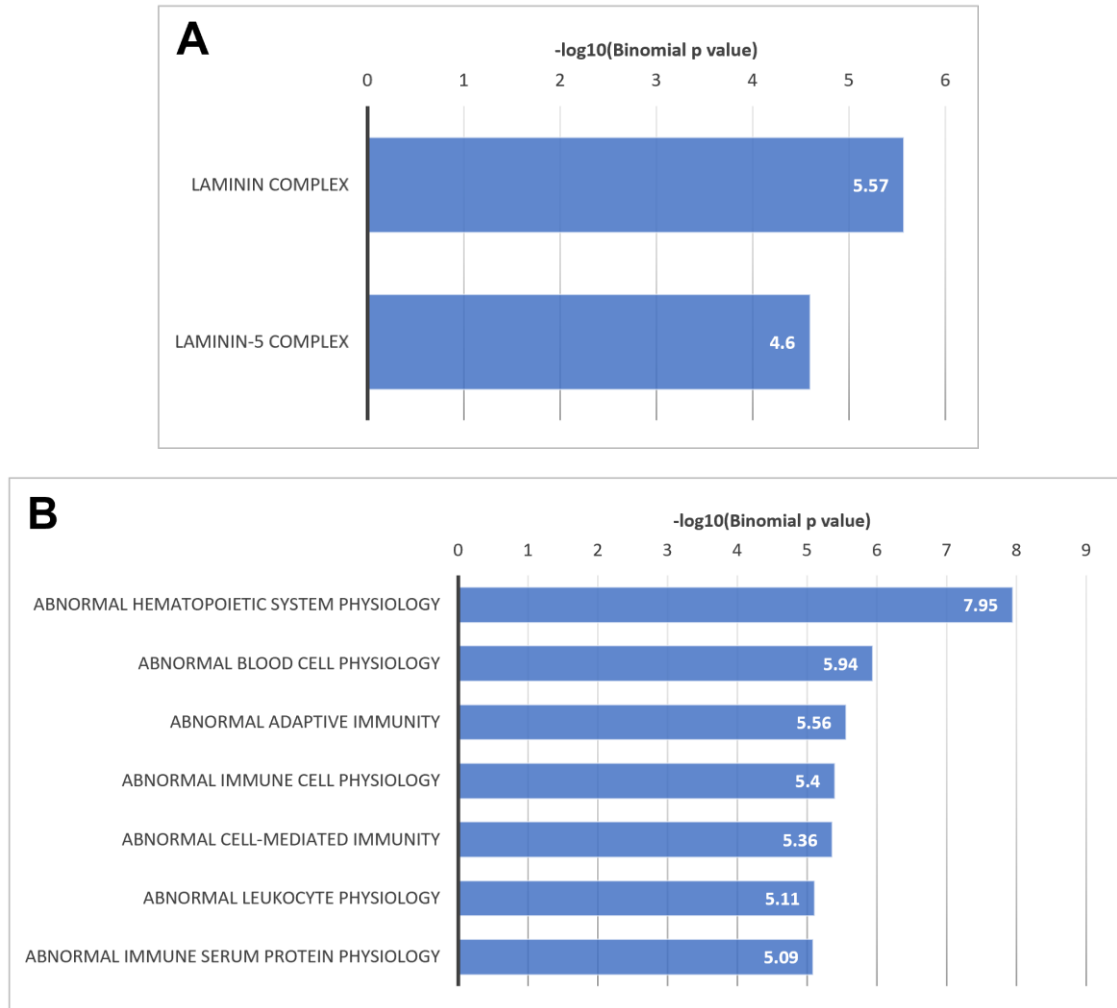
Figure 5.10 shows the most significant GREAT biological processes and mouse phenotype terms for genes associated with the decreased accessibility peaks. Due to the smaller number of genes in this category, no GO biological processes terms were significantly enriched. Two terms were however enriched in GO cellular component (Figure 5.10 A), laminin complex and laminin-5 complex. Neither of these terms are immune cell related, however, looking at the mouse phenotype terms (Figure 5.10 B), six of the seven most significantly enriched terms describe immune-related phenotypes including abnormal







**Figure 5.9. GREAT GO terms for increased accessibility peaks.** GREAT was used to determine which biological processes and mouse phenotypes are enriched within the genes associated with increased accessibility after ionomycin treatment. **(A)** GO Biological processes. **(B)** Mouse phenotype.



**Figure 5.10. GREAT GO terms for decreased accessibility peaks.** GREAT was used to determine which biological processes and mouse phenotypes are enriched in the genes associated with decreased accessibility after ionomycin treatment. **(A)** GO Cellular Component. **(B)** Mouse phenotype.

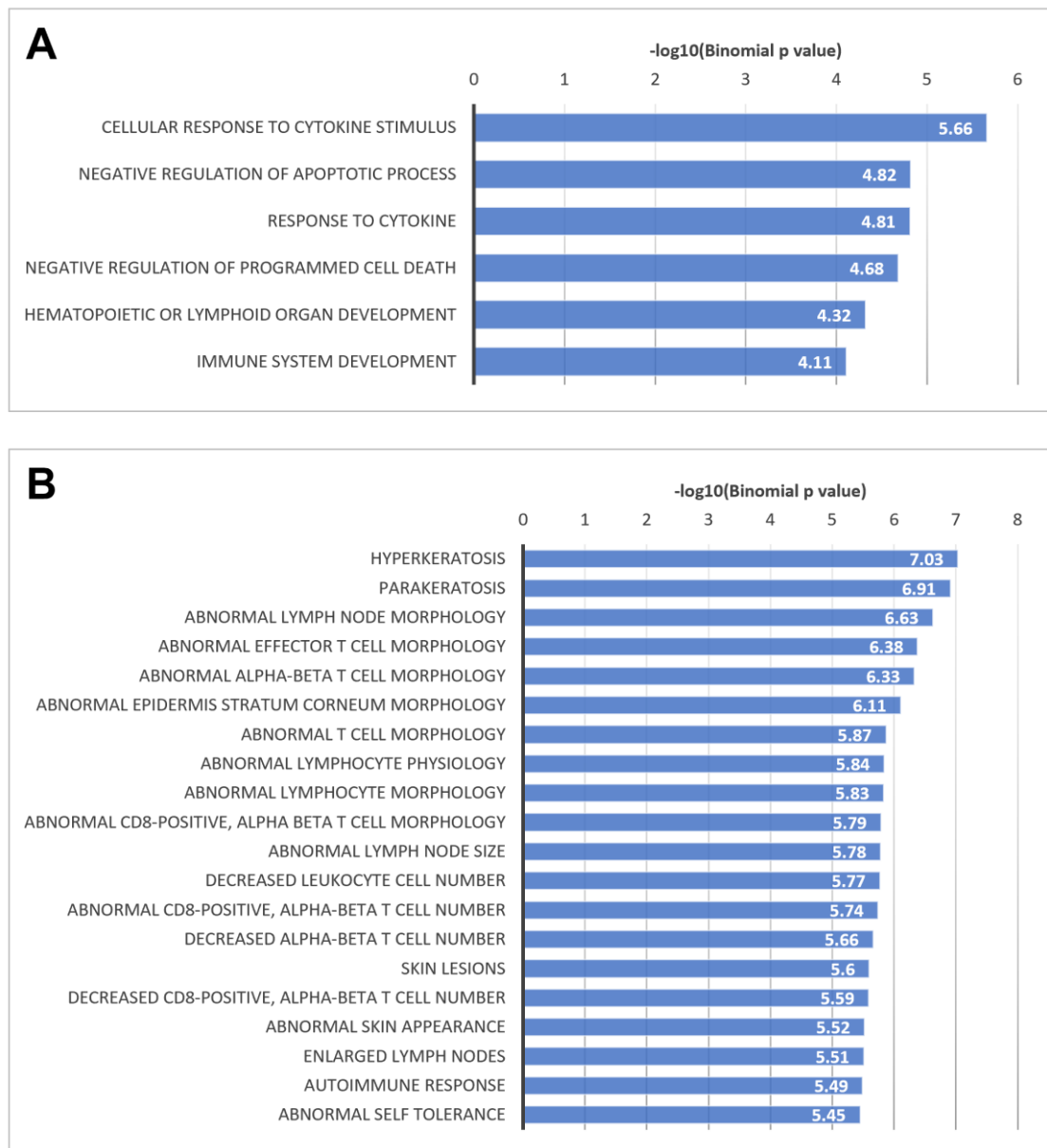
adaptive immunity, abnormal immune cell physiology and abnormal cell-mediated immunity. Genes associated with both increased and decreased accessibility appear to have some involvement in immunity-related processes, suggesting that  $\text{Ca}^{2+}$  signalling may regulate key immune functions in microglia-like cells.

The genes associated with MDARs (see above) were also analysed using GREAT. Figure 5.11 A shows the GO biological processes terms significantly enriched in this gene set. All six terms either relate to immune-specific processes or cell death and include cellular response to cytokine stimulus, negative regulation of apoptotic process and immune system development. A significant proportion of the mouse phenotype terms (Figure 5.11 B) also related to immune cells including abnormal lymphocyte morphology, abnormal effector T-

cell morphology, and autoimmune response. This suggests that Mef2c could be involved in regulating a set of genes that are important for immunity in a  $\text{Ca}^{2+}$ -dependent manner.

### 5.2.6 MAGMA

MAGMA was used to assess the relevance of  $\text{Ca}^{2+}$ -regulated genes to AD-risk. Only genes associated with differentially accessible peaks were tested. No significant enrichment of AD association signals was detected within the gene list ( $p=0.56407$ ), suggesting that genes associated with  $\text{Ca}^{2+}$ -regulated peaks in BV2 cells are not significantly associated with AD-risk.



**Figure 5.11. GREAT GO terms for MDARs.** GREAT was used to determine which biological processes and mouse phenotypes are enriched in the genes associated with MDARs. **(A)** GO Biological Processes. **(B)** Mouse phenotype.

### 5.3 Discussion

The dysregulation of  $\text{Ca}^{2+}$  signalling is a key pathogenic pathway in AD so understanding how  $\text{Ca}^{2+}$  signalling influences chromatin accessibility through transcription factors, potentially including Mef2c, in microglia-like cells is particularly important. In this chapter, ATAC-seq has been used to assess the chromatin accessibility of ionomycin-stimulated and unstimulated BV2 cells. A substantial number of differentially accessible regions were identified, and these sites were assigned to specific genes including three AD-risk genes. The motifs for three transcription factors, Atf4, NFATC3 and p53 were overrepresented in sites associated with ionomycin-induced changes in chromatin accessibility in BV2 cells. While the Mef2c motif was not enriched at differentially accessible chromatin, a targeted analysis did reveal that some MDARs are evident in ionomycin-treated cells.

#### 5.3.1 Increases in intracellular $[\text{Ca}^{2+}]$ result in changes to the chromatin landscape

The data presented in this chapter suggest that, similarly to peripheral immune cells (Brignall et al., 2017; Zhu et al., 2021), increases in intracellular  $[\text{Ca}^{2+}]$  can alter chromatin accessibility in microglia-like cells. Around 1,500 sites, with a fold change of  $\geq 1.5$ , were found to be differentially accessible between ionomycin-stimulated and unstimulated conditions highlighting a change to the chromatin landscape of these cells in elevated intracellular  $[\text{Ca}^{2+}]$  conditions. As  $[\text{Ca}^{2+}]$  is increased in microglia in AD (McLarnon et al., 2005), this may be reflective of chromatin accessibility changes in microglia in this disease-state.

#### 5.3.2 Atf4, NFATC3 and p53 motifs are associated with ionomycin-induced changes in chromatin accessibility in BV2 cells

Motif enrichment analysis on the differentially accessible peaks revealed that Atf4, NFATC3 and p53 motifs are present at differentially accessible sites. Splitting the differentially accessible regions into increased and decreased accessibility revealed that these changes are associated with different transcription factor motifs. As emerging evidence points to an involvement of transcription factors in initiating chromatin remodelling (Klemm et al., 2019), the identification of these motifs could suggest that these transcription factors are involved in initiating  $\text{Ca}^{2+}$ -induced changes to chromatin accessibility in microglia-like cells. However, it is not explicitly clear what proteins or mechanisms are primarily responsible for mediating changes in chromatin accessibility or whether these transcription factors are directly bound to these motifs. Further investigation is required before firm conclusions can

be made about the involvement of these transcription factors in initiating  $\text{Ca}^{2+}$ -induced changes to chromatin accessibility.

Regions associated with increased accessibility after ionomycin stimulation appear to be enriched for Atf4 and NFATC3 binding sites. Motifs for these transcription factors were found in 40.13% and 30.62% of the increased accessibility regions, respectively. NFATC3 is a well-documented  $\text{Ca}^{2+}$ -responsive protein (Crabtree & Olson, 2002) indicating that intracellular  $[\text{Ca}^{2+}]$  is changing chromatin accessibility in BV2 cells. As described in section 5.1, activation of the TREM2/PLC $\gamma$ 2 pathway results in the propagation of  $\text{Ca}^{2+}$  signalling which may lead to the translocation of NFAT to the nucleus and an initiation of gene transcription (Hansen et al., 2018; Hogan et al., 2003). The identification of the NFATC3 binding site as one of the top motifs adds to the understanding of NFAT as a downstream effector of the TREM2/PLC $\gamma$ 2 pathway. It suggests that, as a result of TREM2 signalling and subsequent NFAT translocation, NFAT may be involved in initiating ionomycin-induced changes in chromatin accessibility and gene expression. As both *TREM2* and *PLC $\gamma$ 2* are well-established AD-risk genes (Guerreiro et al., 2013; Sims et al., 2017), this pathway may contribute to AD genetic risk (Hansen et al., 2018). These data suggest that in AD, alterations in gene expression as a consequence of changes to TREM2 signalling may result in altered mediation of  $\text{Ca}^{2+}$ -induced changes in chromatin accessibility potentially by NFAT.

The Atf4 motif was also enriched in  $\text{Ca}^{2+}$ -induced increased accessibility regions. Atf4 has also been implicated in AD. For example, protein levels of ATF4 in human AD brains are increased by 1.9 fold compared to controls (Ohno, 2014). ChIP-seq has also revealed that ATF4 binds to the regulatory region of human *PSEN1* which is important for the processing of APP and production of  $\text{A}\beta$  (Mitsuda et al., 2007). The data presented in this chapter suggest that Atf4 may be involved in initiating increases in chromatin accessibility induced by  $\text{Ca}^{2+}$ . As  $\text{Ca}^{2+}$  signalling is dysregulated in AD this may result in changes in chromatin accessibility and altered gene expression potentially mediated by Atf4. This may affect biological processes like autophagy as the eIF2 $\alpha$ /ATF4 pathway is thought to direct an autophagy gene transcriptional program in response to endoplasmic reticulum stress or amino acid starvation. ATF4 is specifically required to increase the transcription of genes important for the function, formation, and elongation of the autophagosome including autophagy related 16 like 1 (*Atg16l1*), microtubule-associated proteins 1A/1B light chain 3B (*Map1lc3b*), autophagy related 12 (*Atg12*), Atg3, beclin-1 (*Becn1*) and GABA type A receptor associated protein like 2 (*Gabarapl2*) (B'Chir et al., 2013). However, none of these autophagy genes were associated with sites of open chromatin that contained Atf4 motifs

after increases in intracellular  $[Ca^{2+}]$  suggesting that a similar phenomenon in which autophagy genes are transcribed in response to stress may not occur in response to increases in intracellular  $[Ca^{2+}]$ . Thus, the genes assigned to  $Ca^{2+}$ -dependent regions of open chromatin containing Atf4 motifs are likely important for different biological processes in microglia-like cells.

Investigating GO terms enriched within the genes assigned to increased accessibility (Figure 5.8) reveals potential roles of these genes in several immune-related processes including glial cell development and B cell activation involved in immune response, and processes regulating cell death. Thus, as a consequence of  $Ca^{2+}$ -induced increases in accessibility, genes important for immune cell development and activation and cell death may be regulated. As Atf4 and NFATC3 motifs were enriched within these regions, these transcription factors could be responsible for the regulation of these regions and subsequent gene expression.

Regions of open chromatin that have decreased accessibility after ionomycin stimulation could be regulated by p53. Motifs for this transcription factor were found in 37.36% of the decreased accessibility regions. p53 is thought to be essential for the activation of microglia pro-inflammatory behaviours. In the absence of p53, phagocytosis and gene expression linked to anti-inflammatory and tissue repair functions are activated (Jayadev et al., 2011). This suggests that p53 is a key regulator of the immune response in microglia. p53 is thought to regulate microglial behaviour as a direct transcriptional activator, p53 regulates several miRNAs that modulate microglial pro-inflammatory responses (Aloia et al., 2015; Su et al., 2014). Furthermore, the GO terms enriched within genes associated with decreased accessibility also point to an involvement of p53 in the microglial immune response. Six out of seven enriched terms described immune-related mouse phenotypes (Figure 5.10). These included abnormal adaptive immunity, abnormal immune cell physiology and abnormal cell-mediated immunity. Thus, increases in intracellular  $[Ca^{2+}]$ , which result in decreased accessibility in regions containing p53 motifs, may potentially result in p53-driven transcription being attenuated, modulating microglial activation and pro-inflammatory responses. This could be reflective of the consequences of dysregulated  $Ca^{2+}$  signalling in AD.

The top motifs present at differentially accessible sites are different to those identified in other ionomycin-treated cell types. For example, Brignall et al (2017) used ATAC-seq to investigate the chromatin landscape of T-cells after ionomycin stimulation. The top motifs

enriched within ionomycin-specific peaks included runt-related transcription factor (RUNX) (59% of targets), NFAT (45% of targets) and activator protein 1 (AP-1) (21% of targets). The NFAT motif is enriched in both cell types which is not surprising as the activity of these proteins are tightly regulated by calcineurin and  $\text{Ca}^{2+}$  signalling. However, the other top motifs do differ with Atf4 and p53 in microglia-like cells and RUNX and AP-1 in T-cells. This suggests that, although there are some similarities,  $\text{Ca}^{2+}$  has different effects on different types of immune cell and that these effects potentially involve different sets of transcription factors. This is not unexpected as it has been suggested that the microglial molecular signature is distinct from other myeloid or immune cells (Butovsky et al., 2014). This also highlights that it is important to carry out these experiments in cell-specific models.

### 5.3.3 *App* and immune-specific processes are potentially regulated by Mef2c in a $\text{Ca}^{2+}$ -dependent fashion

$\text{Ca}^{2+}$ -dependent changes in chromatin accessibility were not enriched for the Mef2c motif. However, Mef2c may still contribute to  $\text{Ca}^{2+}$ -sensitive activity, especially since  $\text{Ca}^{2+}$  releases Hdac- and Cabin1-induced repression, potentially allowing Mef2c to be transcriptionally active (Chapter 4, sections 4.2.7 and 4.3.4).

Therefore, to identify  $\text{Ca}^{2+}$ -dependent changes in accessibility linked to Mef2c, differentially accessible peaks were directly searched for instances of the Mef2c motif. 202 MDARs were identified with 88.6% of these regions associated with increased accessibility. This suggests that the Mef2c motif is predominantly associated with increased accessibility regions. MDARs did not include any of Mef2c's interactors (identified in Chapters 3 and 4) suggesting that Mef2c is not likely to regulate the expression of any of its putative interactors in a  $\text{Ca}^{2+}$ -dependent fashion. However, the Mef2c motif was found in an open chromatin region associated to the AD-risk gene *App*. This suggests that Mef2c may contribute to the regulation this region in a  $\text{Ca}^{2+}$ -dependent manner. In APP processing, the APP intracellular domain (AICD) is translocated to the nucleus where it modulates  $\text{Ca}^{2+}$  (Leissring et al., 2002) suggesting that it may form a feedback loop. In AD, where  $\text{Ca}^{2+}$  signalling is dysregulated, the regulation of *App* gene expression, potentially by Mef2c, may become disrupted, potentially resulting in further modulation of  $\text{Ca}^{2+}$  signalling by the AICD. The processing of APP also results in the production of  $\text{A}\beta$  which increases intracellular  $[\text{Ca}^{2+}]$  which may further exacerbate  $\text{Ca}^{2+}$  dysregulation in AD (Mattson, 1994; Mattson et al., 1992). In microglia, oligomeric  $\text{A}\beta$  interacts with APP to promote microglial activation and drive microgliosis associated with AD brains (Manocha et al., 2016). Therefore



speculatively, increases in intracellular  $[Ca^{2+}]$  and the subsequent regulation of the *App* gene, potentially by Mef2c, may result in dysregulated *App* expression, interaction of APP with oligomeric A $\beta$ , and finally the promotion of microglial activation. However, changes in gene expression of *App* as a result of increases in  $[Ca^{2+}]$  and the direct binding of Mef2c to this region would need to be investigated to validate this proposed mechanism.

To determine the key processes that may be regulated by Mef2c in a  $Ca^{2+}$ -dependent fashion, genes associated with MDARs were analysed using GREAT (Figure 5.10). The MDARs regulated by changes in  $Ca^{2+}$  were found to be associated with genes involved in several biological processes including cellular response to cytokine stimulus and negative regulation of programmed cell death. The remaining terms also related to either the immune system and the inflammatory response or cell death.

The potential of role of Mef2c in mediating responses to cytokine stimuli and an involvement in the inflammatory response is of particular interest and fits well with previous research. Mef2c is thought to function as a microglial 'off' factor which limits microglial activation to immune challenges. Mef2c downregulation by interferon type 1 (IFN-1) results in an unrestrained microglial response to inflammatory stimuli (Deczkowska et al., 2017). The strict regulation of the microglial immune response is very important as immune activities in the brain can be detrimental to the surrounding environment (Hanisch & Kettenmann, 2007). As a microglial 'off' factor, in normal circumstances Mef2c regulates the response of microglia to immune challenges perhaps through the recruitment of repressive proteins like Hdac or Cabin1 or through mediating the expression of specific genes important for regulating responses to cytokines in response to changes in  $Ca^{2+}$ . If increases in intracellular  $[Ca^{2+}]$  affect the activity of Mef2c by removing repressive proteins and changing what genes Mef2c is potentially regulating than this may lead to abnormal control of the microglial inflammatory response in AD.

5.3.4  $Ca^{2+}$  potentially regulates genes and processes important for immune cell function which link to TREM2 signalling

The differentially accessible peaks were assigned to genes using HOMER. This revealed several genes that are potentially regulated by changes in  $Ca^{2+}$ . However, changes in chromatin accessibility do not equivocally correspond to quantitative changes in gene expression. Four of the top five significant peaks have increased accessibility after ionomycin stimulation and were assigned to the genes *Bcar1*, *Tbc1d16*, *Stc2* and *Fgf21*. The

most significant peak had decreased accessibility after ionomycin stimulation and was assigned to the *Cbfa2t3* gene.

Stc2 is a secreted glycoprotein hormone and is widely expressed throughout the body (Byun et al., 2010). It is closely related to *Stc1* which is induced by elevated  $\text{Ca}^{2+}$  levels in human neural crest-derived Paju cells (Zhang et al., 2000). The amino acid sequences of *Stc1* and *Stc2* are well-conserved, especially at their N-termini, implying that they have similar biological functions (Chang et al., 2008; Wagner & Dlimattia, 2006). In BV2 cells, *Stc2* has been shown to inhibit the activation of microglia and the release of proinflammatory cytokines and nitric oxide (Byun et al., 2010). Thus, the regulation of *Stc2* by  $\text{Ca}^{2+}$  may exert protective effects, if *Stc2* is upregulated as a result, by attenuating cell death and microglial activation. However, this could have an opposite effect if *Stc2* is downregulated. This would be particularly interesting to determine.

*Fgf21* is a member of the fibroblast growth factor (FGF) family and is predominantly expressed in the thymus and liver. *Fgf21* regulates lipid metabolism and glucose uptake (Rydén, 2009; Wang et al., 2020). In the CNS FGF21 is an important neuroprotective factor that plays a vital role in alleviating brain ischemia. After transient middle cerebral artery occlusion (MCAO)/reperfusion in mice, FGF21 is produced by microglia. As a result, FGF21 is thought to activate astrocytes which in turn contribute to the upregulation of neurotrophic factors and promote neuronal survival (Liu et al., 2020, unpublished). FGF21 can also modulate microglia-mediated neuroinflammation and reduce the expression of pro-inflammatory genes (Wang et al., 2020). Furthermore, FGF21 is thought to be a protective factor in AD. FGF21 may reduce BACE1 expression resulting in a reduction the generation of  $\text{A}\beta$ . The fact that  $\text{Ca}^{2+}$  may regulate *Fgf21* suggests that, in AD, it may be abnormally expressed. Whether it is upregulated, downregulated, or unaffected is important to determine due to its potential protective properties.

*Cbfa2t3* plays a vital role in T-cell development and proliferation (Hunt et al., 2011). It has been linked to therapy-related acute myeloid leukaemia (AML) as *CBFA2T3* is expressed in AML patient samples. Patients expressing high levels are associated with poorer prognosis as *CBFA2T3* is essential for the maintenance of AML cell proliferation (Steinauer et al., 2019). As *Cbfa2t3* is important for cell proliferation, if decreased accessibility is reflective of *Cbfa2t3* being downregulated in microglia-like cells after increases in intracellular  $[\text{Ca}^{2+}]$ , then this could result in reductions in cell proliferation. However, both the regulation directionality and the function of *CBFA2T3* in microglia cells requires further investigation.

Investigating biological processes regulated by  $\text{Ca}^{2+}$  has revealed a potential link to TREM2. Activation of TREM2 activates a  $\text{Ca}^{2+}$  signalling cascade that may lead to the translocation of NFAT to the nucleus. The identification of the NFATC3 motif in differentially accessible regions and the proposal that transcription factors are involved in initiating changes to chromatin accessibility (Klemm et al., 2019), suggests that NFAT may contribute to the initiation of  $\text{Ca}^{2+}$ -induced chromatin accessibility changes in BV2s. This could occur as a result of changes in TREM2 signalling in AD. The identified genes and processes potentially regulated by  $\text{Ca}^{2+}$  are very similar to known functions of TREM2. For example, TREM2 regulates microglial populations by cell proliferation and survival. TREM2 deficiency results in decreased microglia cell proliferation and increases in microglial apoptosis (Wang et al., 2015; Zheng et al., 2017). As *Cbfa2t3* is important for cell proliferation and *Fgf21* and *Stc2* are protective against cell death, TREM2 may regulate these processes via the modulation of these genes. Additionally, the data reveals that  $\text{Ca}^{2+}$  may regulate several biological processes that relate to the immune response. TREM2 is thought to be involved in the regulation of the inflammatory response (Jay et al., 2017), thus, this regulation may be mediated through changes in  $\text{Ca}^{2+}$ -induced accessibility. The specific activation of TREM2, as opposed to ionomycin treatment, could be useful to understand TREM2 signalling and its impact on chromatin accessibility.

#### 5.3.5 Genes associated with $\text{Ca}^{2+}$ -regulated peaks are not enriched for AD-risk association signals

Within the annotated genes several AD-risk genes including *App*, *Kansl1* and *Cr1l* were identified. GWAS risk loci may operate in specific microglial activation states, therefore, to assess whether AD-risk genes are enriched in  $\text{Ca}^{2+}$ -dependent microglial activation the gene-set analysis tool MAGMA (de Leeuw et al., 2015) was used. This revealed that genes assigned to  $\text{Ca}^{2+}$ -dependent differentially accessible regions were not significantly enriched with AD-risk association signals. Thus, the activation of microglial via  $\text{Ca}^{2+}$  signalling appears to differ from other forms of microglial activation, including  $\text{A}\beta$  activation, that do appear to be enriched for AD-risk genes (Sierksma et al., 2020). Perhaps  $\text{Ca}^{2+}$  activation of microglia induces more global changes in gene expression rather than specific to AD-risk. It may also indirectly target AD-risk pathways or genes via other non-associated genes hence a lack of AD-risk gene enrichment.

### 5.3.6 Limitations

There are several limitations with these experiments which should be addressed. The motif analysis on all BV2 peaks, showed that BV2 cells and microglia express similar transcription factors including PU.1, C/EBPD and MEF2. BV2 cells also express phenotypical, morphological and functional characteristics of primary microglia (Henn et al., 2009). However, there are still limitations with using BV2 cells as a model of microglia which need to be considered. For example, BV2 cells are transformed which can result in increased proliferation and adhesion (Horvath et al., 2008; Stansley et al., 2012). Additionally, in response to LPS, the upregulation of inflammation-related genes is less pronounced in BV2 cells compared to microglia (Henn et al., 2009). Finally, the *de novo* enrichment analysis does not provide direct evidence showing whether transcription factors are directly bound in these locations and are driving changes in accessibility or gene expression, further investigation would be required to address this.

### 5.3.7 Conclusions

Using a genome-wide approach, this chapter has revealed that using ionomycin treatment to increase intracellular  $[Ca^{2+}]$  results in robust changes to a relatively small proportion of accessible chromatin in BV2 cells. This is likely to be reflective of changes to gene expression that would require verification with RNA-seq. The motifs of three transcription factors, Atf4, NFATc3 and p53, were identified as enriched at sites with  $Ca^{2+}$ -induced changes in accessibility, which tentatively points to a potential role for these transcription factors in mediating  $Ca^{2+}$ -induced changes in chromatin function and gene expression. Atf4 and NFATC3 motifs were enriched within regions associated with increased accessibility whereas the p53 motif was enriched within regions associated with decreased accessibility. These transcription factors could be good targets for novel therapeutic strategies to reprogram chromatin profiles of microglia in response to increases in intracellular  $[Ca^{2+}]$  in AD. However, further experiments to confirm the direct binding of these transcription factors at these motif-containing regions and to determine whether these factors are driving chromatin accessibility changes are required. Contrary to what was hypothesised, differentially accessible regions were not enriched for the Mef2c motif suggesting that this motif is not one of the major motifs associated with ionomycin-induced changes in chromatin accessibility. Nevertheless, a targeted analysis did reveal that some MDARs are evident in ionomycin-treated cells. Functional annotation of genes associated to MDARs revealed that increases in intracellular  $Ca^{2+}$  may result in the regulation, potentially by Mef2c, of genes important for the control of the microglial inflammatory response. In AD,

Ca<sup>2+</sup> dysregulation may result in the abnormal control of this response by Mef2c.

Integrating these results with Chapters 3 and 4 will provide insights into two mechanisms by which Ca<sup>2+</sup> potentially influences gene regulation in BV2 cells; altered Mef2c protein interactions and chromatin accessibility. This will be discussed in the following and final chapter.

## Chapter 6 General Discussion

*MEF2C* is an AD-risk gene that encodes a transcription factor which is expressed in microglia cells (Escott-Price et al., 2015; Jean Charles Lambert et al., 2013). In microglia and macrophages, AD-risk SNPs are enriched in regions of open chromatin that contain MEF2C DNA binding motifs (Tansey et al., 2018). This could result in impaired transcriptional control by MEF2C as the genetic variation at these sites may lead to disrupted DNA binding and subsequent gene expression changes. This identifies MEF2C's transcriptional network as a potential underlying AD-risk mechanism. This thesis comprised of a series of experiments which aimed to investigate this further and to elucidate how MEF2C is regulated through protein interactions and how MEF2C regulates gene expression and therefore AD-risk.

To achieve this aim, three major research objectives were pursued:

- 1) To define the interactome of Mef2c in microglia-like cells (Chapter 3)
- 2) To investigate stimulus-dependent interactions of Mef2c (Chapter 4)
- 3) To investigate the effects of Ca<sup>2+</sup> signalling on chromatin accessibility (Chapter 5)

Identifying protein-protein interactions is particularly important for understanding the regulation, biological role, and molecular mechanisms of protein function. This may help to elucidate mechanisms of disease pathology or highlight new therapeutic targets (Goehler et al., 2004; Pedley et al., 2020). In Chapter 3, using co-IP-MS, the first interactome for endogenous Mef2c in microglia-like cells was delineated. The data revealed that Mef2c exists as two predominant isoforms in BV2 cells which may have different functions and/or interacting partners. Additionally, potential regulators and cofactors that are important for understanding Mef2c function in unstimulated BV2 cells were identified revealing that Mef2c is largely being held in a transcriptionally inactive state by three main proteins, Hdac4, Hdac5 and Cabin1. These proteins may also be binding to specific Mef2c isoforms, but this requires further investigation. To address the main limitations with co-IP-MS, initial validation experiments were carried out on two of the identified interactors. A direct interaction between Hdac4 and Mef2c in microglia-like cells was verified. These data are consistent with previous research which found an interaction between these two proteins in HEK293T cells and yeast (Wang et al., 1999; Wang et al., 2005). The work presented herein shows that this interaction occurs physiologically between endogenous proteins in BV2 cells removing the reliance on overexpression models or reconstituted protein complexes. This biochemical interaction was further supported using a reporter system to

show a functional consequence of this interaction. Hdac4 reduced the ability of Mef2c to transactivate reporter gene expression suggesting that Hdac4 represses Mef2c in microglia-like cells and highlights a non-enzymatic role for HDAC proteins in this cell type.

Having established that Mef2c is partially repressed in unstimulated BV2 cells, I aimed to alleviate this repression using ionomycin stimulation to increase intracellular  $[Ca^{2+}]$  and determine the stimulus-dependent interactions of Mef2c. This is of particular importance as very few dynamic interactomes are mapped. In muscle cells, the activation of CaMKI/IV by  $Ca^{2+}$  signalling results in the dissociation of HDAC4 and HDAC5 from MEF2 allowing MEF2 to bind to other cofactors and promote gene expression (Mckinsey et al., 2000; Stewart & Crabtree, 2000). Similarly, increases in  $[Ca^{2+}]$  levels result in the release of CABIN1 from the HIRA/MEF2D complex leading to enhanced transcriptional activity of MEF2D (Jang et al., 2007; Robinson & Dilworth, 2018; Youn & Liu, 2000). Thus, a similar phenomenon may occur in BV2 cells allowing Mef2c to form new interactions. In Chapter 4, the antibiotic ionomycin was used to elevate intracellular  $[Ca^{2+}]$  levels prior to the isolation of Mef2c and its interacting proteins from BV2 cells via co-IP-MS. This resulted in the partial dissociation of the main repressing proteins from Mef2c and allowed Mef2c to form some new interactions including associations with two microglial  $A\beta$  response proteins Yes1 and Smpd13b. However, no well characterised transcriptional co-activators appeared to be recruited to the remodelled Mef2c complex.

After demonstrating that ionomycin treatment alters the Mef2c interactome and partially releases Mef2c from its repressed state, I aimed to determine what effect ionomycin may have on chromatin accessibility. Analysing differential accessibility may highlight  $Ca^{2+}$ -regulated transcriptional processes in BV2 cells. In Chapter 5, ATAC-seq was used to explore the effect of elevated intracellular  $[Ca^{2+}]$  levels on chromatin accessibility in BV2 cells, and to identify the transcription factor motifs enriched at these ionomycin-responsive differentially accessible sites. The motifs of three transcription factors, Atf4, NFATc3 and p53, were identified as enriched at sites with  $Ca^{2+}$ -induced changes in accessibility. Atf4 and NFATC3 motifs were enriched within regions associated with increased accessibility whereas the p53 motif was enriched within regions associated with decreased accessibility. Due to the proposal that transcription factors are involved in initiating changes to chromatin accessibility (Klemm et al., 2019), these identified transcription factors may contribute to the initiation of  $Ca^{2+}$ -induced chromatin accessibility changes in BV2s. This work also contributes to our understanding of NFAT's role as a downstream effector of the

TREM2/PLCy2 pathway (Hansen et al., 2018). NFAT could be involved in initiating  $\text{Ca}^{2+}$ -induced accessibility changes as a direct result of changes in TREM2 signalling.

Contrary to what was hypothesised, differentially accessible regions were not enriched for Mef2c motifs beyond the background frequency. However, as Mef2c is a  $\text{Ca}^{2+}$ -sensitive transcription factor it was hypothesised that it may still contribute to  $\text{Ca}^{2+}$ -dependent activity. Therefore, the ATAC-seq data was searched for instances of Mef2c motif-containing differentially accessible regions (MDARs). A MDAR was associated to the AD-risk gene *App* suggesting that Mef2c may be involved in its regulation in elevated intracellular  $[\text{Ca}^{2+}]$  conditions. Additionally, the functional annotation of genes assigned to MDARs revealed a potential involvement of Mef2c in cell death and the regulation of the immune response after increases in intracellular  $[\text{Ca}^{2+}]$ .

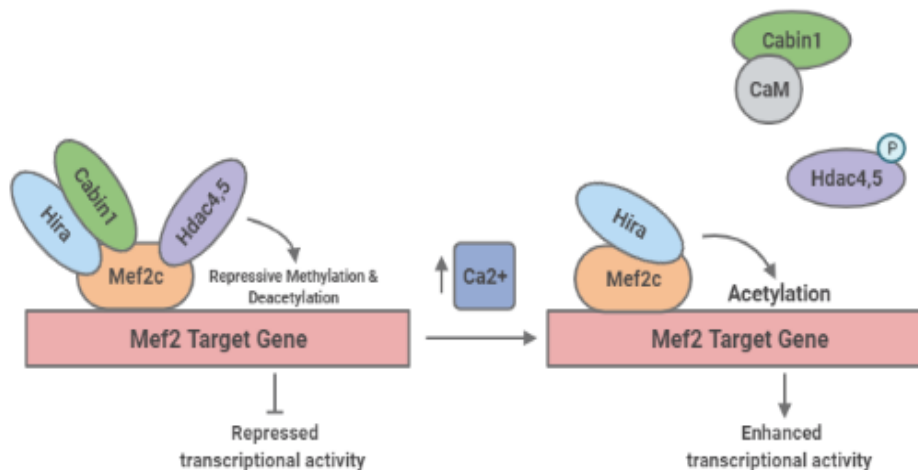
### 6.1 Elevated intracellular $[\text{Ca}^{2+}]$ levels and Mef2c

Data presented herein show that protein-protein interactions hold Mef2c in a partially repressed state in BV2 cells suggesting the Mef2c is unlikely to be transcriptionally active. Ionomycin stimulation resulted in the partial dissociation of the three main repressing proteins which allows Mef2c to form some new interactions and potentially become transcriptionally active. As discussed in Chapter 3 section 3.3.2, Mef2c would be expected to interact with other transcription factors as these proteins exist in multi-protein complexes that regulate target gene expression (Adcock & Caramori, 2009; Martin, 1991). However, no new, well characterised coactivators or transcription factors were identified suggesting that there is no Mef2c activating complex that facilitates transcriptional activation of Mef2c. Despite this, the histone regulator Hira, which was identified as an interactor in Chapter 3, was still co-immunoprecipitated alongside Mef2c after increases in intracellular  $[\text{Ca}^{2+}]$ . In the absence of CABIN1, HIRA has been shown to interact with MEF2D and enhance transcriptional activity (Yang et al., 2011). Thus, as the abundance of Cabin1 has been reduced, this could allow Hira to enhance Mef2c transcriptional activity and contribute to the activation of Mef2c target genes. In microglia, this interaction may be important for the activation of specific target genes by Mef2c when  $[\text{Ca}^{2+}]$  is increased. Additionally, in elevated  $[\text{Ca}^{2+}]$  conditions, despite the dissociation of repressor proteins from Mef2c, these data reveal that differentially accessible regions are not enriched for Mef2c motifs beyond the background frequency. The true frequency of changes in chromatin accessibility at Mef2c bound sites will require the identification of genuine



Mef2c-bound regions of the genome using ChIP-seq. A working model of the response of Mef2c to increases in intracellular  $[Ca^{2+}]$  in BV2 cells is presented in Figure 6.1.

The reporter data presented in section 3.2.6 may suggest that Mef2c becomes more transcriptionally active after the release of Hdac4 repression. However, this experiment was conducted in HEK293T cells in the absence of endogenous BV2 cell stimuli that may affect the transcriptional status of Mef2c. In BV2 cells, it is not clear whether Mef2c is transcriptionally active after the release of repression. It was postulated in Chapter 4 that additional, currently unidentified, signals may be required to reconstitute a Mef2c activating complex which may promote Mef2c transcriptional activity. Mef2c is regulated by a range of signalling pathways and interactions which in turn regulate the transcriptional activity of Mef2c (section 1.4.5). These signals may be required to activate Mef2c, potentially through additional co-activator binding, after the release of repression. For example, the phosphorylation of Mef2c is particularly important in its regulation. MEF2C can be phosphorylated by the mitogen activated protein kinases (MAPK) p38 and ERK5 which bind to the transcription activation domain to enhance transcriptional activity (Yang et al., 1998; Zhao et al., 1999). Additionally, previous research has shown that the



**Figure 6.1. The repression of Mef2c in microglia-like cells.** In unstimulated BV2 cells Mef2c appears to be held in a repressed state by Hdac4, Hdac5 and Cabin1. Stimulating BV2 cells with ionomycin prior to co-IP-MS alleviates the repression of Mef2c by these proteins. As described in muscle cells by Mckinsey et al (2002), the initiation of  $Ca^{2+}$  signalling within the cell may activate CaMKI/IV resulting in the phosphorylation of Hdac4 and Hdac5 and their dissociation from Mef2c. As described by Robinson and Dilworth (2018) in muscle cells, increases in intracellular  $[Ca^{2+}]$  allow for the binding of calmodulin (CaM) to Cabin1, releasing it from Hira. This may also be the case in microglia-like cells, allowing Hira to facilitate the activation of Mef2c target genes. However, no additional Mef2c activating complex seems to aid Hira-mediated Mef2c activity. Additionally, in elevated  $[Ca^{2+}]$  conditions, despite the dissociation of repressor proteins from Mef2c, differentially accessible regions are not enriched for Mef2c motifs beyond the background frequency. Created with BioRender.com.

interaction between ERK5 and MEF2 is regulated by  $\text{Ca}^{2+}$  and the co-repressor Cabin1 (Kasler et al., 2000), thus the removal of Cabin1 repression may allow ERK5 to bind to and phosphorylate Mef2c to enhance activity however, an interaction between these proteins was not detected in BV2 cells. This may be due the location of the antibody epitope preventing binding or this interaction may not endogenously occur in BV2 cells as it has only been shown in Y2H screens and muscle cells (Han et al., 1997; Kato et al., 1997). However, changes in Mef2c phosphorylation may still be attenuating the transcriptional activation of Mef2c.

It is noteworthy that the inclusion of the  $\gamma$  domain in the Mef2c isoforms identified in BV2 cells creates a MEF2C isoform that has a phosphoserine-dependent transrepressor function (Zhu & Gulick, 2004). Accordingly, if Mef2c is phosphorylated in the  $\gamma$  domain by kinases such as p38 or ERK5 it may result in transcriptional repression, rather than activation, of Mef2c activity. Thus, despite the dissociation of the main repressing proteins, Mef2c still may not be transcriptionally active in BV2 cells.

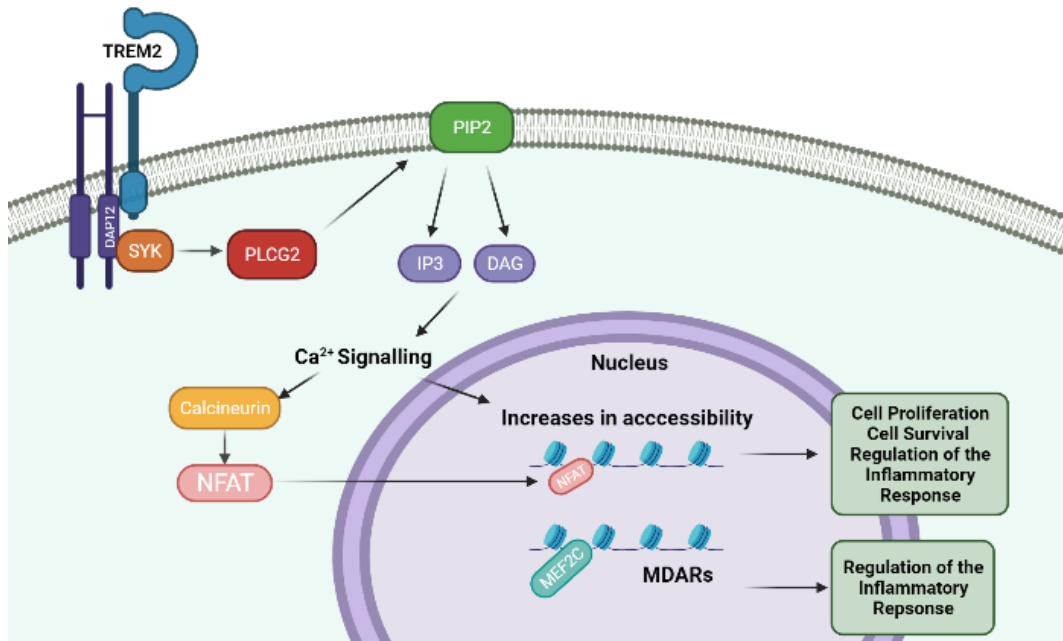
## 6.2 Increases in intracellular $[\text{Ca}^{2+}]$ may result in the regulation of the microglia inflammatory response by Mef2c

The results presented in this thesis collectively highlight an important role for Mef2c in the microglial immune response. Mef2c is thought to be important for restraining the response and activation of microglia to pro-inflammatory stimuli - it acts as a microglial 'off' factor (Deczkowska et al., 2017). The recruitment of repressive proteins like Hdac or Cabin1 in unstimulated conditions to attenuate Mef2c activity (Chapter 3) and the partial release of this repression after increases in intracellular  $[\text{Ca}^{2+}]$  (Chapter 4) may be one mechanism for regulating the response of microglia to inflammatory stimuli. In response to changes in  $\text{Ca}^{2+}$ , Mef2c may also regulate the expression of specific genes that play a role in the response to cytokines (Chapter 5). Furthermore, after increases in intracellular  $[\text{Ca}^{2+}]$  Mef2c may interact with other proteins including Smpd13b which is important for modulating pro-inflammatory mechanisms (Heinz et al., 2015). These proteins may work together to regulate the response of microglia to immune challenges in elevated  $[\text{Ca}^{2+}]$  conditions. Increases in intracellular  $[\text{Ca}^{2+}]$  appear to affect the transcriptional activity of Mef2c by removing repressive proteins, remodelling the Mef2c interactome, and potentially altering what genes Mef2c is regulating. Therefore, in AD where  $\text{Ca}^{2+}$  is dysregulated, this may lead to abnormal control of the microglia inflammatory response by Mef2c, thereby contributing to or exacerbating cognitive loss and disease pathology (Simen et al., 2011).

### 6.3 NFAT and Mef2c as downstream effectors of TREM2 signalling

As discussed in Chapter 5 (section 5.1), both MEF2C and NFAT are thought to be downstream effectors of the TREM2/PLC $\gamma$ 2 signalling pathway. This thesis provides evidence to add to the understanding of NFAT and Mef2c as important players at the end point of this AD genetic risk pathway. NFATC3 motifs were enriched within Ca<sup>2+</sup>-dependent differentially accessible regions, which may point to a role of NFAT in initiating Ca<sup>2+</sup>-induced chromatin accessibility changes. Additionally, in Chapter 4, another NFAT family member, Nfatc2, was used as a positive control to investigate the effect of ionomycin treatment on BV2 cells. Western blots revealed that after ionomycin stimulation an additional band, likely to represent dephosphorylated Nfatc2, was visible. This suggests that in microglia-like cells, NFAT is being dephosphorylated and potentially translocated to the nucleus where it may be involved in initiating Ca<sup>2+</sup>-induced changes in chromatin accessibility and ultimately gene transcription. In AD, this could happen in response to changes to the TREM2/PLC $\gamma$ 2 signalling pathway as several of the identified Ca<sup>2+</sup>-regulated biological processes were similar to the biological functions of TREM2 including cell proliferation, survival, and regulation of the inflammatory response. However, the consequences of changes to TREM2 signalling and activation on the chromatin landscape would need to be investigated separately to confirm this. Although the Mef2c motif was not found to be enriched in ionomycin-induced differentially accessible regions, it does not mean that Mef2c is not a downstream component of this pathway. Hansen et al (2018) postulate that Mef2c translocates to the nucleus upon activation of TREM2 signalling, however, this thesis provides no evidence of Mef2c present in the cytoplasm in BV2 cells (section 4.2.5.4). Additionally, no phosphorylation changes in Mef2c were detected after ionomycin-treatment unlike NFAT (section 4.2.1). These data suggest that Mef2c is likely already in the nucleus, which does not support a model of translocation in BV2 cells. Increases in intracellular [Ca<sup>2+</sup>], perhaps due to the activation of TREM2, may result in the potential targeting of MDARs by Mef2c, which is already present in the nucleus, and the regulation of the microglia inflammatory response by Mef2c. However, further work which determines genuine Mef2c-bound sites is required to support this concept. A working model of the potential involvement of NFAT and Mef2c downstream of TREM2 signalling is presented in Figure 6.2.

In peripheral immune cells NFAT and MEF2 have been found to interact (Blaeser et al., 2000; Kipanyula et al., 2016). NFAT recruits coactivators like the histone acetylase p300 to MEF2 target genes to facilitate the expression of MEF2 target genes (Sun et al., 2010; Youn



**Figure 6.2. A role for Mef2c and NFAT downstream of AD-risk genes TREM2 and PLC $\gamma$ 2.**

Interaction of TREM2 and the cell-surface adapter protein DAP12, recruits the tyrosine kinase SYK. SYK activates PLC $\gamma$ 2 which cleaves PIP2 into two secondary messengers; IP3 and DAG which activate Ca<sup>2+</sup> signalling. This, and the subsequent activation of calcineurin may result in the translocation of NFAT to the nucleus. Here, NFAT may be involved in initiating increases in accessibility induced by Ca<sup>2+</sup> signalling resulting in the regulation of genes important for cell proliferation, survival, and the regulation of the inflammatory response. Ca<sup>2+</sup> signalling may also result in the targeting Ca<sup>2+</sup>-dependent MDARs by Mef2c and the transcription of genes important for the regulation of the inflammatory response in microglia. Figure adapted from Hansen et al., (2018). Created with BioRender.com.

et al., 2000). Thus, a similar interaction may be expected in microglia. However, no NFAT proteins were found to interact with Mef2c in BV2 cells under unstimulated or stimulated conditions (Chapters 3 and 4). This may signify that, as discussed above, despite the relief of repression after ionomycin stimulation, Mef2c may remain in a transcriptionally inactive state, unable to interact with other transcription factors. However, NFAT proteins have never been directly associated with Mef2c specifically, and neither has the interaction between NFAT and MEF2 been confirmed in BV2 cells or microglia. Thus, this interaction may be restricted to other MEF2 family members or specific to certain cell types.

## 6.4 Future directions

This work has defined the first endogenous Mef2c interactomes in unstimulated and ionomycin-stimulated microglia-like cells, however, interactions cannot be considered direct until further validation. In Chapter 3 (section 3.2.6), some interactions were tested and the interaction between Hdac4 and Mef2c was verified. However, due to time

constraints and the lack of appropriate high-quality antibodies no further interactions could be successfully validated. Therefore, to strengthen the conclusions of this thesis, it is important to validate the remaining interactors of interest using techniques like HEK293T co-IP and reporter assays as described in Chapter 2 (sections 2.3.3 and 2.5.6). Additionally, BV2 cells were found to predominantly express two Mef2c isoforms. These isoforms contain different  $\alpha$  exons which sit close to the MEF2 binding domain. Thus, these isoforms may not only have different functions but also different binding partners. It was postulated in Chapter 3 that these two isoforms may be repressed by two separate complexes; the  $\alpha 1$  isoform may be primarily repressed by the Hdac complex whereas the  $\alpha 2$  isoform may be repressed by the Hira/Cabin1 complex. Attempts were made to verify if these interactions were isoform specific but due to the limitations described above this was not possible. Thus, determining whether these Mef2c isoforms do have different binding partners and therefore involved in different biological processes is an important future direction.

Within this thesis, ATAC-seq revealed that certain motifs are enriched in ionomycin-induced differentially accessible regions. However, this experiment does not provide direct evidence as to whether the transcription factors assigned to these motifs are bound at these locations and are driving changes in chromatin accessibility. Future work should seek to address this question. For example, computational footprinting techniques have been developed to predict transcription factor binding sites from ATAC-seq data (Li et al., 2019). This method detects transcription factor footprints which are troughs in read coverage in accessible regions of relatively high read coverage. These locations represent regions within peaks where transcription factors are bound. These troughs occur as the Tn5 transposase enzyme, which normally cuts DNA reasonably indiscriminately throughout nucleosome free regions, is prevented from cleaving DNA when a transcription factor is present resulting in small regions, within high coverage peaks, where read coverage drops suddenly (transcription factor footprint). However, due to time constraints this additional analysis could not be completed. Another, more direct, method that could be used to measure genome-wide occupancy of specific transcription factors in BV2 cells, and perhaps help to determine the true frequency of changes in chromatin accessibility at Mef2c bound sites, is chromatin immunoprecipitation with sequencing (ChIP-seq). In this assay, chromatin is fragmented and then incubated with antibodies that target specific DNA-binding proteins or histone modifications. These protein-bound DNA fragments are subsequently immunoprecipitated and sequenced (Park, 2009). Similarly, to ATAC-seq, reads are then aligned to a reference genome and identified peaks indicate the genomic

loci that are associated with the transcription factor or histone modification of interest. ChIP-seq could have been used to identify the binding sites of Mef2c in BV2 cells to get a clearer idea of what Mef2c is regulating. However, as Chapters 3 and 4 revealed that Mef2c is not in a transcriptionally active complex, ATAC-seq, which offers a more global look at accessibility changes and potential transcription factor binding induced by  $\text{Ca}^{2+}$ , was a more appropriate choice for this thesis. It has also identified other  $\text{Ca}^{2+}$ -responsive transcription factors that perhaps may be important in AD.

The ATAC-seq data presented in this thesis could be overlaid with currently available Mef2c ChIP-seq data which has been generated in a number of cell types including cortical neurons, B lymphocytes, cardiomyocytes and endothelial cells (Gertz et al., 2013; Liu et al., 2011; Maejima et al., 2014; Papait et al., 2017; Telese et al., 2015). However, there is no Mef2c ChIP-seq data from microglia or BV2 cells that is currently publicly available. Overlaying this ATAC-seq data with ChIP-seq from microglia would be more appropriate as sites of open chromatin and motif enrichment differs between peripheral immune cells and BV2 cells (Brignall et al., 2017, section 5.3.2) so it is likely that the same is true for Mef2c ChIP-seq in different cell types. Data is publicly available for the histone mark H3K27ac in BV2 cells (Kumar et al., 2016; Liu et al., 2011) which could be integrated with the ATAC-seq data to identify active enhancers within the dataset. This would help to understand more about potential gene regulation at sites of open chromatin.

This thesis has also identified several genes that may be regulated in a  $\text{Ca}^{2+}$ -dependent manner. However, whether these genes are upregulated, downregulated, or unaffected cannot be determined with ATAC-seq data alone. Addressing this limitation would provide more information regarding how  $\text{Ca}^{2+}$ -induced changes in accessibility correlate with gene expression. RNA-sequencing (RNA-seq) can provide a transcriptome-wide readout of (differential) gene expression and could be used to investigate the effect of  $\text{Ca}^{2+}$  signalling on the gene expression profile. The association between changes in chromatin accessibility and changes in gene expression could then be established by integrating RNA-seq data with the ATAC-seq data presented in Chapter 5. Combining ATAC-seq with RNA-seq on stimulated and unstimulated BV2 cells would provide more information about gene regulatory changes in response to  $[\text{Ca}^{2+}]$  increases which would be applicable to AD.

As discussed in the General Introduction (section 1.3.3.3), AD patient-derived microglia have a decreased amplitude and longer-lasting  $\text{Ca}^{2+}$  response compared to controls (McLarnon et al., 2005). Thus, to ensure the results of these experiments are more

translationally relevant to AD, it would also be important to determine what form of  $\text{Ca}^{2+}$  signalling is propagated by stimulating BV2 cells with ionomycin, whether it is continuous, low-amplitude  $\text{Ca}^{2+}$  transients as in AD or transient, high-amplitude  $\text{Ca}^{2+}$  spikes.

Furthermore, alternative stimulation strategies in BV2 cells should be explored as these cells can be activated by range of exogenous stimuli. For example, lipopolysaccharide (LPS) has been widely used to model neuroinflammation associated with neurodegeneration (Batista et al., 2019). More specifically, LPS levels in the brain have been associated with AD pathology, it is abundant in the hippocampus and neocortex of AD-patient brains (Zhao et al., 2017). Thus, experimental models that use LPS could be helpful in understanding the disease process of AD. The main target of LPS is TLR4 and in BV2 cells, LPS stimulation results in increases in IL-1 $\beta$  and TNF- $\alpha$  (Bachstetter et al., 2011). Therefore, LPS could be used to stimulate BV2 cells prior to ATAC-seq to reveal the effect of neuroinflammation associated with AD on chromatin accessibility and provide information on how gene regulation may be affected in AD brains. Additionally, as discussed in Chapter 5 (section 5.3.4), investigating the effect of specific TREM2 activation on the BV2 chromatin landscape would shed more light on the role of the AD genetic risk pathway on chromatin accessibility and gene regulation in this disease. Using these alternative stimulation strategies in BV2 cells may provide information about the chromatin landscape of these cells which is more applicable to AD.

Completing the experiments described in this thesis in BV2 cells has provided a good insight into the role of Mef2c and  $\text{Ca}^{2+}$ -signalling in microglia-like cells. The BV2 cell line was generated by transducing neonatal mouse primary microglia with the v-raf/v-myc carrying J2 retrovirus creating an immortalised microglial line (Blasi et al., 1990). BV2 cells express macrophage markers including macrophage antigen 1 and 2 (MAC1/2) and are negative for the astrocyte and oligodendrocyte markers glial fibrillary acidic protein (GFAP) and galactocerebroside (GalC). BV2 cells have been used extensively in neurodegeneration research, including AD and Parkinson's Disease, as they are easily maintained, freely available and have an ability to proliferate in an unrestricted manner making them useful for assays that require high cell numbers (Gao et al., 2013; Griciuc et al., 2013; Timmerman et al., 2018). Additionally, data presented herein which shows that motifs for several microglial-related transcription factors including PU.1, C/EBP $\beta$  and MEF2 are enriched in BV2 open chromatin regions, validates the microglial-like chromatin profile of BV2 cells and strengthens the use of these cells in these experiments. However, there are several limitations with using BV2 cells as a model of microglia. The immortalisation process

includes a retrovirus to introduce oncogenes to the microglial genome which result in increased proliferation and adhesion and differences in cell morphology when compared to primary microglia (Horvath et al., 2008; Branden Stansley et al., 2012). This means that BV2 cells do not accurately represent the precise *in vivo* state of microglia. This must be considered when interpreting these results and future work should aim to investigate the Mef2c interactome and the influence of  $\text{Ca}^{2+}$  signalling on the chromatin landscape in primary microglia or induced pluripotent stem cell (iPSC)-derived microglia.

## 6.5 Final conclusions

Throughout this final chapter, the most pertinent findings from this thesis have been presented and discussed. Two mechanisms by which  $[\text{Ca}^{2+}]$  levels potentially influence gene regulation; altered protein interactions and chromatin accessibility have been investigated. Collectively, the findings show that Mef2c can be partially released from its transcriptionally inactive state in unstimulated BV2 cells by increasing intracellular  $[\text{Ca}^{2+}]$  and is associated with remodelling of the Mef2c interactome. However, no well characterised transcriptional co-activators appeared to be recruited to the remodelled Mef2c complex. In addition to a remodelling of the Mef2c interactome, this thesis also revealed that ionomycin treatment alters the chromatin landscape in BV2 cells. The motifs of three transcription factors, Atf4, NFATc3 and p53, were identified as enriched at sites with  $\text{Ca}^{2+}$ -induced changes in chromatin accessibility, which tentatively points to a potential role for these transcription factors in mediating  $\text{Ca}^{2+}$ -induced changes in chromatin function and gene expression. By contrast to Atf4, NFATC3 and p53, differentially accessible regions were not enriched for Mef2c motifs beyond the background frequency. However, directly investigating Mef2c motif-containing differentially accessible regions (MDARs) revealed that increases in intracellular  $[\text{Ca}^{2+}]$  may result in the regulation of the microglia inflammatory response by Mef2c. The ATAC-seq data also added to the understanding of the involvement of NFAT and Mef2c as downstream effectors of the TREM2/PLC $\gamma$ 2 pathway, with NFAT potentially involved in initiating  $\text{Ca}^{2+}$ -induced accessibility changes as a direct result of changes in TREM2 signalling. Collectively, these results highlight several potential novel therapeutic targets for the potential manipulation of Mef2c activity and chromatin accessibility in BV2 cells. These data further contribute to our understanding of the transcription factor Mef2c,  $\text{Ca}^{2+}$  signalling, and chromatin function in microglia-like cells.



## References

- Abdul, H. M., Sama, M. A., Furman, J. L., Mathis, D. M., Beckett, T. L., Weidner, A. M., Patel, E. S., Baig, I., Murphy, M. P., LeVine, H., Kraner, S. D., & Norris, C. M. (2009). Cognitive decline in Alzheimer's disease is associated with selective changes in calcineurin/NFAT signaling. *Journal of Neuroscience*, *29*(41), 12957–12969. <https://doi.org/10.1523/JNEUROSCI.1064-09.2009>
- Adcock, I. M., & Caramori, G. (2009). Transcription Factors. In *Asthma and COPD: Basic Mechanisms and Clinical Management* (pp. 373–380). <https://doi.org/10.1016/B978-0-12-374984-0.01552-7>
- Aizenstein, H. J., Nebes, R. D., Saxton, J. A., Price, J. C., Mathis, C. A., Tsopelas, N. D., Ziolkowski, S. K., James, J. A., Snitz, B. E., Houck, P. R., Bi, W., Cohen, A. D., Lopresti, B. J., DeKosky, S. T., Halligan, E. M., & Klunk, W. E. (2008). Frequent amyloid deposition without significant cognitive impairment among the elderly. *Archives of Neurology*, *65*(11), 1509–1517. <https://doi.org/10.1001/archneur.65.11.1509>
- Ajami, B., Bennett, J. L., Krieger, C., Tetzlaff, W., & Rossi, F. M. V. (2007). Local self-renewal can sustain CNS microglia maintenance and function throughout adult life. *Nature Neuroscience*, *10*(12), 1538–1543. <https://doi.org/10.1038/nn2014>
- Akerblom, I. E., Slater, E. P., Beato, M., Baxter, J. D., & Mellon, P. L. (1988). Negative regulation by glucocorticoids through interference with a cAMP responsive enhancer. *Science*, *241*(4863), 350–353. <https://doi.org/10.1126/science.2838908>
- Albert, M. S., DeKosky, S. T., Dickson, D., Dubois, B., Feldman, H. H., Fox, N. C., Gamst, A., Holtzman, D. M., Jagust, W. J., Petersen, R. C., Snyder, P. J., Carrillo, M. C., Thies, B., & Phelps, C. H. (2011). The diagnosis of mild cognitive impairment due to Alzheimer's disease: Recommendations from the National Institute on Aging-Alzheimer's Association workgroups on diagnostic guidelines for Alzheimer's disease. *Alzheimer's and Dementia*, *7*(3), 270–279. <https://doi.org/10.1016/j.jalz.2011.03.008>
- Alexander, G. C., Emerson, S., & Kesselheim, A. S. (2021). Evaluation of Aducanumab for Alzheimer Disease Scientific Evidence and Regulatory Review Involving Efficacy, Safety, and Futility. *JAMA*, *325*, 1717–1718. <https://doi.org/10.1111/cts.12617>
- Allis, C. D., & Jenuwein, T. (2016). The molecular hallmarks of epigenetic control. *Nature Reviews Genetics*, *17*(8), 487–500. <https://doi.org/10.1038/nrg.2016.59>
- Aloia, M. S., Sub, W., & Garden, G. A. (2015). The p53 Transcriptional Network Influences Microglia Behavior and Neuroinflammation. *Critical Reviews in Immunology*, *35*(5), 401–415.
- Alvarez-Buylla, A., & Lim, D. A. (2004). For the long run: Maintaining germinal niches in the adult brain. *Neuron*, *41*(5), 683–686. [https://doi.org/10.1016/S0896-6273\(04\)00111-4](https://doi.org/10.1016/S0896-6273(04)00111-4)
- Alzheimer's Association. (2020). 2020 Alzheimer's disease facts and figures. *Alzheimer's and Dementia*, *16*(3), 391–460. <https://doi.org/10.1002/alz.12068>
- Alzheimer, A. (1907). Allgemeine Zeitschrift für Psychiatrie und Psychisch-Gerichtliche Medizin. *Allgemeine Zeitschrift Für Psychiatrie Und Psychisch-Gerichtliche Medizin.*, *64*, 146.
- Amanchy, R., Balamurugan, Periaswamy, Mathivanan, S., Reddy, R., Tattikota, S. G., & Pandey, A. (2007). A curated compendium of phosphorylation motifs. *Nature*

*Biotechnology*, 25(3), 285–286.

- Amat, R., Planavila, A., Chen, S. L., Iglesias, R., Giralt, M., & Villarroya, F. (2009). SIRT1 controls the transcription of the peroxisome proliferator-activated receptor- $\gamma$  co-activator-1 $\alpha$ (PGC-1 $\alpha$ ) gene in skeletal muscle through the PGC-1 $\alpha$  autoregulatory loop and interaction with MyoD. *Journal of Biological Chemistry*, 284(33), 21872–21880. <https://doi.org/10.1074/jbc.M109.022749>
- Amati, B., & Land, H. (1994). Myc-Max-Mad: a transcription factor network controlling cell cycle progression, differentiation and death. *Current Opinion in Genetics and Development*, 4(1), 102–108. [https://doi.org/10.1016/0959-437X\(94\)90098-1](https://doi.org/10.1016/0959-437X(94)90098-1)
- Amemiya, H. M., Kundaje, A., & Boyle, A. P. (2019). The ENCODE Blacklist: Identification of Problematic Regions of the Genome. *Scientific Reports*, 9(9354), 1–5. <https://doi.org/10.1038/s41598-019-45839-z>
- American Psychiatric Association. (2013). *Diagnostic and statistical manual of mental disorders, fifth edition*. American Psychiatric Publishing.
- Anderson, C. M., Hu, J., Barnes, R. M., Heidt, A. B., Cornelissen, I., & Black, B. L. (2015). Myocyte enhancer factor 2C function in skeletal muscle is required for normal growth and glucose metabolism in mice. *Skeletal Muscle*, 5(1), 1–10. <https://doi.org/10.1186/s13395-015-0031-0>
- Andreone, B. J., Przybyla, L., Llapashtica, C., Rana, A., Davis, S. S., van Lengerich, B., Lin, K., Shi, J., Mei, Y., Astarita, G., Di Paolo, G., Sandmann, T., Monroe, K. M., & Lewcock, J. W. (2020). Alzheimer's-associated PLC $\gamma$ 2 is a signaling node required for both TREM2 function and the inflammatory response in human microglia. *Nature Neuroscience*, 23(8), 927–938. <https://doi.org/10.1038/s41593-020-0650-6>
- Andres, V., Cervera, M., & Mahdavi, V. (1995). Determination of the consensus binding site for MEF2 expressed in muscle and brain reveals tissue-specific sequence constraints. *Journal of Biological Chemistry*, 270(40), 23246–23249. <https://doi.org/10.1074/jbc.270.40.23246>
- Andrews, S. (2010). *FastQC: A Quality Control Tool for High Throughput Sequence Data [Online]*. Babraham Bioinformatics. <http://www.bioinformatics.babraham.ac.uk/projects/fastqc/>
- Ankarcrona, M., Mangialasche, F., & Winblad, B. (2010). Rethinking Alzheimer's disease therapy: Are mitochondria the key? *Journal of Alzheimer's Disease*, 20(SUPPL.2). <https://doi.org/10.3233/JAD-2010-100327>
- Apostolova, L. G. (2016). Alzheimer Disease. *Continuum*, 22(2), 419–434. [www.ContinuumJournal.com](http://www.ContinuumJournal.com)
- Arbel-Ornath, M., Hudry, E., Boivin, J. R., Hashimoto, T., Takeda, S., Kuchibhotla, K. V., Hou, S., Lattarulo, C. R., Belcher, A. M., Shakerdige, N., Trujillo, P. B., Muzikansky, A., Betensky, R. A., Hyman, B. T., & Bacskai, B. J. (2017). Soluble oligomeric amyloid- $\beta$  induces calcium dyshomeostasis that precedes synapse loss in the living mouse brain. *Molecular Neurodegeneration*, 12(1), 1–14. <https://doi.org/10.1186/s13024-017-0169-9>
- Arber, C., Toombs, J., Lovejoy, C. C., Ryan, N. S., Paterson, R. W., Willumsen, N., Gkanatsiou, E., Portelius, E., Blennow, K., Heslegrave, A., Schott, J. M., Hardy, J., Lashley, T., Fox, N. C., Zetterberg, H., & Wray, S. (2019). Familial Alzheimer's disease patient-derived

- neurons reveal distinct mutation-specific effects on amyloid beta. *Molecular Psychiatry*. <https://doi.org/10.1038/s41380-019-0410-8>
- Arnold, S. E., Hyman, B. T., Flory, J., Damasio, A. R., & Van Hoesen, G. W. (1991). The topographical and neuroanatomical distribution of neurofibrillary tangles and neuritic plaques in the cerebral cortex of patients with Alzheimer's disease. *Cerebral Cortex*, *1*(1), 103–116. <https://doi.org/10.1093/cercor/1.1.103>
- Arriagada, P. V, Marzloff, K., & Hyman, B. T. (1992). Distribution of Alzheimer-type pathologic changes in nondemented elderly individuals matches the pattern in Alzheimer's disease. *Neurology*, *42*(9), 1681–1688. <https://doi.org/10.1212/wnl.42.9.1681>
- B'Chir, W., Maurin, A. C., Carraro, V., Averous, J., Jousse, C., Muranishi, Y., Parry, L., Stepien, G., Fafournoux, P., & Bruhat, A. (2013). The eIF2 $\alpha$ /ATF4 pathway is essential for stress-induced autophagy gene expression. *Nucleic Acids Research*, *41*(16), 7683–7699. <https://doi.org/10.1093/nar/gkt563>
- Bachiller, S., Jiménez-Ferrer, I., Paulus, A., Yang, Y., Swanberg, M., Deierborg, T., & Boza-Serrano, A. (2018). Microglia in neurological diseases: A road map to brain-disease dependent-inflammatory response. *Frontiers in Cellular Neuroscience*, *12*(December), 1–17. <https://doi.org/10.3389/fncel.2018.00488>
- Bachstetter, A. D., Xing, B., de Almeida, L., Dimayuga, E. R., Watterson, D. M., & Van Eldik, L. J. (2011). Microglial p38 $\alpha$  MAPK is a key regulator of proinflammatory cytokine up-regulation induced by toll-like receptor (TLR) ligands or beta-amyloid (A $\beta$ ). *Journal of Neuroinflammation*, *8*(1), 79. <https://doi.org/10.1186/1742-2094-8-79>
- Backs, J., Backs, T., Bezprozvannaya, S., McKinsey, T. A., & Olson, E. N. (2008). Histone Deacetylase 5 Acquires Calcium/Calmodulin-Dependent Kinase II Responsiveness by Oligomerization with Histone Deacetylase 4. *Molecular and Cellular Biology*, *28*(10), 3437–3445. <https://doi.org/10.1128/mcb.01611-07>
- Bali, J., Gheinani, A. H., Zurbriggen, S., & Rajendran, L. (2012). Role of genes linked to sporadic Alzheimer's disease risk in the production of  $\beta$ -amyloid peptides. *Proceedings of the National Academy of Sciences*, *109*(38), 15307. <https://doi.org/10.1073/pnas.1201632109>
- Bandyopadhyay, S., Chiang, C. Y., Srivastava, J., Gersten, M., White, S., Bell, R., Kurschner, C., Martin, C. H., Smoot, M., Sahasrabudhe, S., Barber, D. L., Chanda, S. K., & Ideker, T. (2010). A human MAP kinase interactome. *Nature Methods*, *7*(10), 801–805. <https://doi.org/10.1038/nmeth.1506>
- Banerji, J., Rusconi, S., & Schaffner, W. (1981). Expression of a  $\beta$ -globin gene is enhanced by remote SV40 DNA sequences. *Cell*, *27*(2 PART 1), 299–308. [https://doi.org/10.1016/0092-8674\(81\)90413-X](https://doi.org/10.1016/0092-8674(81)90413-X)
- Banumathy, G., Somaiah, N., Zhang, R., Tang, Y., Hoffmann, J., Andrade, M., Ceulemans, H., Schultz, D., Marmorstein, R., & Adams, P. D. (2009). Human UBN1 Is an Ortholog of Yeast Hpc2p and Has an Essential Role in the HIRA/ASF1a Chromatin-Remodeling Pathway in Senescent Cells. *Molecular and Cellular Biology*, *29*(3), 758–770. <https://doi.org/10.1128/mcb.01047-08>
- Barbosa, A. C., Kim, M. S., Ertunc, M., Adachi, M., Nelson, E. D., McAnally, J., Richardson, J. A., Kavalali, E. T., Monteggia, L. M., Bassel-Duby, R., & Olson, E. N. (2008). MEF2C, a transcription factor that facilitates learning and memory by negative regulation of

- synapse numbers and function. *Proceedings of the National Academy of Sciences of the United States of America*, *105*(27), 9391–9396.  
<https://doi.org/10.1073/pnas.0802679105>
- Bateman, A., Martin, M. J., Orchard, S., Magrane, M., Agivetova, R., Ahmad, S., Alpi, E., Bowler-Barnett, E. H., Britto, R., Bursteinas, B., Bye-A-Jee, H., Coetzee, R., Cukura, A., Silva, A. Da, Denny, P., Dogan, T., Ebenezer, T. G., Fan, J., Castro, L. G., ... Zhang, J. (2021). UniProt: The universal protein knowledgebase in 2021. *Nucleic Acids Research*, *49*(D1), D480–D489. <https://doi.org/10.1093/nar/gkaa1100>
- Bateman, R. J., Aisen, P. S., De Strooper, B., Fox, N. C., Lemere, C. A., Ringman, J. M., Salloway, S., Sperling, R. A., Windisch, M., & Xiong, C. (2011). Autosomal-dominant Alzheimer's disease: A review and proposal for the prevention of Alzheimer's disease. *Alzheimer's Research and Therapy*, *2*(6), 1–13. <https://doi.org/10.1186/alzrt59>
- Batista, C. R. A., Gomes, G. F., Candelario-Jalil, E., Fiebich, B. L., & Oliveira, A. C. P. de. (2019). Lipopolysaccharide-Induced Neuroinflammation as a Bridge to Understand Neurodegeneration. *International Journal of Molecular Sciences*, *20*(2293).
- Bekris, L. M., Yu, C., Bird, T. D., & Tsuang, D. W. (2010). Genetics of Alzheimer's disease. *Journal of Geriatric Psychiatry and Neurology*, *23*(4), 213–227.  
<https://doi.org/10.1201/9781315381572>
- Benner, C., Heinz, S., & Glass, C. K. (2017). *HOMER - Software for motif discovery and next generation sequencing analysis*.
- Bennett, M. L., Bennett, F. C., Liddelow, S. A., Ajami, B., Zamanian, J. L., Fernhoff, N. B., Mulinyawe, S. B., Bohlen, C. J., Adil, A., Tucker, A., Weissman, I. L., Chang, E. F., Li, G., Grant, G. A., Hayden Gephart, M. G., & Barres, B. A. (2016). New tools for studying microglia in the mouse and human CNS. *Proceedings of the National Academy of Sciences of the United States of America*, *113*(12), E1738–E1746.  
<https://doi.org/10.1073/pnas.1525528113>
- Benson, M. A., Tinsley, C. L., Waite, A. J., Carlisle, F. A., Sweet, S. M. M., Ehler, E., George, C. H., Lai, F. A., Martin-Rendon, E., & Blake, D. J. (2017). Ryanodine receptors are part of the myospryn complex in cardiac muscle. *Scientific Reports*, *7*(1), 1–12.  
<https://doi.org/10.1038/s41598-017-06395-6>
- Bernstein, B. E., Humphrey, E. L., Erlich, R. L., Schneider, R., Bouman, P., Liu, J. S., Kouzarides, T., & Schreiber, S. L. (2002). Methylation of histone H3 Lys 4 in coding regions of active genes. *Proceedings of the National Academy of Sciences of the United States of America*, *99*(13), 8695–8700.  
<https://doi.org/10.1073/pnas.082249499>
- Berridge, M. J. (2009). Inositol trisphosphate and calcium signalling mechanisms. *Biochimica et Biophysica Acta - Molecular Cell Research*, *1793*(6), 933–940.  
<https://doi.org/10.1016/j.bbamcr.2008.10.005>
- Berridge, M. J., Bootman, M. D., & Lipp, P. (1998). Calcium- a life and death signal. *Nature*, *395*, 645–648. <https://doi.org/10.1038/120001a0>
- Berridge, M. J., Lipp, P., & Bootman, M. D. (2000). The versatility and universality of calcium signalling. *Nature Reviews*, *1*(October), 11–21.
- Bertram, L., Lange, C., Mullin, K., Parkinson, M., Hsiao, M., Hogan, M. F., Schjeide, B. M. M., Hooli, B., DiVito, J., Ionita, I., Jiang, H., Laird, N., Moscarillo, T., Ohlsen, K. L., Elliott, K.,

- Wang, X., Hu-Lince, D., Ryder, M., Murphy, A., ... Tanzi, R. E. (2008). Genome-wide Association Analysis Reveals Putative Alzheimer's Disease Susceptibility Loci in Addition to APOE. *American Journal of Human Genetics*, *83*(5), 623–632. <https://doi.org/10.1016/j.ajhg.2008.10.008>
- Bhatt, D., & Ghosh, S. (2014). Regulation of the NF- $\kappa$ B-mediated transcription of inflammatory genes. *Frontiers in Immunology*, *5*(FEB), 1–9. <https://doi.org/10.3389/fimmu.2014.00071>
- Birks, J. (2006). Cholinesterase inhibitors for Alzheimer's disease. *Cochrane Database Syst Rev*, *1*, CD005593. <https://doi.org/10.1002/14651858.CD005593>
- Black, B. L., Ligon, K. L., Zhang, Y., & Olson, E. N. (1996). Cooperative transcriptional activation by the neurogenic basic helix-loop-helix protein MASH1 and members of the myocyte enhancer factor-2 (MEF2) family. *Journal of Biological Chemistry*, *271*(43), 26659–26663. <https://doi.org/10.1074/jbc.271.43.26659>
- Black, B. L., Molkenin, J. D., & Olson, E. N. (1998). Multiple Roles for the MyoD Basic Region in Transmission of Transcriptional Activation Signals and Interaction with MEF2. *Molecular and Cellular Biology*, *18*(1), 69–77. <https://doi.org/10.1128/mcb.18.1.69>
- Black, B. L., & Olson, E. N. (1998). TRANSCRIPTIONAL CONTROL OF MUSCLE DEVELOPMENT BY MYOCYTE ENHANCER FACTOR-2 (MEF2) PROTEINS. In *Annu. Rev. Cell Dev. Biol* (Vol. 14). [www.annualreviews.org](http://www.annualreviews.org)
- Blackwood, E. M., & Kadonaga, J. T. (1998). Going the distance: A current view of enhancer action. *Science*, *281*(5373), 60–63. <https://doi.org/10.1126/science.281.5373.60>
- Blaeser, F., Ho, N., Prywes, R., & Chatila, T. A. (2000). *Ca 2-dependent Gene Expression Mediated by MEF2 Transcription Factors\**. <http://www.jbc.org/>
- Blasi, E., Barluzzi, R., Bocchini, V., Mazzolla, R., & Bistoni, F. (1990). Immortalization of murine microglial cells by a v-raf / v-myc carrying retrovirus. *Journal of Neuroimmunology*, *27*(2–3), 229–237.
- Bogenhagen, D. F. (2012). Mitochondrial DNA nucleoid structure. *Biochimica et Biophysica Acta - Gene Regulatory Mechanisms*, *1819*(9–10), 914–920. <https://doi.org/10.1016/j.bbagr.2011.11.005>
- Bootman, M. D., Collins, T. J., Peppiatt, C. M., Prothero, L. S., MacKenzie, L., De Smet, P., Travers, M., Tovey, S. C., Seo, J. T., Berridge, M. J., Ciccolini, F., & Lipp, P. (2001). Calcium signalling - An overview. *Seminars in Cell and Developmental Biology*, *12*(1), 3–10. <https://doi.org/10.1006/scdb.2000.0211>
- Borghi, S., Molinari, S., Razzini, G., Parise, R., Battini, R., & Ferrari, S. (2001). The nuclear localization domain of the MEF2 family of transcription factors shows member-specific features and mediates the nuclear import of histone deacetylase 4. *Journal of Cell Science*, *114*(24), 4477–4483.
- Braak, H., & Braak, E. (1991). Neuropathological staging of Alzheimer-related changes. *Acta Neuropathologica*, *82*(4), 239–259. <https://doi.org/10.1007/BF00308809>
- Bradshaw, E. M., Chibnik, L. B., Keenan, B. T., Ottoboni, L., Raj, T., Tang, A., Rosenkrantz, L. L., Imboywa, S., Lee, M., Von Korff, A., Morris, M. C., Evans, D. A., Johnson, K., Sperling, R. A., Schneider, J. A., Bennett, D. A., & De Jager, P. L. (2013). CD33 Alzheimer's disease locus: Altered monocyte function and amyloid biology. *Nature*

- Neuroscience*, 16(7), 848–850. <https://doi.org/10.1038/nn.3435>
- Breitbart, R. E., Liang -s., C., Smoot, L. B., Laheru, D. A., Mahdavi, V., & Nadal-Ginard, B. (1993). A fourth human MEF2 transcription factor, hMEF2D, is an early marker of the myogenic lineage. *Development*, 118(4), 1095–1106.
- Brignall, R., Cauchy, P., Bevington, S. L., Gorman, B., Pisco, A. O., Bagnall, J., Boddington, C., Rowe, W., England, H., Rich, K., Schmidt, L., Dyer, N. P., Travis, M. A., Ott, S., Jackson, D. A., Cockerill, P. N., & Paszek, P. (2017). Integration of Kinase and Calcium Signaling at the Level of Chromatin Underlies Inducible Gene Activation in T Cells. *The Journal of Immunology*, 199(8), 2652–2667. <https://doi.org/10.4049/jimmunol.1602033>
- Brion, J.-P., Flament-Durand, J., & Dustin, P. (1986). Alzheimer’s Disease and Tau Proteins. *The Lancet.*, 328(8515), 1098. [https://doi.org/10.1016/S0140-6736\(86\)90495-2](https://doi.org/10.1016/S0140-6736(86)90495-2)
- Bryois, J., Garrett, M. E., Song, L., Safi, A., Giusti-Rodriguez, P., Johnson, G. D., Shieh, A. W., Buil, A., Fullard, J. F., Roussos, P., Sklar, P., Akbarian, S., Haroutunian, V., Stockmeier, C. A., Wray, G. A., White, K. P., Liu, C., Reddy, T. E., Ashley-Koch, A., ... Crawford, G. E. (2018). Evaluation of chromatin accessibility in prefrontal cortex of individuals with schizophrenia. *Nature Communications*, 9(1). <https://doi.org/10.1038/s41467-018-05379-y>
- Bucher, P. (1990). Weight matrix descriptions of four eukaryotic RNA polymerase II promoter elements derived from 502 unrelated promoter sequences. *Journal of Molecular Biology*, 212(4), 563–578. [https://doi.org/10.1016/0022-2836\(90\)90223-9](https://doi.org/10.1016/0022-2836(90)90223-9)
- Buenrostro, J. D., Giresi, P. G., Zaba, L. C., Chang, H. Y., & Greenleaf, W. J. (2013). Transposition of native chromatin for fast and sensitive epigenomic profiling of open chromatin, DNA-binding proteins and nucleosome position. *Nature Methods*, 10(12), 1213–1218. <https://doi.org/10.1038/nmeth.2688>
- Buscà, R., Pouysségur, J., & Lenormand, P. (2016). ERK1 and ERK2 map kinases: Specific roles or functional redundancy? *Frontiers in Cell and Developmental Biology*, 4(JUN), 1–23. <https://doi.org/10.3389/fcell.2016.00053>
- Buskin, J. N., & Hauschka, S. D. (1989). Identification of a Myocyte Nuclear Factor That Binds to the Muscle-Specific Enhancer of the Mouse Muscle Creatine Kinase Gene. *MOLECULAR AND CELLULAR BIOLOGY*.
- Butovsky, O., Jedrychowski, M. P., Moore, C. S., Cialic, R., Lanser, A. J., Gabriely, G., Koeglsperger, T., Dake, B., Wu, P. M., Doykan, C. E., Fanek, Z., Liu, L., Chen, Z., Rothstein, J. D., Ransohoff, R. M., Gygi, S. P., Antel, J. P., & Weiner, H. L. (2014). Identification of a unique TGF- $\beta$ -dependent molecular and functional signature in microglia. *Nature Neuroscience*, 17(1), 131–143. <https://doi.org/10.1038/nn0914-1286d>
- Byun, J. S., Lee, J. W., Kim, S. Y., Kwon, K. J., Sohn, J. H., Lee, K., Oh, D., Kim, S. S., Chun, W., & Lee, H. J. (2010). Neuroprotective effects of stanniocalcin 2 following kainic acid-induced hippocampal degeneration in ICR mice. *Peptides*, 31(11), 2094–2099. <https://doi.org/10.1016/j.peptides.2010.08.002>
- Calvo-Rodriguez, M., Kharitonova, E. K., & Bacskaï, B. J. (2020). Therapeutic Strategies to Target Calcium Dysregulation in Alzheimer’s Disease. *Cells*, 9(11). <https://doi.org/10.3390/cells9112513>
- Canté-Barrett, K., Pieters, R., & Meijerink, J. P. P. (2014). Myocyte enhancer factor 2C in

- hematopoiesis and leukemia. *Oncogene*, *33*(4), 403–410.  
<https://doi.org/10.1038/onc.2013.56>
- Cao, L. L., Guan, P. P., Liang, Y. Y., Huang, X. S., & Wang, P. (2019). Calcium ions stimulate the hyperphosphorylation of tau by activating microsomal prostaglandin E synthase 1. *Frontiers in Aging Neuroscience*, *11*(108), 1–16.  
<https://doi.org/10.3389/fnagi.2019.00108>
- Carotta, S., Wu, L., & Nutt, S. L. (2010). Surprising new roles for PU.1 in the adaptive immune response. *Immunological Reviews*, *238*(1), 63–75.  
<https://doi.org/10.1111/j.1600-065X.2010.00955.x>
- Chami, M., & Checler, F. (2020). Alterations of the Endoplasmic Reticulum (ER) Calcium Signaling Molecular Components in Alzheimer's Disease. *Cells*, *9*(12), 1–23.  
<https://doi.org/10.3390/cells9122577>
- Chan, J. K. L., Sun, L., Yang, X. J., Zhu, G., & Wu, Z. (2003). Functional characterization of an amino-terminal region of HDAC4 that possesses MEF2 binding and transcriptional repressive activity. *Journal of Biological Chemistry*, *278*(26), 23515–23521.  
<https://doi.org/10.1074/jbc.M301922200>
- Chang, A. C. M., Hook, J., Lemckert, F. A., McDonald, M. M., Nguyen, M. A. T., Hardeman, E. C., Little, D. G., Gunning, P. W., & Reddel, R. R. (2008). The murine stanniocalcin 2 gene is a negative regulator of postnatal growth. *Endocrinology*, *149*(5), 2403–2410.  
<https://doi.org/10.1210/en.2007-1219>
- Chavez, S. (2000). A protein complex containing Tho2, Hpr1, Mft1 and a novel protein, Thp2, connects transcription elongation with mitotic recombination in *Saccharomyces cerevisiae*. *The EMBO Journal*, *19*(21), 5824–5834.  
<https://doi.org/10.1093/emboj/19.21.5824>
- Chen, H. H., Mullett, S. J., & Stewart, A. F. R. (2004). Vgl-4, a novel member of the vestigial-like family of transcription cofactors, regulates  $\alpha$ 1-adrenergic activation of gene expression in cardiac myocytes. *Journal of Biological Chemistry*, *279*(29), 30800–30806. <https://doi.org/10.1074/jbc.M400154200>
- Chen, R., Chan, P. T., Chu, H., Lin, Y. C., Chang, P. C., Chen, C. Y., & Chou, K. R. (2017). Treatment effects between monotherapy of donepezil versus combination with memantine for Alzheimer disease: A meta-analysis. *PLoS ONE*, *12*(8), 1–14.  
<https://doi.org/10.1371/journal.pone.0183586>
- Chen, S. L., Dowhan, D. H., Hosking, B. M., & Muscat, G. E. O. (2000). The steroid receptor coactivator, GRIP-1, is necessary for MEF-2C- dependent gene expression and skeletal muscle differentiation. *Genes and Development*, *14*(10), 1209–1228.  
<https://doi.org/10.1101/gad.14.10.1209>
- Cherry, J. D., Olschowka, J. A., & O'Banion, M. K. (2014). Neuroinflammation and M2 microglia: The good, the bad, and the inflamed. *Journal of Neuroinflammation*, *11*(1), 1–15. <https://doi.org/10.1186/1742-2094-11-98>
- Chávez-Gutiérrez, L., Bammens, L., Benilova, I., Vandersteen, A., Benurwar, M., Borgers, M., Lismont, S., Zhou, L., Van Cleynenbreugel, S., Esselmann, H., Wiltfang, J., Serneels, L., Karran, E., Gijzen, H., Schymkowitz, J., Rousseau, F., Broersen, K., & De Strooper, B. (2012). The mechanism of  $\gamma$ -Secretase dysfunction in familial Alzheimer disease. *EMBO Journal*, *31*(10), 2261–2274. <https://doi.org/10.1038/emboj.2012.79>

- Chiu, I. M., Morimoto, E. T. A., Goodarzi, H., Liao, J. T., O'Keefe, S., Phatnani, H. P., Muratet, M., Carroll, M. C., Levy, S., Tavazoie, S., Myers, R. M., & Maniatis, T. (2013). A neurodegeneration-specific gene-expression signature of acutely isolated microglia from an amyotrophic lateral sclerosis mouse model. *Cell Reports*, *4*(2), 385–401. <https://doi.org/10.1016/j.celrep.2013.06.018>
- Chu, Y., Jin, X., Parada, I., Pesic, A., Stevens, B., Barres, B., & Prince, D. A. (2010). Enhanced synaptic connectivity and epilepsy in C1q knockout mice. *Proceedings of the National Academy of Sciences of the United States of America*, *107*(17), 7975–7980. <https://doi.org/10.1073/pnas.0913449107>
- Clapier, C. R., & Cairns, B. R. (2009). The Biology of Chromatin Remodeling Complexes. *Annual Review of Biochemistry*, *78*(1), 273–304. <https://doi.org/10.1146/annurev.biochem.77.062706.153223>
- Colonna, M., & Butovsky, O. (2017). Microglia Function in the Central Nervous System During Health and Neurodegeneration. *Annual Review of Immunology*, *35*(1), 441–468. <https://doi.org/10.1146/annurev-immunol-051116-052358>
- Combs, C. K., Johnson, D. E., Cannady, S. B., Lehman, T. M., & Landreth, G. E. (1999). Identification of microglial signal transduction pathways mediating a neurotoxic response to amyloidogenic fragments of  $\beta$ -amyloid and prion proteins. *Journal of Neuroscience*, *19*(3), 928–939. <https://doi.org/10.1523/jneurosci.19-03-00928.1999>
- Condello, C., Yuan, P., Schain, A., & Grutzendler, J. (2015). Microglia constitute a barrier that prevents neurotoxic protofibrillar A $\beta$ 42 hotspots around plaques. *Nature Communications*, *6*(May 2014). <https://doi.org/10.1038/ncomms7176>
- Corces, M. R., Buenrostro, J. D., Wu, B., Greenside, P. G., Chan, S. M., Koenig, J. L., Snyder, M. P., Pritchard, J. K., Kundaje, A., Greenleaf, W. J., Majeti, R., & Chang, H. Y. (2016). Lineage-specific and single-cell chromatin accessibility charts human hematopoiesis and leukemia evolution. *Nature Genetics*, *48*(10), 1193–1203. <https://doi.org/10.1038/ng.3646>
- Corces, M. R., Trevino, A. E., Hamilton, E. G., Greenside, P. G., Sinnott-Armstrong, N. A., Vesuna, S., Satpathy, A. T., Rubin, A. J., Montine, K. S., Wu, B., Kathiria, A., Cho, S. W., Mumbach, M. R., Carter, A. C., Kasowski, M., Orloff, L. A., Risca, V. I., Kundaje, A., Khavari, P. A., ... Chang, H. Y. (2017). An improved ATAC-seq protocol reduces background and enables interrogation of frozen tissues. *Nature Methods*, *14*(10), 959–962. <https://doi.org/10.1101/181206>
- Corder, E. H., Saunders, A. M., Risch, N. J., Strittmatter, W. J., Schmechel, D. E., Gaskell, P. C., Rimmler, J. B., Locke, P. A., Conneally, P. M., Schmechel, K. E., Small, G. W., Roses, A. D., Haines, J. L., & Pericak-Vance, M. A. (1994). Protective effect of apolipoprotein E type 2 allele for late onset Alzheimer disease. *Nature Genetics*, *7*(2), 180–184. <https://doi.org/10.1038/ng0694-180>
- Cowie, P., Hay, E. A., & Mackenzie, A. (2015). The noncoding human genome and the future of personalised medicine. *Expert Reviews in Molecular Medicine*, *17*(January 2015). <https://doi.org/10.1017/erm.2014.23>
- Crabtree, G. R., & Olson, E. N. (2002). NFAT signaling: Choreographing the social lives of cells. *Cell*, *109*(2 SUPPL. 1), 67–79. [https://doi.org/10.1016/S0092-8674\(02\)00699-2](https://doi.org/10.1016/S0092-8674(02)00699-2)
- Crehan, H., Holton, P., Wray, S., Pocock, J., Guerreiro, R., & Hardy, J. (2012). Complement receptor 1 (CR1) and Alzheimer's disease. *Immunobiology*, *217*(2), 244–250.



<https://doi.org/10.1016/j.imbio.2011.07.017>

- Creyghton, M. P., Cheng, A. W., Welstead, G. G., Kooistra, T., Carey, B. W., Steine, E. J., Hanna, J., Lodato, M. A., Frampton, G. M., Sharp, P. A., Boyer, L. A., Young, R. A., & Jaenisch, R. (2010). Histone H3K27ac separates active from poised enhancers and predicts developmental state. *Proceedings of the National Academy of Sciences of the United States of America*, *107*(50), 21931–21936. <https://doi.org/10.1073/pnas.1016071107>
- Cunningham, C. L., Martínez-Cerdeño, V., & Noctor, S. C. (2013). Microglia regulate the number of neural precursor cells in the developing cerebral cortex. *Journal of Neuroscience*, *33*(10), 4216–4233. <https://doi.org/10.1523/JNEUROSCI.3441-12.2013>
- Dai, M. H., Zheng, H., Zeng, L. D., & Zhang, Y. (2018). The genes associated with early-onset Alzheimer's disease. *Oncotarget*, *9*(19), 15132–15143. <https://doi.org/10.18632/oncotarget.23738>
- Davalos, D., Grutzendler, J., Yang, G., Kim, J. V., Zuo, Y., Jung, S., Littman, D. R., Dustin, M. L., & Gan, W. B. (2005). ATP mediates rapid microglial response to local brain injury in vivo. *Nature Neuroscience*, *8*(6), 752–758. <https://doi.org/10.1038/nn1472>
- Davies, G., Armstrong, N., Bis, J. C., Bressler, J., Chouraki, V., Giddaluru, S., Hofer, E., Ibrahim-Verbaas, C. A., Kirin, M., Lahti, J., Van Der Lee, S. J., Le Hellard, S., Liu, T., Marioni, R. E., Oldmeadow, C., Postmus, I., Smith, A. V., Smith, J. A., Thalamuthu, A., ... Deary, I. J. (2015). Genetic contributions to variation in general cognitive function: A meta-analysis of genome-wide association studies in the CHARGE consortium (N=53 949). *Molecular Psychiatry*, *20*(2), 183–192. <https://doi.org/10.1038/mp.2014.188>
- de Leeuw, C. A., Mooij, J. M., Heskes, T., & Posthuma, D. (2015). MAGMA: Generalized Gene-Set Analysis of GWAS Data. *PLoS Computational Biology*, *11*(4), 1–19. <https://doi.org/10.1371/journal.pcbi.1004219>
- De Munter, S., Görnemann, J., Derua, R., Lesage, B., Qian, J., Heroes, E., Waelkens, E., Van Eynde, A., Beullens, M., & Bollen, M. (2017). Split-BioID: a proximity biotinylation assay for dimerization-dependent protein interactions. *FEBS Letters*, *591*(2), 415–424. <https://doi.org/10.1002/1873-3468.12548>
- Deane, R., Sagare, A., Hamm, K., Parisi, M., Lane, S., Finn, M. B., Holtzman, D. M., & Zlokovic, B. V. (2008). apoE isoform – specific disruption of amyloid  $\beta$  peptide clearance from mouse brain. Deane, R., Sagare, A., Hamm, K., Parisi, M., Lane, S., Finn, M. B., ... Zlokovic, B. V. (2008). apoE isoform – specific disruption of amyloid  $\beta$  peptide clearance from mouse br. *The Journal of Clinical Investigation*, *118*(12), 4002–4013. <https://doi.org/10.1172/JCI36663DS1>
- Deczkowska, A., Matcovitch-Natan, O., Tzitsou-Kampeli, A., Ben-Hamo, S., Dvir-Szternfeld, R., Spinrad, A., Singer, O., David, E., Winter, D. R., Smith, L. K., Kertser, A., Baruch, K., Rosenzweig, N., Terem, A., Prinz, M., Villeda, S., Citri, A., Amit, I., & Schwartz, M. (2017). Mef2C restrains microglial inflammatory response and is lost in brain ageing in an IFN-I-dependent manner. *Nature Communications*, *8*(1). <https://doi.org/10.1038/s41467-017-00769-0>
- Deture, M. A., & Dickson, D. W. (2019). The neuropathological diagnosis of Alzheimer's disease. *Molecular Neurodegeneration*, *14*(1), 1–18. <https://doi.org/10.1186/s13024-019-0333-5>
- Dhavan, R., & Tsai, L. H. (2001). A decade of CDK5. *Nature Reviews Molecular Cell Biology*,

- 2(10), 749–759. <https://doi.org/10.1038/35096019>
- Di Giorgio, E., Gagliostro, E., Clocchiatti, A., & Brancolini, C. (2015). The Control Operated by the Cell Cycle Machinery on MEF2 Stability Contributes to the Downregulation of CDKN1A and Entry into S Phase. *Molecular and Cellular Biology*, 35(9), 1633–1647. <https://doi.org/10.1128/mcb.01461-14>
- Dodou, E., Xu, S. M., & Black, B. L. (2003). Mef2C Is Activated Directly By Myogenic Basic Helix-Loop-Helix Proteins During Skeletal Muscle Development in Vivo. *Mechanisms of Development*, 120(9), 1021–1032. [https://doi.org/10.1016/S0925-4773\(03\)00178-3](https://doi.org/10.1016/S0925-4773(03)00178-3)
- Dong, C., Yang, X. Z., Zhang, C. Y., Liu, Y. Y., Zhou, R. Bin, Cheng, Q. Di, Yan, E. K., & Yin, D. C. (2017). Myocyte enhancer factor 2C and its directly-interacting proteins: A review. *Progress in Biophysics and Molecular Biology*, 126, 22–30. <https://doi.org/10.1016/j.pbiomolbio.2017.02.002>
- Dressel, U., Bailey, P. J., Wang, S. C. M., Downes, M., Evans, R. M., & Muscat, G. E. O. (2001). A Dynamic Role for HDAC7 in MEF2-mediated Muscle Differentiation. *Journal of Biological Chemistry*, 276(20), 17007–17013. <https://doi.org/10.1074/jbc.M101508200>
- Drummond, E., & Wisniewski, T. (2017). Alzheimer’s Disease: Experimental Models and Reality. *Acta Neuropathologica*, 133(2), 155–175. <https://doi.org/10.1016/j.physbeh.2017.03.040>
- Ecco, G., Imbeault, M., & Trono, D. (2017). KRAB zinc finger proteins. *Development (Cambridge)*, 144(15), 2719–2729. <https://doi.org/10.1242/dev.132605>
- Edmondson, D. G., Lyons, G. E., Martin, J. F., & Olson, E. N. (1994). Mef2 gene expression marks the cardiac and skeletal muscle lineages during mouse embryogenesis. *Development*, 120(5), 1251–1263.
- Efthymiou, A. G., & Goate, A. M. (2017). Late onset Alzheimer’s disease genetics implicates microglial pathways in disease risk. *Molecular Neurodegeneration*, 12(1), 1–12. <https://doi.org/10.1186/s13024-017-0184-x>
- Ejarque-Ortiz, A., Gresa-Arribas, N.´ria, Straccia, M., Mancera, P., Sola, C., Tusell, J. M., Serratos, J., & Saura, J. (2010). CCAAT Enhancer Binding Protein Delta in Microglial Activation. In *Journal of Neuroscience Research* (pp. 1113–1123). <https://doi.org/10.32388/sth5fq>
- El Khoury, J. B., Moore, K. J., Means, T. K., Leung, J., Terada, K., Toft, M., Freeman, M. W., & Luster, A. D. (2003). CD36 mediates the innate host response to  $\beta$ -amyloid. *Journal of Experimental Medicine*, 197(12), 1657–1666. <https://doi.org/10.1084/jem.20021546>
- Emptage, N. J., Reid, C. A., & Fine, A. (2001). Calcium stores in hippocampal synaptic boutons mediate short-term plasticity, store-operated Ca<sup>2+</sup> entry, and spontaneous transmitter release. *Neuron*, 29(1), 197–208. [https://doi.org/10.1016/S0896-6273\(01\)00190-8](https://doi.org/10.1016/S0896-6273(01)00190-8)
- ENCODE. (2004). The ENCODE (ENCyclopedia Of DNA Elements) Project. *Science (New York, N.Y.)*, 306(5696), 636–640. <https://doi.org/10.1126/science.1105136>
- Engels, H., Wohlleber, E., Zink, A., Hoyer, J., Ludwig, K. U., Brockschmidt, F. F., Wiczorek, D., Moog, U., Hellmann-Mersch, B., Weber, R. G., Willatt, L., Kreiß-Nachtsheim, M., Firth, H. V., & Rauch, A. (2009). A novel microdeletion syndrome involving 5q14.3-q15: Clinical and molecular cytogenetic characterization of three patients. *European*

- Journal of Human Genetics*, 17(12), 1592–1599. <https://doi.org/10.1038/ejhg.2009.90>
- Escott-Price, V., Sims, R., Bannister, C., Harold, D., Vronskaya, M., Majounie, E., Badarinarayan, N., Morgan, K., Passmore, P., Holmes, C., Powell, J., Brayne, C., Gill, M., Mead, S., Goate, A., Cruchaga, C., Lambert, J. C., van Duijn, C., Maier, W., ... Consortium, I. (2015). Common polygenic variation enhances risk prediction for Alzheimer's disease. *Brain*, 138, 3673–3684. <https://doi.org/10.1093/brain/awv268>
- Färber, K., & Kettenmann, H. (2006). Functional Role of Calcium Signals for Microglial Function. *Glia*, 54(7), 656–665. <https://doi.org/10.1002/glia>
- Farlow, M. R., Miller, M. L., & Pejovic, V. (2008). Treatment Options in Alzheimer's Disease: Maximizing Benefit, Managing Expectations. *Dementia and Geriatric Cognitive Disorders*, 25(5), 408–422. <https://doi.org/10.1159/000122962>
- Fernández, M., Gobartt, A. L., & Balañá, M. (2010). Behavioural symptoms in patients with Alzheimer's disease and their association with cognitive impairment. *BMC Neurology*, 10. <https://doi.org/10.1186/1471-2377-10-87>
- Fields, S., & Song, O. K. (1989). A novel genetic system to detect protein-protein interactions. *Nature*, 340(6230), 245–246. <https://doi.org/10.1038/340245a0>
- Filipescu, D., Müller, S., & Almouzni, G. (2014). Histone H3 Variants and Their Chaperones During Development and Disease: Contributing to Epigenetic Control. *Annual Review of Cell and Developmental Biology*, 30(1), 615–646. <https://doi.org/10.1146/annurev-cellbio-100913-013311>
- Flavell, S. W., Cowan, C. W., Kim, T. K., Greer, P. L., Lin, Y., Paradis, S., Griffith, E. C., Hu, L. S., Chen, C., & Greenberg, M. E. (2006). Activity-dependent regulation of MEF2 transcription factors suppresses excitatory synapse number. *Science*, 311(5763), 1008–1012. <https://doi.org/10.1126/science.1122511>
- Forner, S., Baglietto-Vargas, D., Martini, A. C., Trujillo-Estrada, L., & LaFerla, F. M. (2017). Synaptic Impairment in Alzheimer's Disease: A Dysregulated Symphony. *Trends in Neurosciences*, 40(6), 347–357. <https://doi.org/10.1016/j.tins.2017.04.002>
- Frade, J. M., & Barde, Y. A. (1998). Microglia-derived nerve growth factor causes cell death in the developing retina. *Neuron*, 20(1), 35–41. [https://doi.org/10.1016/S0896-6273\(00\)80432-8](https://doi.org/10.1016/S0896-6273(00)80432-8)
- Franco, R., & Fernández-Suárez, D. (2015). Alternatively activated microglia and macrophages in the central nervous system. *Progress in Neurobiology*, 131, 65–86.
- Frautschy, S. A., Yang, F., Irrizarry, M., Hyman, B., Saido, T. C., Hsiao, K., & Cole, G. M. (1998). Microglial response to amyloid plaques in APPsw transgenic mice. *Am J Pathol*, 152(1), 307–317. <https://www.ncbi.nlm.nih.gov/pubmed/9422548>
- Free, R. B., Hazelwood, L. A., & Sibley, D. R. (2009). Identifying novel protein-protein interactions using co-immunoprecipitation and mass spectroscopy. *Current Protocols in Neuroscience*, SUPPL. 46, 1–19. <https://doi.org/10.1002/0471142301.ns0528s46>
- Frietze, S., & Farnham, P. J. (2011). Transcription factor effector domains. *Sub-Cellular Biochemistry*, 52, 261–277. [https://doi.org/10.1007/978-90-481-9069-0\\_12](https://doi.org/10.1007/978-90-481-9069-0_12)
- Fullard, J. F., Hauberg, M. E., Bendl, J., Egervari, G., Cirnaru, M. D., Reach, S. M., Motl, J., Ehrlich, M. E., Hurd, Y. L., & Roussos, P. (2018). An atlas of chromatin accessibility in the adult human brain. *Genome Research*, 28(8), 1243–1252.

<https://doi.org/10.1101/gr.232488.117>

- Fulton, D. L., Sundararajan, S., Badis, G., Hughes, T. R., Wasserman, W. W., Roach, J. C., & Sladek, R. (2009). TFCat: The curated catalog of mouse and human transcription factors. *Genome Biology*, *10*(3). <https://doi.org/10.1186/gb-2009-10-3-r29>
- Gage, F. H. (2002). Neurogenesis in the adult brain. *The Journal of Neuroscience*, *22*(3), 612–613. <https://doi.org/10.1023/A:1021150525223>
- Gao, C., Cheng, X., Lam, M., Liu, Y., Liu, Q., Chang, K., & Kao, H. (2008). Signal-dependent Regulation of Transcription by Histone Deacetylase 7 Involves Recruitment to Promyelocytic Leukemia Protein Nuclear Bodies. *Molecular Biology of the Cell*, *19*(July), 3020–3027. <https://doi.org/10.1091/mbc.E07>
- Gao, F., Chen, D., Hu, Q., & Wang, G. (2013). Rotenone Directly Induces BV2 Cell Activation via the p38 MAPK Pathway. *PLoS ONE*, *8*(8), 1–9. <https://doi.org/10.1371/journal.pone.0072046>
- Gatz, M., Reynolds, C. A., Fratiglioni, L., Johansson, B., Mortimer, J. A., Berg, S., Fiske, A., & Pedersen, N. L. (2006). Role of genes and environments for explaining Alzheimer disease. *Archives of General Psychiatry*, *63*(2), 168–174. <https://doi.org/10.1001/archpsyc.63.2.168>
- Gertz, J., Savic, D., Varley, K. E., Partridge, E. C., Safi, A., Jain, P., Cooper, G. M., Reddy, T. E., Crawford, G. E., & Myers, R. M. (2013). Distinct properties of cell-type-specific and shared transcription factor binding sites. *Molecular Cell*, *52*(1), 25–36. <https://doi.org/10.1016/j.molcel.2013.08.037>
- Ghisletti, S., Barozzi, I., Mietton, F., Polletti, S., De Santa, F., Venturini, E., Gregory, L., Lonie, L., Chew, A., Wei, C. L., Ragoussis, J., & Natoli, G. (2010). Identification and Characterization of Enhancers Controlling the Inflammatory Gene Expression Program in Macrophages. *Immunity*, *32*(3), 317–328. <https://doi.org/10.1016/j.immuni.2010.02.008>
- Giannakopoulos, P., Herrmann, F. R., Bussi ere, T., Bouras, C., Kovari, E., Perl, D. P., Morrison, J. H., Gold, G., & Hof, P. R. (2003). Tangle and neuron numbers, but not amyloid load, predict cognitive status in Alzheimer’s disease. *Neurology*, *60*(9), 1495–1500. <https://doi.org/10.1212/01.wnl.0000063311.58879.01>
- Gibson, G. E., Vestling, M., Zhang, H., Szolosi, S., Alkon, D., Lannfelt, L., Gandy, S., & Cowburn, R. F. (1997). Abnormalities in Alzheimer’s disease fibroblasts bearing the APP670/671 mutation. *Neurobiology of Aging*, *18*(6), 573–580. [https://doi.org/10.1016/S0197-4580\(97\)00149-8](https://doi.org/10.1016/S0197-4580(97)00149-8)
- Gibson, G., & Peterson, C. (1987). Calcium and the aging nervous system. *Neurobiology of Aging*, *8*(4), 329–343. [https://doi.org/10.1016/0197-4580\(87\)90083-2](https://doi.org/10.1016/0197-4580(87)90083-2)
- Ginhoux, F., Greter, M., Leboeuf, M., Nandi, S., See, P., Gokhan, S., Mehler, M. F., Conway, S. J., Ng, L. G., Stanley, E. R., Samokhvalov, I. M., & Merad, M. (2010). Fate Mapping Analysis Reveals That Adult Microglia Derive from Primitive Macrophages. *Science*, *701*(November), 841–845. <https://doi.org/10.1126/science.1194637>
- Ginhoux, F., & Prinz, M. (2015). Origin of microglia: Current concepts and past controversies. *Cold Spring Harbor Perspectives in Biology*, *7*(8), 1–15. <https://doi.org/10.1101/cshperspect.a020537>
- Glenner, G. G., & Wong, C. W. (1984). Alzheimer’s disease and Down’s syndrome: sharing

- of a unique cerebrovascular amyloid fibril protein. *Biochem Biophys Res Commun*, 122(3), 1131–1135. <https://www.ncbi.nlm.nih.gov/pubmed/6236805>
- Go, C. D., Knight, J. D. R., Rajasekharan, A., Rathod, B., Hesketh, G. G., Abe, K. T., Youn, J. Y., Samavarchi-Tehrani, P., Zhang, H., Zhu, L. Y., Popiel, E., Lambert, J. P., Coyaud, É., Cheung, S. W. T., Rajendran, D., Wong, C. J., Antonicka, H., Pelletier, L., Palazzo, A. F., ... Gingras, A. C. (2021). A proximity-dependent biotinylation map of a human cell. *Nature*, 595(7865), 120–124. <https://doi.org/10.1038/s41586-021-03592-2>
- Gocke, C. B., Yu, H., & Kang, J. (2005). Systematic identification and analysis of mammalian small ubiquitin-like modifier substrates. *Journal of Biological Chemistry*, 280(6), 5004–5012. <https://doi.org/10.1074/jbc.M411718200>
- Goehler, H., Lalowski, M., Stelzl, U., Waelter, S., Stroedicke, M., Worm, U., Droege, A., Lindenberg, K. S., Knoblich, M., Haenig, C., Herbst, M., Suopanki, J., Scherzinger, E., Abraham, C., Bauer, B., Hasenbank, R., Fritzsche, A., Ludewig, A. H., Buessow, K., ... Wanker, E. E. (2004). A protein interaction network links GIT1, an enhancer of huntingtin aggregation, to Huntington's disease. *Molecular Cell*, 15(6), 853–865. <https://doi.org/10.1016/j.molcel.2004.09.016>
- Goldman, J., Hahn, S., Catania, J. W., Larusse-Eckert, S., Butson, M. B., Rumbaugh, M., Strecker, M., Roberts, J. S., Burke, W., Mayeux, R., & Bird, T. (2011). Genetic counseling and testing for Alzheimer disease: Joint practice guidelines of the American College of Medical Genetics and the National Society of Genetic Counselors. *Genetics in Medicine*, 13(6), 597. <https://doi.org/10.1097/GIM.0b013e31821d69b8>
- Goldmann, T., & Prinz, M. (2013). Role of microglia in CNS autoimmunity. *Clinical and Developmental Immunology*, 2013(88). <https://doi.org/10.1155/2013/208093>
- Gong, X. Q., & Li. (2002). Dermo-1, a multifunctional basic helix-loop-helix protein, represses MyoD transactivation via the HLH domain, MEF2 interaction, and chromatin deacetylation. *Journal of Biological Chemistry*, 277(14), 12310–12317. <https://doi.org/10.1074/jbc.M110228200>
- Gonzalez-Salvador, T., Lyketsos, C. G., Baker, A., Hovanec, L., Roques, C., Brandt, J., & Steele, C. (2000). Quality of life in dementia patients in long-term care. *International Journal of Geriatric Psychiatry*, 15(2), 181–189. [https://doi.org/10.1002/\(SICI\)1099-1166\(200002\)15:2<181::AID-GPS96>3.0.CO;2-I](https://doi.org/10.1002/(SICI)1099-1166(200002)15:2<181::AID-GPS96>3.0.CO;2-I)
- Gosselin, D., Link, V. M., Romanoski, C. E., Fonseca, G. J., Eichenfield, D. Z., Spann, N. J., Stender, J. D., Chun, H. B., Garner, H., Geissmann, F., & Glass, C. K. (2014). Environment drives selection and function of enhancers controlling tissue-specific macrophage identities. *Cell*, 159(6), 1327–1340. <https://doi.org/10.1016/j.cell.2014.11.023>
- Gossett, L. A., Kelvin, D. J., Sternberg, E. A., & Olson, E. N. (1989). A New Myocyte-Specific Enhancer-Binding Factor That Recognizes a Conserved Element Associated with Multiple Muscle-Specific Genes. In *MOLECULAR AND CELLULAR BIOLOGY* (Vol. 9, Issue 11).
- Greer, E. L., & Shi, Y. (2014). Histone methylation: a dynamic mark in health, disease and inheritance. *Nature Reviews Genetics*, 13(5), 343–357. <https://doi.org/10.1038/nrg3173>.Histone
- Griciuc, A., Serrano-Pozo, A., Parrado, A. R., Lesinski, A. N., Asselin, C. N., Mullin, K., Hooli, B., Choi, S. H., Hyman, B. T., & Tanzi, R. E. (2013). Alzheimer's disease risk gene cd33

- inhibits microglial uptake of amyloid beta. *Neuron*, 78(4), 631–643.  
<https://doi.org/10.1016/j.neuron.2013.04.014>
- Griffin, W. S. T., Sheng, J. G., Roberts, G. W., & Mrak, R. E. (1995). Interleukin-1 Expression in Different Plaque Types in Alzheimer's Disease: Significance in Plaque Evolution. *Journal of Neuropathology & Experimental Neurology*, 54(2), 276–281.  
<https://doi.org/10.1097/00005072-199503000-00014>
- Groth, D., Hartmann, S., Klie, S., & Selbig, J. (2013). Principal Components Analysis. In *Reisfeld B., Mayeno A. (eds) Computational Toxicology. Methods in Molecular Biology (Methods and Protocols)* (vol 930). Humana Press.
- Grozinger, C. M., & Schreiber, S. L. (2000). Regulation of histone deacetylase 4 and 5 and transcriptional activity by 14-3-3-dependent cellular localization. *PNAS*, 97(14), 7835–7840. [www.pnas.org](http://www.pnas.org)
- Grüter, P., Tabernero, C., Von Kobbe, C., Schmitt, C., Saavedra, C., Bachi, A., Wilm, M., Felber, B. K., & Izaurralde, E. (1998). TAP, the human homolog of Mex67p, mediates CTE-dependent RNA export from the nucleus. *Molecular Cell*, 1(5), 649–659.  
[https://doi.org/10.1016/S1097-2765\(00\)80065-9](https://doi.org/10.1016/S1097-2765(00)80065-9)
- Guenther, M. G., Levine, S. S., Boyer, L. A., Jaenisch, R., & Young, R. A. (2007). A Chromatin Landmark and Transcription Initiation at Most Promoters in Human Cells. *Cell*, 130(1), 77–88. <https://doi.org/10.1016/j.cell.2007.05.042>
- Guerreiro, R., Wojtas, A., Bras, J., Carrasquillo, M., Rogaeva, E., Majounie, E., Cruchaga, C., Sassi, C., Kauwe, J. S. K., Younkin, S., Hazrati, L., Collinge, J., Pocock, J., Lashley, T., Williams, J., Lambert, J. C., Amouyel, P., Goate, A., Rademakers, R., ... Hardy, J. (2013). TREM2 variants in Alzheimer's disease. *New England Journal of Medicine*, 368(2), 117–127. <https://doi.org/10.1056/NEJMoa1211851>
- Haeberlein, S. B., von Hehn, C., Tian, Y., Chalkias, S., Muralidharan, K. K., Chen, T., Wu, S., Skordos, L., Nisenbaum, L., Rajagovindan, R., Dent, G., Harrison, K., Nestorov, I., Zhu, Y., Mallinckrodt, C., & Sandrock, A. (2019). *Emerge and Engage topline results: Phase 3 studies of aducanumab in early Alzheimer's disease*.  
<https://doi.org/10.1002/alz.047259>
- Hakim, N. H. A., Kounishi, T., Alam, A. H. M. K., Tsukahara, T., & Suzuki, H. (2010). Alternative splicing of Mef2c promoted by Fox-1 during neural differentiation in P19 cells. *Genes to Cells*, 15(3), 255–267. <https://doi.org/10.1111/j.1365-2443.2009.01378.x>
- Han, A., He, J., Wu, Y., Liu, J. O., & Chen, L. (2005). Mechanism of recruitment of class II histone deacetylases by myocyte enhancer factor-2. *Journal of Molecular Biology*.  
<https://doi.org/10.1016/j.jmb.2004.10.033>
- Han, A., Pan, F., Stroud, J. C., Youn, H. D., Liu, J. O., & Chen, L. (2003). Sequence-specific recruitment of transcriptional co-repressor Cabin1 by myocyte enhancer factor-2. *Nature*, 422(6933), 730–734. <https://doi.org/10.1038/nature01555>
- Han, J., Jiang, Y., Li, Z., Kravchenko, V. V., & J, U. R. (1997). Activation of the transcription factor MEF2C by the MAP kinase p38 in inflammation. *Nature*, 386, 296–299.  
<https://doi.org/10.1038/255242a0>
- Han, Jaeseok, Back, S. H., Hur, J., Lin, Y. H., Gildersleeve, R., Shan, J., Yuan, C. L., Krokowski, D., Wang, S., Hatzoglou, M., Kilberg, M. S., Sartor, M. A., & Kaufman, R. J. (2013). ER-

- stress-induced transcriptional regulation increases protein synthesis leading to cell death. *Nature Cell Biology*, 15(5), 481–490. <https://doi.org/10.1038/ncb2738>
- Hanisch, U. K., & Kettenmann, H. (2007). Microglia: Active sensor and versatile effector cells in the normal and pathologic brain. *Nature Neuroscience*, 10(11), 1387–1394. <https://doi.org/10.1038/nn1997>
- Hansen, D. V., Hanson, J. E., & Sheng, M. (2018). Microglia in Alzheimer's disease. *Journal of Cell Biology*, 217(2), 459–472.
- Hardy, J. A., & Higgins, G. A. (1992). Alzheimer's disease: The amyloid cascade hypothesis. *Science*, 256(5054), 184–185. <https://doi.org/10.1126/science.1566067>
- Hardy, J., & Allsop, D. (1991). Amyloid deposition as the central event in the aetiology of Alzheimer's disease. In *Trends in Pharmacological Sciences* (Vol. 12, Issue C, pp. 383–388). [https://doi.org/10.1016/0165-6147\(91\)90609-V](https://doi.org/10.1016/0165-6147(91)90609-V)
- Harold, D., Abraham, R. A., Hollingworth, P., Sims, R., Gerrish, A., Hamshere, M. L., Pahwa, J. S., Escott-Price, V., Dowzell, K. F., Williams, A., Denning, N., Thomas, C., Stretton, A., Morgan, A. R., Lovestone, S., Powell, J., Proitsi, P., Lupton, M. K., Brayne, C., ... Williams, J. (2009). *Genome-wide association study identifies variants at CLU and PICALM associated with Alzheimer's disease [Letter]*.
- Harrow, J., Frankish, A., Gonzalez, J. M., Tapanari, E., Diekhans, M., Kokocinski, F., Aken, B. L., Barrell, D., Zadissa, A., Searle, S., Barnes, I., Bignell, A., Boychenko, V., Hunt, T., Kay, M., Mukherjee, G., Rajan, J., Despacio-Reyes, G., Saunders, G., ... Hubbard, T. J. (2012). GENCODE: The reference human genome annotation for the ENCODE project. *Genome Research*, 22(9), 1760–1774. <https://doi.org/10.1101/gr.135350.111>
- Havugimana, P. C., Hart, G. T., Nepusz, T., Yang, H., Turinsky, A. L., Li, Z., Wang, P. I., Boutz, D. R., Fong, V., Phanse, S., Babu, M., Craig, S. A., Hu, P., Wan, C., Vlasblom, J., Dar, V. U. N., Bezginov, A., Clark, G. W., Wu, G. C., ... Emili, A. (2012). A census of human soluble protein complexes. *Cell*, 150(5), 1068–1081. <https://doi.org/10.1016/j.cell.2012.08.011>
- Hayashi, M., Kim, S., Imanaka-Yoshida, K., Yoshida, T., Abel, E. D., Eliceiri, B., Yang, Y., Ulevitch, R. J., & Lee, J. (2004). Targeted deletion of BMK1/ERK5 in adult mice perturbs vascular integrity and leads to endothelial failure. *The Journal of Clinical Investigation*, 113(8), 1138–1148.
- Hayley, M., Perspicace, S., Schulthess, T., & Seelig, J. (2009). Calcium enhances the proteolytic activity of BACE1: An in vitro biophysical and biochemical characterization of the BACE1-calcium interaction. *Biochimica et Biophysica Acta - Biomembranes*, 1788(9), 1933–1938. <https://doi.org/10.1016/j.bbamem.2009.05.015>
- Head, E., Silverman, W., Patterson, D., & Lott, I. T. (2012). Aging and down syndrome. *Current Gerontology and Geriatrics Research*, 2012. <https://doi.org/10.1155/2012/412536>
- Heintzman, N. D., Stuart, R. K., Hon, G., Fu, Y., Ching, C. W., Hawkins, R. D., Barrera, L. O., Van Calcar, S., Qu, C., Ching, K. A., Wang, W., Weng, Z., Green, R. D., Crawford, G. E., & Ren, B. (2007). Distinct and predictive chromatin signatures of transcriptional promoters and enhancers in the human genome. *Nature Genetics*, 39(3), 311–318. <https://doi.org/10.1038/ng1966>
- Heinz, L. X., Baumann, C. L., Köberlin, M. S., Snijder, B., Gawish, R., Shui, G., Sharif, O.,

- Aspalter, I. M., Müller, A. C., Kandasamy, R. K., Breitwieser, F. P., Pichlmair, A., Bruckner, M., Rebsamen, M., Blüml, S., Karonitsch, T., Fauster, A., Colinge, J., Bennett, K. L., ... Superti-Furga, G. (2015). The Lipid-Modifying Enzyme SMPDL3B Negatively Regulates Innate Immunity. *Cell Reports*, *11*(12), 1919–1928. <https://doi.org/10.1016/j.celrep.2015.05.006>
- Heinz, S., Romanoski, C. E., Benner, C., Allison, K. A., Kaikkonen, M. U., Orozco, L. D., & Glass, C. K. (2013). Effect of natural genetic variation on enhancer selection and function. *Nature*, *503*(7477), 487–492. <https://doi.org/10.1038/nature12615>
- Heinz, Sven, Benner, C., Spann, N., Bertolino, E., Lin, Y. c, Laslo, P., Cheng, J. X., Murre, C., Singh, H., & Glass, C. K. (2010). Simple combinations of lineage-determining transcription factors prime cis-regulatory elements required for macrophage and B cell identities. *Molecular Cell*, *38*(4), 576–589. <https://doi.org/10.1016/j.molcel.2010.05.004>.Simple
- Hemonnot, A. L., Hua, J., Ulmann, L., & Hirbec, H. (2019). Microglia in Alzheimer disease: Well-known targets and new opportunities. *Frontiers in Cellular and Infection Microbiology*, *9*(JUL), 1–20. <https://doi.org/10.3389/fnagi.2019.00233>
- Heneka, M. T., Golenbock, D. T., & Latz, E. (2015). Innate immunity in Alzheimer’s disease. *Nature Immunology*, *16*(3), 229–236. <https://doi.org/10.1038/ni.3102>
- Heneka, M. T., Kummer, M. P., Stutz, A., Delekate, A., Schwartz, S., Vieira-Saecker, A., Griep, A., Axt, D., Remus, A., Tzeng, T. C., Gelpi, E., Halle, A., Korte, M., Latz, E., & Golenbock, D. T. (2013). NLRP3 is activated in Alzheimer’s disease and contributes to pathology in APP/PS1 mice. *Nature*, *493*(7434), 674–678. <https://doi.org/10.1038/nature11729>
- Henn, A., Lund, S., Hedtjärn, M., Schrattenholz, A., Pörzgen, P., & Leist, M. (2009). The Suitability of BV2 Cells as Alternative Model System for Primary Microglia Cultures or for Animal Experiments Examining Brain Inflammation Doerenkamp-Zbinden Chair for alternative in vitro methods to replace animal experiments. *Altex*, *26*(January), 83–94.
- Hickman, S. E., Allison, E. K., & El Khoury, J. (2008). Microglial dysfunction and defective  $\beta$ -amyloid clearance pathways in aging alzheimer’s disease mice. *Journal of Neuroscience*, *28*(33), 8354–8360. <https://doi.org/10.1523/JNEUROSCI.0616-08.2008>
- Hoffmann, A., Kann, O., Ohlemeyer, C., Hanisch, U. K., & Kettenmann, H. (2003). Elevation of basal intracellular calcium as a central element in the activation of brain macrophages (microglia): Suppression of receptor-evoked calcium signaling and control of release function. *Journal of Neuroscience*, *23*(11), 4410–4419. <https://doi.org/10.1523/jneurosci.23-11-04410.2003>
- Hogan, P. G., Chen, L., Nardone, J., & Rao, A. (2003). Transcriptional regulation by calcium, calcineurin, and NFAT. *Genes and Development*, *17*(18), 2205–2232. <https://doi.org/10.1101/gad.1102703>
- Holtman, I. R., Skola, D., & Glass, C. K. (2017). Transcriptional control of microglia phenotypes in health and disease. *Journal of Clinical Investigation*, *127*(9), 3220–3229. <https://doi.org/10.1172/jci90604>
- Holtzman, D. M., Morris, J. C., & Goate, A. M. (2011). Alzheimer’s disease: The challenge of the second century. *Science Translational Medicine*, *3*(77). <https://doi.org/10.1126/scitranslmed.3002369>



- Hooper, C., Meimaridou, E., Tavassoli, M., Melino, G., Lovestone, S., & Killick, R. (2007). p53 is upregulated in Alzheimer's disease and induces tau phosphorylation in HEK293a cells. *Neuroscience Letters*, *418*(1), 34–37. <https://doi.org/10.1016/j.neulet.2007.03.026>
- Horvath, R. J., Nutilo-McMenemy, N., Alkaitis, M. S., & DeLeo, J. A. (2008). Differential migration, LPS-induced cytokine, chemokine, and NO expression in immortalized BV-2 and HAPI cell lines and primary microglial cultures. *Journal of Neurochemistry*, *107*(2), 557–569. <https://doi.org/10.1111/j.1471-4159.2008.05633.x>
- Hosking, B. M., Wang, S. C. M., Chen, S. L., Penning, S., Koopman, P., & Muscat, G. E. O. (2001). SOX18 directly interacts with MEF2C in endothelial cells. *Biochemical and Biophysical Research Communications*, *287*(2), 493–500. <https://doi.org/10.1006/bbrc.2001.5589>
- Howard, R., McShane, R., Lindsay, J., Ritchie, C., Baldwin, A., Barber, R., Burns, A., Denning, T., Findlay, D., Holmes, C., Jones, R., Jones, R., McKeith, I., Macharouthu, A., O'Brien, J., Sheehan, B., Juszczak, E., Katona, C., Hills, R., ... Phillips, P. P. J. (2015). Nursing home placement in the Donepezil and Memantine in Moderate to Severe Alzheimer's Disease (DOMINO-AD) trial: Secondary and post-hoc analyses. *The Lancet Neurology*, *14*(12), 1171–1181. [https://doi.org/10.1016/S1474-4422\(15\)00258-6](https://doi.org/10.1016/S1474-4422(15)00258-6)
- Hu, X., Kim, H., Stahl, E., Plenge, R., Daly, M., & Raychaudhuri, S. (2011). Integrating autoimmune risk loci with gene-expression data identifies specific pathogenic immune cell subsets. *American Journal of Human Genetics*, *89*(4), 496–506. <https://doi.org/10.1016/j.ajhg.2011.09.002>
- Huang, J., Tu, Z., & Lee, F. S. (2003). Mutations in protein kinase subdomain X differentially affect MEKK2 and MEKK1 activity. *Biochemical and Biophysical Research Communications*, *303*(2), 532–540. [https://doi.org/10.1016/S0006-291X\(03\)00387-5](https://doi.org/10.1016/S0006-291X(03)00387-5)
- Huang, K. L., Marcora, E., Pimenova, A. A., Di Narzo, A. F., Kapoor, M., Jin, S. C., Harari, O., Bertelsen, S., Fairfax, B. P., Czajkowski, J., Chouraki, V., Grenier-Boley, B., Bellenguez, C., Deming, Y., McKenzie, A., Raj, T., Renton, A. E., Budde, J., Smith, A., ... Alzheimer's Dis, N. (2017). A common haplotype lowers PU.1 expression in myeloid cells and delays onset of Alzheimer's disease. *Nature Neuroscience*, *20*(8), 1052–1066. <https://doi.org/10.1038/nn.4587>
- Hunt, A., Fischer, M., Engel, M. E., & Hiebert, S. W. (2011). Mtg16/Eto2 Contributes to Murine T-Cell Development. *Molecular and Cellular Biology*, *31*(13), 2544–2551. <https://doi.org/10.1128/mcb.01458-10>
- Hunter, T., & Karin, M. (1992). The regulation of transcription by phosphorylation. *Cell*, *70*(3), 375–387. [https://doi.org/10.1016/0092-8674\(92\)90162-6](https://doi.org/10.1016/0092-8674(92)90162-6)
- Huttlin, E. L., Bruckner, R. J., Paulo, J. A., Cannon, J. R., Ting, L., Baltier, K., Colby, G., Gebreab, F., Gygi, M. P., Parzen, H., Szpyt, J., Tam, S., Zarraga, G., Pontano-Vaites, L., Swarup, S., White, A. E., Schweppe, D. K., Rad, R., Erickson, B. K., ... Wade Harper, J. (2017). Architecture of the human interactome defines protein communities and disease networks. *Nature*, *545*(7655), 505–509. <https://doi.org/10.1038/nature22366>
- Huttlin, E. L., Jedrychowski, M. P., Elias, J. E., Goswami, T., Rad, R., Beausoleil, S. A., Villén, J., Haas, W., Sowa, M. E., & Gygi, S. P. (2010). A tissue-specific atlas of mouse protein phosphorylation and expression. *Cell*, *143*(7), 1174–1189. <https://doi.org/10.1016/j.cell.2010.12.001>

## References

- Hyde, C. L., Nagle, M. W., Tian, C., Chen, X., Paciga, S. A., Wendland, J. R., Tung, J. Y., Hinds, D. A., Perlis, R. H., & Winslow, A. R. (2016). Identification of 15 genetic loci associated with risk of major depression in individuals of European descent. *Nature Genetics*, *48*(9), 1031–1036. <https://doi.org/10.1038/ng.3623>
- Infantino, V., Convertini, P., Menga, A., & Iacobazzi, V. (2013). MEF2C exon  $\alpha$ : Role in gene activation and differentiation. *Gene*. <https://doi.org/10.1016/j.gene.2013.08.044>
- Itagaki, S., McGeer, P. L., Akiyama, H., Zhu, S., & Selkoe, D. (1989). Relationship of microglia and astrocytes to amyloid deposits of Alzheimer disease. *Journal of Neuroimmunology*, *24*(3), 173–182. [https://doi.org/10.1016/0165-5728\(89\)90115-X](https://doi.org/10.1016/0165-5728(89)90115-X)
- Iwafuchi-Doi, M., & Zaret, K. S. (2014). Pioneer transcription factors in cell reprogramming. *Genes and Development*, *28*(24), 2679–2692. <https://doi.org/10.1101/gad.253443.114>
- Jahn, H. (2013). Memory loss in Alzheimer's disease. *Dialogues in Clinical Neuroscience*, *15*(4), 445–454. <https://doi.org/10.4324/9780429314384-1>
- Jang, H., Choi, D. E., Kim, H., Cho, E. J., & Youn, H. D. (2007). Cabin1 represses MEF2 transcriptional activity by association with a methyltransferase, SUV39H1. *Journal of Biological Chemistry*, *282*(15), 11172–11179. <https://doi.org/10.1074/jbc.M611199200>
- Janson, C. G., Chen, Y., Li, Y., & Leifer, D. (2001). Functional regulatory regions of human transcription factor MEF2C. *Molecular Brain Research*. [https://doi.org/10.1016/S0169-328X\(01\)00187-5](https://doi.org/10.1016/S0169-328X(01)00187-5)
- Janssen, S. M., Moscona, R., Elchebly, M., Papadakis, A. I., Redpath, M., Wang, H., Rubin, E., van Kempen, L. C., & Spatz, A. (2020). BORIS/CTCF promotes a switch from a proliferative towards an invasive phenotype in melanoma cells. *Cell Death Discovery*, *6*(1), 1–17. <https://doi.org/10.1038/s41420-019-0235-x>
- Jarrett, J., Berger, E., & Lansbury, P. (1993). The Carboxy Terminus of the Beta-Amyloid Protein is Critical for the Seeding of Amyloid Formation- Implications for the Pathogenesis of Alzheimer's-Disease. *Biochemistry*, *32*(18), 4693–4697. <https://doi.org/10.1021/bi00069a001>
- Jay, T. R., Von Saucken, V. E., & Landreth, G. E. (2017). TREM2 in Neurodegenerative Diseases. In *Molecular Neurodegeneration* (Vol. 12, Issue 1). Molecular Neurodegeneration. <https://doi.org/10.1186/s13024-017-0197-5>
- Jayadev, S., Nesser, N. K., Hopkins, S., Myers, S. J., Case, A., Lee, R. J., Seaburg, L. A., Uo, T., Murphy, S. P., Morrison, R. S., & Garden, G. A. (2011). The Transcription Factor p53 Influences Microglial Activation Phenotype. *Glia*, *59*(10), 1402–1413. <https://doi.org/10.1016/j.pestbp.2011.02.012>. Investigations
- Jellinger, K. A. (2002). Alzheimer disease and cerebrovascular pathology: An update. *Journal of Neural Transmission*, *109*(5–6), 813–836. <https://doi.org/10.1007/s007020200068>
- Jia, J., Jia, J., Zhou, W., Xu, M., Chu, C., Yan, X., & Sun, Y. (2004). Differential acetylcholine and choline concentrations in the cerebrospinal fluid of patients with Alzheimer's disease and vascular dementia. *Chinese Medical Journal*, *117*(8), 1161–1164.
- Joe, E., & Ringman, J. M. (2019). Cognitive symptoms of Alzheimer's disease: Clinical management and prevention. In *The BMJ* (Vol. 367). BMJ Publishing Group. <https://doi.org/10.1136/bmj.l6217>

- John, L. B., & Ward, A. C. (2011). The Ikaros gene family: Transcriptional regulators of hematopoiesis and immunity. *Molecular Immunology*, *48*(9–10), 1272–1278. <https://doi.org/10.1016/j.molimm.2011.03.006>
- Johnson, J. L., Georgakilas, G., Petrovic, J., Kurachi, M., Cai, S., Harly, C., Pear, W. S., Bhandoola, A., Wherry, E. J., & Vahedi, G. (2018). Lineage-Determining Transcription Factor TCF-1 Initiates the Epigenetic Identity of T Cells. *Immunity*, *48*(2), 243-257.e10. <https://doi.org/10.1016/j.immuni.2018.01.012>
- Johnson, P. F., & McKnight, S. L. (1989). Eukaryotic transcriptional regulatory proteins. *Annual Review of Biochemistry*, *58*, 799–839. <https://doi.org/10.1146/annurev.bi.58.070189.004055>
- Johnston, H., Boutin, H., & Allan, S. M. (2011). Assessing the contribution of inflammation in models of Alzheimer's disease. *Biochemical Society Transactions*, *39*(4), 886–890. <https://doi.org/10.1042/BST0390886>
- Jones, L., Lambert, J., Wang, L., Choi, S., Harold, D., Vedernikov, A., Escott-Price, V., Stone, T., Richards, A., Bellenguez, C., & Al., E. (2015). Convergent genetic and expression data implicate immunity in Alzheimer's disease. *Alzheimer's & Dementia*, *11*(6), 658–671. <https://doi.org/10.1016/j.physbeh.2017.03.040>
- Jonsson, T., Stefansson, H., Steinberg, S., Jonsdottir, I., Jonsson, P. V., Snaedal, J., Bjornsson, S., Huttenlocher, J., Levey, A. I., Lah, J. J., Rujescu, D., Hampel, H., Giegling, I., Andreassen, O. A., Engedal, K., Ulstein, I., Djurovic, S., Ibrahim-Verbaas, C., Hofman, A., ... Stefansson, K. (2013). Variant of TREM2 Associated with the Risk of Alzheimer's Disease. *The New England Journal of Medicine*, *368*(2), 107–116. <https://doi.org/10.1056/NEJMoa1211103>
- Joshi, P., Greco, T. M., Guise, A. J., Luo, Y., Yu, F., Nesvizhskii, A. I., & Cristea, I. M. (2013). The functional interactome landscape of the human histone deacetylase family. *Molecular Systems Biology*, *9*(1), 1–21. <https://doi.org/10.1038/msb.2013.26>
- Jung, J., Lee, M. K., Rosales, J. L., & Lee, K. Y. (2011). Clues for c-Yes involvement in the cell cycle and cytokinesis. *Cell Cycle*, *10*(9), 1502–1503. <https://doi.org/10.4161/cc.10.9.15495>
- Jurica, M. S., & Moore, M. J. (2003). Pre-mRNA splicing: Awash in a sea of proteins. In *Molecular Cell*. [https://doi.org/10.1016/S1097-2765\(03\)00270-3](https://doi.org/10.1016/S1097-2765(03)00270-3)
- Kadauke, S., & Blobel, G. A. (2009). Chromatin loops in gene regulation. *Biochimica et Biophysica Acta - Gene Regulatory Mechanisms*, *1789*(1), 17–25. <https://doi.org/10.1016/j.bbagr.2008.07.002>
- Kadavath, H., Hofele, R. V., Biernat, J., Kumar, S., Tepper, K., Urlaub, H., Mandelkow, E., & Zweckstetter, M. (2015). Tau stabilizes microtubules by binding at the interface between tubulin heterodimers. *Proceedings of the National Academy of Sciences of the United States of America*, *112*(24), 7501–7506. <https://doi.org/10.1073/pnas.1504081112>
- Kalaria, R. N., & Ballard, C. (1999). Overlap between pathology of Alzheimer disease and vascular dementia. *Alzheimer Disease and Associated Disorders*, *13* Suppl 3, S115-23. <https://doi.org/10.1097/00002093-199912003-00017>
- Kang, J., Gocke, C. B., & Yu, H. (2006). Phosphorylation-facilitated sumoylation of MEF2C negatively regulates its transcriptional activity. *BMC Biochemistry*, *7*, 1–14.

<https://doi.org/10.1186/1471-2091-7-5>

- Kanhere, A., & Bansal, M. (2005). Structural properties of promoters: Similarities and differences between prokaryotes and eukaryotes. *Nucleic Acids Research*, *33*(10), 3165–3175. <https://doi.org/10.1093/nar/gki627>
- Kaoru, S., & Christopher, K. G. (2011). Microglial cell origin and phenotypes in health and disease. *Nature Reviews Immunology*, *11*(11), 775. <https://doi.org/10.1038/nri3086>
- Karantzoulis, S., & Galvin, J. E. (2011). Distinguishing Alzheimer's disease from other major forms of dementia. *Expert Review of Neurotherapeutics*, *11*(11), 1579–1591. <https://doi.org/10.1586/ern.11.155>
- Karasseva, N., Tsika, G., Ji, J., Zhang, A., Mao, X., & Tsika, R. (2003). Transcription Enhancer Factor 1 Binds Multiple Muscle MEF2 and A/T-Rich Elements during Fast-to-Slow Skeletal Muscle Fiber Type Transitions. *Molecular and Cellular Biology*, *23*(15), 5143–5164. <https://doi.org/10.1128/mcb.23.15.5143-5164.2003>
- Karch, C. M., Jeng, A. T., Nowotny, P., Cady, J., Cruchaga, C., & Goate, A. M. (2012). Expression of Novel Alzheimer's Disease Risk Genes in Control and Alzheimer's Disease Brains. *PLoS ONE*, *7*(11). <https://doi.org/10.1371/journal.pone.0050976>
- Kasler, H. G., Victoria, J., Duramad, O., & Winoto, A. (2000). ERK5 Is a Novel Type of Mitogen-Activated Protein Kinase Containing a Transcriptional Activation Domain. In *MOLECULAR AND CELLULAR BIOLOGY* (Vol. 20, Issue 22).
- Katahira, J. (2015). Nuclear export of messenger RNA. *Genes*, *6*(2), 163–184. <https://doi.org/10.3390/genes6020163>
- Kato, Y., Kravchenko, V. V., Tapping, R. I., Han, J., Ulevitch, R. J., & Lee, J.-D. (1997). BMK1/ERK5 regulates serum-induced early gene expression through transcription factor MEF2C. In *The EMBO Journal* (Vol. 16, Issue 23).
- Kelemen, O., Convertini, P., Zhang, Z., Wen, Y., Shen, M., Falaleeva, M., & Stamm, S. (2013). Function of alternative splicing. *Gene*, *514*(1), 1–30. <https://doi.org/10.1016/j.gene.2012.07.083>
- Khachaturian, Z S. (1989). The role of calcium regulation in brain aging: reexamination of a hypothesis. *Aging (Milan, Italy)*, *1*(1), 17–34. <https://doi.org/10.1007/BF03323872>
- Khachaturian, Zaven S. (1987). Hypothesis on the Regulation of Cytosol Calcium Concentration and the Aging Brain. *Neurobiology of Aging*, *8*(4), 345–346. [https://doi.org/10.1016/0197-4580\(87\)90073-X](https://doi.org/10.1016/0197-4580(87)90073-X)
- Kidd, M. (1963). Paired Helical Filaments in Electron Microscopy of Alzheimer's Disease. *Nature*, *197*, 192–193.
- Kierdorf, K., Erny, D., Goldmann, T., Sander, V., Schulz, C., Wieghofer, P., Heinrich, A., Riemke, P., Hölscher, C., Luckow, B., Broucker, T., Debowski, K., Fritz, G., Opdenakker, G., Diefenbach, A., Biber, K., Heikenwalder, M., Geissmann, F., Rosenbauer, F., & P. M. (2013). Microglia emerge from erythromyeloid precursors via Pu.1- and Irf8-dependent pathways. *Nature Neuroscience*, *16*(3), 273. <https://doi.org/10.1038/nn.3318>
- Kigerl, K. A., Vaccari, J. P., Dietrich, W. D., Popovich, P. G., & Keane, R. W. (2014). Pattern recognition receptors and central nervous system repair. *Experimental Neurology*, *258*, 5–16. <https://doi.org/10.1016/j.physbeh.2017.03.040>

- Kim, S., Yu, N. K., & Kaang, B. K. (2015). CTCF as a multifunctional protein in genome regulation and gene expression. *Experimental & Molecular Medicine*, 47(December 2014), e166. <https://doi.org/10.1038/emm.2015.33>
- Kimura, K., Wakamatsu, A., Suzuki, Y., Ota, T., Nishikawa, T., Yamashita, R., Yamamoto, J., Sekine, M., Tsuritani, K., Wakaguri, H., Ishii, S., Sugiyama, T., Saito, K., Isono, Y., Irie, R., Kushida, N., Yoneyama, T., Otsuka, R., Kanda, K., ... Sugano, S. (2006). Diversification of transcriptional modulation: Large-scale identification and characterization of putative alternative promoters of human genes. *Genome Research*, 16(1), 55–65. <https://doi.org/10.1101/gr.4039406.1>
- Kipanyula, M. J., Kimaro, W. H., & Etet, P. F. S. (2016). The Emerging Roles of the Calcineurin-Nuclear Factor of Activated T-Lymphocytes Pathway in Nervous System Functions and Diseases. In *Journal of Aging Research* (Vol. 2016). Hindawi Limited. <https://doi.org/10.1155/2016/5081021>
- Kitamura, Y., Shimohama, S., Kamoshima, W., Matsuoka, Y., Nomura, Y., & Taniguchi, T. (1997). Changes of p53 in the brains of patients with Alzheimer's disease. *Biochemical and Biophysical Research Communications*, 232(2), 418–421. <https://doi.org/10.1006/bbrc.1997.6301>
- Kleinberger, G., Yamanishi, Y., Suárez-Calvet, M., Czirr, E., Lohmann, E., Cuyvers, E., Struyfs, H., Pettkus, N., Wenninger-Weinzierl, A., Mazaheri, F., Tahirovic, S., Lleó, A., Alcolea, D., Fortea, J., Willem, M., Lammich, S., Molinuevo, J. L., Sánchez-Valle, R., Antonell, A., ... Haass, C. (2014). TREM2 mutations implicated in neurodegeneration impair cell surface transport and phagocytosis. *Science Translational Medicine*, 6(243). <https://doi.org/10.1126/scitranslmed.3009093>
- Klemm, S. L., Shipony, Z., & Greenleaf, W. J. (2019). Chromatin accessibility and the regulatory epigenome. *Nature Reviews Genetics*, 20(4), 207–220. <https://doi.org/10.1038/s41576-018-0089-8>
- Knapp, M., King, D., Romeo, R., Adams, J., Baldwin, A., Ballard, C., Banerjee, S., Barber, R., Bentham, P., Brown, R. G., Burns, A., Dening, T., Findlay, D., Holmes, C., Johnson, T., Jones, R., Katona, C., Lindesay, J., Macharouthu, A., ... Howard, R. (2017). Cost-effectiveness of donepezil and memantine in moderate to severe Alzheimer's disease (the DOMINO-AD trial). *International Journal of Geriatric Psychiatry*, 32(12), 1205–1216. <https://doi.org/10.1002/gps.4583>
- Knight, R., Khondoker, M., Magill, N., Stewart, R., & Landau, S. (2018). A systematic review and meta-analysis of the effectiveness of acetylcholinesterase inhibitors and memantine in treating the cognitive symptoms of dementia. *Dementia and Geriatric Cognitive Disorders*, 45(3–4), 131–151. <https://doi.org/10.1159/000486546>
- Knopman, D. S., Jones, D. T., & Greicius, M. D. (2021). Failure to demonstrate efficacy of aducanumab: An analysis of the EMERGE and ENGAGE trials as reported by Biogen, December 2019. *Alzheimer's and Dementia*, 17(4), 696–701. <https://doi.org/10.1002/alz.12213>
- Knopman, D. S., & Perlmutter, J. S. (2021). Prescribing Aducanumab in the Face of Meager Efficacy and Real Risks. *Neurology*, 97(11), 545–547. <https://doi.org/10.1212/WNL.0000000000012452>
- Kober, D. L., Alexander-Brett, J. M., Karch, C. M., Cruchaga, C., Colonna, M., Holtzman, M. J., & Brett, T. J. (2016). Neurodegenerative disease mutations in TREM2 reveal a functional surface and distinct loss-of-function mechanisms. *ELife*, 5(DECEMBER2016),

- 1–24. <https://doi.org/10.7554/eLife.20391>
- Koh, G. C. K. W., Porras, P., Aranda, B., Hermjakob, H., & Orchard, S. E. (2012). Analyzing Protein-Protein Interaction Networks. *Journal of Proteome Research*, *11*(4), 2014–2031. <https://doi.org/10.1002/9783527619368.ch31>
- Kouzarides, T. (2007). Chromatin Modifications and Their Function. *Cell*, *128*(4), 693–705. <https://doi.org/10.1016/j.cell.2007.02.005>
- Kozhemyakina, E., Cohen, T., Yao, T.-P., & Lassar, A. B. (2009). Parathyroid Hormone-Related Peptide Represses Chondrocyte Hypertrophy through a Protein Phosphatase 2A/Histone Deacetylase 4/MEF2 Pathway. *Molecular and Cellular Biology*, *29*(21), 5751–5762. <https://doi.org/10.1128/mcb.00415-09>
- Krainc, D., Bai, G., Okamoto, S. I., Carles, M., Kusiak, J. W., Brent, R. N., & Lipton, S. A. (1998). Synergistic activation of the N-methyl-D-aspartate receptor subunit 1 promoter by myocyte enhancer factor 2C and Sp1. *Journal of Biological Chemistry*, *273*(40), 26218–26224. <https://doi.org/10.1074/jbc.273.40.26218>
- Krueger, K. R., Wilson, R. S., Kamenetsky, J. M., Barnes, L. L., Bienias, J. L., & Bennett, D. A. (2009). Social engagement and cognitive function in old age. *Experimental Aging Research*, *35*(1), 45–60. <https://doi.org/10.1161/CIRCULATIONAHA.110.956839>
- Kruiswijk, F., Labuschagne, C. F., & Vousden, K. H. (2015). P53 in survival, death and metabolic health: A lifeguard with a licence to kill. *Nature Reviews Molecular Cell Biology*, *16*(7), 393–405. <https://doi.org/10.1038/nrm4007>
- Kuchibhotla, K. V., Goldman, S. T., Lattarulo, C. R., Wu, H. Y., Hyman, B. T., & Bacskai, B. J. (2008). A $\beta$  Plaques Lead to Aberrant Regulation of Calcium Homeostasis In Vivo Resulting in Structural and Functional Disruption of Neuronal Networks. *Neuron*, *59*(2), 214–225. <https://doi.org/10.1016/j.neuron.2008.06.008>
- Kuenzi, B. M., Borne, A. L., Li, J., Haura, E. B., Eschrich, S. A., Koomen, J. M., Rix, U., & Stewart, P. A. (2016). APOSTL: An Interactive Galaxy Pipeline for Reproducible Analysis of Affinity Proteomics Data. *Journal of Proteome*, *15*(12), 4747–4754. <https://doi.org/10.1021/acs.jproteome.6b00660.APOSTL>
- Kuller, L. H., & Lopez, O. L. (2021). ENGAGE and EMERGE: Truth and consequences? *Alzheimer's & Dementia : The Journal of the Alzheimer's Association*, *17*(4), 692–695. <https://doi.org/10.1002/alz.12286>
- Kumar, V., Rayan, N. A., Muratani, M., Lim, S., Elanggovan, B., Xin, L., Lu, T., Makhija, H., Poschmann, J., Lufkin, T., Ng, H. H., & Prabhakar, S. (2016). Comprehensive benchmarking reveals H2BK20 acetylation as a distinctive signature of cell-statespecific enhancers and promoters. *Genome Research*, *26*(5), 612–623. <https://doi.org/10.1101/gr.201038.115>
- Kunkle, B. W., Grenier-Boley, B., Sims, R., Bis, J. C., Damotte, V., Naj, A. C., Boland, A., Vronskaya, M., van der Lee, S. J., Amlie-Wolf, A., Bellenguez, C., Frizatti, A., Chouraki, V., Martin, E. R., Sleegers, K., Badarinarayan, N., Jakobsdottir, J., Hamilton-Nelson, K. L., Moreno-Grau, S., ... Pericak-Vance, M. A. (2019). Genetic meta-analysis of diagnosed Alzheimer's disease identifies new risk loci and implicates A $\beta$ , tau, immunity and lipid processing. *Nature Genetics*, *51*(3), 414–430. <https://doi.org/10.1038/s41588-019-0358-2>
- LaFerla, F. M. (2002). Calcium dyshomeostasis and intracellular signalling in Alzheimer's

- disease. *Nature Reviews Neuroscience*, 3(11), 862–872.  
<https://doi.org/10.1038/nrn960>
- Lambert, Jean Charles, Heath, S., Even, G., Campion, D., Sleegers, K., Hiltunen, M., Combarros, O., Zelenika, D., Bullido, M. J., Tavernier, B., Letenneur, L., Bettens, K., Berr, C., Pasquier, F., Fiévet, N., Barberger-Gateau, P., Engelborghs, S., De Deyn, P., Mateo, I., ... Pilotto, A. (2009). Genome-wide association study identifies variants at *CLU* and *CR1* associated with Alzheimer's disease. *Nature Genetics*, 41(10), 1094–1099. <https://doi.org/10.1038/ng.439>
- Lambert, Jean Charles, Ibrahim-Verbaas, C. A., Harold, D., Naj, A. C., Sims, R., Bellenguez, C., Jun, G., DeStefano, A. L., Bis, J. C., Beecham, G. W., Grenier-Boley, B., Russo, G., Thornton-Wells, T. A., Jones, N., Smith, A. V., Chouraki, V., Thomas, C., Ikram, M. A., Zelenika, D., ... Seshadri, S. (2013). Meta-analysis of 74,046 individuals identifies 11 new susceptibility loci for Alzheimer's disease. *Nature Genetics*, 45(12), 1452–1458. <https://doi.org/10.1038/ng.2802>
- Lambert, M. P., Barlow, A. K., Chromy, B. A., Edwards, C., Freed, R., Liosatos, M., Morgan, T. E., Rozovsky, I., Trommer, B., Viola, K. L., Wals, P., Zhang, C., Finch, C. E., Krafft, G. A., & Klein, W. L. (1998). Diffusible, nonfibrillar ligands derived from A $\beta$ 1–42 are potent central nervous system neurotoxins. *Proceedings of the National Academy of Sciences of the United States of America*, 95(11), 6448–6453.  
<https://doi.org/10.1073/pnas.95.11.6448>
- Lambert, S. A., Jolma, A., Campitelli, L. F., Das, P. K., Yin, Y., Albu, M., Chen, X., Taipale, J., Hughes, T. R., & Weirauch, M. T. (2018). The Human Transcription Factors. *Cell*, 172(4), 650–665. <https://doi.org/10.1016/j.cell.2018.01.029>
- Lander, E. S., Linton, L. M., Birren, B., Nusbaum, C., Zody, M. C., Baldwin, J., Devon, K., Dewar, K., Doyle, M., Fitzhugh, W., Funke, R., Gage, D., Harris, K., Heaford, A., Howland, J., Kann, L., Lehoczky, J., Levine, R., McEwan, P., ... Chen, Y. J. (2001). Erratum: Initial sequencing and analysis of the human genome: International Human Genome Sequencing Consortium (Nature (2001) 409 (860-921)). *Nature*, 412(6846), 565–566. <https://doi.org/10.1038/35087627>
- Lane, C. A., Hardy, J., & Schott, J. M. (2018). Alzheimer's disease. *European Journal of Neurology*, 25(1), 59–70. <https://doi.org/10.1111/ene.13439>
- Längst, G., & Manelyte, L. (2015). Chromatin remodelers: From function to dysfunction. *Genes*, 6(2), 299–324. <https://doi.org/10.3390/genes6020299>
- Lanzillotta, A., Porrini, V., Bellucci, A., Benarese, M., Branca, C., Parrella, E., Spano, P. F., & Pizzi, M. (2015). NF- $\kappa$ B in innate neuroprotection and age-related neurodegenerative diseases. *Frontiers in Neurology*, 6(MAY), 1–8.  
<https://doi.org/10.3389/fneur.2015.00098>
- Larsen, M. R., Sørensen, G. L., Fey, S. J., Larsen, P. M., & Roepstorff, P. (2001). Phospho-proteomics: Evaluation of the use of enzymatic de-phosphorylation and differential mass spectrometric peptide mass mapping for site specific phosphorylation assignment in proteins separated by gel electrophoresis. *Proteomics*, 1(2), 223–238.  
[https://doi.org/10.1002/1615-9861\(200102\)1:2<223::AID-PROT223>3.0.CO;2-B](https://doi.org/10.1002/1615-9861(200102)1:2<223::AID-PROT223>3.0.CO;2-B)
- Lau, S. F., Chen, C., Fu, W. Y., Qu, J. Y., Cheung, T. H., Fu, A. K. Y., & Ip, N. Y. (2020). IL-33-PU.1 Transcriptome Reprogramming Drives Functional State Transition and Clearance Activity of Microglia in Alzheimer's Disease. *Cell Reports*, 31(3), 107530.  
<https://doi.org/10.1016/j.celrep.2020.107530>

- Laver, K., Dyer, S., Whitehead, C., Clemson, L., & Crotty, M. (2016). Interventions to delay functional decline in people with dementia: A systematic review of systematic reviews. *BMJ Open*, *6*(4). <https://doi.org/10.1136/bmjopen-2015-010767>
- Lavin, Y., Winter, D., Blecher-Gonen, R., David, E., Keren-Shaul, H., Merad, M., Jung, S., & Amit, I. (2014). Tissue-resident macrophage enhancer landscapes are shaped by the local microenvironment. *Cell*, *159*(6), 1312–1326. <https://doi.org/10.1016/j.cell.2014.11.018>
- Lazaro, J. B., Bailey, P. J., & Lassar, A. B. (2002). Cyclin D-cdk4 activity modulates the subnuclear localization and interaction of MEF2 with SRC-family coactivators during skeletal muscle differentiation. *Genes and Development*, *16*(14), 1792–1805. <https://doi.org/10.1101/gad.U-9988R>
- Le Meur, N., Holder-Espinasse, M., Jaillard, S., Goldenberg, A., Joriot, S., Amati-Bonneau, P., Guichet, A., Barth, M., Charollais, A., Journel, H., Auvin, S., Boucher, C., Kerckaert, J.-P., David, V., Manouvrier-Hanu, S., Saugier-veber, P., Frébourg, T., Dubourg, C., Andrieux, J., & Bonneau, D. (2010). MEF2C haploinsufficiency caused by either microdeletion of the 5q14.3 region or mutation is responsible for severe mental retardation with stereotypic movements, epilepsy and/or cerebral malformations. *Journal of Medical Genetics*, *47*(1), 22–29. <https://doi.org/10.1136/jmg.2009.069732>
- Lee, H. K., & Oh, J. E. (2016). OASL1 deficiency promotes antiviral protection against genital herpes simplex virus type 2 infection by enhancing type I interferon production. *The Journal of Immunology*, *196*(1). <https://doi.org/10.1038/srep19089>
- Lee, M. S., Kim, B., Oh, G. T., & Kim, Y. J. (2013). OASL1 inhibits translation of the type I interferon-regulating transcription factor IRF7. *Nature Immunology*, *14*(4), 346–355. <https://doi.org/10.1038/ni.2535>
- Lehnardt, S. (2010). Innate immunity and neuroinflammation in the CNS: The role of microglia in toll-like receptor-mediated neuronal injury. *Glia*, *58*(3), 253–263. <https://doi.org/10.1002/glia.20928>
- Leifer, D., Golden, J., & Kowall, N. W. (1994). Myocyte-specific enhancer binding factor 2C expression in human brain development. *Neuroscience*, *63*(4), 1067–1079. [https://doi.org/10.1016/0306-4522\(94\)90573-8](https://doi.org/10.1016/0306-4522(94)90573-8)
- Leifer, D., Krainc, D., Yu, Y. T., McDermott, J., Breitbart, R. E., Heng, J., Neve, R. L., Kosofsky, B., Nadal-Ginard, B., & Lipton, S. A. (1993). MEF2C, a MADS/MEF2-family transcription factor expressed in a laminar distribution in cerebral cortex. *Proceedings of the National Academy of Sciences of the United States of America*, *90*(4), 1546–1550. <https://doi.org/10.1073/pnas.90.4.1546>
- Leissring, M. A., Murphy, M. P., Mead, T. R., Akbari, Y., Sugarman, M. C., Saftig, P., Strooper, B. De, Jannatipour, M., Anliker, B., Mu, U., Wolfe, M. S., Golde, T. E., & Laferla, F. M. (2002). A physiologic signaling role for the  $\gamma$ -secretase-derived intracellular fragment of APP. *PNAS*, *99*(7), 4697–4702.
- Lewerenz, J., & Maher, P. (2009). Basal levels of eIF2 $\alpha$  phosphorylation determine cellular antioxidant status by regulating ATF4 and xCT expression. *Journal of Biological Chemistry*, *284*(2), 1106–1115. <https://doi.org/10.1074/jbc.M807325200>
- Li, Hao, Radford, J. C., Ragusa, M. J., Shea, K. L., McKercher, S. R., Zaremba, J. D., Soussou, W., Nie, Z., Kang, Y. J., Nakanishi, N., Okamoto, S. I., Roberts, A. J., Schwarz, J. J., & Lipton, S. A. (2008). Transcription factor MEF2C influences neural stem/progenitor cell



- differentiation and maturation in vivo. *Proceedings of the National Academy of Sciences of the United States of America*, 105(27), 9397–9402.  
<https://doi.org/10.1073/pnas.0802876105>
- Li, Heng, & Durbin, R. (2009). Fast and accurate short read alignment with Burrows-Wheeler transform. *Bioinformatics*, 25(14), 1754–1760.  
<https://doi.org/10.1093/bioinformatics/btp324>
- Li, Heng, Handsaker, B., Wysoker, A., Fennell, T., Ruan, J., Homer, N., Marth, G., Abecasis, G., & Durbin, R. (2009). The Sequence Alignment/Map format and SAMtools. *Bioinformatics*, 25(16), 2078–2079. <https://doi.org/10.1093/bioinformatics/btp352>
- Li, L., Stefan, M. I., & Le Novère, N. (2012). Calcium Input Frequency, Duration and Amplitude Differentially Modulate the Relative Activation of Calcineurin and CaMKII. *PLoS ONE*, 7(9). <https://doi.org/10.1371/journal.pone.0043810>
- Li, X. L., Hu, N., Tan, M. S., Yu, J. T., & Tan, L. (2014). Behavioral and Psychological Symptoms in Alzheimer's Disease. *BioMed Research International*, 2014. <https://doi.org/10.1155/2014/927804>
- Li, X., Wang, W., Wang, J., Malovannaya, A., Xi, Y., Li, W., Guerra, R., Hawke, D. H., Qin, J., & Chen, J. (2015). Proteomic analyses reveal distinct chromatin-associated and soluble transcription factor complexes. *Molecular Systems Biology*, 11(1), 775. <https://doi.org/10.15252/msb.20145504>
- Li, Z., Schulz, M. H., Look, T., Begemann, M., Zenke, M., & Costa, I. (2019). Identification of transcription factor binding sites using ATAC-seq. *Genome Biology*, 20(45). <https://doi.org/10.1109/ISDA.2006.171>
- Liddel, S. A., Guttenplan, K. A., Clarke, L. E., Bennett, F. C., Bohlen, C. J., Schirmer, L., Bennett, M. L., & Münch, A. E. (2017). Neurotoxic reactive astrocytes are induced by activated microglia. *Nature*, 541(7638), 481–487. <https://doi.org/10.1016/j.physbeh.2017.03.040>
- Lin, Q., Lu, J., Yanagisawa, H., Webb, R., Lyons, G. E., Richardson, J. A., & Olson, E. N. (1998). Requirement of the MADS-box transcription factor MEF2C for vascular development. *Development*, 125(22), 4565–4574.
- Lin, Q., Schwarz, J., Bucana, C., & Olson, E. N. (1997). Control of mouse cardiac morphogenesis and myogenesis by transcription factor MEF2C. *Science*, 276(5317), 1404–1407. <https://doi.org/10.1126/science.276.5317.1404>
- Linnartz-Gerlach, B., Mathews, M., & Neumann, H. (2014). Sensing the neuronal glycocalyx by glial sialic acid binding immunoglobulin-like lectins. *Neuroscience*, 275, 113–124. <https://doi.org/10.1016/j.neuroscience.2014.05.061>
- Liu, F., Wang, D., Zhu, L., Du, J., Lin, P., Liang, F., Wang, X., Tan, X., & Lin, L. (2020). Microglia-derived FGF21 as a modulator of astrocytic phenotype and cerebral ischemia injury. <https://doi.org/10.21203/rs.3.rs-15781/v1>
- Liu, J., Li, M., Luo, X. J., & Su, B. (2018). Systems-level analysis of risk genes reveals the modular nature of schizophrenia. *Schizophrenia Research*, 201, 261–269. <https://doi.org/10.1016/j.schres.2018.05.015>
- Liu, M. L., Olson, A. L., Edgington, N. P., Moye-Rowley, W. S., & Pessin, J. E. (1994). Myocyte enhancer factor 2 (MEF2) binding site is essential for C2C12 myotube-specific expression of the rat GLUT4/muscle-adipose facilitative glucose transporter gene.

- Journal of Biological Chemistry*, 269(45), 28514–28521.
- Liu, T., Ortiz, J. A., Taing, L., Meyer, C. A., Lee, B., Zhang, Y., Shin, H., Wong, S. S., Ma, J., Lei, Y., Pape, U. J., Poidinger, M., Chen, Y., Yeung, K., Brown, M., Turpaz, Y., & Liu, X. S. (2011). Cistrome: An integrative platform for transcriptional regulation studies. *Genome Biology*, 12(8), R83. <https://doi.org/10.1186/gb-2011-12-8-r83>
- Love, M. I., Huber, W., & Anders, S. (2014). Moderated estimation of fold change and dispersion for RNA-seq data with DESeq2. *Genome Biology*, 15(550). <https://doi.org/10.1186/s13059-014-0550-8>
- Lu, J., McKinsey, T. A., Nicol, R. L., & Olson, E. N. (2000a). Signal-dependent activation of the MEF2 transcription factor by dissociation from histone deacetylases. *Proceedings of the National Academy of Sciences of the United States of America*, 97(8), 4070–4075. <https://doi.org/10.1073/pnas.080064097>
- Lu, J., McKinsey, T. A., Zhang, C. L., & Olson, E. N. (2000b). Regulation of skeletal myogenesis by association of the MEF2 transcription factor with class II histone deacetylases. *Molecular Cell*. [https://doi.org/10.1016/S1097-2765\(00\)00025-3](https://doi.org/10.1016/S1097-2765(00)00025-3)
- Luengo-Fernandez, R., Leal, J., & Gray, A. (2015). *UK research spend in 2008 and 2012: comparing stroke, cancer, coronary heart disease and dementia* (Vol. 5). British Medical Journal Publishing Group. <https://doi.org/10.1136/bmjopen-2014-006648>
- Luger, K., Mäder, A. W., Richmond, R. K., Sargent, D. F., & Richmond, T. J. (1997). Crystal structure of the nucleosome core particle at 2.8 Å resolution. *Nature*, 389(6648), 251–260. <https://doi.org/10.1038/38444>
- Lun, A. T. L., & Smyth, G. K. (2016). csaw: A Bioconductor package for differential binding analysis of ChIP-seq data using sliding windows. *Nucleic Acids Research*, 44(5). <https://doi.org/10.1093/nar/gkv1191>
- Luoma, J. I., & Zirpel, L. (2008). Deafferentation-induced activation of NFAT (Nuclear Factor of Activated T-Cells) in cochlear nucleus neurons during a developmental critical period: A role for NFATc4-dependent apoptosis in the CNS. *Journal of Neuroscience*, 28(12), 3159–3169. <https://doi.org/10.1523/JNEUROSCI.5227-07.2008>
- Lyketsos, C. G., Steele, G., Baker, L., Galik, E., Kopunek, S., Steinberg, M., & Warren, A. (1997). Major and minor depression in Alzheimer's disease: prevalence and impact. *The Journal of Neuropsychiatry*, 9(4), 556–561.
- Lynch, J., Guo, L., Gelebart, P., Chilibeck, K., Xu, J., Molkentin, J. D., Agellon, L. B., & Michalak, M. (2005). Calreticulin signals upstream of calcineurin and MEF2C in a critical Ca<sup>2+</sup>-dependent signaling cascade. *Journal of Cell Biology*, 170(1), 37–47. <https://doi.org/10.1083/jcb.200412156>
- Lyons, G. E., Micales, B. K., Schwarz, J., Martin, J. F., & Olson, E. N. (1995). Expression of mef2 genes in the mouse central nervous system suggests a role in neuronal maturation. *Journal of Neuroscience*, 15(8), 5727–5738. <https://doi.org/10.1523/jneurosci.15-08-05727.1995>
- Madeira, F., Park, Y. M., Lee, J., Buso, N., Gur, T., Madhusoodanan, N., Basutkar, P., Tivey, A. R. N., Potter, S. C., Finn, R. D., & Lopez, R. (2019). The EMBL-EBI search and sequence analysis tools APIs in 2019. *Nucleic Acids Research*, 47(W1), W636–W641. <https://doi.org/10.1093/nar/gkz268>
- Maeda, T., Chapman, D. L., & Stewart, A. F. R. (2002). Mammalian vestigial-like 2, a cofactor

- of TEF-1 and MEF2 transcription factors that promotes skeletal muscle differentiation. *Journal of Biological Chemistry*, 277(50), 48889–48898. <https://doi.org/10.1074/jbc.M206858200>
- Maejima, T., Inoue, T., Kanki, Y., Kohro, T., Li, G., Ohta, Y., Kimura, H., Kobayashi, M., Taguchi, A., Tsutsumi, S., Iwanari, H., Yamamoto, S., Aruga, H., Dong, S., Stevens, J. F., Poh, H. M., Yamamoto, K., Kawamura, T., Mimura, I., ... Wada, Y. (2014). Direct evidence for pitavastatin induced chromatin structure change in the KLF4 gene in endothelial cells. *PLoS ONE*, 9(5). <https://doi.org/10.1371/journal.pone.0096005>
- Majidi, S. P., Reddy, N. C., Moore, M. J., Chen, H., Yamada, T., Andzelm, M. M., Cherry, T. J., Hu, L. S., Greenberg, M. E., & Bonni, A. (2019). Chromatin Environment and Cellular Context Specify Compensatory Activity of Paralogous MEF2 Transcription Factors. *Cell Reports*, 29(7), 2001-2015.e5. <https://doi.org/10.1016/j.celrep.2019.10.033>
- Manocha, G. D., Floden, A. M., Rausch, K., Kulas, J. A., McGregor, B. A., Rojanathammanee, L., Puig, K. R., Puig, K. L., Karki, S., Nichols, M. R., Darland, D. C., Porter, J. E., & Combs, C. K. (2016). APP regulates microglial phenotype in a mouse model of alzheimer's disease. *Journal of Neuroscience*, 36(32), 8471–8486. <https://doi.org/10.1523/JNEUROSCI.4654-15.2016>
- Mao, Z., Bonni, A., Xia, F., Nadal-Vicens, M., & Greenberg, M. E. (1999). Neuronal Activity-Dependent Cell Survival Mediated by Transcription Factor MEF2. In *Source: Science, New Series* (Vol. 286, Issue 5440).
- Marian, A. J. (2014). Sequencing your genome: what does it mean? *Methodist DeBaakey Cardiovascular Journal*, 10(1), 3–6. <https://doi.org/10.14797/mdcj-10-1-3>
- Marín-Teva, J. L., Dusart, I., Colin, C., Gervais, A., Van Rooijen, N., & Mallat, M. (2004). Microglia Promote the Death of Developing Purkinje Cells. *Neuron*, 41(4), 535–547. [https://doi.org/10.1016/S0896-6273\(04\)00069-8](https://doi.org/10.1016/S0896-6273(04)00069-8)
- Marinissen, M. J., Chiariello, M., Pallante, M., & Gutkind, J. S. (1999). A Network of Mitogen-Activated Protein Kinases Links G Protein-Coupled Receptors to the c-jun Promoter: a Role for c-Jun NH 2-Terminal Kinase, p38s, and Extracellular Signal-Regulated Kinase 5. In *MOLECULAR AND CELLULAR BIOLOGY* (Vol. 19, Issue 6). <http://mcb.asm.org/>
- Markesbery, W. R. (1997). Oxidative stress hypothesis in Alzheimer's disease. *Free Radical Biology and Medicine*, 23(1), 134–147. [https://doi.org/10.1016/S0891-5849\(96\)00629-6](https://doi.org/10.1016/S0891-5849(96)00629-6)
- Marks, P. A., Miller, T., & Richon, V. M. (2003). Histone deacetylases. In *Current Opinion in Pharmacology*. [https://doi.org/10.1016/S1471-4892\(03\)00084-5](https://doi.org/10.1016/S1471-4892(03)00084-5)
- Martin, J F, Miano, J. M., Hustad, C. M., Copeland, N. G., Jenkins, N. A., & Olson, E. N. (1994). A Mef2 gene that generates a muscle-specific isoform via alternative mRNA splicing. *Molecular and Cellular Biology*, 14(3), 1647–1656. <https://doi.org/10.1128/mcb.14.3.1647>
- Martin, James F., Schwarz, J. J., & Olson, E. N. (1993). Myocyte enhancer factor (MEF) 2C: A tissue-restricted member of the MEF-2 family of transcription factors. *Proceedings of the National Academy of Sciences of the United States of America*, 90(11), 5282–5286. <https://doi.org/10.1073/pnas.90.11.5282>
- Martin, K. (1991). The interactions of transcription factors and their adaptors, coactivators

- and accessory proteins. *BioEssays*, 13(10), 499–503.
- Maston, G. A., Evans, S. K., & Green, M. R. (2006). Transcriptional Regulatory Elements in the Human Genome. *Annual Review of Genomics and Human Genetics*, 7(1), 29–59. <https://doi.org/10.1146/annurev.genom.7.080505.115623>
- Matcovitch-Natan, O., Winter, D. R., Giladi, A., Aguilar, S. V., Spinrad, A., Sarrazin, S., Ben-Yehuda, H., David, E., González, F. Z., Perrin, P., Keren-Shaul, H., Gury, M., Lara-Astaiso, D., Thaiss, C. A., Cohen, M., Halpern, K. B., Baruch, K., Deczkowska, A., Lorenzo-Vivas, E., ... Amit, I. (2016). Microglia development follows a stepwise program to regulate brain homeostasis. *Science*, 353(6301). <https://doi.org/10.1126/science.aad8670>
- Mattson, M. P. (1994). Calcium and Neuronal Injury in Alzheimer's Disease. *Annals of The New York Academy of Sciences*, 747(1), 50–76.
- Mattson, M. P., Cheng, B., Davis, D., Bryant, K., Lieberburg, I., & Rydel, E. R. (1992). B-Amyloid Peptides Destabilize Calcium Homeostasis and Render Human Cortical Neurons Vulnerable to Excitotoxicity. *The Journal of Neuroscience*, 12(2), 376–389.
- McDaid, J., Mustaly-Kalimi, S., & Stutzmann, G. E. (2020). Ca<sup>2+</sup> Dyshomeostasis Disrupts Neuronal and Synaptic Function in Alzheimer's Disease. *Cells*, 9(12), 1–25. <https://doi.org/10.3390/cells9122655>
- McDermott, J. C., Cardoso, M. C., Yu, Y. T., Andres, V., Leifer, D., Krainc, D., Lipton, S. A., & Nadal-Ginard, B. (1993). hMEF2C gene encodes skeletal muscle- and brain-specific transcription factors. *Molecular and Cellular Biology*, 13(4), 2564–2577. <https://doi.org/10.1128/mcb.13.4.2564>
- McGee, S. L., Sparling, D., Olson, A., & Hargreaves, M. (2006). Exercise increases MEF2- and GEF DNA-binding activities in human skeletal muscle. *The FASEB Journal*, 20(2), 348–349. <https://doi.org/10.1096/fj.05-4671fje>
- McKhann, G. M., Knopman, D. S., Chertkow, H., Hyman, B. T., Jack, C. R., Kawas, C. H., Klunk, W. E., Koroshetz, W. J., Manly, J. J., Mayeux, R., Mohs, R. C., Morris, J. C., Rossor, M. N., Scheltens, P., Carrillo, M. C., Thies, B., Weintraub, S., & Phelps, C. H. (2011). The diagnosis of dementia due to Alzheimer's disease: Recommendations from the National Institute on Aging-Alzheimer's Association workgroups on diagnostic guidelines for Alzheimer's disease. *Alzheimer's and Dementia*, 7(3), 263–269. <https://doi.org/10.1016/j.jalz.2011.03.005>
- McKinsey, T. A., Zhang, C. L., & Olson, E. N. (2000a). Activation of the myocyte enhancer factor-2 transcription factor by calcium/calmodulin-dependent protein kinase-stimulated binding of 14-3-3 to histone deacetylase 5. *Proceedings of the National Academy of Sciences of the United States of America*, 97(26), 14400–14405. <https://doi.org/10.1073/pnas.260501497>
- McKinsey, T. A., Zhang, C. L., & Olson, E. N. (2001a). Control of muscle development by dueling HATs and HDACs. In *Current Opinion in Genetics and Development*. [https://doi.org/10.1016/S0959-437X\(00\)00224-0](https://doi.org/10.1016/S0959-437X(00)00224-0)
- McKinsey, T. A., Zhang, C. L., & Olson, E. N. (2001b). Identification of a Signal-Responsive Nuclear Export Sequence in Class II Histone Deacetylases. *Molecular and Cellular Biology*, 21(18), 6312–6321. <https://doi.org/10.1128/mcb.21.18.6312-6321.2001>
- McKinsey, T. A., Zhang, C., Lu, J., & Olson, E. N. (2000b). Signal-dependent nuclear export of

- a histone deacetylase regulates muscle differentiation. *408*(6808), 106–111.  
<https://doi.org/10.1038/35040593>.Signal-dependent
- McKinsey, Timothy A., Zhang, C. L., & Olson, E. N. (2002). MEF2: A calcium-dependent regulator of cell division, differentiation and death. In *Trends in Biochemical Sciences*.  
[https://doi.org/10.1016/S0968-0004\(01\)02031-X](https://doi.org/10.1016/S0968-0004(01)02031-X)
- McLarnon, J. G., Choi, H. B., Lue, L. F., Walker, D. G., & Kim, S. U. (2005). Perturbations in calcium-mediated signal transduction in microglia from Alzheimer's disease patients. *Journal of Neuroscience Research*, *81*(3), 426–435. <https://doi.org/10.1002/jnr.20487>
- McLean, C. Y., Bristor, D., Hiller, M., Clarke, S. L., Schaar, B. T., Lowe, C. B., Wenger, A. M., & Bejerano, G. (2010). GREAT improves functional interpretation of cis-regulatory regions. *Nature Biotechnology*, *28*(5), 495–501. <https://doi.org/10.1038/nbt.1630>
- Mcshane, R., Westby, M., Roberts, E., Minakaran, N., Schneider, L., Farrimond, L., Maayan, N., Ware, J., & Debarros, J. (2019). Memantine for dementia [Systematic Review]. *Cochrane Database of Systematic Reviews*, *1*.  
<https://doi.org/10.1002/14651858.CD003154.pub6>.www.cochranelibrary.com
- Mehta, D., Jackson, R., Paul, G., Shi, J., Sabbagh, M., Network, V. H., & Division, M. D. (2017). Why do trials for Alzheimer's disease drugs keep failing? *Expert Opin Investig Drugs*, *26*(6), 735–739. <https://doi.org/10.1080/13543784.2017.1323868>.Why
- Mellacheruvu, D., Wright, Z., Couzens, A. L., Lambert, J. P., St-Denis, N. A., Li, T., Miteva, Y. V., Hauri, S., Sardi, M. E., Low, T. Y., Halim, V. A., Bagshaw, R. D., Hubner, N. C., Al-Hakim, A., Bouchard, A., Faubert, D., Fermin, D., Dunham, W. H., Goudreault, M., ... Nesvizhskii, A. I. (2013). The CRAPome: A contaminant repository for affinity purification-mass spectrometry data. *Nature Methods*, *10*(8), 730–736.  
<https://doi.org/10.1038/nmeth.2557>
- Menche, J., Sharma, A., Kitsak, M., Ghiassian, S., Vidal, M., Loscalzo, J., & Barabási, A. (2015). Uncovering disease-disease relationships through the incomplete human interactome. *Science*, *347*(6224). <https://doi.org/10.1016/j.physbeh.2017.03.040>
- Merle, N. S., Church, S. E., Fremeaux-Bacchi, V., & Roumenina, L. T. (2015). Complement system part I - molecular mechanisms of activation and regulation. *Frontiers in Immunology*, *6*(JUN), 1–30. <https://doi.org/10.3389/fimmu.2015.00262>
- Michalak, M., Parker, J. M. R., & Opas, M. (2002). Ca<sup>2+</sup> signaling and calcium binding chaperones of the endoplasmic reticulum. *Cell Calcium*, *32*(5–6), 269–278.  
<https://doi.org/10.1016/S0143416002001884>
- Micheli, L., Leonardi, L., Conti, F., Buanne, P., Canu, N., Caruso, M., & Tirone, F. (2005). PC4 Coactivates MyoD by Relieving the Histone Deacetylase 4-Mediated Inhibition of Myocyte Enhancer Factor 2C. *Molecular and Cellular Biology*, *25*(6), 2242–2259.  
<https://doi.org/10.1128/mcb.25.6.2242-2259.2005>
- Mielcarek, M., Zielonka, D., Carnemolla, A., Marcinkowski, J. T., & Guidez, F. (2015). HDAC4 as a potential therapeutic target in neurodegenerative diseases: A summary of recent achievements. *Frontiers in Cellular Neuroscience*, *9*(FEB), 1–9.  
<https://doi.org/10.3389/fncel.2015.00042>
- Mills, M. A., Yang, N., Weinberger, R., Vander Woude, D. L., Beggs, A. H., Easteal, S., & North, K. N. (2001). Differential expression for the actin-binding proteins,  $\alpha$ -actinin-2 and -3, in different species: Implications for the evolution of functional redundancy.

- Human Molecular Genetics*, 10(13), 1335–1346.  
<https://doi.org/10.1093/hmg/10.13.1335>
- Minghetti, L., & Levi, G. (1998). Microglia as effector cells in brain damage and repair: Focus on prostanoids and nitric oxide. *Progress in Neurobiology*, 54(1), 99–125.  
[https://doi.org/10.1016/S0301-0082\(97\)00052-X](https://doi.org/10.1016/S0301-0082(97)00052-X)
- Miska, E. A., Langley, E., Wolf, D., Karlsson, C., Pines, J., & Kouzarides, T. (2001). Differential localization of HDAC4 orchestrates muscle differentiation. *Nucleic Acids Research*, 29(16), 3439–3447. <https://doi.org/10.1093/nar/29.16.3439>
- Miska, Eric A., Karlsson, C., Langley, E., Nielsen, S. J., Pines, J., & Kouzarides, T. (1999). HDAC4 deacetylase associates with and represses the MEF2 transcription factor. *EMBO Journal*, 18(18), 5099–5107. <https://doi.org/10.1093/emboj/18.18.5099>
- Mitchell, A. C., Javidfar, B., Pothula, V., Ibi, D., Shen, E. Y., Peter, C. J., Bicks, L. K., Fehr, T., Jiang, Y., Brennand, K. J., Neve, R. L., Gonzalez-Maeso, J., & Akbarian, S. (2018). MEF2C transcription factor is associated with the genetic and epigenetic risk architecture of schizophrenia and improves cognition in mice. *Molecular Psychiatry*, 23(1), 123–132. <https://doi.org/10.1038/mp.2016.254>
- Mitrofanova, A., Mallela, S. K., Ducasa, G. M., Yoo, T. H., Rosenfeld-Gur, E., Zelnik, I. D., Molina, J., Varona Santos, J., Ge, M., Sloan, A., Kim, J. J., Pedigo, C., Bryn, J., Volosenco, I., Faul, C., Zeidan, Y. H., Garcia Hernandez, C., Mendez, A. J., Leibiger, I., ... Feroni, A. (2019). SMPDL3b modulates insulin receptor signaling in diabetic kidney disease. *Nature Communications*, 10(1). <https://doi.org/10.1038/s41467-019-10584-4>
- Mitsuda, T., Hayakawa, Y., Itoh, M., Ohta, K., & Nakagawa, T. (2007). ATF4 regulates  $\gamma$ -secretase activity during amino acid imbalance. *Biochemical and Biophysical Research Communications*, 352(3), 722–727. <https://doi.org/10.1016/j.bbrc.2006.11.075>
- Mittelbronn, M., Dietz, K., Schluesener, H. J., & Meyermann, R. (2001). Local distribution of microglia in the normal adult human central nervous system differs by up to one order of magnitude. *Acta Neuropathologica*, 101(3), 249–255.  
<https://doi.org/10.1007/s004010000284>
- Molkentin, J D, Black, B. L., Martin, J. F., & Olson, E. N. (1996a). Mutational analysis of the DNA binding, dimerization, and transcriptional activation domains of MEF2C. *Molecular and Cellular Biology*, 16(6), 2627–2636.  
<https://doi.org/10.1128/mcb.16.6.2627>
- Molkentin, Jeffery D., Li, L., & Olson, E. N. (1996b). Phosphorylation of the MADS-box transcription factor MEF2C enhances its DNA binding activity. *Journal of Biological Chemistry*, 271(29), 17199–17204. <https://doi.org/10.1074/jbc.271.29.17199>
- Molkentin, Jeffery D, Black, B. L., Martin, J. F., & Olson, E. N. (1995). Cooperative Activation of Muscle Gene Expression by MEF2 and Myogenic bHLH Proteins. In *Cell* (Vol. 63).
- Monasor, L. S., Müller, S. A., Colombo, A. V., Tanriover, G., König, J., Roth, S., Liesz, A., Berghofer, A., Piechotta, A., Prestel, M., Saito, T., Saido, T. C., Herms, J., Willem, M., Haass, C., Lichtenthaler, S. F., & Tahirovic, S. (2020). Fibrillar  $\alpha\beta$  triggers microglial proteome alterations and dysfunction in alzheimer mouse models. *ELife*, 9, 1–33.  
<https://doi.org/10.7554/eLife.54083>
- Moreau, P., Hen, R., Wasylyk, B., Everett, R., Gaub, M. P., & Chambon, P. (1981). The SV40 72 base repair repeat has a striking effect on gene expression both in SV40 and other

- chimeric recombinants. *Nucleic Acids Research*, 9(22), 6047–6068.  
<https://doi.org/10.1093/nar/9.22.6047>
- Morgan, R. G., Ridsdale, J., Payne, M., Heesom, K. J., Wilson, M. C., Davidson, A., Greenhough, A., Davies, S., Williams, A. C., Blair, A., Waterman, M. L., Tonks, A., & Darley, R. L. (2019). LEF-1 drives aberrant  $\beta$ -catenin nuclear localization in myeloid leukemia cells. *Haematologica*, 104(7), 1365–1377.  
<https://doi.org/10.3324/haematol.2018.202846>
- Morganti, J. M., Riparip, L. K., & Rosi, S. (2016). Call off the dog(ma): M1/M2 polarization is concurrent following traumatic brain injury. *PLoS ONE*, 11(1), 1–13.  
<https://doi.org/10.1371/journal.pone.0148001>
- Morin, S., Charron, F., Robitaille, L., & Nemer, M. (2000). GATA-dependent recruitment of MEF2 proteins to target promoters. *The EMBO Journal*, 19(9), 2046–2055.  
<https://doi.org/10.1093/emboj/19.9.2046>
- Morisaki, T., & Holmes, E. W. (1993). Functionally distinct elements are required for expression of the AMPD1 gene in myocytes. *Molecular and Cellular Biology*, 13(9), 5854–5860. <https://doi.org/10.1128/mcb.13.9.5854>
- Muller, P. A. J., & Vousden, K. H. (2013). P53 mutations in cancer. *Nature Cell Biology*, 15(1), 2–8. <https://doi.org/10.1038/ncb2641>
- Naj, A. C., Jun, G., Beecham, G. W., Wang, L. S., Vardarajan, B. N., Buross, J., Gallins, P. J., Buxbaum, J. D., Jarvik, G. P., Crane, P. K., Larson, E. B., Bird, T. D., Boeve, B. F., Graff-Radford, N. R., De Jager, P. L., Evans, D., Schneider, J. A., Carrasquillo, M. M., Ertekin-Taner, N., ... Schellenberg, G. D. (2011). Common variants at MS4A4/MS4A6E, CD2AP, CD33 and EPHA1 are associated with late-onset Alzheimer's disease. *Nature Genetics*, 43(5), 436–443. <https://doi.org/10.1038/ng.801>
- Naya, F. J., & Olson, E. (1999). MEF2: A transcriptional target for signaling pathways controlling skeletal muscle growth and differentiation. *Current Opinion in Cell Biology*, 11(6), 683–688. [https://doi.org/10.1016/S0955-0674\(99\)00036-8](https://doi.org/10.1016/S0955-0674(99)00036-8)
- Nayak, D., Roth, T. L., & McGavern, D. B. (2014). Microglia Development and Function. In *Annu. Rev. Immunol.* (Vol. 32, pp. 367–402). <https://doi.org/10.1146/annurev-immunol-032713-120240>
- Ndoja, A., Reja, R., Lee, S. H., Webster, J. D., Ngu, H., Rose, C. M., Kirkpatrick, D. S., Modrusan, Z., Chen, Y. J. J., Dugger, D. L., Gandham, V., Xie, L., Newton, K., & Dixit, V. M. (2020). Ubiquitin Ligase COP1 Suppresses Neuroinflammation by Degrading c/EBP $\beta$  in Microglia. *Cell*, 182(5), 1156–1169.e12. <https://doi.org/10.1016/j.cell.2020.07.011>
- Nerlov, C., & Graf, T. (1998). PU.1 induces myeloid lineage commitment in multipotent hematopoietic progenitors. *Genes and Development*, 12(15), 2403–2412. <https://doi.org/10.1101/gad.12.15.2403>
- Nilsen, T. W. (2003). The spliceosome: The most complex macromolecular machine in the cell? *BioEssays*, 25(12), 1147–1149. <https://doi.org/10.1002/bies.10394>
- Nimmerjahn, A., Kirchhoff, F., & Helmchen, F. (2005). Neuroscience: Resting microglial cells are highly dynamic surveillants of brain parenchyma in vivo. *Science*, 308(5726), 1314–1318. <https://doi.org/10.1126/science.1110647>
- Norman, C., Runswick, M., Pollock, R., & Treisman, R. (1988). Isolation and properties of

- cDNA clones encoding SRF, a transcription factor that binds to the c-fos serum response element. *Cell*, 55(6), 989–1003. [https://doi.org/10.1016/0092-8674\(88\)90244-9](https://doi.org/10.1016/0092-8674(88)90244-9)
- Nott, A., Holtman, I. R., Coufal, N. G., Schlachetzki, J. C. M., Yu, M., Hu, R., Han, C. Z., Pena, M., Xiao, J., Wu, Y., Keulen, Z., Pasillas, M. P., O'Connor, C., Nickl, C. K., Schafer, S. T., Shen, Z., Rissman, R. A., Brewer, J. B., Gosselin, D., ... Glass, C. K. (2019). Brain cell type-specific enhancer-promoter interactome maps and disease-risk association. *Science*, 366(6469), 1134–1139. <https://doi.org/10.1126/science.aay0793>
- Nurnberger, J. I., Koller, D. L., Jung, J., Edenberg, H. J., Foroud, T., Guella, I., Vawter, M. P., Kelsoe, J. R., Sklar, P., Ripke, S., Scott, L. J., Andreassen, O. A., Cichon, S., Craddock, N., Rietschel, M., Blackwood, D., Corvin, A., Flickinger, M., Guan, W., ... Purcell, S. M. (2014). Identification of pathways for bipolar disorder: A meta-analysis. *JAMA Psychiatry*, 71(6), 657–664. <https://doi.org/10.1001/jamapsychiatry.2014.176>
- Office for National Statistics. (2021). *Deaths registered in England and Wales*. Office of National Statistics. <https://www.ons.gov.uk/peoplepopulationandcommunity/birthsdeathsandmarriages/deaths/datasets/deathsregisteredinenglandandwalesseriesdrreferencetables>
- Ogbourne, S., & Antalis, T. M. (1998). Transcriptional control and the role of silencers in transcriptional regulation in eukaryotes. *Biochemical Journal*, 331, 1–14.
- Ohno, M. (2014). Roles of eIF2 $\alpha$  kinases in the pathogenesis of Alzheimer's disease. *Frontiers in Molecular Neuroscience*, 7(1 APR), 1–8. <https://doi.org/10.3389/fnmol.2014.00022>
- Okamura, H., Aramburu, J., García-Rodríguez, C., Viola, J. P. B., Raghavan, A., Tahiliani, M., Zhang, X., Qin, J., Hogan, P. G., & Rao, A. (2000). Concerted dephosphorylation of the transcription factor NFAT1 induces a conformational switch that regulates transcriptional activity. *Molecular Cell*, 6(3), 539–550. [https://doi.org/10.1016/S1097-2765\(00\)00053-8](https://doi.org/10.1016/S1097-2765(00)00053-8)
- Olins, A. L., & Olins, D. E. (1974). Spheroid chromatin units (v bodies). *Science*, 183(4122), 330–332. <https://doi.org/10.1126/science.183.4122.330>
- Olins, D. E., & Olins, A. L. (2003). Chromatin history: our view from the bridge. *Molecular Cell Biology*, 4, 909–914. <https://doi.org/10.1038/nrm1225>
- Olson, E. N., Perry, M., & Schulz, R. A. (1995). Regulation of Muscle Differentiation by the MEF2 Family of MADS Box Transcription Factors. *Developmental Biology*. <https://doi.org/10.1006/dbio.1995.0002>
- Olson, J. K., & Miller, S. D. (2004). Microglia Initiate Central Nervous System Innate and Adaptive Immune Responses through Multiple TLRs. *The Journal of Immunology*, 173(6), 3916–3924. <https://doi.org/10.4049/jimmunol.173.6.3916>
- Overk, C. R., & Masliah, E. (2014). Pathogenesis of synaptic degeneration in Alzheimer's disease and Lewy body disease. *Biochemical Pharmacology*, 88(4), 508–516. <https://doi.org/10.1016/j.bcp.2014.01.015>
- Panne, D. (2008). The enhanceosome. *Current Opinion in Structural Biology*, 18(2), 236–242. <https://doi.org/10.1016/j.sbi.2007.12.002>
- Paolicelli, R. C., Bolasco, G., Pagani, F., Maggi, L., Scianni, M., Panzanelli, P., Giustetto, M., Ferreira, T. A., Guiducci, E., Dumas, L., Ragozzino, D., & Gross, C. T. (2011). Synaptic



- pruning by microglia is necessary for normal brain development. *Science*, 333(6048), 1456–1458. <https://doi.org/10.1126/science.1202529>
- Papait, R., Serio, S., Pagiatakis, C., Rusconi, F., Carullo, P., Mazzola, M., Salvarani, N., Miragoli, M., & Condorelli, G. (2017). Histone methyltransferase G9a is required for cardiomyocyte homeostasis and hypertrophy. *Circulation*, 136(13), 1233–1246. <https://doi.org/10.1161/CIRCULATIONAHA.117.028561>
- Park, P. J. (2009). ChIP-seq: Advantages and challenges of a maturing technology. *Nature Reviews Genetics*, 10(10), 669–680. <https://doi.org/10.1038/nrg2641>
- Passmore, S., Maine, G., Elble, R., Christ, C., & Tye, B. (1988). *Saccharomyces cerevisiae* protein involved in plasmid maintenance is necessary for mating of MAT $\alpha$  cells. *Journal of Molecular Biology*, 204(3), 593–606.
- PCNS. (2020). Combined FDA and Biogen briefing information for the November 6, 2020 meeting of the Peripheral and Central Nervous System Drugs Advisory Committee. *Peripheral and Central Nervous System (PCNS) Drugs Advisory Committee Meeting*.
- Pedley, R., King, L. E., Mallikarjun, V., Wang, P., Swift, J., Brennan, K., & Gilmore, A. P. (2020). BioID-based proteomic analysis of the Bid interactome identifies novel proteins involved in cell-cycle-dependent apoptotic priming. *Cell Death and Disease*, 11(10). <https://doi.org/10.1038/s41419-020-03091-8>
- Pennacchio, L. A., Bickmore, W., Dean, A., Nobrega, M. A., & Bejerano, G. (2013). Enhancers: Five essential questions. *Nature Reviews Genetics*, 14(4), 288–295. <https://doi.org/10.1038/nrg3458>
- Pérez-Bercoff, Å., Hudson, C. M., & Conant, G. C. (2013). A Conserved Mammalian Protein Interaction Network. *PLoS ONE*, 8(1). <https://doi.org/10.1371/journal.pone.0052581>
- Perl, D. P. (2010). Neuropathology of Alzheimer's Disease. *Mount Sinai Journal of Medicine*, 77, 32–42. <https://doi.org/10.1002/MSJ>
- Pfurr, S., Chu, Y. H., Bohrer, C., Greulich, F., Beattie, R., Mammadzada, K., Hils, M., Arnold, S. J., Taylor, V., Schachtrup, K., Henriette Uhlenhaut, N., & Schachtrup, C. (2017). The E2A splice variant E47 regulates the differentiation of projection neurons via p57(KIP2) during cortical development. In *Development (Cambridge)* (Vol. 144, Issue 21). <https://doi.org/10.1242/dev.145698>
- Picard Tools*. (2009). Broad Institute. <http://broadinstitute.github.io/picard/>
- Pitale, P. M., Gorbatyuk, O., & Gorbatyuk, M. (2017). Neurodegeneration: Keeping ATF4 on a tight leash. *Frontiers in Cellular Neuroscience*, 11(410), 1–8. <https://doi.org/10.3389/fncel.2017.00410>
- Poliani, P. L., Wang, Y., Fontana, E., Robinette, M. L., Yamanishi, Y., Gilfillan, S., & Colonna, M. (2015). TREM2 sustains microglial expansion during aging and response to demyelination. *Journal of Clinical Investigation*, 125(5), 2161–2170. <https://doi.org/10.1172/JCI77983>
- Potthoff, M. J., Arnold, M. A., McAnally, J., Richardson, J. A., Bassel-Duby, R., & Olson, E. N. (2007). Regulation of Skeletal Muscle Sarcomere Integrity and Postnatal Muscle Function by Mef2c. *Molecular and Cellular Biology*, 27(23), 8143–8151. <https://doi.org/10.1128/mcb.01187-07>
- Potthoff, Matthew J., & Olson, E. N. (2007). MEF2: A central regulator of diverse

- developmental programs. *Development*, 134(23), 4131–4140.  
<https://doi.org/10.1242/dev.008367>
- Prince, M., Knapp, M., Guerchet, M., McCrone, P., Prina, M., Comas-Herrera, A., Wittenberg, R., Adelaja, B., Hu, B., King, D., Rehill, A., & Salimkumar, D. (2014). *Dementia UK: Second Edition*. Alzheimer's Society.
- Purcell, S. M., Moran, J. L., Fromer, M., Ruderfer, D., Solovieff, N., Roussos, P., O'Dushlaine, C., Chambert, K., Bergen, S. E., Kähler, A., Duncan, L., Stahl, E., Genovese, G., Fernández, E., Collins, M. O., Komiyama, N. H., Choudhary, J. S., Magnusson, P. K. E., Banks, E., ... Sklar, P. (2014). A polygenic burden of rare disruptive mutations in schizophrenia. *Nature*, 506(7487), 185–190. <https://doi.org/10.1038/nature12975>
- Putney, J. W., & Tomita, T. (2012). Phospholipase C Signaling and Calcium Influx. *Advances in Biological Regulation*, 52(1), 152–164.  
<https://doi.org/10.1016/j.advenzreg.2011.09.005>.Phospholipase
- Puzzo, D., Lee, L., Palmeri, A., Calabrese, G., & Arancio, O. (2014). Behavioral assays with mouse models of Alzheimer's disease: practical considerations and guidelines. *Biochemical Pharmacology*, 88(4), 450–467.  
<https://doi.org/10.1016/j.bcp.2014.01.011>.Behavioral
- Qian, W., He, X., Chan, E., Xu, H., & Zhang, J. (2011). Measuring the evolutionary rate of protein - Protein interaction. *Proceedings of the National Academy of Sciences of the United States of America*, 108(21), 8725–8730.  
<https://doi.org/10.1073/pnas.1104695108>
- Quinn, Z. A., Yang, C. C., Wrana, J. L., & McDermott, J. C. (2001). Smad proteins function as co-modulators for MEF2 transcriptional regulatory proteins. *Nucleic Acids Research*, 29(3), 732–742. <https://doi.org/10.1093/nar/29.3.732>
- R Core Team. (2020). *R: A language and environment for statistical computing*. Foundation for Statistical Computing, Vienna, Austria.
- Rai, T. S., Puri, A., McBryan, T., Hoffman, J., Tang, Y., Pchelintsev, N. A., van Tuyn, J., Marmorstein, R., Schultz, D. C., & Adams, P. D. (2011). Human CABIN1 Is a Functional Member of the Human HIRA/UBN1/ASF1a Histone H3.3 Chaperone Complex. *Molecular and Cellular Biology*, 31(19), 4107–4118.  
<https://doi.org/10.1128/mcb.05546-11>
- Rajan, K. B., Weuve, J., Barnes, L. L., McAninch, E. A., Wilson, R. S., & Evans, D. A. (2021). Population estimate of people with clinical Alzheimer's disease and mild cognitive impairment in the United States (2020–2060). *Alzheimer's and Dementia*, October 2020, 1966–1975. <https://doi.org/10.1002/alz.12362>
- Ransohoff, R. M. (2016). A polarizing question: Do M1 and M2 microglia exist. *Nature Neuroscience*, 19(8), 987–991. <https://doi.org/10.1038/nn.4338>
- Rao, V. S., Srinivas, K., Sujini, G. N., & Kumar, G. N. S. (2014). Protein-Protein Interaction Detection: Methods and Analysis. *International Journal of Proteomics*.  
<https://doi.org/10.1201/9781315213743>
- Rashid, A. J., Cole, C. J., & Josselyn, S. A. (2014). Emerging roles for MEF2 transcription factors in memory. *Genes, Brain and Behavior*, 13(1), 118–125.  
<https://doi.org/10.1111/gbb.12058>
- Ravasi, T., Suzuki, H., Cannistraci, C. V., Katayama, S., Bajic, V. B., Tan, K., Akalin, A.,

- Schmeier, S., Kanamori-Katayama, M., Bertin, N., Carninci, P., Daub, C. O., Forrest, A. R., Gough, J., Grimmond, S., Han, J. H., Hashimoto, T., Hide, W., Hofmann, O., ... Hayashizaki, Y. (2010). An Atlas of Combinatorial Transcriptional Regulation in Mouse and Man. *Cell*, *140*(5), 744–752. <https://doi.org/10.1016/j.cell.2010.01.044>
- Reiter, F., Wienerroither, S., & Stark, A. (2017). Combinatorial function of transcription factors and cofactors. *Current Opinion in Genetics and Development*, *43*, 73–81. <https://doi.org/10.1016/j.gde.2016.12.007>
- Ren, J., Wen, L., Gao, X., Jin, C., Xue, Y., & Yao, X. (2009). DOG 1.0: Illustrator of protein domain structures. *Cell Research*, *19*(2), 271–273. <https://doi.org/10.1038/cr.2009.6>
- Rendeiro, A. F., Schmidl, C., Strefford, J. C., Walewska, R., Davis, Z., Farlik, M., Oscier, D., & Bock, C. (2016). Chromatin accessibility maps of chronic lymphocytic leukaemia identify subtype-specific epigenome signatures and transcription regulatory networks. *Nature Communications*, *7*(May). <https://doi.org/10.1038/ncomms11938>
- Reske, J. J., Wilson, M. R., & Chandler, R. L. (2020). ATAC-seq normalization method can significantly affect differential accessibility analysis and interpretation. *Epigenetics and Chromatin*, *13*(1), 1–17. <https://doi.org/10.1186/s13072-020-00342-y>
- Réu, P., Khosravi, A., Bernard, S., Mold, J. E., Salehpour, M., Alkass, K., Perl, S., Tisdale, J., Possnert, G., Druid, H., & Frisén, J. (2017). The Lifespan and Turnover of Microglia in the Human Brain. *Cell Reports*, *20*(4), 779–784. <https://doi.org/10.1016/j.celrep.2017.07.004>
- Rio-Hortega, P. (1919). El “tercer elemento” de los centros nerviosos. I. La microglia en estado normal. *Bol Soc Esp Biol*, *VIII*, 67–82.
- Ripke, S., Neale, B. M., Corvin, A., Walters, J. T. R., Farh, K., Holmans, P. A., Lee, P., Bulik-Sullivan, B., & Collier, D. A. (2014). Biological Insights From 108 Schizophrenia-Associated Genetic Loci. *Nature*, *511*(7510), 421–427. <https://doi.org/10.1038/nature13595>
- Rippe, K., Schrader, A., Riede, P., Strohner, R., Lehmann, E., & Längst, G. (2007). DNA sequence- and conformation-directed positioning of nucleosomes by chromatin-remodeling complexes. *Proceedings of the National Academy of Sciences of the United States of America*, *104*(40), 15635–15640. <https://doi.org/10.1073/pnas.0702430104>
- Robinson, D. C. L., & Dilworth, F. J. (2018). Epigenetic Regulation of Adult Myogenesis. In *Current Topics in Developmental Biology* (1st ed., Vol. 126). Elsevier Inc. <https://doi.org/10.1016/bs.ctdb.2017.08.002>
- Robinson, J. T., Thorvaldsdóttir, H., Winckler, W., Guttman, M., Lander, E. S., Getz, G., & Mesirov, J. P. (2011). Integrative genomics viewer. *Nature Biotechnology*, *29*(1), 24–26. <https://doi.org/10.1038/nbt.1754>
- Robinson, M. D., & Oshlack, A. (2010). A scaling normalization method for differential expression analysis of RNA-seq data. *Genome Biology*, *11*(R25). <http://genomebiology.com/2010/11/3/R25>
- Robinson, P. J., & Rhodes, D. (2006). Structure of the “30 nm” chromatin fibre: A key role for the linker histone. *Current Opinion in Structural Biology*, *16*(3), 336–343. <https://doi.org/10.1016/j.sbi.2006.05.007>
- Rock, R. B., Gekker, G., Hu, S., Sheng, W. S., Cheeran, M., Lokensgard, J. R., & Peterson, P. K. (2004). Role of microglia in central nervous system infections. *Clinical Microbiology*

- Reviews*, 17(4), 942–964. <https://doi.org/10.1128/CMR.17.4.942-964.2004>
- Roundtree, I. A., Luo, G. Z., Zhang, Z., Wang, X., Zhou, T., Cui, Y., Sha, J., Huang, X., Guerrero, L., Xie, P., He, E., Shen, B., & He, C. (2017). YTHDC1 mediates nuclear export of N6-methyladenosine methylated mRNAs. *ELife*, 6, 1–28. <https://doi.org/10.7554/eLife.31311>
- Roux, K. J., Kim, D. I., Burke, B. E., & May, D. G. (2018). BioID : A Screen for Protein-Protein Interactions. *Current Protocols in Protein Science*, 91, 19.23.1–19.23.15. <https://doi.org/10.1002/cpps.51.BioID>
- Roux, K. J., Kim, D. I., Raida, M., & Burke, B. (2012). A promiscuous biotin ligase fusion protein identifies proximal and interacting proteins in mammalian cells. *Journal of Cell Biology*, 196(6), 801–810. <https://doi.org/10.1083/jcb.201112098>
- Ruiz, A., Heilmann, S., Becker, T., Hernández, I., Wagner, H., Thelen, M., Mauleón, A., Rosende-Roca, M., Bellenguez, C., Bis, J. C., Harold, D., Gerrish, A., Sims, R., Sotolongo-Grau, O., Espinosa, A., Alegret, M., Arrieta, J. L., Lacour, A., Leber, M., ... Ramírez, A. L. (2014). Follow-up of loci from the International Genomics of Alzheimer's Disease Project identifies TRIP4 as a novel susceptibility gene. *Translational Psychiatry*, 4(December 2013), 2–5. <https://doi.org/10.1038/tp.2014.2>
- Rusnak, F., & Mertz, P. (2000). Calcineurin: Form and Function. *Physiological Reviews*, 80(4), 1483–1521. <http://physrev.physiology.org>
- Rydén, M. (2009). Fibroblast growth factor 21: an overview from a clinical perspective. *Cellular and Molecular Life Sciences*, 66, 2067–2073.
- Sainsbury, S., Bernecky, C., & Cramer, P. (2015). Structural basis of transcription initiation by RNA polymerase II. *Nature Reviews Molecular Cell Biology*, 16(3), 129–143. <https://doi.org/10.1038/nrm3952>
- Sajeev, G., Weuve, J., Jackson, J. W., Vanderweele, T. J., Bennett, D. A., Grodstein, F., & Blacker, D. (2016). Late-life cognitive activity and dementia. *Epidemiology*, 27(5), 732–742. <https://doi.org/10.1097/EDE.0000000000000513>
- Sando, S. B., Melquist, S., Cannon, A., Hutton, M., Sletvold, O., Saltvedt, I., White, L. R., Lydersen, S., & Aasly, J. (2008). Risk-reducing effect of education in Alzheimer's disease. *International Journal of Geriatric Psychiatry*, 23(11), 1156–1162. <https://doi.org/10.1002/gps.2043>
- Sartorelli, V., Huang, J., Hamamori, Y., & Kedes, L. (1997). Molecular mechanisms of myogenic coactivation by p300: direct interaction with the activation domain of MyoD and with the MADS box of MEF2C. *Molecular and Cellular Biology*, 17(2), 1010–1026. <https://doi.org/10.1128/mcb.17.2.1010>
- Saunders, A. M., Schmeider, K., Breitner, J. C., Benson, M. D., Brown, W. T., Goldfarb, L., Goldgaber, D., Manwaring, M. G., Szymanski, M. H., & McCown, N. (1993). Apolipoprotein E epsilon 4 allele distributions in late-onset Alzheimer's disease and in other amyloid-forming diseases. *Lancet (London, England)*, 342(8873), 710–711. [https://doi.org/10.1016/0140-6736\(93\)91709-u](https://doi.org/10.1016/0140-6736(93)91709-u)
- Sauvé, F., McBroom, L. D. B., Gallant, J., Moraitis, A. N., Labrie, F., & Giguère, V. (2001). CIA, a Novel Estrogen Receptor Coactivator with a Bifunctional Nuclear Receptor Interacting Determinant. *Molecular and Cellular Biology*, 21(1), 343–353. <https://doi.org/10.1128/mcb.21.1.343-353.2001>

- Schafer, D. P., Lehrman, E. K., Kautzman, A. G., Koyama, R., Mardinly, A. R., Yamasaki, R., Ransohoff, R. M., Greenberg, M. E., Barres, B. A., & Stevens, B. (2012). Microglia Sculpt Postnatal Neural Circuits in an Activity and Complement-Dependent Manner. *Neuron*, *74*(4), 691–705. <https://doi.org/10.1016/j.neuron.2012.03.026>
- Schaub, M. A., Boyle, A. P., Kundaje, A., Batzoglou, S., & Snyder, M. (2012). Linking disease associations with regulatory information in the human genome. *Genome Research*, *22*(9), 1748–1759. <https://doi.org/10.1101/gr.136127.111>
- Schitteck, B., & Sinnberg, T. (2014). Biological functions of casein kinase 1 isoforms and putative roles in tumorigenesis. *Molecular Cancer*, *13*(1), 1–14. <https://doi.org/10.1186/1476-4598-13-231>
- Schoenfelder, S., & Fraser, P. (2019). Long-range enhancer–promoter contacts in gene expression control. *Nature Reviews Genetics*, *20*(8), 437–455. <https://doi.org/10.1038/s41576-019-0128-0>
- Schwartzentruber, J., Cooper, S., Liu, J. Z., Barrio-hernandez, I., Bello, E., Kumasaka, N., Young, A. M. H., Franklin, R. J. M., Estrada, K., Gaffney, D. J., Beltrao, P., & Bassett, A. (2021). *Genome-wide meta-analysis, fine-mapping, and integrative prioritization implicate new Alzheimer’s disease risk genes* (Vol. 53, Issue 3). <https://doi.org/10.1038/s41588-020-00776-w>. Genome-wide
- Sedel, F., Béchade, C., Vyas, S., & Triller, A. (2004). Macrophage-Derived Tumor Necrosis Factor  $\alpha$ , an Early Developmental Signal for Motoneuron Death. *Journal of Neuroscience*, *24*(9), 2236–2246. <https://doi.org/10.1523/JNEUROSCI.4464-03.2004>
- Serrano-Pozo, A., Frosch, M. P., Masliah, E., & Hyman, B. T. (2011a). Neuropathological alterations in Alzheimer disease. *Cold Spring Harbor Perspectives in Medicine*, *1*(1), 1–24. <https://doi.org/10.1101/cshperspect.a006189>
- Serrano-Pozo, A., Mielke, M. L., Gómez-Isla, T., Betensky, R. A., Growdon, J. H., Frosch, M. P., & Hyman, B. T. (2011b). Reactive glia not only associates with plaques but also parallels tangles in Alzheimer’s disease. *American Journal of Pathology*, *179*(3), 1373–1384. <https://doi.org/10.1016/j.ajpath.2011.05.047>
- Seshadri, S., Fitzpatrick, A. L., Ikram, M. A., DeStefano, A. L., Gudnason, V., Boada, M., Bis, J. C., Smith, A. V., Carassquillo, M. M., Lambert, J. C., Harold, D., Schrijvers, E. M. C., Ramirez-Lorca, R., Debette, S., Longstreth, W. T., Janssens, A. C. J. W., Pankratz, V. S., Dartigues, J. F., Hollingworth, P., ... Breteler, M. M. B. (2010). Genome-wide analysis of genetic loci associated with Alzheimer disease. *JAMA - Journal of the American Medical Association*, *303*(18), 1832–1840. <https://doi.org/10.1001/jama.2010.574>
- Shadrin, A. A., Smeland, O. B., Zayats, T., Schork, A. J., Frei, O., Bettella, F., Witoelar, A., Li, W., Eriksen, J. A., Krull, F., Djurovic, S., Faraone, S. V., Reichborn-Kjennerud, T., Thompson, W. K., Johansson, S., Haavik, J., Dale, A. M., Wang, Y., & Andreassen, O. A. (2018). Novel Loci Associated With Attention-Deficit/Hyperactivity Disorder Are Revealed by Leveraging Polygenic Overlap With Educational Attainment. *Journal of the American Academy of Child and Adolescent Psychiatry*, *57*(2), 86–95. <https://doi.org/10.1016/j.jaac.2017.11.013>
- Shaji, K. S., George, R. K., Prince, M. J., & Jacob, K. S. (2009). Behavioral symptoms and caregiver burden in dementia. *Indian Journal of Psychiatry*, *51*(1), 45–49. <https://doi.org/10.4103/0019-5545.44905>
- Shalizi, A. K., & Bonni, A. (2005). Brawn for Brains: The Role of MEF2 Proteins in the

- Developing Nervous System. In *Current Topics in Developmental Biology*.  
[https://doi.org/10.1016/S0070-2153\(05\)69009-6](https://doi.org/10.1016/S0070-2153(05)69009-6)
- Sharan, R., Suthram, S., Kelley, R. M., Kuhn, T., McCuine, S., Uetz, P., Sittler, T., Karp, R. M., & Ideker, T. (2005). Conserved patterns of protein interaction in multiple species. *Proceedings of the National Academy of Sciences*, *102*(6), 1974–1979.  
<https://doi.org/10.1073/PNAS.0409522102>
- Sherrington, R., Froelich, S., Sorbi, S., Campion, D., Chi, H., Rogaeva, E. A., Levesque, G., Rogaev, E. I., Lin, C., Liang, Y., Ikeda, M., Mar, L., Brice, A., Agid, Y., Percy, M. E., Clerget-Darpoux, F., Piacentini, S., Marcon, G., Nacmias, B., ... St George-Hyslop, P. H. (1996). Alzheimer's disease associated with mutations in presenilin 2 is rare and variably penetrant. *Human Molecular Genetics*, *5*(7), 985–988.  
<https://doi.org/10.1093/hmg/5.7.985>
- Sherwood, R. I., Hashimoto, T., O'Donnell, C. W., Lewis, S., Barkal, A. A., Van Hoff, J. P., Karun, V., Jaakkola, T., & Gifford, D. K. (2014). Discovery of directional and nondirectional pioneer transcription factors by modeling DNase profile magnitude and shape. *Nature Biotechnology*, *32*(2), 171–178. <https://doi.org/10.1038/nbt.2798>
- Shi, L., Wen, H., & Shi, X. (2017). The histone variant H3.3 in transcriptional regulation and human disease. *Journal of Molecular Biology*, *429*(13), 1934–1945.  
<https://doi.org/10.1016/j.jmb.2016.03.011>
- Shioda, N., Han, F., Moriguchi, S., & Fukunaga, K. (2007). Constitutively active calcineurin mediates delayed neuronal death through Fas-ligand expression via activation of NFAT and FKHR transcriptional activities in mouse brain ischemia. *Journal of Neurochemistry*, *102*(5), 1506–1517. <https://doi.org/10.1111/j.1471-4159.2007.04600.x>
- Shore, P., & Sharrocks, A. D. (1995). The MADS-Box Family of Transcription Factors. *European Journal of Biochemistry*, *229*(1), 1–13. <https://doi.org/10.1111/j.1432-1033.1995.tb20430.x>
- Sica, A., & Mantovani, A. (2012). Macrophage plasticity and polarization: in vivo veritas. *Journal of Clinical Investigation*, *122*(3), 787–795.  
<https://doi.org/10.1172/JCI59643DS1>
- Sierksma, A., Lu, A., Mancuso, R., Fattorelli, N., Thrupp, N., Salta, E., Zoco, J., Blum, D., Buée, L., De Strooper, B., & Fiers, M. (2020). Novel Alzheimer risk genes determine the microglia response to amyloid- $\beta$  but not to TAU pathology. *EMBO Molecular Medicine*, 1–30. <https://doi.org/10.15252/emmm.201910606>
- Sierra, A., de Castro, F., del Río-Hortega, J., Rafael Iglesias-Rozas, J., Garrosa, M., & Kettenmann, H. (2016). The “Big-Bang” for modern glial biology: Translation and comments on Pío del Río-Hortega 1919 series of papers on microglia. *Glia*, *64*(11), 1801–1840. <https://doi.org/10.1002/glia.23046>
- Sierra, A., Encinas, J. M., Deudero, J. J. P., Chancey, J. H., Enikolopov, G., Overstreet-Wadiche, L. S., Tsirka, S. E., & Maletic-Savatic, M. (2010). Microglia shape adult hippocampal neurogenesis through apoptosis-coupled phagocytosis. *Cell Stem Cell*, *7*(4), 483–495. <https://doi.org/10.1016/j.stem.2010.08.014>
- Sim, C. K., Lee, J. H., Baek, I. J., Lee, S. W., & Lee, M. S. (2019). Enhanced antitumor immune response in 2'-5'oligoadenylate synthetase-like 1- (OASL1-) deficient mice upon cisplatin chemotherapy and radiotherapy. *Journal of Immunology Research*, 2019.

<https://doi.org/10.1155/2019/7596786>

- Simen, A. A., Bordner, K. A., Martin, M. P., Moy, L. A., & Barry, L. C. (2011). Cognitive dysfunction with aging and the role of inflammation. *Therapeutic Advances in Chronic Disease*, 2(3), 175–195. <https://doi.org/10.1177/2040622311399145>
- Sims, R., Hill, M., & Williams, J. (2020). The multiplex model of the genetics of Alzheimer's disease. *Nature Neuroscience*, 23, 311–322. <https://doi.org/10.1038/s41593-020-0599-5>
- Sims, R., Van Der Lee, S. J., Naj, A. C., Bellenguez, C., Badarinarayan, N., Jakobsdottir, J., Kunkle, B. W., Boland, A., Raybould, R., Bis, J. C., Martin, E. R., Grenier-Boley, B., Heilmann-Heimbach, S., Chouraki, V., Kuzma, A. B., Sleegers, K., Vronskaya, M., Ruiz, A., Graham, R. R., ... Schellenberg, G. D. (2017). Rare coding variants in PLCG2, ABI3, and TREM2 implicate microglial-mediated innate immunity in Alzheimer's disease. *Nature Genetics*, 49(9), 1373–1384. <https://doi.org/10.1038/ng.3916>
- Skene, N. G., & Grant, S. G. N. (2016). Identification of vulnerable cell types in major brain disorders using single cell transcriptomes and expression weighted cell type enrichment. *Frontiers in Neuroscience*, 10(JAN), 1–11. <https://doi.org/10.3389/fnins.2016.00016>
- Smale, S. T., & Kadonaga, J. T. (2003). The RNA Polymerase II Core Promoter. *Annual Review of Biochemistry*, 72(1), 449–479. <https://doi.org/10.1146/annurev.biochem.72.121801.161520>
- Smith, A. M., Davey, K., Tsartsalis, S., Khozoie, C., Fancy, N., Tang, S. S., Liaptsi, E., Weinert, M., McGarry, A., Muirhead, R. C. J., Gentleman, S., Owen, D. R., & Matthews, P. M. (2022). Diverse human astrocyte and microglial transcriptional responses to Alzheimer's pathology. *Acta Neuropathologica*, 143(1), 75–91. <https://doi.org/10.1007/s00401-021-02372-6>
- Sommer, H., Beltrán, J. P., Huijser, P., Pape, H., Lönnig, W. E., Saedler, H., & Schwarz-Sommer, Z. (1990). Deficiens, a homeotic gene involved in the control of flower morphogenesis in *Antirrhinum majus*: the protein shows homology to transcription factors. *The EMBO Journal*, 9(3), 605–613. <https://doi.org/10.1002/j.1460-2075.1990.tb08152.x>
- Song, Z., Wang, Y., Zhang, F., Yao, F., & Sun, C. (2019). Calcium signaling pathways: Key pathways in the regulation of obesity. *International Journal of Molecular Sciences*, 20(11). <https://doi.org/10.3390/ijms20112768>
- Soufi, A., Donahue, G., & Zaret, K. S. (2012). Facilitators and impediments of the pluripotency reprogramming factors' initial engagement with the genome. *Cell*, 151(5), 994–1004. <https://doi.org/10.1016/j.cell.2012.09.045>
- Speliotis, E. K., Kowall, N. W., Shanti, B. F., Kosofsky, B., Finklestein, S. P., & Leifer, D. (1996). Myocyte-specific enhancer binding factor 2C expression in gerbil brain following global cerebral ischemia. *Neuroscience*, 70(1), 67–77. [https://doi.org/10.1016/0306-4522\(95\)00301-X](https://doi.org/10.1016/0306-4522(95)00301-X)
- Sperling, R. A., Aisen, P. S., Beckett, L. A., Bennett, D. A., Craft, S., Fagan, A. M., Iwatsubo, T., Jack, C. R., Kaye, J., Montine, T. J., Park, D. C., Reiman, E. M., Rowe, C. C., Siemers, E., Stern, Y., Yaffe, K., Carrillo, M. C., Thies, B., Morrison-Bogorad, M., ... Phelps, C. H. (2011). Toward defining the preclinical stages of Alzheimer's disease: Recommendations from the National Institute on Aging-Alzheimer's Association

- workgroups on diagnostic guidelines for Alzheimer's disease. *Alzheimer's and Dementia*, 7(3), 280–292. <https://doi.org/10.1016/j.jalz.2011.03.003>
- Stansley, B., Post, J., & Hensley, K. (2012). A comparative review of cell culture systems for the study of microglial biology in Alzheimer's disease. *Journal of Neuroinflammation*, 9(115). <https://doi.org/10.1086/302477>
- Stansley, Branden, Post, J., & Hensley, K. (2012). A comparative review of cell culture systems for the study of microglial biology in Alzheimer's disease. *Journal of Neuroinflammation*, 9(1), 115. <https://doi.org/10.1186/1742-2094-9-115>
- Stark, R., & Brown, G. (2011). *DiffBind: differential binding analysis of ChIP-Seq peak data*. <http://bioconductor.org/packages/release/bioc/vignettes/DiffBind/inst/doc/DiffBind.pdf>
- Stäßer, K., Masuda, S., Mason, P., Pfannstiel, J., Oppizzi, M., Rodriguez-Navarro, S., Rondón, A. G., Aguilera, A., Struhl, K., Reed, R., & Hurt, E. (2002). TREX is a conserved complex coupling transcription with messenger RNA export. *Nature*, 417(6886), 304–308. <https://doi.org/10.1038/nature746>
- Steele, C., Rovner, B., Chase, G. A., & Folstein, M. (1990). Psychiatric symptoms and nursing home placement of patients with Alzheimer's disease. *The American Journal of Psychiatry*, 147(8), 1049–1051. <https://doi.org/10.1176/ajp.147.8.1049>
- Steinauer, N., Guo, C., Huang, C., Wong, M., Tu, Y., Freter, C. E., & Zhang, J. (2019). Myeloid translocation gene CBFA2T3 directs a relapse gene program and determines patient-specific outcomes in AML. *Blood Advances*, 3(9), 1379–1393. <https://doi.org/10.1182/bloodadvances.2018028514>
- Stevens, B., Allen, N. J., Vazquez, L. E., Howell, G. R., Christopherson, K. S., Nouri, N., Micheva, K. D., Mehalow, A. K., Huberman, A. D., Stafford, B., Sher, A., Litke, A. M. M., Lambris, J. D., Smith, S. J., John, S. W. M., & Barres, B. A. (2007). The Classical Complement Cascade Mediates CNS Synapse Elimination. *Cell*, 131(6), 1164–1178. <https://doi.org/10.1016/j.cell.2007.10.036>
- Stewart, S., & Crabtree, G. R. (2000). Transcription: Regulation of the regulators. *Nature*, 408(6808), 46–47. <https://doi.org/10.1038/35040690>
- Strittmatter, W. J., Saunders, A. M., Schmechel, D., Pericak-Vance, M., Enghild, J., Salvesen, G. S., & Roses, A. D. (1993). Apolipoprotein E: High-avidity binding to  $\beta$ -amyloid and increased frequency of type 4 allele in late-onset familial Alzheimer disease. *Proceedings of the National Academy of Sciences of the United States of America*, 90(5), 1977–1981. <https://doi.org/10.1073/pnas.90.5.1977>
- Su, W., Hopkins, S., Nesser, N. K., Sopher, B., Silvestroni, A., Ammanuel, S., Jayadev, S., Möller, T., Weinstein, J., & Garden, G. A. (2014). The p53 transcription factor modulates microglia behavior through microRNA dependent regulation of c-Maf. *Journal of Immunology*, 192(1), 358–366. <https://doi.org/10.4049/jimmunol.1301397>
- Sun, H., Yang, X., Zhu, J., Lv, T., Chen, Y., Chen, G., Zhong, L., Li, Y., Huang, X., Huang, G., & Tian, J. (2010). Inhibition of p300-HAT results in a reduced histone acetylation and down-regulation of gene expression in cardiac myocytes. *Life Sciences*. <https://doi.org/10.1016/j.lfs.2010.10.009>
- Sun, L., Youn, H. D., Loh, C., Stolow, M., He, W., & Liu, J. O. (1998). Cabin 1, a negative



- regulator for calcineurin signaling in T lymphocytes. *Immunity*.  
[https://doi.org/10.1016/S1074-7613\(00\)80575-0](https://doi.org/10.1016/S1074-7613(00)80575-0)
- Suter, B., Kittanakom, S., & Stagljar, I. (2008). Two-hybrid technologies in proteomics research. *Current Opinion in Biotechnology*, *19*(4), 316–323.  
<https://doi.org/10.1016/j.copbio.2008.06.005>
- Swinnen, N., Smolders, S., Avila, A., Notelaers, K., Paesen, R., Ameloot, M., Brône, B., Legendre, P., & Rigo, J. M. (2013). Complex invasion pattern of the cerebral cortex by microglial cells during development of the mouse embryo. *Glia*, *61*(2), 150–163.  
<https://doi.org/10.1002/glia.22421>
- Szklarczyk, D., Gable, A. L., Lyon, D., Junge, A., Wyder, S., Huerta-Cepas, J., Simonovic, M., Doncheva, N. T., Morris, J. H., Bork, P., Jensen, L. J., & Von Mering, C. (2019). STRING v11: Protein-protein association networks with increased coverage, supporting functional discovery in genome-wide experimental datasets. *Nucleic Acids Research*, *47*(D1), D607–D613. <https://doi.org/10.1093/nar/gky1131>
- Tacke, R., Tohyama, M., Ogawa, S., & Manley, J. L. (1998). Human Tra2 proteins are sequence-specific activators of pre-mRNA splicing. *Cell*, *93*(1), 139–148.  
[https://doi.org/10.1016/S0092-8674\(00\)81153-8](https://doi.org/10.1016/S0092-8674(00)81153-8)
- Tagami, H., Ray-Gallet, D., Almouzni, G., & Nakatani, Y. (2004). Histone H3.1 and H3.3 Complexes Mediate Nucleosome Assembly Pathways Dependent or Independent of DNA Synthesis. *Cell*, *116*(1), 51–61. [https://doi.org/10.1016/S0092-8674\(03\)01064-X](https://doi.org/10.1016/S0092-8674(03)01064-X)
- Takahashi, Kazutoshi, & Yamanaka, S. (2006). Induction of Pluripotent Stem Cells from Mouse Embryonic and Adult Fibroblast Cultures by Defined Factors. *Cell*, *126*(4), 663–676. <https://doi.org/10.1016/j.cell.2006.07.024>
- Takahashi, Kazuya, Prinz, M., Stagi, M., Chechneva, O., & Neumann, H. (2007). TREM2-transduced myeloid precursors mediate nervous tissue debris clearance and facilitate recovery in an animal model of multiple sclerosis. *PLoS Medicine*, *4*(4), 675–689.  
<https://doi.org/10.1371/journal.pmed.0040124>
- Takahashi, Kazuya, Rochford, C. D. P., & Neumann, H. (2005). Clearance of apoptotic neurons without inflammation by microglial triggering receptor expressed on myeloid cells-2. *Journal of Experimental Medicine*, *201*(4), 647–657.  
<https://doi.org/10.1084/jem.20041611>
- Takeuchi, O., & Akira, S. (2001). Toll-like receptors; their physiological role and signal transduction system. *International Immunopharmacology*, *1*(4), 625–635.  
[https://doi.org/10.1016/S1567-5769\(01\)00010-8](https://doi.org/10.1016/S1567-5769(01)00010-8)
- Tansey, K. E., Cameron, D., & Hill, M. J. (2018). Genetic risk for Alzheimer’s disease is concentrated in specific macrophage and microglial transcriptional networks. *Genome Medicine*, *10*. <https://doi.org/10.1186/s13073-018-0523-8>
- Tauzin, S., Chaigne-Delalande, B., Selva, E., Khadra, N., Daburon, S., Contin-Bordes, C., Blanco, P., Le Seyec, J., Ducret, T., Counillon, L., Moreau, J. F., Hofman, P., Vacher, P., & Legembre, P. (2011). The naturally processed CD95L Elicits a c-fos/Calcium/PI3K-driven cell migration pathway. *PLoS Biology*, *9*(6).  
<https://doi.org/10.1371/journal.pbio.1001090>
- Tay, T. L., Savage, J. C., Hui, C. W., Bisht, K., & Tremblay, M. È. (2017). Microglia across the lifespan: from origin to function in brain development, plasticity and cognition.

- Journal of Physiology*, 595(6), 1929–1945. <https://doi.org/10.1113/JP272134>
- Tedde, A., Nacmias, B., Ciantelli, M., Forleo, P., Cellini, E., Bagnoli, S., Piccini, C., Caffarra, P., Ghidoni, E., Paganini, M., Bracco, L., & Sorbi, S. (2003). Identification of New Presenilin Gene Mutations in Early-Onset Familial Alzheimer Disease. *Archives of Neurology*, 60(11), 1541–1544. <https://doi.org/10.1001/archneur.60.11.1541>
- Telese, F., Ma, Q., Perez, P. M., Notani, D., Oh, S., Li, W., Comoletti, D., Ohgi, K. A., Taylor, H., & Rosenfeld, M. G. (2015). LRP8-Reelin-regulated Neuronal (LRN) Enhancer Signature Underlying Learning and Memory Formation. *Neuron*, 86(3), 696–710. <https://doi.org/10.1016/j.neuron.2015.03.033>
- Teo, G., Liu, G., Zhang, J., Nesvizhskii, A. I., Gingras, A.-C., & Choi, H. (2014). SAINTExpress. *Proteomics*, 23(1), 1–7. <https://doi.org/10.1038/jid.2014.371>
- Teri, L. (1997). Behavior and caregiver burden: Behavioral problems in patients with Alzheimer disease and its association with caregiver distress. In *Alzheimer Disease and Associated Disorders* (Vol. 11, Issue Suppl 4, pp. S35–S38). Lippincott Williams & Wilkins.
- Terry, R. D., Masliah, E., Salmon, D. P., Butters, N., DeTeresa, R., Hill, R., Hansen, L. A., & Katzman, R. (1991). Physical basis of cognitive alterations in alzheimer's disease: Synapse loss is the major correlate of cognitive impairment. *Annals of Neurology*, 30(4), 572–580. <https://doi.org/10.1002/ana.410300410>
- Tessarz, P., & Kouzarides, T. (2014). Histone core modifications regulating nucleosome structure and dynamics. *Nature Reviews Molecular Cell Biology*, 15(11), 703–708. <https://doi.org/10.1038/nrm3890>
- Thomas, J. O., & Kornberg, R. D. (1975). An octamer of histones in chromatin and free in solution. *Proceedings of the National Academy of Sciences of the United States of America*, 72(7), 2626–2630. <https://doi.org/10.1073/pnas.72.7.2626>
- Thurman, R. E., Rynes, E., Humbert, R., Vierstra, J., Maurano, M. T., Haugen, E., Sheffield, N. C., Stergachis, A. B., Wang, H., Vernet, B., Garg, K., John, S., Sandstrom, R., Bates, D., Boatman, L., Canfield, T. K., Diegel, M., Dunn, D., Ebersol, A. K., ... Stamatoyannopoulos, J. A. (2012). The accessible chromatin landscape of the human genome. *Nature*, 489(7414), 75–82. <https://doi.org/10.1038/nature11232>
- Timmerman, R., Burm, S. M., & Bajramovic, J. J. (2018). An overview of in vitro methods to study microglia. *Frontiers in Cellular Neuroscience*, 12(August), 1–12. <https://doi.org/10.3389/fncel.2018.00242>
- Tolar, M., Keller, J. N., Chan, S., Mattson, M. P., Marques, M. A., & Crutcher, K. A. (1999). Truncated apolipoprotein E (ApoE) causes increased intracellular calcium and may mediate ApoE neurotoxicity. *Journal of Neuroscience*, 19(16), 7100–7110. <https://doi.org/10.1523/jneurosci.19-16-07100.1999>
- Tong, B. C. K., Wu, A. J., Li, M., & Cheung, K. H. (2018). Calcium signaling in Alzheimer's disease & therapies. *Biochimica et Biophysica Acta - Molecular Cell Research*, 1865(11), 1745–1760. <https://doi.org/10.1016/j.bbamcr.2018.07.018>
- Tremblay, M. È., Stevens, B., Sierra, A., Wake, H., Bessis, A., & Nimmerjahn, A. (2011). The role of microglia in the healthy brain. *Journal of Neuroscience*, 31(45), 16064–16069. <https://doi.org/10.1523/JNEUROSCI.4158-11.2011>
- Trowsdale, J., & Knight, J. C. (2013). Major histocompatibility complex genomics and human

- disease. *Annual Review of Genomics and Human Genetics*, 14(67), 301–323. <https://doi.org/10.1146/annurev-genom-091212-153455>
- Tyagi, M., Imam, N., Verma, K., & Patel, A. K. (2016). Chromatin remodelers: We are the drivers!! *Nucleus*, 7(4), 388–404. <https://doi.org/10.1080/19491034.2016.1211217>
- Uhlén, M., Fagerberg, L., Hallström, B. M., Lindskog, C., Oksvold, P., Mardinoglu, A., Sivertsson, Å., Kampf, C., Sjöstedt, E., Asplund, A., Olsson, I. M., Edlund, K., Lundberg, E., Navani, S., Szigartyo, C. A. K., Odeberg, J., Djureinovic, D., Takanen, J. O., Hober, S., ... Pontén, F. (2015). Tissue-based map of the human proteome. *Science*, 347(6220). <https://doi.org/10.1126/science.1260419>
- US Food and Drug Administration. (2021). *FDA Grants Accelerated Approval for Alzheimer's Drug*. [fda.gov/news-events/press-announcements/fdagrants-accelerated-approval-alzheimers-drug](https://www.fda.gov/news-events/press-announcements/fdagrants-accelerated-approval-alzheimers-drug)
- Vaquerezas, J. M., Kummerfeld, S. K., Teichmann, S. A., & Luscombe, N. M. (2009). A census of human transcription factors: Function, expression and evolution. *Nature Reviews Genetics*, 10(4), 252–263. <https://doi.org/10.1038/nrg2538>
- Verghese, P. B., Castellano, J. M., & Holtzman, D. M. (2011). Roles of Apolipoprotein E in Alzheimer's Disease and Other Neurological Disorders. *Lancet Neurology*, 10(3), 241–252. <https://doi.org/10.1038/jid.2014.371>
- Verney, C., Monier, A., Fallet-Bianco, C., & Gressens, P. (2010). Early microglial colonization of the human forebrain and possible involvement in periventricular white-matter injury of preterm infants. *Journal of Anatomy*, 217(4), 436–448. <https://doi.org/10.1111/j.1469-7580.2010.01245.x>
- Vernimmen, D., & Bickmore, W. A. (2015). The Hierarchy of Transcriptional Activation: From Enhancer to Promoter. *Trends in Genetics*, 31(12), 696–708. <https://doi.org/10.1016/j.tig.2015.10.004>
- Villemagne, V. L., Pike, K. E., Chételat, G., Ellis, K. A., Mulligan, R. S., Bourgeat, P., Ackermann, U., Jones, G., Szoeke, C., Salvado, O., Martins, R., O'Keefe, G., Mathis, C. A., Klunk, W. E., Ames, D., Masters, C. L., & Rowe, C. C. (2011). Longitudinal assessment of A $\beta$  and cognition in aging and Alzheimer disease. *Annals of Neurology*, 69(1), 181–192. <https://doi.org/10.1002/ana.22248>
- Vousden, K. H., & Lane, D. P. (2007). P53 in Health and Disease. *Nature Reviews Molecular Cell Biology*, 8(4), 275–283. <https://doi.org/10.1038/nrm2147>
- Vrečar, I., Innes, J., Jones, E., Kingston, H., Reardon, W., Kerr, B., Clayton-Smith, J., & Douzgou, S. (2017). Further Clinical Delineation of the MEF2C Haploinsufficiency Syndrome: Report on New Cases and Literature Review of Severe Neurodevelopmental Disorders Presenting with Seizures, Absent Speech, and Involuntary Movements. *Journal of Pediatric Genetics*, 06(03), 129–141. <https://doi.org/10.1055/s-0037-1601335>
- Wagner, G. F., & Dimattia, G. E. (2006). The Stanniocalcin Family of Proteins. *Journal of Experimental Zoology*, 305, 769–780. <https://doi.org/10.1002/jez.a>
- Wang, A. H., & Yang, X.-J. (2001). Histone Deacetylase 4 Possesses Intrinsic Nuclear Import and Export Signals. *Molecular and Cellular Biology*, 21(17), 5992–6005. <https://doi.org/10.1128/mcb.21.17.5992-6005.2001>
- Wang, Audrey H., Bertos, N. R., Vezmar, M., Pelletier, N., Crosato, M., Heng, H. H., Th'ng, J.,

- Han, J., & Yang, X.-J. (1999). HDAC4, a Human Histone Deacetylase Related to Yeast HDA1, Is a Transcriptional Corepressor. *Molecular and Cellular Biology*, *19*(11), 7816–7827. <https://doi.org/10.1128/mcb.19.11.7816>
- Wang, Audrey H., Grégoirei, S., Zika, E., Xiao, L., Li, C. S., Li, H., Wright, K. L., Ting, J. P., & Yang, X. J. (2005). Identification of the ankyrin repeat proteins ANKRA and RFXANK as novel partners of class IIa histone deacetylases. *Journal of Biological Chemistry*, *280*(32), 29117–29127. <https://doi.org/10.1074/jbc.M500295200>
- Wang, D., Liu, F., Zhu, L., Lin, P., Han, F., Wang, X., Tan, X., Xiong, Y., & Lin, L. (2020). FGF21 alleviates neuroinflammation following ischemic stroke by modulating the temporal and spatial dynamics of microglia/macrophages. *Journal of Neuroinflammation*, *17*(257), 1–17. <https://doi.org/10.21203/rs.2.24026/v1>
- Wang, J., Huo, K., Ma, L., Tang, L., Li, D., Huang, X., Yuan, Y., Li, C., Wang, W., Guan, W., Chen, H., Jin, C., Wei, J., Zhang, W., Yang, Y., Liu, Q., Zhou, Y., Zhang, C., Wu, Z., ... Yang, X. (2011). Toward an understanding of the protein interaction network of the human liver. *Molecular Systems Biology*, *7*(536), 1–10. <https://doi.org/10.1038/msb.2011.67>
- Wang, Y., Cella, M., Mallinson, K., Ulrich, J. D., Young, K. L., Robinette, M. L., Gilfillan, S., Krishnan, G. M., Sudhakar, S., Zinselmeyer, B. H., Holtzman, D. M., Cirrito, J. R., & Colonna, M. (2015). TREM2 lipid sensing sustains the microglial response in an Alzheimer's disease model. *Cell*, *160*(6), 1061–1071. <https://doi.org/10.1016/j.cell.2015.01.049>
- Wang, Y., Ulland, T. K., Ulrich, J. D., Song, W., Tzaferis, J. A., Hole, J. T., Yuan, P., Mahan, T. E., Shi, Y., Gilfillan, S., Cella, M., Grutzendler, J., DeMattos, R. B., Cirrito, J. R., Holtzman, D. M., & Colonna, M. (2016). TREM2-mediated early microglial response limits diffusion and toxicity of amyloid plaques. *Journal of Experimental Medicine*, *213*(5), 667–675. <https://doi.org/10.1084/jem.20151948>
- Weill, U., Krieger, G., Avihou, Z., Milo, R., Schuldiner, M., & Davidi, D. (2019). Assessment of GFP Tag Position on Protein Localization and Growth Fitness in Yeast. *Journal of Molecular Biology*, *431*(3), 636–641. <https://doi.org/10.1016/j.jmb.2018.12.004>
- Wes, P. D., Holtman, I. R., Boddeke, E. W. G. M., Möller, T., & Eggen, B. J. L. (2016). Next generation transcriptomics and genomics elucidate biological complexity of microglia in health and disease. *Glia*, *64*(2), 197–213. <https://doi.org/10.1002/glia.22866>
- Wilker, P. R., Kohyama, M., Sandau, M. M., Albring, J. C., Nakagawa, O., Schwarz, J. J., & Murphy, K. M. (2008). Transcription factor Mef2c is required for B cell proliferation and survival after antigen receptor stimulation. *Nature Immunology*, *9*(6), 603–612. <https://doi.org/10.1038/ni.1609>
- Wilson-Rawls, J., Molkentin, J. D., Black, B. L., & Olson, E. N. (1999). Activated Notch Inhibits Myogenic Activity of the MADS-Box Transcription Factor Myocyte Enhancer Factor 2C. *Molecular and Cellular Biology*, *19*(4), 2853–2862. <https://doi.org/10.1128/mcb.19.4.2853>
- Wilson, M. R., Reske, J. J., Holladay, J., Wilber, G. E., Rhodes, M., Koeman, J., Adams, M., Johnson, B., Su, R. W., Joshi, N. R., Patterson, A. L., Shen, H., Leach, R. E., Teixeira, J. M., Fazleabas, A. T., & Chandler, R. L. (2019). ARID1A and PI3-kinase pathway mutations in the endometrium drive epithelial transdifferentiation and collective invasion. *Nature Communications*, *10*(1). <https://doi.org/10.1038/s41467-019-11403-6>

## References

- Wisdom, R., Johnson, R. S., & Moore, C. (1999). c-Jun regulates cell cycle progression and apoptosis by distinct mechanisms. In *The EMBO Journal* (Vol. 18, Issue 1).
- Wise, E. A., Rosenberg, P. B., Lyketsos, C. G., & Leoutsakos, J. M. (2019). Time course of neuropsychiatric symptoms and cognitive diagnosis in National Alzheimer's Coordinating Centers volunteers. *Alzheimer's and Dementia: Diagnosis, Assessment and Disease Monitoring*, *11*, 333–339. <https://doi.org/10.1016/j.dadm.2019.02.006>
- Wisniewski, K. E., Wisniewski, H. M., & Wen, G. Y. (1985). Occurrence of neuropathological changes and dementia of Alzheimer's disease in Down's syndrome. *Annals of Neurology*, *17*(3), 278–282. <https://doi.org/10.1002/ana.410170310>
- Wittenberg, R., Hu, B., Barraza-Araiza, L. F., & Rehill, A. (2019). Projections of Older People with Dementia and Costs of Dementia Care in the United Kingdom, 2019-2040. In *Care Policy and Evaluation Centre* (Issue November). [https://www.alzheimers.org.uk/sites/default/files/2019-11/cpec\\_report\\_november\\_2019.pdf](https://www.alzheimers.org.uk/sites/default/files/2019-11/cpec_report_november_2019.pdf)
- Woronicz, J. D., Lina, A., Calnan, B. J., Szychowski, S., Cheng, L., & Winoto, A. (1995). Regulation of the Nur77 orphan steroid receptor in activation-induced apoptosis. *Molecular and Cellular Biology*, *15*(11), 6364–6376. <https://doi.org/10.1128/mcb.15.11.6364>
- Wu, H., Naya, F. J., McKinsey, T. A., Mercer, B., Shelton, J. M., Chin, E. R., Simard, A. R., Michel, R. N., Bassel-Duby, R., Olson, E. N., & Williams, R. S. (2000). MEF2 responds to multiple calcium-regulated signals in the control of skeletal muscle fiber type. *The EMBO Journal*, *19*(9), 1963–1973.
- Wu, W., de Folter, S., Shen, X., Zhang, W., & Tao, S. (2011). Vertebrate paralogous MEF2 genes: Origin, conservation, and evolution. *PLoS ONE*, *6*(3). <https://doi.org/10.1371/journal.pone.0017334>
- Xiang, Z., Haroutunian, V., Ho, L., Purohit, D., & Pasinetti, G. M. (2006). Microglia activation in the brain as inflammatory biomarker of Alzheimer's disease neuropathology and clinical dementia. *Disease Markers*, *22*, 95–102.
- Xie, Z., Yang, X., Deng, X., Ma, M., & Shu, K. (2017). A genome-wide association study and complex network identify four core hub genes in bipolar disorder. *International Journal of Molecular Sciences*, *18*(12). <https://doi.org/10.3390/ijms18122763>
- Xiong, C., Wen, Z., Yu, J., Chen, J., Liu, C. P., Zhang, X., Chen, P., Xu, R. M., & Li, G. (2018). UBN1/2 of HIRA complex is responsible for recognition and deposition of H3.3 at cis-regulatory elements of genes in mouse ES cells. *BMC Biology*, *16*(1), 1–18. <https://doi.org/10.1186/s12915-018-0573-9>
- Xu, W., Tan, L., Wang, H. F., Jiang, T., Tan, M. S., Tan, L., Zhao, Q. F., Li, J. Q., Wang, J., & Yu, J. T. (2015). Meta-analysis of modifiable risk factors for Alzheimer's disease. *Journal of Neurology, Neurosurgery and Psychiatry*, *86*(12), 1299–1306. <https://doi.org/10.1136/jnnp-2015-310548>
- Xue, F., Tian, J., Yu, C., Du, H., & Guo, L. (2021). Type I interferon response-related microglial Mef2c deregulation at the onset of Alzheimer's pathology in 5x*FAD* mice. *Neurobiology of Disease*, *152*, 105272. <https://doi.org/10.1016/j.nbd.2021.105272>
- Yang, C. C., Ornatsky, O. I., McDermott, J. C., Cruz, T. F., & Prody, C. A. (1998). Interaction of myocyte enhancer factor 2 (MEF2) with a mitogen-activated protein kinase,

- ERK5/BMK1. *Nucleic Acids Research*, 26(20), 4771–4777.  
<https://doi.org/10.1093/nar/26.20.4771>
- Yang, J. H., Choi, J. H., Jang, H., Park, J. Y., Han, J. W., Youn, H. D., & Cho, E. J. (2011). Histone chaperones cooperate to mediate Mef2-targeted transcriptional regulation during skeletal myogenesis. *Biochemical and Biophysical Research Communications*, 407(3), 541–547. <https://doi.org/10.1016/j.bbrc.2011.03.055>
- Yang, S.-H., Galanis, A., & Sharrocks, A. D. (1999). Targeting of p38 Mitogen-Activated Protein Kinases to MEF2 Transcription Factors. *Molecular and Cellular Biology*, 19(6), 4028–4038. <https://doi.org/10.1128/mcb.19.6.4028>
- Yang, Y., Liu, L., Naik, I., Braunstein, Z., Zhong, J., & Ren, B. (2017). Transcription factor C/EBP homologous protein in health and diseases. *Frontiers in Immunology*, 8(NOV). <https://doi.org/10.3389/fimmu.2017.01612>
- Yanofsky, M. F., Ma, H., Bowman, J. L., Drews, G. N., Feldmann, K. A., & Meyerowitz, E. M. (1990). The protein encoded by the Arabidopsis homeotic gene *agamous* resembles transcription factors. *Nature*, 346(6279), 35–39. <https://doi.org/10.1038/346035a0>
- Yao, Y., & Fu, K. Y. (2020). Serum-deprivation leads to activation-like changes in primary microglia and BV-2 cells but not astrocytes. *Biomedical Reports*, 13(5), 1–8. <https://doi.org/10.3892/br.2020.1358>
- Yoo, T. H., Pedigo, C. E., Guzman, J., Correa-Medina, M., Wei, C., Villarreal, R., Mitrofanova, A., Leclercq, F., Faul, C., Li, J., Kretzler, M., Nelson, R. G., Lehto, M., Forsblom, C., Groop, P. H., Reiser, J., Burke, G. W., Fornoni, A., & Merscher, S. (2015). Sphingomyelinase-like phosphodiesterase 3b expression levels determine podocyte injury phenotypes in glomerular disease. *Journal of the American Society of Nephrology*, 26(1), 133–147. <https://doi.org/10.1681/ASN.2013111213>
- Youn, H., Chatila, T. A., & Liu, J. O. (2000). Integration of calcineurin and MEF2 signals by the coactivator p300 during T-cell apoptosis. *The EMBO Journal*, 19(16), 4323–4331.
- Youn, H. D., & Liu, J. O. (2000). Cabin1 represses MEF2-dependent Nur77 expression and T cell apoptosis by controlling association of histone deacetylases and acetylases with MEF2. *Immunity*, 13(1), 85–94. [https://doi.org/10.1016/S1074-7613\(00\)00010-8](https://doi.org/10.1016/S1074-7613(00)00010-8)
- Youn, H. D., Sun, L., Prywes, R., & Liu, J. O. (1999). Apoptosis of T cells mediated by Ca<sup>2+</sup>-induced release of the transcription factor MEF2. *Science*, 286(5440), 790–793. <https://doi.org/10.1126/science.286.5440.790>
- Young, A. M. H., Kumasaka, N., Calvert, F., Hammond, T. R., Knights, A., Panousis, N., Park, J. S., Schwartzenuber, J., Liu, J., Kundu, K., Segel, M., Murphy, N. A., McMurrin, C. E., Bulstrode, H., Correia, J., Budohoski, K. P., Joannides, A., Guilfoyle, M. R., Trivedi, R., ... Gaffney, D. J. (2021). A map of transcriptional heterogeneity and regulatory variation in human microglia. *Nature Genetics*, 53(6), 861–868. <https://doi.org/10.1038/s41588-021-00875-2>
- Yu, Y. T., Breitbart, R. E., Smoot, L. B., Lee, Y., Mahdavi, V., & Nadal-Ginard, B. (1992). Human myocyte-specific enhancer factor 2 comprises a group of tissue-restricted MADS box transcription factors. *Genes and Development*, 6(9), 1783–1798. <https://doi.org/10.1101/gad.6.9.1783>
- Yuan, P., Condello, C., Keene, C. D., Wang, Y., Bird, T. D., Paul, S. M., Luo, W., Colonna, M., Baddeley, D., & Grutzendler, J. (2016). TREM2 Haplodeficiency in Mice and Humans

- Impairs the Microglia Barrier Function Leading to Decreased Amyloid Compaction and Severe Axonal Dystrophy. *Neuron*, 90(4), 724–739.  
<https://doi.org/10.1016/j.neuron.2016.05.003>
- Yusufzai, T. M., Tagami, H., Nakatani, Y., & Felsenfeld, G. (2004). CTCF Tethers an Insulator to Subnuclear Sites, Suggesting Shared Insulator Mechanisms across Species. *Molecular Cell*, 13(2), 291–298. [https://doi.org/10.1016/S1097-2765\(04\)00029-2](https://doi.org/10.1016/S1097-2765(04)00029-2)
- Zaret, K. S., & Carroll, J. S. (2011). Pioneer transcription factors : establishing competence for gene expression Parameters affecting transcription factor access to target sites in chromatin Initiating events in chromatin : pioneer factors bind first. *Genes and Development*, 2227–2241. <https://doi.org/10.1101/gad.176826.111.GENES>
- Zatti, G., Ghidoni, R., Barbiero, L., Binetti, G., Pozzan, T., Fasolato, C., & Pizzo, P. (2004). The presenilin 2 M239I mutation associated with familial Alzheimer’s disease reduces Ca<sup>2+</sup> release from intracellular stores. *Neurobiology of Disease*, 15(2), 269–278.  
<https://doi.org/10.1016/j.nbd.2003.11.002>
- Zetser, A., Gredinger, E., & Bengal, E. (1999). *p38 Mitogen-activated Protein Kinase Pathway Promotes Skeletal Muscle Differentiation PARTICIPATION OF THE MEF2C TRANSCRIPTION FACTOR\**. <http://www.jbc.org/>
- Zhang, K. Z., Lindsberg, P. J., Tatlisumak, T., Kaste, M., Olsen, H. S., & Andersson, L. C. (2000). Stanniocalcin: A molecular guard of neurons during cerebral ischemia. *Proceedings of the National Academy of Sciences of the United States of America*, 97(7), 3637–3642. <https://doi.org/10.1073/pnas.97.7.3637>
- Zhang, M., Zhu, B., & Davie, J. (2015). Alternative splicing of MEF2C pre-mRNA controls its activity in normal myogenesis and promotes tumorigenicity in rhabdomyosarcoma cells. *Journal of Biological Chemistry*, 290(1), 310–324.  
<https://doi.org/10.1074/jbc.M114.606277>
- Zhang, Y., Liu, T., Meyer, C. A., Eeckhoutte, J., Johnson, D. S., Bernstein, B. E., Nussbaum, C., Myers, R. M., Brown, M., Li, W., & Shirley, X. S. (2008). Model-based analysis of ChIP-Seq (MACS). *Genome Biology*, 9(9). <https://doi.org/10.1186/gb-2008-9-9-r137>
- Zhao, M., New, L., Kravchenko, V. V., Kato, Y., Gram, H., di Padova, F., Olson, E. N., Ulevitch, R. J., & Han, J. (1999). Regulation of the MEF2 Family of Transcription Factors by p38. *Molecular and Cellular Biology*, 19(1), 21–30. <https://doi.org/10.1128/mcb.19.1.21>
- Zhao, Yan, & Zhao, B. (2013). Oxidative Stress and the Pathogenesis of Alzheimer’s Disease. *Oxidative Medicine and Cellular Longevity*, 2013. <https://doi.org/10.1155>
- Zhao, Yuhai, Cong, L., Jaber, V., & Lukiw, W. J. (2017). Microbiome-derived lipopolysaccharide enriched in the perinuclear region of Alzheimer’s disease brain. *Frontiers in Immunology*, 8(SEP), 1–6. <https://doi.org/10.3389/fimmu.2017.01064>
- Zheng, H., Jia, L., Liu, C. C., Rong, Z., Zhong, L., Yang, L., Chen, X. F., Fryer, J. D., Wang, X., Zhang, Y. W., Xu, H., & Bu, G. (2017). TREM2 promotes microglial survival by activating wnt/β-catenin pathway. *Journal of Neuroscience*, 37(7), 1772–1784.  
<https://doi.org/10.1523/JNEUROSCI.2459-16.2017>
- Zhou, H., Di Palma, S., Preisinger, C., Peng, M., Polat, A. N., Heck, A. J. R., & Mohammed, S. (2013). Toward a Comprehensive Characterization of a Human Cancer Cell Phosphoproteome. *Journal of Proteome Research*, 12(1), 260–271.
- Zhou, X., Marks, P. A., Rifkind, R. A., & Richon, V. M. (2001). *Cloning and characterization of*

*a histone deacetylase, HDAC9.* [www.pnas.org/cgi/doi/10.1073/pnas.191375098](http://www.pnas.org/cgi/doi/10.1073/pnas.191375098)

- Zhou, Y., Zhou, B., Pache, L., Chang, M., Khodabakhshi, A. H., Tanaseichuk, O., Benner, C., & Chanda, S. K. (2019). Metascape provides a biologist-oriented resource for the analysis of systems-level datasets. *Nature Communications*, *10*(1). <https://doi.org/10.1038/s41467-019-09234-6>
- Zhu, B., & Gulick, T. (2004). Phosphorylation and Alternative Pre-mRNA Splicing Converge To Regulate Myocyte Enhancer Factor 2C Activity. *Molecular and Cellular Biology*, *24*(18), 8264–8275. <https://doi.org/10.1128/mcb.24.18.8264-8275.2004>
- Zhu, Bangmin, Ramachandran, B., & Gulick, T. (2005). Alternative pre-mRNA splicing governs expression of a conserved acidic transactivation domain in myocyte enhancer factor 2 factors of striated muscle and brain. *Journal of Biological Chemistry*, *280*(31), 28749–28760. <https://doi.org/10.1074/jbc.M502491200>
- Zhu, J., Ghosh, A., & Sarkar, S. N. (2015a). OASL – a new player in controlling antiviral innate immunity. *Current Opinion in Virology*, *12*, 15–19. <https://doi.org/10.1016/j.physbeh.2017.03.040>
- Zhu, X. C., Tan, L., Wang, H. F., Jiang, T., Cao, L., Wang, C., Wang, J., Tan, C. C., Meng, X. F., & Yu, J. T. (2015b). Rate of early onset Alzheimer’s disease: A systematic review and meta-analysis. *Annals of Translational Medicine*, *3*(3). <https://doi.org/10.3978/j.issn.2305-5839.2015.01.19>
- Zhu, Y., Denholtz, M., Lu, H., & Murre, C. (2021). Calcium signaling instructs NIPBL recruitment at active enhancers and promoters via distinct mechanisms to reconstruct genome compartmentalization. *Genes and Development*, *35*(1), 65–81. <https://doi.org/10.1101/GAD.343475.120>
- Zweier, M., & Rauch, A. (2012). The MEF2C-related and 5q14.3q15 microdeletion syndrome. *Molecular Syndromology*, *2*(3–5), 164–170. <https://doi.org/10.1159/000337496>



## Appendix

### Appendix 1. Known interactors of Mef2c

**Appendix Table 1. Known MEF2C interactors.** Known interactors of human MEF2C downloaded from the National Center for Biotechnology Information (NCBI). Interactors are supported by a range of experimental evidence including yeast two-hybrid and affinity capture western. Descriptions of each interactor have been extracted from their corresponding NCBI entry. Interactors identified in the current data set that survive the filtering process are highlighted in red. Sources of the interaction data include the Biomolecular Interaction Network Database (BIND), the Biological General Repository for Interaction Datasets (BioGRID) and the Human Protein Reference Database (HPRD).

Interactor	Description	Source	Experimental Evidence	Cell/Tissue Type	Publication
<b>ASCL1</b>	Member of the basic helix-loop-helix (BHLH) family of transcription factors. Plays a role in the neuronal commitment and differentiation and in the generation of olfactory and autonomic neurons.	BioGRID	Two-hybrid	10T1/2 fibroblasts	Black et al (1996)
<b>CCNB1</b>	Regulatory protein involved in mitosis. Is necessary for proper control of the G2/M phase of the cell cycle.	HPRD	<i>In vitro</i> kinase assay	N/A ( <i>in vitro</i> )	Kang et al (2006)
<b>CDK1</b>	Member of the serine/threonine kinase family. Is essential for G1/S and G2/M phase transitions of the cell cycle	HPRD	<i>In vitro</i> kinase assay	N/A ( <i>in vitro</i> )	Kang et al (2006)
<b>COP55</b>	One of the eight subunits of COP9 signalosome, a highly conserved protein complex that functions as an important regulator in multiple signalling pathways.	BioGRID	Two-hybrid	Yeast	Bandyopadhyay et al (2010)
<b>CSNK2A1</b>	Casein Kinase II is a serine/threonine protein kinase that phosphorylates acidic proteins such as casein. It is involved in various cellular processes, including cell cycle control, apoptosis, and circadian rhythm.	HPRD	Phosphoamino acid analysis	COS Fibroblasts	Molkentin et al (1996b)
<b>EP300 (p300)</b>	Transcriptional coactivator protein. It functions as histone acetyltransferase that regulates transcription via	BioGRID HPRD	Phenotypic Enhancement; Reconstituted Complex	NIH-3T3 embryo fibroblasts	Sartorelli et al (1997)

Appendix

	chromatin remodelling and is important in the processes of cell proliferation and differentiation.				
<b>EPAS1</b>	Transcription factor involved in the induction of genes regulated by oxygen. Is induced as oxygen levels fall.	BioGRID	Two-hybrid	Yeast	Bandyopadhyay et al (2010)
<b>GATA4</b>	Member of the GATA family of zinc-finger transcription factors. Regulates genes involved in embryogenesis and in myocardial differentiation and function and is necessary for normal testicular development.	HPRD	<i>In vitro</i> pull-down assay	N/A ( <i>in vitro</i> )	Morin et al (2000)
<b>HDAC7</b>	Class II member of histone deacetylase family. Possesses histone deacetylase activity and represses transcription when tethered to a promoter.	BioGRID	Affinity Capture-Western; Reconstituted Complex	COS-7 fibroblasts, HeLa cancer cells	Dressel et al (2001); Gao et al (2008)
<b>HDAC9</b>	Class II member of histone deacetylase family. Possesses histone deacetylase activity and represses transcription when tethered to a promoter.	BioGRID	Two-hybrid	Yeast	Bandyopadhyay et al (2010); Ravasi et al (2010)
<b>IFRD1</b>	Immediate early gene that encodes a protein related to interferon-gamma. May function as a transcriptional co-activator/repressor that controls the growth and differentiation of specific cell types during embryonic development and tissue regeneration.	BioGRID	Affinity Capture-Western; Reconstituted Complex	C2C7 myoblasts, C2C12 myoblasts	Micheli et al (2005)
<b>MAPK14 (p38)</b>	Member of the MAP kinase family. Involved in the downstream signalling processes of various receptor molecules. It regulates transcription factor activity via phosphorylation.	BioGRID HPRD	Two-hybrid	Yeast, COS-7 fibroblasts	Bandyopadhyay et al., 2010; Han et al., 1997; Yang et al., 1999
<b>MAPK7 (ERK5)</b>	Member of the MAP kinase family. Involved in the downstream signalling processes of various receptor molecules. It regulates transcription factor activity via phosphorylation.	BioGRID BIND HPRD	Biochemical Activity; Reconstituted Complex; Two-hybrid	Yeast, primary rat myotubes, COS-1 fibroblasts	Bandyopadhyay et al (2010); Huang et al (2003); Kato et al (1997); Yang et al (1998)

Appendix

<b>MEF2B</b>	Member of the MADS box transcription enhancer factor 2 (MEF2) family of proteins, which play a role in myogenesis.	BioGRID	Affinity Capture-MS	HEK293T (stable OE)	Huttlin et al (2017)
<b>MEF2D</b>	Member of the MADS box transcription enhancer factor 2 (MEF2) family of proteins, which play a role in myogenesis.	HPRD	Electrophoretic mobility shift assay (EMSA)	HEK293T	Zhao et al (1999)
<b>MYOD1</b>	Member of the basic helix-loop-helix family of transcription factors and the myogenic factors subfamily. Regulates muscle cell differentiation by inducing cell cycle arrest, a prerequisite for myogenic initiation.	BioGRID	Reconstituted Complex; Two-hybrid	10T1/2 fibroblasts	Black et al (1998); Micheli et al (2005)
<b>MYOG</b>	Member of the helix-loop-helix (HLH) proteins. Myogenin is a muscle-specific transcription factor that can induce myogenesis, it is essential for the development of functional skeletal muscle.	BioGRID	Reconstituted Complex	10T1/2 fibroblasts	Molkentin et al (1995)
<b>NCOA2</b>	Transcriptional coactivator for nuclear hormone receptors, including steroid, thyroid, retinoid, and vitamin D receptors.	BioGRID HPRD	Reconstituted Complex	C2C12 myoblasts, C3H-10T1/2 fibroblasts, COS7 cells	Lazaro et al (2002)
<b>NOTCH1</b>	Member of the NOTCH family of proteins. It is proteolytically processed to generate two polypeptide chains that heterodimerize to form the mature cell-surface receptor. This receptor plays a role in the development of numerous cell and tissue types.	HPRD	Two-hybrid; Immunoprecipitation- Western	10T1/2 fibroblasts, COS fibroblasts	Wilson-Rawls et al (1999)
<b>PLA2G12A</b>	Group XII secreted phospholipase A2 (sPLA2) enzyme. Liberates arachidonic acid from phospholipids for production of eicosanoids.	BioGRID	Two-hybrid	Yeast	Wang et al (2011)
<b>SIRT1</b>	Class I member of the sirtuin family of proteins. Human sirtuins may function as intracellular regulatory proteins with mono-ADP-ribosyltransferase activity.	BioGRID	Co-localization	C2C12 myotubes	Amat et al (2009)
<b>SKP2</b>	Fbls class member of the F-box protein family. Essential element of the cyclin A-CDK2 S-phase kinase.	BioGRID	Affinity Capture-Western	BJ/TERT fibroblasts	Di Giorgio et al (2015)

Appendix

<b>SMAD2</b>	Member of the SMAD family. Mediates the signal of the transforming growth factor (TGF)-beta, and thus regulates multiple cellular processes, such as cell proliferation, apoptosis, and differentiation.	BioGRID HPRD	Reconstituted Complex	C2C12 myoblasts/ myotubes, COS fibroblasts	Quinn et al (2001)
<b>SOX18</b>	Member of the SOX family of transcription factors. Acts as a transcriptional regulator.	BioGRID BIND HPRD	Affinity Capture-Western; Reconstituted Complex	SVEC4-10 endothelial cells	Hosking et al (2001)
<b>SP1</b>	Zinc finger transcription factor that binds to GC-rich motifs of many promoters. It is involved in many cellular processes, including cell differentiation, cell growth, apoptosis, immune responses, response to DNA damage, and chromatin remodelling.	BioGRID HPRD	Affinity Capture-Western; Two-hybrid	Yeast, HeLa cancer cells	Krinc et al (1998)
<b>SPTBN1</b>	Member of a family of beta-spectrin genes. Spectrin is an actin crosslinking and molecular scaffold protein that links the plasma membrane to the actin cytoskeleton, and functions in the determination of cell shape, arrangement of transmembrane proteins, and organization of organelles.	BioGRID	Two-hybrid	Yeast	Bandyopadhyay et al (2010)
<b>TEAD1</b>	Member of the TEA/ATTS domain family. Ubiquitous transcriptional enhancer factor that directs the transactivation of a wide variety of genes.	BioGRID HPRD	Affinity Capture-Western; Reconstituted Complex	Control plantaris (muscle), MOV-P adult mouse muscle	Karasseva et al (2003)
<b>TWIST2</b>	Basic helix-loop-helix type transcription factor. Thought to inhibit osteoblast maturation and maintain cells in a preosteoblast phenotype during osteoblast development.	BioGRID HPRD	Affinity Capture-Western	COS fibroblasts	Gong & Li (2002)
<b>UBE2I</b>	Member of the E2 ubiquitin-conjugating enzyme family. The modification of proteins with ubiquitin is an important cellular mechanism for targeting abnormal or short-lived proteins for degradation.	BioGRID	Biochemical Activity	HeLa cancer cells	Gocke et al (2005)

## Appendix

<b>VGLL2</b>	Member of the Vestigial-like family. Thought to act as a co-factor of TEF-1 regulated gene expression during skeletal muscle development.	HPRD	Two-hybrid	Cardiac myocytes	Maeda et al (2002a)
<b>VGLL4</b>	Member of the Vestigial-like family. Transcriptional cofactor thought to modulate the activity of TEF-1 factors.	HPRD	Two-hybrid	Cardiac myocytes	Chen et al (2004)
<b>YWHAZ</b>	Member of the 14-3-3 family of proteins which mediate signal transduction by binding to phosphoserine-containing proteins.	BioGRID	Two-hybrid	Yeast	Bandyopadhyay et al (2010)

## Appendix 2. MDARs identified by HOMER

**Appendix Table 2. Mef2c motif-containing differentially accessible regions.** MDARs identified by HOMER. Chromosome positions, genes associated with these regions, and motif information are presented.

Chromosome_Start_End	Gene Name	Accessibility	Mef2c Motif Distance From Peak (sequence, strand, conservation)
chr1_107419538_107419938	Serpib7	Increased	139(GCTATTTTGAAA,-,0.00)
chr1_118689855_118690255	Tfcp2l1	Increased	13(TCTATTTCTGGA,-,0.00)
chr1_128514248_128514648	Cxcr4	Increased	235(TCTAAAATTAGA,+,0.00)
chr1_138919971_138920371	1700019P21Rik	Increased	87(TGCAGAAATAGC,+,0.00),115(ACCCAAAATAGC,+,0.00)
chr1_152083867_152084267	1700025G04Rik	Increased	333(ACAAAAAATAGC,+,0.00)
chr1_152992260_152992660	Nmnat2	Decreased	218(CCTATTTTATAG,-,0.00)
chr1_172289605_172290005	Atp1a2	Increased	25(GTTATTTATGTA,-,0.00)
chr1_172918467_172918867	Apcs	Increased	55(ATTATTTTGGC,-,0.00),152(GCTATTTCCAGA,-,0.00)
chr1_191169599_191169999	Fam71a	Increased	310(ATTAAAAATAAA,+,0.00),316(AATAAAAATAGA,+,0.00)
chr1_20634822_20635222	Pkhd1	Increased	325(TCCAAGAATAGC,+,0.00)

Appendix

chr1_36304799_36305199	Arid5a	Increased	120(TCTATTTCAAGC,-,0.00)
chr1_37386427_37386827	Inpp4a	Increased	231(TCTAATTTAAGC,-,0.00)
chr1_37951810_37952210	Lyg1	Increased	273(TCTCTAAATAGA,+,0.00)
chr1_47468267_47468667	Mir6350	Increased	219(GCTATTTTTAGA,-,0.00)
chr1_58524886_58525286	Orc2	Increased	257(TTTATTTTTACA,-,0.00),302(TCTATTTTTAAG,-,0.00), 346(CTTATTTTTGGA,-,0.00)
chr1_60859839_60860239	Ctla4	Increased	357(ACTCAAATAAA,+,0.00)
chr1_71395991_71396391	Abca12	Increased	59(GATAGAAATAGC,+,0.00)
chr1_74147114_74147514	Cxcr2	Decreased	185(TCCTAAAATAGA,+,0.00)
chr1_80221151_80221551	Fam124b	Decreased	310(AGCAAAAATAGA,+,0.00)
chr1_89622644_89623044	4933400F21Rik	Increased	148(CCTATTTTTGGA,-,0.00)
chr10_21029136_21029536	Ahi1	Increased	380(TATATTTTTGGC,-,0.00)
chr10_21535535_21535935	1700020N01Rik	Increased	47(TCTCAAATAAA,+,0.00)
chr10_39324327_39324727	Fyn	Increased	270(ACTAAAATAAT,+,0.00)
chr10_44135346_44135746	Crybg1	Decreased	56(GCTAAAATACA,+,0.00),180(GGTATAAATAGA,+,0.00)
chr10_53765507_53765907	Fam184a	Increased	72(TCTATAAATAAA,+,0.00)
chr10_56024555_56024955	Msl3l2	Increased	115(GCTATTTTTACA,-,0.00)
chr10_58872052_58872452	Sh3rf3	Increased	84(GCTATTTTTGGT,-,0.00)
chr10_95336700_95337100	2310039L15Rik	Increased	272(TCTATTCTGTA,-,0.00)
chr10_95914467_95914867	Eea1	Increased	342(ACCTAAAATAAA,+,0.00)
chr10_96093937_96094337	4930459C07Rik	Increased	365(GATAAAATTAGC,+,0.00)
chr10_96410037_96410437	4930459C07Rik	Increased	22(TCTATTTCTGCC,-,0.00)
chr10_96863290_96863690	4930556N09Rik	Increased	40(GCTATTTTCATT,-,0.00),199(GCTATTCTTGGT,-,0.00)
chr10_98728784_98729184	Atp2b1	Increased	333(AATATAAATAGA,+,0.00)

Appendix

chr11_111331656_111332056	Kcnj2	Increased	53(TTTATAAATAGA,+0.00),197(TCTATTTTACA,-0.00)
chr11_111801042_111801442	Kcnj2	Increased	360(ACTATTTTGGGT,-0.00)
chr11_11417339_11417739	Zbp1	Increased	36(AATAAAAATAGA,+0.00)
chr11_17043837_17044237	Cnrip1	Increased	114(CTTAAAAATAGC,+0.00)
chr11_29778070_29778470	4931440F15Rik	Decreased	56(GGCAAAAATAGC,+0.00),242(GCCTGAAATAGC,+0.00)
chr11_32029344_32029744	Nsg2	Increased	45(AATAAAAATAAA,+0.00),246(TCCAAAAATAGC,+0.00)
chr11_54151914_54152314	P4ha2	Increased	200(TCTATTTTAATC,-0.00)
chr11_78648464_78648864	Nlk	Increased	279(ACTAGAAATAAC,+0.00)
chr11_88586322_88586722	0610039H22Rik	Increased	240(TCTATAAATACC,+0.00)
chr11_9897152_9897552	Abca13	Increased	194(TCCAAAATTAAC,+0.00),383(GATAAAAATATC,+0.00)
chr12_100575798_100576198	Ttc7b	Increased	324(TACAAAATAAC,+0.00)
chr12_119170111_119170511	Itgb8	Increased	35(TCCAAAATAAA,+0.00),340(TTTTAAAATAGC,+0.00),367(GCTAAAATA TA,+0.00)
chr12_16160604_16161004	Trib2	Increased	236(CCCAGAAATAGC,+0.00)
chr12_16473850_16474250	Lpin1	Increased	104(ACTGAAAATAAA,+0.00)
chr12_38861218_38861618	Etv1	Increased	316(TCTATTTATAAC,-0.00)
chr12_38951712_38952112	Etv1	Increased	36(GTTATATTTGGA,-0.00),228(TCTGGAAATAGA,+0.00)
chr12_51517126_51517526	Coch	Increased	26(TCTATTTAAGGT,-0.00)
chr12_72953878_72954278	Six6	Decreased	182(CCTATTTTATC,-0.00)
chr12_73895485_73895885	Hif1a	Increased	255(GCTATTTTGGAG,-0.00)
chr12_79759342_79759742	9430078K24Rik	Increased	287(GTTATAAATAAC,+0.00)
chr12_85256029_85256429	Mir6938	Increased	302(CCTATTTCTGGA,-0.00)
chr13_102576636_102577036	Cd180	Increased	218(GCTATTTTAAA,-0.00)
chr13_103077686_103078086	Mast4	Increased	384(AATAAAATAGC,+0.00)

Appendix

chr13_118024789_118025189	4933413L06Rik	Increased	232(TTTATATTTGGC,-,0.00)
chr13_19451261_19451661	9330199G10Rik	Increased	279(TCTATTTTGAGA,-,0.00)
chr13_19822888_19823288	Gpr141	Increased	273(GCCAAAATTAAC,+,0.00)
chr13_24203836_24204236	Carmil1	Increased	88(GTTATTTCTGGC,-,0.00)
chr13_3551050_3551450	Gdi2	Increased	131(GTCAAAAATAGT,+,0.00),181(AATATAAATAGC,+,0.00)
chr13_40137093_40137493	Ofcc1	Increased	319(TCTATTTATAGA,-,0.00)
chr13_41431807_41432207	Nedd9	Increased	279(TCCAGAAATAGA,+,0.00),333(TTTATTTTGTAGT,-,0.00)
chr13_63970605_63971005	Hsd17b3	Increased	222(GCTCAAAATAGC,+,0.00)
chr13_64361479_64361879	Ctsl	Increased	88(TTTATTTCTAGT,-,0.00)
chr13_90251106_90251506	Tmem167	Increased	84(TTTATTTTGGGC,-,0.00)
chr13_9304893_9305293	Dip2c	Increased	321(ACTATAATTAGC,+,0.00)
chr14_57101789_57102189	Gjb2	Increased	187(TCTATATATGGC,-,0.00)
chr14_62835236_62835636	Wdfy2	Increased	109(TCTATTTATGAC,-,0.00)
chr14_63013106_63013506	Defb43	Increased	110(GTTATTTATAGA,-,0.00)
chr14_65270250_65270650	Fbxo16	Increased	363(TACAAAATAAAA,+,0.00)
chr14_86017625_86018025	4930529K09Rik	Increased	323(ATTAAAAATAAAA,+,0.00)
chr15_14374457_14374857	Cdh6	Increased	104(CCTATTTATGGT,-,0.00)
chr15_15370430_15370830	Cdh9	Increased	102(TCTATATTTGGA,-,0.00)
chr15_37443385_37443785	Gm15941	Increased	356(GCTATATTTGTT,-,0.00)
chr15_37950756_37951156	Rrm2b	Increased	301(GGTATTTTGTGC,-,0.00)
chr15_4012484_4012884	Oxct1	Increased	212(TCTCAAAATAGC,+,0.00)
chr15_5355364_5355764	Ptger4	Increased	47(ACTATATTTAGA,-,0.00)
chr15_62271452_62271852	H2afy3	Increased	192(TGTATTTTGTAGC,-,0.00)
chr15_67397297_67397697	1700012111Rik	Increased	340(TCTATTTTGGGA,-,0.00)



Appendix

chr16_19848722_19849122	A930003A15Rik	Decreased	83(GTCAAAATTAGC,+0.00)
chr16_23932397_23932797	Rtp2	Increased	368(ACTAATTTTAGC,-0.00)
chr16_24840027_24840427	Lpp	Increased	271(TCTATTTTTGCA,-0.00),297(TCTAAATATAGA,+0.00)
chr16_27354381_27354781	Uts2b	Increased	54(GCTATTTTCAGA,-0.00)
chr16_48585345_48585745	Morc1	Decreased	366(TTTATTTTTGAA,-0.00)
chr16_55723169_55723569	Nfkbiz	Increased	205(GCCAAAAAAGA,+0.00)
chr16_55735479_55735879	Nfkbiz	Increased	305(GCCAAAAATAGT,+0.00)
chr16_56352164_56352564	Abi3bp	Increased	44(AATAAAAATAAC,+0.00),373(TCTAAAAATAGA,+0.00)
chr16_60247136_60247536	Epha6	Increased	76(TCTATTATAGC,-0.00)
chr16_67284622_67285022	Cadm2	Increased	63(TCCATTTTTAGT,-0.00),306(GTTATTATATT,-0.00)
chr16_70510104_70510504	D16Ert519e	Increased	3(TTTATAAATAAC,+0.00),145(CCTAAAAATAGT,+0.00)
chr16_85247285_85247685	App	Increased	175(GATATTTTTAGC,-0.00)
chr17_30309200_30309600	Gm6402	Increased	18(AATAAAAATAAC,+0.00)
chr17_37167498_37167898	Olfr93	Increased	213(GATAAAAATAGG,+0.00)
chr17_38531558_38531958	Esp34	Increased	89(TTTATTTTAGGT,-0.00)
chr17_44215537_44215937	Clic5	Increased	250(GCTATATTGAGC,-0.00)
chr17_65939831_65940231	Twsg1	Increased	57(GTTATTATATA,-0.00)
chr17_70007647_70008047	Dlgap1	Increased	118(TCCAGAAATAAC,+0.00)
chr17_73081351_73081751	Lclat1	Increased	148(ACTATAAATAGC,+0.00)
chr17_78268048_78268448	Crim1	Increased	189(ACTTTAAATAGA,+0.00)
chr17_81899019_81899419	Slc8a1	Increased	38(TCTATTTATAAT,-0.00)
chr17_83982971_83983371	8430430B14Rik	Decreased	144(ATTAAAAATAGC,+0.00)
chr17_87275930_87276330	4833418N02Rik	Increased	191(TCTAAAATTAAC,+0.00)
chr17_94012405_94012805	Mettl4	Increased	356(TTTATTTGGGT,-0.00)

Appendix

chr18_21079005_21079405	Mep1b	Increased	302(TCTTTAAATAGA,+,0.00)
chr18_21203870_21204270	Garem1	Increased	195(GCTATAAATAAC,+,0.00)
chr18_38861100_38861500	Gm5820	Increased	326(TTTATTTTTATC,-,0.00)
chr18_43994706_43995106	Spink5	Increased	222(ACTATTTTTGGT,-,0.00)
chr18_90541250_90541650	Tmx3	Increased	291(GCTAATTATAGT,-,0.00)
chr19_25641853_25642253	2610016A17Rik	Increased	222(GGTATTTTTATC,-,0.00)
chr19_36891778_36892178	Fgfbp3	Increased	241(GCTATTTTTACT,-,0.00)
chr19_44351748_44352148	Scd4	Decreased	245(CCTATTATAGA,-,0.00)
chr19_57199398_57199798	Ablim1	Increased	327(GTTATTTTTGTC,-,0.00)
chr19_60795294_60795694	Eif3a	Increased	304(GCTAAAATTAGC,+,0.00)
chr2_102934868_102935268	Cd44	Increased	245(TCTATAAATAAA,+,0.00)
chr2_108579143_108579543	Mettl15	Increased	362(TCTATTTTTAGT,-,0.00)
chr2_109331726_109332126	Kif18a	Increased	122(ACCAGAAATAGA,+,0.00),234(GCTATTATTAGC,-,0.00)
chr2_120500019_120500419	Capn3	Decreased	119(GCTTTTTTTAGT,-,0.00)
chr2_136860607_136861007	Slx4ip	Increased	12(GATAAAAATATC,+,0.00),213(AGCAAAAATAGA,+,0.00)
chr2_145401255_145401655	Gm14092	Increased	356(TCCAGAAATAAA,+,0.00)
chr2_160435663_160436063	Mafb	Decreased	78(TACCAAAATAGA,+,0.00)
chr2_165411498_165411898	Ocstamp	Increased	153(TCTATTCTATT,-,0.00),159(TCTATTCTATT,-,0.00)
chr2_29102816_29103216	Setx	Increased	203(ACCAAAAATACC,+,0.00)
chr2_5094892_5095292	Optn	Increased	269(TTTATTTTTGGC,-,0.00)
chr2_51323013_51323413	Gm13497	Decreased	46(GCCAAAATAAA,+,0.00)
chr2_57833043_57833443	Galnt5	Increased	70(ACTATTTTTACC,-,0.00)
chr2_90015053_90015453	Olfr1263	Increased	342(TTTATTTATGGC,-,0.00)
chr2_93416855_93417255	Mir7001	Increased	206(GCTATTTCAATA,-,0.00),344(GCTTTTTTTGGC,-,0.00)

Appendix

chr3_100421513_100421913	4930406D18Rik	Increased	18(GCTATTTTAGAT,-,0.00),103(GCCTGAAATAGC,+,0.00)
chr3_107576792_107577192	Alx3	Increased	129(TTTATTTTGTGTA,-,0.00)
chr3_115038919_115039319	Olfm3	Increased	268(CTTAAAAATAGA,+,0.00)
chr3_117044230_117044630	1700061117Rik	Increased	33(TCTATTTCTAAC,-,0.00)
chr3_124066668_124067068	Tram1l1	Increased	369(TTTAAATATAGC,+,0.00)
chr3_125441934_125442334	Ndst4	Increased	102(ACTATAAATAGA,+,0.00)
chr3_130282848_130283248	Col25a1	Increased	265(GCTAAATATAGT,+,0.00)
chr3_130810043_130810443	Rpl34	Increased	243(TTTATTTTGTGTT,-,0.00)
chr3_132927637_132928037	Npnt	Increased	143(TCTATAATTAGA,+,0.00)
chr3_158140640_158141040	Lrrc40	Increased	331(TCTTAAAATAGA,+,0.00)
chr3_19260629_19261029	Pde7a	Decreased	82(GCTATTTTCAGGT,-,0.00)
chr3_21963830_21964230	Tbl1xr1	Increased	46(GTTAAAAATAAAA,+,0.00),263(GCTATTATTAGA,-,0.00)
chr3_37821174_37821574	Gm20755	Increased	35(GGTAAAAATAGA,+,0.00),387(CATAGAAATAGA,+,0.00)
chr3_60124346_60124746	Sucnr1	Increased	137(TCTAAAAATAAAA,+,0.00)
chr3_68529096_68529496	Schip1	Increased	348(TCTAGAAATAGA,+,0.00)
chr3_86196458_86196858	Lrba	Decreased	327(TTTAAAATTAGC,+,0.00)
chr3_89491495_89491895	Kcnn3	Increased	133(GCTAATTTTAGG,-,0.00)
chr4_124755494_124755894	Gm12915	Increased	243(ACTATTTATATC,-,0.00)
chr4_143263130_143263530	Pdpm	Increased	74(TTTATTTTGAGA,-,0.00)
chr4_145096821_145097221	Vps13d	Increased	66(TCTATTTTAGAT,-,0.00)
chr4_31969918_31970318	Map3k7	Decreased	93(TCTATTTCTATC,-,0.00)
chr4_55670219_55670619	Klf4	Increased	117(TTTATTTTGGGA,-,0.00)
chr4_56231363_56231763	Actl7b	Increased	43(ATTATTTATAGA,-,0.00)
chr5_124185899_124186299	Pitpnm2	Increased	182(TCTATTTAAAGA,-,0.00)

Appendix

chr5_128632953_128633353	Fzd10	Decreased	238(CTTATTTTTGGC,-,0.00)
chr5_147057594_147057994	Lnx2	Increased	143(TCCATTTTTGGT,-,0.00)
chr5_21094417_21094817	Ptpn12	Increased	8(AATCAAAATAGA+,0.00)
chr5_41339996_41340396	Rab28	Increased	22(TCTAAAAATATA+,0.00)
chr5_5618326_5618726	Gm8773	Increased	340(ACTATTTTTGTT,-,0.00)
chr6_100476681_100477081	1700049E22Rik	Decreased	296(ACTTAAAATAAA+,0.00)
chr6_106153500_106153900	Cntn4	Increased	38(CCCATAAATAAC+,0.00),70(CCTATTTTGAGA,-,0.00)
chr6_115457433_115457833	Pparg	Increased	24(GATAAATATAGA+,0.00)
chr6_51633977_51634377	Snx10	Decreased	322(TTTATTTTGAGT,-,0.00)
chr6_52827853_52828253	Jazf1	Increased	157(ACCAAATTAGA+,0.00)
chr6_84965002_84965402	Exoc6b	Increased	223(TGTATTTTGTAGT,-,0.00)
chr7_109541633_109542033	Snora3	Decreased	252(GCTAAAAATACC+,0.00)
chr7_128206181_128206581	Cox6a2	Increased	223(GCTATTTTAGG,-,0.00)
chr7_133220506_133220906	4930483O08Rik	Increased	294(TCTATTATAAC,-,0.00)
chr7_139418167_139418567	Inpp5a	Increased	383(GCTATTTTGGG,-,0.00)
chr7_141932628_141933028	Brsk2	Increased	147(GGTAAAAATAGC+,0.00)
chr7_142074110_142074510	Mob2	Increased	141(TCTATTTAAAGC,-,0.00),161(GCTATTTATAGT,-,0.00)
chr7_142077115_142077515	Mob2	Increased	256(GCTATAAATAGA+,0.00),277(GCTAAAAATACC+,0.00)
chr7_143129290_143129690	Kcnq1	Decreased	148(ATTAAAAATAGC+,0.00)
chr7_16796455_16796855	Slc1a5	Increased	152(TTTATTTTAAAC,-,0.00)
chr7_3322838_3323238	Cacng7	Increased	170(GCTATTTATATC,-,0.00)
chr7_49822111_49822511	Prmt3	Increased	64(TTTATTTTGTAGT,-,0.00)
chr7_72501417_72501817	Mctp2	Increased	234(ACCAAATAAA+,0.00)
chr7_75319930_75320330	Sv2b	Decreased	47(TCTCGAAATAGA+,0.00)

Appendix

chr7_79747696_79748096	Wdr93	Increased	85(GCCAAAATAGC,+0.00)
chr7_92134244_92134644	4930567K12Rik	Increased	304(TCTATTCTTGGA,-0.00)
chr8_111834386_111834786	Cfdp1	Increased	93(GCTATTATTAGC,-0.00)
chr8_11206499_11206899	Col4a2	Increased	234(GATAAAAATAGT,+0.00)
chr8_124283927_124284327	Galnt2	Increased	163(TCTAAAATTTAAA,+0.00)
chr8_127876245_127876645	Mir21c	Increased	295(CATAAAAATAGC,+0.00)
chr8_22726930_22727330	lkbkb	Increased	181(GATAAAAATAAA,+0.00)
chr8_26630578_26630978	2310008N11Rik	Increased	76(ACTTGAAATAGC,+0.00)
chr8_31749174_31749574	Nrg1	Increased	315(TCTATTTATGTT,-0.00)
chr8_8441628_8442028	Efnb2	Increased	179(TCTATTATTAGC,-0.00)
chr9_111619271_111619671	Stac	Increased	168(TTTAAAATAGC,+0.00)
chr9_13057231_13057631	4930568E12Rik	Increased	287(TCTATAAATAAA,+0.00)
chr9_49731965_49732365	Ncam1	Increased	166(GTTATATTTAGA,-0.00)
chr9_51286065_51286465	Colca2	Increased	371(TCTATTTTTAAA,-0.00)
chr9_64261007_64261407	Map2k1	Increased	116(TCTACAAATAGC,+0.00)
chr9_76211584_76211984	Gfral	Increased	5(GCTATTTTTACT,-0.00)
chr9_83008675_83009075	Phip	Increased	260(TCTATTTTGGTC,-0.00)
chr9_92377955_92378355	1700057G04Rik	Increased	50(CCTAAAATAAA,+0.00),302(GCTATTTAAGTC,-0.00)
chrX_107432470_107432870	Itm2a	Increased	96(TCTATTTTTAGG,-0.00)
chrX_13606753_13607153	Gpr34	Decreased	230(GCTATTTTTGGT,-0.00)
chrX_156156249_156156649	4930503H13Rik	Increased	110(TCTATTTTTAAA,-0.00)
chrX_159731468_159731868	Sh3kbp1	Increased	63(TCCAGAAATAAA,+0.00)
chrX_169592448_169592848	Mid1	Increased	182(CCTATTTTGAGC,-0.00)
chrX_50697375_50697775	Firre	Increased	357(TTTATTTTGGGA,-0.00)

Appendix

chrX_57373045_57373445	Snord61	Increased	1(GCTATTTTGAAA,-,0.00),288(GGTATTTTATT,-,0.00)
chrX_75848850_75849250	Pls3	Increased	242(GGCAAAAATAAC,+,0.00)